

Identification of novel cold-adapted nitrilase superfamily enzymes

Andrew James Mascré Nel



Identification of novel cold-adapted nitrilase superfamily enzymes

Andrew James Mascré Nel



**A thesis submitted in partial fulfilment of the requirements for the degree of
DOCTOR OF PHILOSOPHY**

Institute of Microbial Biotechnology and Metagenomics (IMBM)

University of the Western Cape

Bellville, Cape Town

Supervisor: Professor D.A. Cowan

June 2009

The financial assistance of the Department of Labour (DoL) toward this research is hereby acknowledged. Opinions expressed and conclusions arrived at, are those of the author and are not necessarily to be attributed to the DoL.

Contents

Abstract	iv
Acknowledgements	vi
Abbreviations	vi
Figures	viii
Tables	x
Chapter 1: Literature review	1
1.1 Bacterial hydrolysis of nitriles and amides	2
1.2 Biotechnological potential of NHases, Nases and amidases	4
1.3 Distribution of nitrile and amide hydrolysing bacteria	6
1.4 NHases	10
1.5 Nases	13
1.6 Aliphatic amidases	16
1.7 The Nitrilase superfamily	19
1.8 Cold adapted enzymes	33
1.8 Aims	35
Chapter 2: Isolation of a cold-adapted nitrile hydrolysing bacterium	36
2.1 Introduction	37
2.2 Materials and methods	38
2.3 Results	45
2.4 Discussion	56
Chapter 3: Gene mining and <i>in silico</i> protein characterisation of nitrile hydrolysing enzymes	58
3.1 Introduction	60
3.2 Materials and Methods	63
3.3 Results	69
3.4 Discussion	93



Chapter 4: Expression and characterisation of the two putative nitrilase proteins, Nit1 and Nit2	97
4.1 Introduction	98
4.2 Materials and methods	99
4.3 Results	105
4.4 Discussion	118
Chapter 5: Crystal structure of Nit2	122
5.1 Introduction	123
5.2 Materials and Methods	123
5.3 Results & discussion	126
Chapter 6: General discussion and future implications	143
Appendix	151
References	162



Abstract

In bacteria, nitrile hydratases and enzymes of nitrilase and signature amidase superfamilies hydrolyse nitriles and amides to their corresponding carboxylic acids releasing ammonia. Bacteria expressing these enzymes are typically isolated where a sole nitrogen and/or carbon source is used to support their growth. The majority of characterised enzymes of industrial potential have been identified for their stabilities at elevated temperatures. To date, no reports of such enzymes have been isolated from cold adapted bacteria.

In this study, an extensive screening program of cold-active microbial isolates for enzymes of this group led to the selection and detailed characterisation of an aliphatic amidase from *Nesterenkonia*.

Nesterenkonia AN1, a new psychrotrophic isolate of the genus, was isolated from soil samples collected from the Miers Valley, Antarctica. AN1 showed significant 16S rRNA sequence identity to known members of the genera, but this is the only strain that had optimal growth at approximately 21°C. AN1, similar to known members, is an obligately alkaliphilic (pH 9-10) and halotolerant (Na⁺ 0-15% (w/v)) strain.

The genome of *Nesterenkonia* AN1, sequenced in-house, revealed two ORFs encoding putative nitrilases, referred to as Nit1 and Nit2. Based on analysis of their deduced protein sequences, both belonged to the nitrilase superfamily. Both sequences showed conserved catalytic residues (EKEC), glycine residues and contained the characteristic monomer fold. Homology modelling using known structures suggested that both genes could encode N-carbamoyl-D-amino acid amidohydrolases, although neither showed conserved residues implicated in the hydrolysis of carbamoyls.

Nit1 and Nit2 were expressed in *Escherichia coli* BL21 (DE3) pLysS as C-terminal and N-terminal hexahistidine tagged fusion proteins, and purified using Ni-chelation chromatography. Nit1 showed no activity towards nitrile, amide and carbamoyl substrates. This protein, unlike members of the multimeric enzymes of

the nitrilase superfamily, was a monomer ~30 kDa protein. It is possible that the C-terminal hexahistidine tag might have prevented Nit1 from forming multimeric proteins.

Nit2 showed substrate specificity similar to known aliphatic amidases with a preference for small amides. Nit2 had maximal activity at 30°C and between pH 6.5 and 7.5, properties compatible with its cold-adapted alkaliphilic origins. In addition, the enzyme was irreversibly inactivated at temperatures above 30°C and had a half-life of approximately 7 mins at 60°C. The crystal structure of Nit2 was solved to 1.66 Å. It revealed a ~45.5 kDa dimer, composed of two tightly bound ~30 kDa monomers. These monomers associated along the A surface forming a sandwich architecture that is conserved in known structures of the nitrilase superfamily.

Nit2 is distinct from known aliphatic amidases in both its structure and enzymic activity: the enzyme did not possess an extended C-terminal region; is active in dimeric form; has high affinity for 3C amides rather than 2C amides; and has a low overall catalytic rate. The short C-terminal region of Nit2 may have contributed to the low stability of the enzyme at elevated temperatures. A dendrogram composed of protein sequences of members of the nitrilase superfamily and Nit2 further supported evidence that this aliphatic amidase falls within a distinct group of enzymes.

This is the first report of the enzymic characterisation and structural analysis of an aliphatic amidase from a psychrotolerant, alkaliphilic and halotolerant extremophile.

Acknowledgements

Professor Don A. Cowan, Director of IMBM. I would like to thank Professor Cowan for providing the opportunity to work under his excellent supervision and for his support and guidance during my research. I am grateful to have been in his laboratory and I am in awe of his many adventures into the extremophilic world and the diversity of his current projects in this field.

Professor Trevor B. Sewell, Dr Brandon Weber and Dr Robert N. Thuku (Electron Microscope Unit, University of Cape Town) - Thank you for the assistance provided in facilitating my attempts at crystallisation and work based on the nitrilase superfamily. Professor Rees and Dr Celton (Genome Sequencing Faculty, University of the Western Cape) – Thank you for providing the sequences of the *Nesterenkonia* AN1 genome for *in silico* gene mining.

I thank Dr Marla I. Tuffin (Deputy Director of IMBM), Dr Ross Wadsworth and Dr Carola van Ijperen, my mentors whose input was so valuable to my doctoral studies over the years. Thank you to Professor Mike Danson for the fantastic experience and kinetic training at the University of Bath, during my visit to the UK.

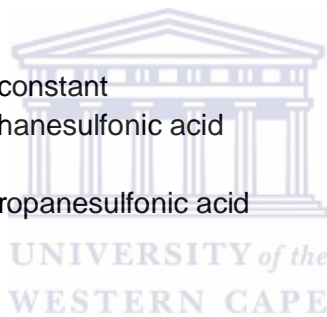
Dr Heide Goodman and fellow assistants are thanked for their crucial day-to-day running of the laboratory and in addition, I thank the current and past members of IMBM (too many to list!) for the many wonderful shared experiences of working in such a vibrant laboratory.

To my family and friends: I would like to thank my parents, Owen & Michèle Nel and my sister Nicole for their love, support, advice and patience during the course of my research and, my late grandfather François Mascré for his love and interest. In addition, I must thank my friend Marié Ting (a.k.a. “Covy”) for listening to my woes and for her support via the internet. I also thank my audiologist, Jenny Perold for easing me into the new world of sound as a bilateral cochlea implantee.

For funding of this research, I gratefully acknowledge the financial support received from the National Research Foundation in the form of a scarce skills scholarship for students with disabilities.

Abbreviations

3D	three dimensional
aa	amino acid
bp	base pair
BSA	bovine serum albumin
CAPS	<i>N</i> -cyclohexyl-3-aminopropanesulfonic acid
CTAB	cetyl-trimethyl-ammonium bromide
C-terminus	carboxy terminus
Da	Dalton
ddH ₂ O	deionised distilled water
DNA	deoxyribonucleic acid
dNTP	deoxynucleoside triphosphate
DTT	dithiothritol
EDTA	ethylene diamine tetraacetic acid
hr(s)	hour(s)
IPTG	isopropyl β -D-thiogalactosidase
k_{cat}	catalytic turnover
kDa	kilo Dalton
K_M	Michaelis-Menten constant
MES	2-(<i>N</i> -morpholino)ethanesulfonic acid
min(s)	minute(s)
MOPS	3-(<i>N</i> -morpholino) propanesulfonic acid
mRNA	messenger RNA
MW	molecular weight
N-terminus	amino-terminus
OD _{x nm}	optical density
ORF	open reading frame
PAGE	polyacrylamide gel electrophoresis
PDB	Protein Data Bank
PCR	polymerase chain reaction
PEG	polyethylene glycol
rbs	ribosome-binding site
rmsd	root mean square distances/deviations
RNA	ribonucleic acid
rpm	revolutions per minute
rRNA	ribosomal RNA
SDS	sodium dodecyl sulphate
sec(s)	second(s)
sp.	specie
TAE	Tris acetic acid EDTA
Tris-HCl	Tris (hydroxymethyl)methylamine hydrochloride
U	units
V_{max}	maximum velocity (rate of enzyme-catalysed reaction at infinite substrate concentration)
X-gal	5-bromo-4-chloro-3-indolyl- β -D-galactoside



Figures

Figure 1.1 Enzymes involved in the hydrolysis of nitriles and amides in bacteria.....	2
Figure 1.2 Negative stained electron microscopy of spiral Nases from <i>R. rhodochrous</i> J1.....	14
Figure 1.3 Proposed gene regulation of <i>P. aeruginosa</i> aliphatic amidase operon.	17
Figure 1.4 Multiple alignment of protein sequences of characterised members of the nitrilase superfamily.....	24
Figure 1.5 The monomer fold of <i>G. pallidus</i> aliphatic amidase.	25
Figure 1.6 A homology model of <i>R. rhodochrous</i> J1 Nase showing the intersubunit interacting surfaces.	27
Figure 1.7 A 3D electron microscopic reconstruction of <i>R. rhodochrous</i> J1 Nase showing the A, C and D intersubunit interacting surfaces.	28
Figure 1.8 The A, C, D, E and F surfaces of spiral forming Nases.....	29
Figure 1.9 Superimposition of the catalytic residues (EKEC) of five nitrilase structures.	30
Figure 1.10 Proposed reaction mechanism for the <i>G. pallidus</i> amidase hydrolysis of amides.	32
Figure 2.1 Colorimetric detection of nitrile hydrolysing activity in the cell free extracts of three isolates.....	48
Figure 2.2 Utilisation of different nitriles as the sole source of nitrogen for growth.....	51
Figure 2.3 Effect of temperature, pH and salinity on the growth rate (μ) of the <i>Nesterenkonia</i> AN1.	52
Figure 2.4 Neighbour-joining phylogenetic dendrogram and 16S rRNA percentage identities showing relationship of AN1 with known <i>Nesterenkonia</i> strains.....	55
Figure 3.1 ClustalW alignment of NHase α -subunit protein sequences used for primer design.....	71
Figure 3.2 ClustalW alignment showing the conservation of the deduced protein sequence of <i>R. erythropolis</i> amplicon with known NHase α -subunits.	73
Figure 3.3 Colorimetric detection of cultures for activity on pyrazinecarbonitrile.	75
Figure 3.4 Multiple alignment of Nit1 and Nit2 protein sequences with known members of the nitrilase superfamily.	84
Figure 3.5 Ramachandran plots for the Nit1 and Nit2 homology models and their structurally similar DCases.	88
Figure 3.6 Superimposition of Nit1 and Nit2 homology models on 1fo6.	90
Figure 4.1 Expression of Nit1 and Nit2 in <i>E. coli</i> BL21 pLyS cells.	106

Figure 4.2 Ni-chelation purification of the His-tagged Nit1 and Nit2.....	107
Figure 4.3 Calculation of ChNit1 and NhNit2 native molecular masses.....	108
Figure 4.4 Determination of the initial rate for NhNit2 using 100 mM acetamide.....	111
Figure 4.5 Effect of temperature on Nhit2 activity.	112
Figure 4.6 Effect of temperature on the stability of NhNit2 activity.....	113
Figure 4.7 Effect of pH on the activity of NhNit2.	115
Figure 5.1 Evidence of high molecular weight Nit2 protein.....	127
Figure 5.2 Crystals of Nit2 in initial crystallisation screens.....	128
Figure 5.3 Single and stacked layers crystals of Nit2 that were produced from seeds in 2 M ammonium sulphate.....	129
Figure 5.4 Hexagonal crystals of Nit2.....	130
Figure 5.5 Structure of Nit2 dimer and monomer fold.....	133
Figure 5.6 Details of the interaction at the A interface.....	134
Figure 5.7 Arrangement of the four catalytic residues (EKEC) of Nit2 compared with <i>G. pallidus</i> aliphatic amidase (2plq)	136
Figure 5.8 Comparison of Nit2 with its homology model.....	138
Figure 5.9 Superimposition of Nit2 on 1j31 and 2plq.....	140
Figure 5.10 The C-terminal region of Nit2 and <i>P. aeruginosa</i> aliphatic amidases.....	141
Figure 6.1 Schematic dendrogram of protein sequences of the nitrilase superfamily.	144
Figure 6.2 Homology model of C-terminal hexahistidine tagged Nit1 in dimer form	146
Figure 6.3 Structure of <i>G. pallidus</i> aliphatic amidase (2uxy) showing the position of the N-terminal hexahistidine tag fused to two monomers.....	148

Tables

Table 1.1 Characteristics of bacterial strains with nitrile and amide hydrolysing capabilities.	7
Table 1.2 13 enzyme branches of the nitrilase superfamily	20
Table 1.3 Eleven atomic structures that have been reported for members of the nitrilase superfamily.....	21
Table 2.1 Chemical composition of four types of media that were modified to NFMM. .	38
Table 2.2 Variations of media used to isolate nitrile hydrolysing bacteria	39
Table 2.3 Description of soil samples collected from Miers Dry Valley, Antarctica.	40
Table 2.4 16S rRNA identification of isolates obtained from NFMM containing nitrile as the sole nitrogen and/or carbon source for growth.....	45
Table 2.5 16S rRNA identification of isolates obtained from alternative types of NFMM supplemented with nitrile as the sole nitrogen source for growth.....	47
Table 2.6 Effects of temperature on growth of isolates.	49
Table 2.7 Utilisation of acetonitrile as the sole nitrogen and/or carbon source for growth.	50
Table 2.8 Comparison of phenotypic characteristics of AN1 with known strains of the genus <i>Nesterenkonia</i>	54
Table 3.1 Primers used for the molecular screening of NHases.	63
Table 3.2 Results of PCR trials using the degenerate primers.	72
Table 3.3 Genetic map of Nit1 and its neighbouring ORFs.....	78
Table 3.4 Genetic map of Nit2 and its neighbouring ORFs.....	79
Table 3.5 Protein sequence conservation (percentage identity) of Nit1 and Nit2 with putative and characterised members of the nitrilase superfamily.....	81
Table 3.6 Alignment of conserved signature sequences of branches of the nitrilase superfamily with Nit1 and Nit2.....	85
Table 4.1 Primers for the cloning of Nit1 and Nit2 ORFs from <i>Nesterenkonia</i> AN1 into pET21a(+) and pET28a(+).	99
Table 4.2 Determination of the substrate range of NhNit2.....	110
Table 4.3 Activity of NhNit2 activity on different amide compounds.....	116
Table 4.4 Kinetic parameters for NhNit2 on acetamide and propionamide.....	117
Table 5.1 Crystallographic data for Nit2	131
Table 5.2 3D superposition analysis of Nit2 with known structures of the nitrilase superfamily.....	139

Chapter 1: Literature review

1.1 Bacterial hydrolysis of nitriles and amides.....	2
1.2 Biotechnological potential of NHases, Nases and amidases	4
1.3 Distribution of nitrile and amide hydrolysing bacteria.....	6
1.4 NHases.....	10
1.4.1 Genes and their regulation.....	10
1.4.2 Recombinant expression of NHases.....	11
1.4.3 Substrate specificity.....	12
1.5 Nases.....	13
1.5.1 A brief background.....	13
1.5.2 Substrate specificity.....	15
1.6 Aliphatic amidases	16
1.6.1 Genes and their regulation.....	16
1.6.2 Substrate specificity.....	18
1.7 The Nitrilase superfamily.....	19
1.7.1 Introduction.....	19
1.7.2 Levels of conservation amongst related members of the nitrilase superfamily	21
Extent of conservation at the protein sequence level.....	22
Extent of structural conservation.....	24
1.7.3 Intersubunit surfaces	26
A surface – conserved in known structures of the nitrilase superfamily	26
B surface	27
C surface	28
D-F surfaces	29
1.7.4 Catalytic cleft of nitrilase structures.....	30
1.7.5 Reaction mechanism	31
1.8 Cold adapted enzymes.....	33
1.8 Aims.....	35

1.1 Bacterial hydrolysis of nitriles and amides

In bacteria, three different enzymes may catalyse the enzymatic hydrolysis of nitriles to the corresponding carboxylic acids releasing ammonia: Nitrilase (Nase) (EC 3.5.5.1), signature amidase-CX₃C motif (EC.3.5), and/or Nitrile Hydratase (NHase) (EC 4.2.1.84) (Figure 1.1). Nase and signature amidase-CX₃C motif hydrolyse nitriles directly to their corresponding carboxylic acids releasing ammonia (Figure 1.1). NHase converts nitriles to amides, which are subsequently hydrolysed by coupled signature or aliphatic amidases (EC 3.5.1.4) (Cameron *et al.*, 2005) (Figure 1.1). These amidases, including non-coupled NHase amidases, hydrolyse carboxylic acid amides (amides) by transferring an acyl group to water with the production of the corresponding carboxylic acids and ammonia.

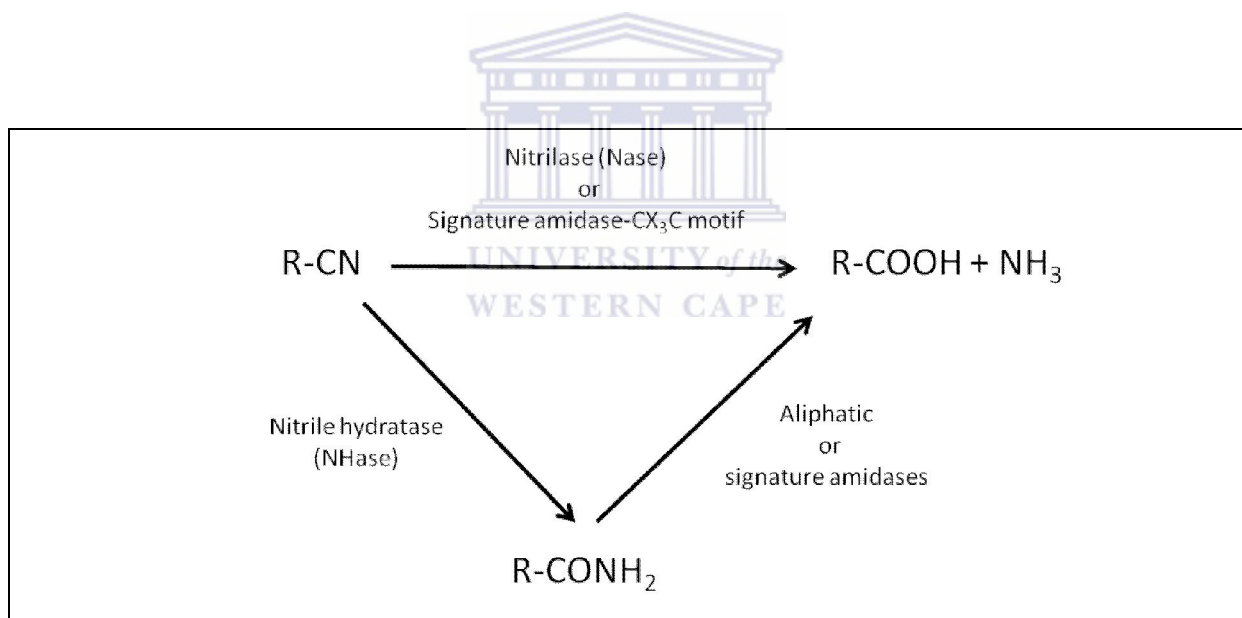


Figure 1.1 Enzymes involved in the hydrolysis of nitriles and amides in bacteria

NHases are metalloproteins consisting of two subunits: a smaller - and a larger -subunit with molecular masses ranging between 22 to 28 kDa (Cowan *et al.*, 2003). Most NHases are heterotetramers (2 2), except for *Rhodococcus rhodochrous* J1 (*R. rhodochrous*) that produces two NHases of differing molecular mass: L-NHase that is heterotetrameric and H-NHase that forms heteromultimers of up to 11 dimers (Kobayashi *et al.*, 1991a). NHases are

classified into either Fe- or Co-type enzymes on the basis of the metal ion coordinated at the active centre (Artaud *et al.*, 1999, Huang *et al.*, 1997, Kobayashi & Shimizu, 1999, Mascharak, 2002, Miyanaga *et al.*, 2001, Nagashima *et al.*, 1998). The type of NHase can also be deduced from the third amino acid position of the highly conserved co-factor binding domain in the α -subunit: V-C-(T/S)-L-C-S-C (Kobayashi & Shimizu, 1998). Co-type NHases have a threonine (T) residue in the third position and Fe-types have a serine (S) residue (Kobayashi and Shimizu, 1998). A sub-group of Fe-type NHases display photoreactivity, and can be activated from an inactive state when irradiated with light *in vivo* and *in vitro* (Bonnet *et al.*, 1997, Duran *et al.*, 1992, Nagamune *et al.*, 1990, Popescu *et al.*, 2001).

The other enzymes are non-metalloproteins and belong to either the amide hydrolase or nitrilase superfamilies (Chebrou *et al.*, 1996, Fournand & Arnaud, 2001, Pace & Brenner, 2001). Enzymes of these superfamilies share a typical α/β hydrolase fold, cleave C–N bonds of different substrates, and can be grouped based on their catalytic site and preferred substrate. Although enzymes vary in substrate specificities and biological functions, their catalysis is mediated by a S–cisS–K catalytic triad for the amide hydrolase superfamily and E–C–K catalytic triad for the nitrilase superfamily (Bracey *et al.*, 2002, Brenner, 2002, Neumann *et al.*, 2002, Pace & Brenner, 2001, Shin *et al.*, 2002).

Signature amidases belong to the amide hydrolase superfamily and are classified by the centrally conserved serine-glycine rich motif (GGSS(S/G)GS) in their protein sequences (Chebrou *et al.*, 1996, Mayaux *et al.*, 1991). These enzymes are typically homodimers of approximately 110 kDa. Although these enzymes share significant protein sequence conservation, they vary greatly in their individual substrate specificities of exclusively mid-length aliphatic amides or aromatic substrates (Chebrou *et al.*, 1996). Signature amidases that have an additional CX₃C motif are capable of nitrile hydrolysis (Kobayashi *et al.*, 1998). An additional C–cisS–K catalytic site has been implicated for nitrile hydrolysis, which may explain the dual specificities of these enzymes (Cilia *et al.*, 2005).

Nases and aliphatic amidases belong to branch 1 and 2 enzymes of the nitrilase superfamily according to the classification of Pace and Brenner (2001). The

quaternary structures of these enzymes are typically multimeric (Thuku *et al.*, 2009). Unlike the signature amidases, these enzymes have subunits of 30-44 kDa that exists as active tetramers, hexamers and octamers. In addition, aliphatic amidases hydrolyse low molecular weight substrates (Asano *et al.*, 1982, Fournand & Arnaud, 2001, Makhongela *et al.*, 2007, Skouloubris *et al.*, 1997). Nases have a subunit size of between 30-45 kDa and may exist in solution as inactive dimers (Banerjee *et al.*, 2002, O'Reilly & Turner, 2003). Active Nases occur as multi-subunit aggregates of 4-22 subunits or as spirals/helices of variable lengths (Thuku *et al.*, 2009). With the exception of Nases, there are 11 crystalline structures of distinct members of the nitrilase superfamily available and these share highly homologous folds (Thuku *et al.*, 2009).

1.2 Biotechnological potential of NHases, Nases and amidases

Although the physiological roles of NHases and Nases are still not clear, it has been suggested that they are involved in the metabolic degradation of aldoximines, a possible intracellular source of nitriles (Kato *et al.*, 1998, Kato *et al.*, 2004). Aldoximines, which are derived from amino acid precursors, are degraded by aldoxime dihydratases to nitriles.

Several reviews have surveyed NHases, Nases and amidases as potential biocatalysts and their use in industry in great detail (Banerjee *et al.*, 2002, Beard & Page, 1998, Bunch, 1998, Cowan *et al.*, 1998, Cowan *et al.*, 2003, Kobayashi & Shimizu, 1998, Martínková & Ken, 2002, Martínková *et al.*, 2008, Ramakrishna *et al.*, 1999, Singh *et al.*, 2006). Biocatalysts are known to be advantageous compared with chemical catalysis, since chemical hydrolysis of nitriles requires the presence of strong acids and/or bases at high temperatures that may result in low yields. Biocatalysts have the potential for improvement of reaction performance under mild conditions and for avoiding deleterious reactions of other sensitive functional groups (Cowan *et al.*, 2003). NHases, Nases and amidases have been reported for their potential for chemically useful chemo-, regio-, and enantio- selective transformations (Chauhan *et al.*, 2003,

Crosby *et al.*, 1994, Dadd *et al.*, 2001, Guranda *et al.*, 2004, Hann *et al.*, 2004, Wang *et al.*, 2007).

The enzymatic conversion of acrylonitrile to acrylamide using NHases is one of the most successful biotransformation processes in the global industrial enzymology field (Cowan *et al.*, 2003, Kobayashi *et al.*, 1992b). A biotechnological application of Nases is the development of transgenic cotton crops expressing a bacterial bromoxynil-specific Nase. The heterologous expression of the bacterial Nase in plants conferred resistance to the herbicide (Stalker *et al.*, 1996, Stalker *et al.*, 1988a, Stalker & McBride, 1987, Stalker *et al.*, 1988b). Amidases are the most widely used amide-hydrolysing enzymes in industry. Several organic compounds, including p-aminobenzoic acid, acrylic acid, nicotinic acid, pyrazinoic acid, and 3-indole acetic acid, are commercially produced through the biotransformation of nitriles using NHase and amidase activities (Banerjee *et al.*, 2002).

Due to the volume of nitriles synthesised in industry, acrylonitrile and nitrile based pesticides are considered an anthropogenic threat to the environment. Acrylonitrile is used extensively in the manufacture of acrylamide for papermaking, waste treatment, and oil recovery (Hughes *et al.*, 1998, Yamada & Kobayashi, 1996). Nitrile based pesticides such as bromoxynil (3,5-dibromo-4-hydroxybenzotrile), ioxynil (3,5-di-iodo-4-hydroxybenzotrile), dichlobenil, and buctril have been extensively used in the agricultural sector (Pollak *et al.*, 1991). Nitrile and amidase hydrolysing microorganisms are potentially useful for the degradation of synthetic nitrile compounds in bioremediation (Banerjee *et al.*, 2002, Madhavan *et al.*, 2005). Bioremediation of acrylonitrile has been reported using a mixture of nitrile hydrolysing enzymes (Battistel *et al.*, 1997, Thompson *et al.*, 1988). In addition, a consortium of nitrile hydrolysing bacteria in an activated sludge system has been successful in bioremediation of acrylonitrile (Thompson *et al.*, 1988).

1.3 Distribution of nitrile and amide hydrolysing bacteria

Since the discovery of NHase and the coupled amidase from *R. rhodochrous* J1 (formerly *Arthrobacter* sp J1) (Asano *et al.*, 1982, Asano *et al.*, 1980) and Nases from plants and bacteria (Hook & Robinson, 1964, Thimann & Mahadevan, 1964), a number of nitrile hydrolysing bacterial species have been isolated from diverse ecosystems including deep sea trenches (Heald *et al.*, 2001), nitrile contaminated soil (Padmakumar & Oriel, 1999) and thermal lake sediments (Brandao *et al.*, 2002, Pereira *et al.*, 1998). Table 1.1 shows the bacterial strains known to express NHase and Nases. Strains expressing aliphatic amidases are included. *Rhodococcus* represents the most prominent group, and a survey of public culture collections showed that more than one-fourth of nitrile-converting strains are of this genus (Martínková & Ken, 2002, Martínková *et al.*, 2009) (Table 1.1).

Nitrile and amide metabolising bacteria are typically isolated using trophic selection strategies, where substrates are used as the sole carbon and/or nitrogen sources to support the growth of these organisms (Cowan *et al.*, 2003). However, standard laboratory cultivation techniques are thought to only access approximately 1% of the true microbial species diversity (Amann *et al.*, 1995, Curtis & Sloan, 2004, Torsvik & Ovreas, 2002, Torsvik *et al.*, 2002)

Novel Nase and NHases sequences have been identified using culture-independent metagenomic based approaches (Schmeisser *et al.*, 2007). In one metagenomic study, 12 novel NHase sequences were detected in a PCR based screening of 3 Gb of environmental DNA using degenerate primers (Liebeton & Eck, 2004). Although it was originally believed that Nases were quite rare in bacterial genomes, two metagenomic studies reported the detection of more than 337 novel Nases (Podar *et al.*, 2005, Robertson *et al.*, 2004).

Although no studies have accessed the metagenomic diversity of aliphatic amidases producing strains, many of these enzymes have been purified and characterised from wild-type isolates.

Table 1.1 Characteristics of bacterial strains with nitrile and amide hydrolysing capabilities. Abbreviations: M/T, mesophilic or thermophilic growth; Co/Fe, metal co-factors of NHases; C/I, constitutive or inducible expression. The substrate (ACA, acetamide, ACR, acrylamide, PRO, propionamide) of the aliphatic amidases are shown in decreasing order based on their reported enzyme specificities. Table 1.1 was taken from Thuku *et al.*, (2009), Cowan *et al.*, (1998 & 2003) and Banerjee (2002).

NHases									
Strain	M / T	Subunit (kDa)	Native (kDa)	°C	pH	Fe / Co	C / I	Specificity	References
<i>Agrobacterium tumefaciens</i>	M	27	27	420	25	6.5-9.5		I	Bauer <i>et al.</i> , 1994
<i>Rhodococcus</i> J1	M	24	27	420				I aliphatic	Asano <i>et al.</i> , 1982
<i>Bacillus alkalinitrilicus</i> ²								aliphatic nitriles	Sorokin <i>et al.</i> , 2008
<i>Bacillus</i> sp BR449	T	25	27		55	7.5	Co	C	Kim & Oriel, 2000
<i>Bacillus smithii</i>	T	26	29		40	7.2	Co	C aliphatic	Takashima <i>et al.</i> , 1998
<i>Bacillus subtilis</i> ZJB-063 ²									Zheng <i>et al.</i> , 2008b
<i>Corynebacterium nitrophilus</i>	M					6-8		aliphatic dinitriles aromatic	Amarant <i>et al.</i> , 1989
<i>Corynebacterium pseudodiphtheriticum</i> ZBB-41	M	25	28	80			Fe	aliphatic	Li <i>et al.</i> , 1992
<i>Corynebacterium</i> sp C5	M	26.9		61			Fe	aliphatic dinitriles cyclic	Yamamoto <i>et al.</i> , 1992b
<i>Geobacillus</i> sp. DAC 521	T	27	29	110	50	7-7.5	Co	C aliphatic	Cramp & Cowan, 1999
<i>Geobacillus pallidus</i> RAPc8	T	28	29	110	60	7	Co	C aliphatic, cyclic, dinitriles	Pereira <i>et al.</i> , 1998
<i>Mesorhizobium</i> sp. F28	M	22.66 28.16			37 -	7.5 45	Co		Feng <i>et al.</i> , 2008a, Feng <i>et al.</i> , 2008b
<i>Microbacterium imperial</i> CBS 498 ²									Cantarella <i>et al.</i> , 2004
<i>Natronocella acetinitrilica</i> ²					11	1			Sorokin <i>et al.</i> , 2007
<i>Nitriliruptor alkaliphilus</i> ²					11	1			Sorokin <i>et al.</i> , 2009
<i>Pseudomonas chlororaphis</i>	M	25	25	100	20	6-7.5	Fe	I aliphatic	Nagasawa <i>et al.</i> , 1987
<i>Pseudomonas putida</i>	M	23	24.1	54/95	30	7.2	Co	C aliphatic, dinitriles,	Payne <i>et al.</i> , 1997
<i>Pseudonocardia thermophila</i>	T	29	32		55		Co		Yamaki <i>et al.</i> , 1997
<i>Rhodococcus equi</i> SHB-121	M	30		30				aliphatic, cyclic, dinitriles	Gilligan <i>et al.</i> , 1993
<i>Rhodococcus erythropolis</i> ³	M	23	24				Fe	C aliphatic, aromatic, heterocyclic	Duran <i>et al.</i> , 1993
<i>Rhodococcus erythropolis</i> BL1 ²	M							I aliphatic, aromatic, heterocyclic	Duran <i>et al.</i> , 1993
<i>Rhodococcus rhodochrous</i> J1 H-NHase	M	23	26		35	6.5-6.8	Co	I aliphatic, aromatic	Komeda <i>et al.</i> , 1996b
<i>Rhodococcus rhodochrous</i> J1 L-NHase	M	23	25		40	8.8	Co	I aliphatic, aromatic	Komeda <i>et al.</i> , 1996c

<i>Rhodococcus</i> sp. AJ270 ²				25	7.6			Song <i>et al.</i> , 2007		
<i>Rhodococcus</i> sp. N-771 ³	M	27	27	70		Fe	I	aliphatic	Ikehata <i>et al.</i> , 1989	
<i>Rhodococcus</i> sp. N-774 ³	M	27	27	70	35	7-8.5	Fe	C	aliphatic	Endo & Watanabe, 1989
<i>Rhodococcus</i> sp. R312 ³	M	23	24	95	35	7-8.5	Fe	C	aliphatic, cyclic, dinitriles	Nagasawa <i>et al.</i> , 1986
<i>Rhodococcus</i> sp. YH3-3					40	7	Co	I		Kato <i>et al.</i> , 1999
Nases										
Strain	M / T	Subunit (kDa)	Native (kDa)	°C	pH	C	I	Specificity	References	
<i>Acidovorax facilis</i> 72W		40	570	65				aliphatic	Chauhan <i>et al.</i> , 2003, Gavagan <i>et al.</i> , 1999	
<i>Acinetobacter</i> sp. AK226	M	41/43	580	50	8	C		aliphatic	Yamamoto & Komatsu, 1991	
<i>Acinetobacter faecalis</i> ATCC 8750	M	32	460	40-45	7.5	I		aliphatic, aromatic, heterocyclic	Yamamoto <i>et al.</i> , 1992a Yamamoto & Komatsu, 1991	
<i>Alcaligenes faecalis</i> JM3	M	38.9 / 44	260/275	45	7.5	I		bromoxynil-specific nitrilase arylaceto-nitrilase	Kobayashi <i>et al.</i> , 1993a, Nagasawa <i>et al.</i> , 1990	
<i>Rhodococcus</i> sp. strain J1	M	30	30	40	8.5	I		aromatic	Bandyopadhyay <i>et al.</i> , 1986	
<i>Bradyrhizobium japonicas</i> USD 110 (gene bl16402)		37	455					bromoxynil-specific nitrilase arylaceto-nitrilase	Zhu <i>et al.</i> , 2007	
<i>Bradyrhizobium japonicas</i> USD 110 (gene blr3397)		34.5	~340	45	7-8			aliphatic	Zhu <i>et al.</i> , 2008	
<i>Comamonas testosteroni</i> sp.	M	38/38.7		30	7			aliphatic	Lévy-Schil <i>et al.</i> , 1995	
<i>Geobacillus pallidus</i> RAPc8	T	41	600	65	7.6			aromatic	Almatawah <i>et al.</i> , 1999	
<i>Klebsiella pneumonia</i> ssp. <i>Ozaena</i>		37/38.1	74	35	9.2			bromoxynil-specific nitrilase arylaceto-nitrilase	Stalker <i>et al.</i> , 1988a	
<i>Nocardia (Rhodococcus)</i> NCIMB 11215	M	45	560	30	7-9.5			aromatic	Harper, 1985	
<i>Nocardia (Rhodococcus)</i> NCIMB 11216	M	45.8	560	30	8			aromatic	Harper, 1977	
<i>Pseudomonas fluorescens</i> EBC 191		37.7		50	6.5			bromoxynil-specific nitrilase arylaceto-nitrilase	Kiziak <i>et al.</i> , 2005	
<i>Pseudomonas fluorescens</i> DSM 7155		38/40	130	55	9			bromoxynil-specific nitrilase arylaceto-nitrilase	Layh <i>et al.</i> , 1998 Brady <i>et al.</i> , 2004	
<i>Pseudomonas putida</i>		43	412	40	7			bromoxynil-specific nitrilase arylaceto-nitrilase	Banerjee <i>et al.</i> , 2006	

<i>Pseudomonas fluorescens</i> Pf-5.	33	138	45	7	dinitrile	Kim <i>et al.</i> , 2009
<i>Pseudomonas</i> sp. S1	41	41			aliphatic	Dhillon <i>et al.</i> , 1999
<i>R. rhodochrous</i> K22	M 41	650	50	5.5	I aliphatic	Kobayashi <i>et al.</i> , 1991b
<i>Rhodococcus rhodochrous</i> ATCC 39484	40/40.3	560	40	7.5	aromatic	Stevenson <i>et al.</i> , 1992
<i>Rhodococcus rhodochrous</i> J1	M ~40	80,410, 480, >1.5 M long helices	45	7.6	I aromatic	Kobayashi <i>et al.</i> , 1992a, Kobayashi <i>et al.</i> , 1992c
<i>Rhodococcus rhodochrous</i> PA-34	45	45	35	7.5	aromatic	Bhalla <i>et al.</i> , 1995
<i>Synechocystis</i> sp. strain PCC6803	~40	390	50	7	aliphatic	Heinemann <i>et al.</i> , 2003

Aliphatic amidases

Strain	M / T	Sub-unit (kDa)	Native (kDa)	°C	pH	Acyl activity	C / I	Specificity	References
<i>Rhodococcus</i> sp. J1		39	320	55	8	Yes	I	ACA ACR PRO	Asano <i>et al.</i> , 1982
<i>Bacillus</i> sp. BR449	T	38.6				Yes			Kim & Oriel, 2000
<i>Bacillus stearothermophilus</i> BR388	T	39.1		55	7	Yes		ACA ACR PRO	Cheong & Oriel, 2000
<i>Geobacillus pallidus</i> RAPc8	T	38	218	50	7	Yes		ACR ACA PRO	Makhongela <i>et al.</i> , 2007
<i>Helicobacter pylori</i> (AmiE)		40	160	55	7	Yes		ACA PRO ACR	Skouloubris <i>et al.</i> , 2001
<i>Helicobacter pylori</i> (AmiF)		34	160	45	6			FOA	Skouloubris <i>et al.</i> , 2001
<i>Pseudomonas aeruginosa</i>	M	38.4	201	55	7.2	Yes		ACA PRO ACR	Karmali <i>et al.</i> , 2001, Kelly & Clarke, 1962
<i>Rhodococcus rhodochrous</i> M8		42	150	55	5-8	Yes	C	ACA PRO ACR	Kotlova <i>et al.</i> , 1999
<i>Rhodococcus</i> sp. R312 (formerly <i>Brevibacterium</i> sp. R312)	M	43	180	40		Yes		ACA ACR PRO	Maestracci <i>et al.</i> , 1984, Thiery <i>et al.</i> , 1988

¹ Optimal growth pH of bacteria strain

² Novel nitrile hydrolysing strain – putative NHase producing strain

³ Subgroup of Fe-type NHases that display photoreactivity

Although an aliphatic amidase was expressed and characterised in this study, the original aim of this research was to identify and characterise a nitrile hydrolysing enzyme from an isolate. A brief discussion of NHases and Nases is therefore included.

1.4 NHases

1.4.1 Genes and their regulation

The genes of the α - and the β -subunit of NHases are of similar size and range from 609 to 660 bp for the α -subunit and from 636 to 706 bp for the β -subunit (Cowan *et al.*, 2003). The genes are encoded within two separate adjacent open reading frames (ORFs) separated by a sequence of 16 to 29 bases (Duran *et al.*, 1993, Kim & Oriol, 2000). *Pseudonocardia thermophila* is an exception as its α - and β -genes overlap by 4 bases (Yamaki *et al.*, 1997). Since NHase takes part in a bi-enzymatic pathway with amidase, the amidase gene in most cases is located 100 bp upstream of the NHase β gene (Cowan *et al.*, 2003). The amidase gene in *R. rhodochrous* J1 is located 1.9 kb downstream of the β -subunit gene of L-NHase (Kobayashi *et al.*, 1993b).

Within the native organism, some NHases are produced constitutively, irrespective of the presence or absence of nitriles or amides, whereas others are shown to be inducible (Cowan *et al.*, 2003) (Table 1.1). It has been reported that apart from nitriles, aldoximines and even amides are good inducers of nitrile-hydrolysing enzymes (Kato *et al.*, 2000, Kobayashi & Shimizu, 1998). The regulation of *R. rhodochrous* J1 high molecular weight NHase and low molecular weight NHase genes has been well characterised (Komeda *et al.*, 1996b). Both genes can be induced by crotonamide. Urea induces H-NHase expression while cyclohexanecarboximide induces L-NHase (Yamada & Kobayashi, 1996). The H-NHase operon contains two regulatory genes, *nhhC* and *nhhD*, located upstream of the NHase gene (Kobayashi & Shimizu, 1998). In the presence of amide, NhhC exhibited a positive regulation on NhhD inducing the H-NHase gene. L-

NHase also has two upstream genes, *nhlD* and *nhlC*, that served positive and negative regulatory roles, respectively (Komeda *et al.*, 1996c).

1.4.2 Recombinant expression of NHases

In some instances, recombinant expression of NHases required the co-expression of additional co-transcribed genes. In the case of Co-type *Pseudomonas putida* NHase, the co-expression of a downstream P14K gene significantly enhanced expression of NHase in *Escherichia coli* (*E. coli*) (Wu *et al.*, 1997). P14K had homology to the N-terminal region of the NHase α -subunit and similar proteins with homology to the NHase α -subunit have been found for *Bacillus* sp. BR449 and *R. rhodochrous* J1 (Kim & Oriel, 2000, Komeda *et al.*, 1996c, Wu *et al.*, 1997). Fe-type NHases of *Pseudomonas chlororaphis*, *Rhodococcus* sp N-771, and *Rhodococcus* sp. R312 required the co-expression of P47K (Bigey *et al.*, 1999, Nishiyama *et al.*, 1991, Nojiri *et al.*, 1999). Studies on the modelled structure of P14K (Cameron *et al.*, 2005) (an activator protein of *Geobacillus pallidus* RAPc8 (*G. pallidus*)) suggested that the protein functions as a subunit-specific chaperone. P14K was suggested to aid NHase α -subunit folding prior to α - β association and the formation of the active heterotetrameric enzyme (Cameron *et al.*, 2005). Co-type NHases required media supplemented with Co^{3+} for enzyme activity (Kobayashi *et al.*, 1991a). *Bacillus* sp. BR449 expresses inactive NHase when cultured in medium containing no cobalt and can be activated upon incubation in 5 μM CoCl_2 (Kim & Oriel, 2000, Kim *et al.*, 2001). Cobalt was suggested to be involved in enhancing protein folding rather than induction of NHase expression (Cowan *et al.*, 1998, Kobayashi *et al.*, 1991a). No information is yet available on the effect of addition of Fe^{3+} ions on the activity of Fe-type NHases (Cowan *et al.*, 2003).

1.4.3 Substrate specificity

The Fe-type NHase of *Rhodococcus erythropolis* (*R. erythropolis*) (Duran *et al.*, 1993) is capable of hydrating aliphatic, aromatic and heterocyclic nitriles. Other Fe-type NHases lack specificity to aromatic nitriles (Nakasako *et al.*, 1999). The Co-type NHases of *Bacillus smithii* (Takashima *et al.*, 1998), *Bacillus pallidus* DAC521 (Cramp *et al.*, 1997), *Bacillus* sp. RAPc8 (Cramp & Cowan, 1999) and *Pseudomonas putida* (Payne *et al.*, 1997) are not specific for aromatic nitriles (Cowan *et al.*, 2003).

In the case of Fe-type NHases, the lack of aromatic substrate specificity could be attributed to the narrow entrance channel enabling only small aliphatic substrates to enter the catalytic site (Nakasako *et al.*, 1999). Structural comparisons between Fe-type NHase of *Rhodococcus* sp. N-771 with Co-type NHase of *Pseudonocardia thermophila* (Miyanaga *et al.*, 2001) confirmed a difference in the catalytic cavity. The Co-type NHases have a conserved non-polar tryptophan residue, W72 for *Pseudonocardia thermophila* NHase, which corresponds to the conserved polar tyrosine residue, Y76 for *Rhodococcus* sp N-771 NHase (Miyanaga *et al.*, 2001). The orientation of the side chain of the tryptophan residue is different from that of the tyrosine residue of Fe-type NHases, which does not clash with aromatic compounds in the catalytic cavity (Miyanaga *et al.*, 2001).

Although *G. pallidus* NHase demonstrated no activity on homoaromatic nitriles such as benzonitrile and benzyl cyanide (Pereira *et al.*, 1998), it accepts heteroaromatic nitrile such as 3-cyanopyridine (Cowan *et al.*, 2003). The lack of enzyme specificity for homoaromatic nitriles was not associated with catalytic cavity volume, but with residues within the catalytic site (Cramp and Cowan, 1999). There are several reports of NHases that display enantioselectivity (Bauer *et al.*, 1994, Fallon *et al.*, 1997). For example, *Agrobacterium tumefaciens* NHase produces (S)-amides from a number of racemic phenylpropionitriles (Bauer *et al.*, 1994).

1.5 Nases

1.5.1 A brief background

Branch 1 enzymes of the nitrilase superfamily consists of three groups of closely related enzymes, the nitrile hydrolysing Nases and two groups of cyanide hydrolysing enzymes, the cyanide hydratases and the cyanide dihydratases (Thuku *et al.*, 2009). The latter two enzymes hydrolyse cyanide only. Several bacterial species produce cyanide dihydratases that hydrolyse cyanide directly to formate and ammonia (Jandhyala *et al.*, 2003, Sewell *et al.*, 2003). The cyanide hydratases, mainly of fungal origin, hydrolyse cyanide to formamide (Dent *et al.*, 2008, Vejvoda *et al.*, 2008, Woodward *et al.*, 2008)

Nases including the cyanide hydrolysing enzymes are inducible and are expressed at very high levels in the presence of nitriles/cyanides in the growth media (Banerjee *et al.*, 2002). *Bacillus subtilis* sp. ZJB-064 is the only exception where its Nase is constitutively expressed (Zheng *et al.*, 2008c). *R. rhodochrous* J1 Nase is expressed up to 35% of the soluble protein of the cell when induced with isovaleronitrile (Komeda *et al.*, 1996a). The expression of J1 Nase is up regulated by a positive regulator, NitR, which ORF is located downstream of the Nase gene. Komeda *et al.*, (1996) showed that expression of NitR is essential for induction of Nase synthesis.

Two Nases from bacterial species *Pseudomonas fluorescens* (Layh *et al.*, 1998), *Comamonas testosteroni* (Lévy-Schil *et al.*, 1995) and thermophilic *G. pallidus* (Almatawah *et al.*, 1999) have been purified with tightly bound chaperonin proteins. The presence of co-purified chaperonin proteins was suggested to stabilise the thermophilic Nase at elevated temperatures (Almatawah *et al.*, 1999). Layh *et al.*, (1998) suggested that the co-purified chaperonin protein, GroE, might play a role in the assembly of the multi-subunit enzyme. The co-expression of *Comamonas testosteroni* Nase with the chaperonin protein in *E. coli* greatly enhanced the solubility and the activity of the enzyme (Lévy-Schil *et al.*, 1995).

The subunits of Nases have been reported to self-associate as a consequence of substrate activation (O'Reilly & Turner, 2003) (Table 1.1). The Nase of *Rhodococcus* NC1B 11216 (Harper, 1976) existed as a monomer with a molecular weight of 47 kDa in the absence of nitrile, but when purified in the presence of the nitrile, its molecular weight was determined to be 560 kDa. The association of subunits also could be dependent on the type of nitrile compound (Harper, 1976). The inactive dimers of *R. rhodochrous* J1 Nase oligomerised to a multi-subunit enzyme in the presence of an aromatic nitrile, benzonitrile, but not in the presence of an alkene aliphatic nitrile, acrylonitrile, for which the enzyme has a higher affinity (Nagasawa *et al.*, 2000). Substrate-dependant subunit association has also been reported for *Rhodococcus* ATCC 39484 and *Alcaligenes faecalis* ATCC8750 (Stevenson *et al.*, 1992, Yamamoto *et al.*, 1992a).

The multi-subunit Nase of *R. rhodochrous* J1 was shown to exist as active spirals in the presence of benzonitrile (Thuku *et al.*, 2007) (Figure 1.2). In addition, the C-terminal region of the Nase subunits was shown to undergo autocatalytic cleavage that was confirmed to be required for spiral formation (Figure 1.2).

UNIVERSITY of the
WESTERN CAPE

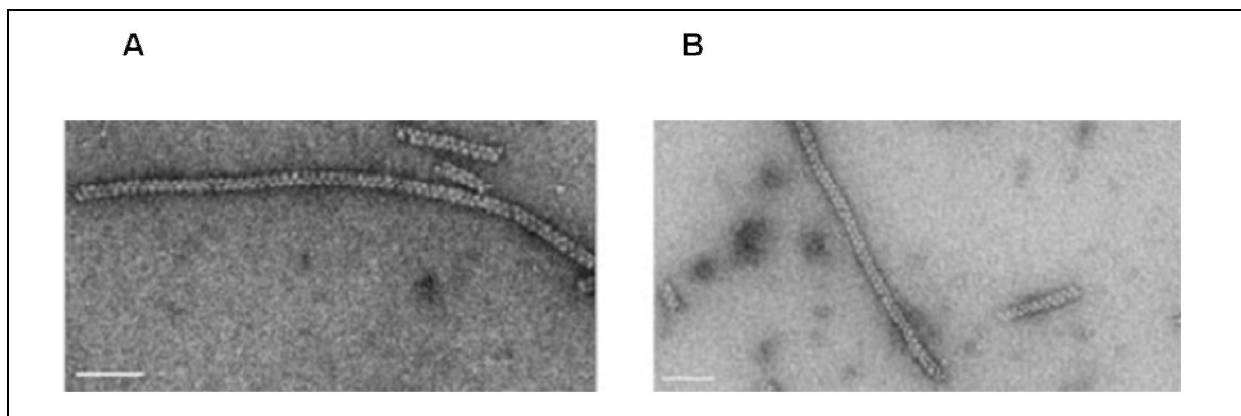


Figure 1.2 Negative stained electron microscopy of spiral Nases from *R. rhodochrous* J1. Panel A, mutant Nase that has 39 residues removed from its C-terminal region. Panel B, wild type Nase. Image was taken from Thuku *et al.*, (2007).

Spiral forming Nases have been reported for many species of the *Rhodococcus* genus (Harper, 1977, Harper, 1985, Hoyle *et al.*, 1998, Stevenson *et al.*, 1992) (Table 1.1). Spiral formation has also been reported for the cyanide hydratases and cyanide dihydratases (Jandhyala *et al.*, 2003, Sewell *et al.*, 2003, Woodward *et al.*, 2008). Some Nases form short, terminating spirals that have a specific number of subunits and others form 14, 18 and 22-subunit spirals (Thuku *et al.*, 2009).

Since no atomic structures have been determined for Nases, a combination of electron microscopy of these spiral structures together with docking of homology models has been used to describe the intersubunit interactions (Thuku *et al.*, 2009). Homology modelling was based on structures of the nitrilase superfamily. A discussion of the nitrilase superfamily and its structural implications to Nases is described later.

1.5.2 Substrate specificity



Nases are generally classified on the basis of their best affinity for a particular substrate such as aromatic and/or heterocyclic nitriles, arylacetonitriles, aliphatic nitriles, or larger compounds such as bromoxynil (Thuku *et al.*, 2009) (Table 1.1). Despite the classification, several Nases have broad substrate ranges. *Synechocystis* spp. 6803 Nase, which is specific for aliphatic nitriles, also hydrolysed 2-acetoxybutenenitrile (Heinemann *et al.*, 2003). The aromatic specific Nases of *R. rhodochrous* J1 and *Rhodococcus* (formerly *Nocardia*) NCIMB 11216 are capable of hydrolysing acrylonitrile and propionitrile, respectively, following activation in the presence of the aromatic nitrile (Hoyle *et al.*, 1998, Nagasawa *et al.*, 2000). Nases that display enantioselective activity are generally associated with arylacetonitrile specific enzymes. Arylacetonitrilases from *Alcaligenes faecalis* ATCC 8750 (Yamamoto *et al.*, 1991) and *Pseudomonas fluorescens* EBC191 (Kiziak *et al.*, 2005) hydrolyse (R,S)-mandelonitrile to (R)-(-) mandelic acid, an important intermediate in the pharmaceutical industry.

Several studies have exploited homology modelling of Nases based on structural homologues of the nitrilase superfamily in order to pin point residues for mutagenesis to optimise catalytic activity (Thuku *et al.*, 2009). For example the putative structure of *R. rhodochrous* ATCC 33278 Nase, which was based on two structures, identified the role of a tryptophan residue (W142) within the catalytic cleft (Yeom *et al.*, 2008). A substitution of W142 with a non-polar aliphatic residue increased the Nase specificity exclusively towards aromatic substrates (Yeom *et al.*, 2008). It was determined that this residue determined the Nase substrate specificity between aliphatic and aromatic nitriles.

1.6 Aliphatic amidases

1.6.1 Genes and their regulation

Amidases identified in NHases operons belonged to either the signature or aliphatic amidase superfamilies (Cameron *et al.*, 2005). Aliphatic amidases have been identified within the NHase operons of *Bacillus* sp. BR449 and *G. pallidus* (Cameron *et al.*, 2005). Their proximity to the NHases suggested that their genes are co-expressed on a single polycistronic mRNA. Only the aliphatic amidase of *R. rhodochrous* M8 is not organised into a single operon with the Co-type NHase despite their common regulation (Pogorelova *et al.*, 1996, Ryabchenko *et al.*, 2006).

The gene regulation of the well characterised non-NHase coupled aliphatic amidase of *Pseudomonas aeruginosa* (*P. aeruginosa*) has been proposed (Wilson *et al.*, 1996, Wilson *et al.*, 1995) (Figure 1.3). *P. aeruginosa* aliphatic amidase is induced from a 5 kb operon when short chained amides are presence in the growth medium (Wilson *et al.*, 1995) (Figure 1.3). Under non-inducing conditions, there is constitutive expression of the operon from the pE promoter, which was suggested to be regulated by catabolite repression that terminates at transcription terminator sequences T1 and T2 (Wilson *et al.*, 1995) (Figure 1.3, panel A). There is basal constitutive expression of the two regulating proteins AmiC and AmiR by the pN1 or pN2 promoters. Under inducing conditions, the

substrate acetamide complexes with AmiC-AmiR causing a conformation change releasing AmiR from the inhibitor AmiC (Wilson *et al.*, 1996). AmiR then induces the expression of other genes in the operon via the anti-termination reaction at T1 (Wilson *et al.*, 1995) (Figure 1.3, panel B). AmiR anti-termination is RNA sequence dependent (Wilson *et al.*, 1995).

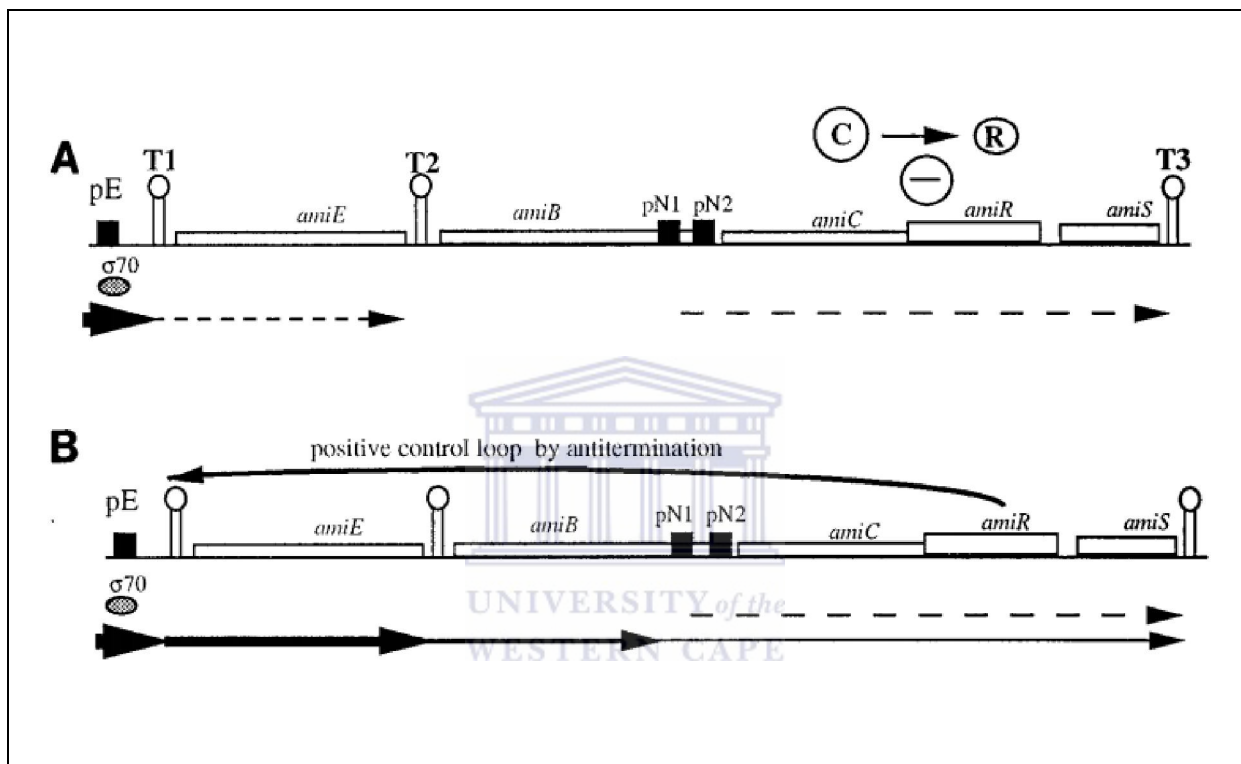


Figure 1.3 Proposed gene regulation of *P. aeruginosa* aliphatic amidase operon. Image was taken from Wilson *et al.*, (1996).

The production of the two paralogous *Helicobacter pylori* aliphatic amidases, AmiE and AmiF, was found to be dependent on the activity of other enzymes involved in nitrogen metabolism (Skouloubris *et al.*, 2001). Their regulation was proposed to maintain intracellular nitrogen balance in order for the bacteria to survive the gastric acidity of the stomach.

1.6.2 Substrate specificity

As shown in Table 1.1, all aliphatic amidases hydrolyse short-chain aliphatic amides such as acetamide, acrylamide and propionamide. According to the substrate preferences, aliphatic amidases (other than AmiF of *Helicobacter pylori* (Skouloubris *et al.*, 2001)) have the highest activity on the 2-carbon amide acetamide, followed by 3-carbon amides (propionamide and acrylamide). *Helicobacter pylori* AmiF hydrolyses exclusively 1-carbon amide (formamide) (Skouloubris *et al.*, 2001).

The substrate preference for *P. aeruginosa* aliphatic amidases was described to be dependent on charge and size of the amides. Its affinity decreased for substrates with increased polarity or size (Pacheco *et al.*, 2005). Point mutations have extended the substrate specificity of *P. aeruginosa* aliphatic amidases to include longer aliphatic amides, such as butyramide, valeramide and aromatic amides, acetanilide and phenylacetamide (Betz & Clarke, 1972, Brown *et al.*, 1969, Brown & Clarke, 1970, Brown & Clarke, 1972).

The aliphatic amidase of the thermophilic *G. pallidus* is capable of hydrolysis on substituted short-chain and mid-length aliphatic amides (Makhongela *et al.*, 2007). In addition, the enzyme exhibited substantial levels of chiral selectivity for D-enantiomers specifically D-lactamide (Makhongela *et al.*, 2007). A W138 residue within the catalytic cleft was proposed to determine the enzyme specificity for D-lactamides due to steric hindrance of L-lactamides (Kimani *et al.*, 2007).

All reported aliphatic amidases are capable of production of hydroxamic acids in the presence of hydroxylamine and aliphatic amides (Table 1.1). This reaction is referred to as the acyl transfer reaction. The amidase transfers acyl groups from the acyl donor (the amide) to the acyl acceptor (water or hydroxylamine) (Fournand *et al.*, 1998). Since hydroxylamine is a better acyl acceptor than water, the bioconversion rates of acyl-transfer reactions to this substrate are usually much higher.

1.7 The Nitrilase superfamily

1.7.1 Introduction

Enzymes of the nitrilase superfamily are classified into 13 branches (Table 1.2), although the enzyme function is known for only nine branches (Brenner, 2002). Only branch 1 has nitrile or cyanide hydrolytic activity and the remaining eight branches have amidase or amide-condensation activities (Brenner, 2002) (Table 1.2). Amidase like activity has been described for aliphatic amidases (branch 2), N-terminal amidase (3), biotinidase (4), and -ureidopropionase (5), N-carbamoyl-D-amino acid amidohydrolases / carbamylases (DCase) (6) and the prokaryotic and eukaryotic NAD synthetases (7 and 8, respectively) (Brenner, 2002, Pace & Brenner, 2001) (Table 1.2). The apolipoprotein N-acyltransferases (branch 9) carry out amide condensation (Brenner, 2002) (Table 1.2). Branch 10 is represented by an atomic structure of a fusion protein, NitFhit (PDB code: 1ems), where a nitrilase domain is fused to a nucleotide-binding Fhit protein (Pace & Brenner, 2001, Pace *et al.*, 2000) (Table 1.3). Enzymes placed in branches 11-13 are grouped according to similar sequence relation (Pace & Brenner, 2001), but have no characterised member. In seven of these branches the nitrilase is fused to another domain (Pace & Brenner, 2001) (Table 1.3). For example, the prokaryotic NAD⁺ synthetase of *Mycobacterium tuberculosis* (Bellinzoni *et al.*, 2005) is composed of a N-terminal amidase fused to NAD⁺ synthetase. The nitrilase domain hydrolyses glutamine, releasing ammonia for the synthesis of NAD⁺.

Table 1.2 13 enzyme branches of the nitrilase superfamily. Parentheses denote domains found in only some members of the branch. The conserved consensus sequences that flank the catalytic triad (EKC) residues for each branch are shown. Shading of residues represents the following: yellow, residue is conserved in all branches; blue, residue is conserved in nine or more branches; green, residue is conserved in six to eight of the branches. Upper case letters indicate 90% or greater consensus levels within a branch, whereas lower case are 50% or greater. Table 1.2 was taken from Pace and Brenner (2001).

		Conserved signature sequences surrounding catalytic triad residues																					
		Glu					Lys					Cys											
Branch	Enzyme	Additional domain																					
1	Nitrilase		f	P	E	A	f	h	R	K	I	.	P	T	I	.	C	W	E	n	.	.	p
2	Aliphatic Amidase		F	P	E	Y	S	Y	R	K	I	P	W	c	i	I	C	d	D	G	n	y	P
3	N-terminal Amidase	(unknown domain)	F	P	E	.	.	Y	r	K	.	F	L	.	.	I	C	M	D	.	.	P	Y
4	Biotinidase	(full/partial nitrilase domain) & carboxyl domain	F	P	E	D	.	Y	r	K	.	h	L	y	F	t	C	F	D	i	I	f	y
5	Beta-ureidopropionase		.	Q	E	A	W	.	R	K	N	H	I	P	N	I	C	Y	G	R	H	H	P
6	Carbamylase		F	p	E	L	A	Y	R	K	I	H	L	P	f	I	C	N	D	R	R	W	P
7	Pro. NAD+ Synthetase	(NAD synthetase domain)	f	P	E	L	.	.	.	K	.	L	P	.	.	I	C	E	D	.	w	.	P
8	Euk. NAD+ Synthetase	NAD synthetase domain	G	P	E	L	E	R	p	K	M	.	I	a	E	i	C	E	E	L	w	.	P
9	ALP N-acyltransferase	Hydrophobic domain & (dolichol phosphate mannose synthetase domain)	w	p	E	.	a	.	.	K	.	.	I	V	.	i	C	y	E	.	.	f	.
10	Nit and NitFhit	(Fhit domain)	L	P	E	.	f	y	r	K	.	H	I	F	.	i	C	Y	D	.	R	f	p
11	NB11		.	q	E	L	f	Y	R	K	.	H	I	P	.	i	C	w	D	q	w	f	p
12	NB12	N-terminal acetyltransferase	F	P	E	I	F	Q	y	K	I	H	i	T	q	I	C	Y	D	I	E	F	P
13	Non-fused Outliers		I	P	E	.	.	y	r	K	.	h	L	f	.	i	C	y	D	.	r	F	P

1.7.2 Levels of conservation amongst related members of the nitrilase superfamily

To describe the extent of conservation amongst members of the nitrilase superfamily at the protein sequence level and at the structural level, an alignment taken from Thuku *et al.*, (2009) is shown in Figure 1.4. Included in this alignment are the protein sequences of eleven members of the nitrilase superfamily for which atomic structures have been determined (Table 1.3). Only the enzyme functions for the aliphatic amidases (branch 2), DCases (6) and a -alanine synthetase (5) are known. Most recently, the structure of a hypothetical protein from mouse (PDB code: 2wlv) has been added to the nitrilase superfamily (Table 1.3) (not shown in alignment).

Table 1.3 Eleven atomic structures that have been reported for members of the nitrilase superfamily.

PDB code	Enzyme	Species	References
2dyu, 2e2k, 2e21, 1uf5	Formamidase (aliphatic amidase)	<i>Helicobacter pylori</i> (AmiF)	(Hung <i>et al.</i> , 2007)
	DCase	<i>Agrobacterium radiobacter</i>	(Hashimoto <i>et al.</i> , 2004) (Nakai <i>et al.</i> , 2000)
1ems	Nitrilase-fragile histidine triad fusion protein	<i>Caenorhabditis elegans</i>	(Pace <i>et al.</i> , 2000)
1f89	Putative CN-hydrolase	<i>Saccharomyces cerevisiae</i>	(Kumaran <i>et al.</i> , 2003)
1fo6, 1erz,	DCase	<i>Agrobacterium</i> strain KNK712	(Wang <i>et al.</i> , 2001)
1j31	Hypothetical protein	<i>Pyrococcus horikoshii</i>	(Sakai <i>et al.</i> , 2004)
2e11	Putative prokaryotic Nit protein	<i>Xanthomonas campestris</i>	(Chin <i>et al.</i> , 2007)
2uxy	Aliphatic amidase	<i>P. aeruginosa</i>	(Andrade <i>et al.</i> , 2007)
2plq	Aliphatic amidase	<i>G. pallidus</i>	(Kimani <i>et al.</i> , 2007)
2vhi, 2vhh	-alanine synthase	<i>Drosophila melanogaster</i>	(Lundgren <i>et al.</i> , 2008)
2wlv	putative nitrilase	<i>Mus musculus</i>	(Barglow <i>et al.</i> , 2008)

The first five sequences included in Thuku *et al.*, (2009) alignment are the branch 1 enzymes that were aligned based on their predicted fold. These enzymes are: Nases from *G. pallidus* (DAC521) and *R. rhodochrous* J1 (RrJ1); cyanide dihydratases, from *Bacillus pumilus* strain C1 (BpumC1) and strain 8A3

(Bpum8A3), and *Pseudomonas stutzeri* AK61 (PstuCDH); cyanide hydratases, from *Gloeocercospora sorghi* (GsorCH) and *Neurospora crassa* (NcraCH) (Figure 1.4).

Extent of conservation at the protein sequence level

All members of the nitrilase superfamily show conserved catalytic triad residues (EKC), as well as an extra glutamate residue (Kimani *et al.*, 2007, Thuku *et al.*, 2009) (Figure 1.4). This extra glutamate residue corresponds to E142 in the structure of *G. pallidus* aliphatic amidase, which has been implicated in the nitrilase reaction mechanism (Kimani *et al.*, 2007). Four glycine residues are also conserved in all members (Thuku *et al.*, 2009) (Figure 1.4). Their role in the structure is not known. Each branch of the nitrilase superfamily has a signature sequence that flanks the catalytic triad (EKC) that is conserved (Pace & Brenner, 2001) (Table 1.3). A signature sequence flanking the extra catalytic glutamate residue has not yet been determined.

Unlike other structures, Nases and aliphatic amidases share an extended C-terminal sequence of 40-100 amino acids (Thuku *et al.*, 2009). The proposed role of the C-terminal region of *G. pallidus* aliphatic amidase is involved in the interlocking of two monomers (Section 1.7.3). In addition to the sequence conservation, only the branch 1 enzymes show the conserved sequence motif DP/FXGHY. Point mutations of the histidine residue within this motif (H296 of the enzyme from *Pseudomonas fluorescens* EBC 191 (Kiziak *et al.*, 2005)(Figure 1.4)), resulted in decreased enzymatic activity and stability (Kiziak *et al.*, 2007).


```

Dac521 1: MEGRNMSNRAQKVKVAVIQA-SSVIM---DRDATTKKAVSLIHQAAEK--G
RzJ1 1: MVEYINTFRKVAAVQA-QPVWF---DAAKTVDKTVSIIAEARN--GC
BpumC1 1: MTSIYPKFRAAVQA-APIYL---NLEASVEKSCELIDEAASN--GA
Bpum8A3 1: MTSIYPKFRAAVQA-APIYL---NLEASVQKSCELIDEAASN--GA
PstuCDH 1: MAHYPKFRAAVQA-APVYL---NLDAVVEKSVKLEEAASN--GA
GsorCH 1: MPINKYKAAVVTs-EPVWE---NLEGGVVKTEFINEAGKA--GC
NcraCH 1: MVLTRYKAAAVTS-EPCWF---DLEGGVRKTIIDFINEAGQA--GC
1j31 1: mvkVGYIQm-ePkIl---eLdkNyskAekLlkeAske--gA
1f89 2: saskiLsqkIkVAVLQI-sGssp---dkmaNlqrAatFlerAmkegpdT
1ems 10: matgrhFIIVQI-sSdn---dlekNFqaAknMerAGekK--C
1erz 1: trqmiLAVGQQgpIaraet---reqVVvLldMltkAasr--gA
1fo6 2: rqmiLAVGQQgpIaraet---reqVVvLldMltkAasr--gV
1uf5 1: trqmiLAVGQQgpIaraet---reqVVvLldMltkAasr--gA
2e11 1: mbLrISLVQI-sT-rwh---dpagNrdyYgalleplagq--S
2duy 13: MGSIGSMGKPIEGFVVAIQFpVpiVns-rkIdhHfIsEirtLhaTkagypgV
2uxy 1: mrhgdissndTVGVAVVNYkMprlht-aaeVldnAkIaemIvymkqgpgM
2plq 1: mrhgdissndTVGVAVVNYkMprlht-kaeVlenAkIaemIvymkqgpgM
2vhi 5: MSAFELKnlndclckhlpdelkevkrilYgveedgtleLptsAkdIaeqngFdlkGyrftAreeqrkrriIvVGAIQnsivipTtapiekGrealvnmkMikAaaAgC
<--β1--> <--α1--> <--αC-->

Dac521 47: KIVVFHAFIPAYPRGLSFGTTIGSRSAEGRKDWYRYSWNSVAVPDLTDLGAAAGVYLVIQ-VTERNEFSGGTLYCSVLFDFSDGQLLGHKRLKPT
RzJ1 42: ELVAFHAFIPGYPYHIWVDS---PLAGMAKFAVRYHENSMTDSPHVQLLAAAHNIIVVVG-ISEBGG---SLYMTQLVIDADGQVAVRRHRLKPT
BpumC1 42: KLVAFAFLPGYPWFALIGH---PEYTRKFYHLYKNAVEIPSLAIQISAAANITVVCIS-CSEKGGG---SLYLAQLWFPNGDILGKHHMRAS
Bpum8A3 42: KLVAFAFLPGYPWFALIGH---PEYTRKFYHLYKNAVEIPSLAIQISAAANITVVCIS-CSEKGGG---SLYLAQLWFPNGDILGKHHMRAS
PstuCDH 41: KLVAFAFLPGYPWFALIGH---PEYTRRFYHLYKNAVEIPSLAIQISAAANITVVCIS-CSEKGGG---SLYLAQLWFPNGDILGKHHMRAS
GsorCH 40: KLIAFHVWIPGYPYWMKVNLYQS---LPLMKAYRENSIAMDSMVAIAANINQIVYVSLG-VSETHA---TLYLTQVLISPLGDVINHRRHKIPT
NcraCH 40: KLVAFHVWIPGYPYWMKVT---YQQSLPMLKRYRENAMAVDSVTFIAANINQIVYVSLG-FAETHA---TLYLAQALIDPTGEVINHRRHKIPT
1j31 36: KLVLFLDFDTPG-ynFe---sreeVfdvlgqIpe-egertTfImeLarelGlyIVAG-TAEKgn---yLynSAAVDPGrg-yigkYKihlF
1f89 47: KLVLFLDFDTPG-ynFe---sreeVfdvlgqIpe-egertTfImeLarelGlyIVAG-TAEKgn---yLynSAAVDPGrg-yigkYKihlF
1ems 48: eMVLFLDFDTPG-Gl---kneqIdlAmaTdeeymekYrelARkhnIwLSLGGlhhkdpS-daahpwTfHlIdsdovtraeYKihlFdlIeipg
1erz 40: nFIVFHLALTLTPFRwhft---deaeLdsfYeteMpggvVrplLefkAaelGIGFNLG-YaelVveggvkrFNTSILVdksGkiyvkYKihlFghkeyeay
1fo6 40: nFIVFHLALTLTPFRwhft---deaeLdsfYeteMpggvVrplLefkAaelGIGFNLG-YaelVveggvkrFNTSILVdksGkiyvkYKihlFghkeyeay
1uf5 40: nFIVFHLALTLTPFRwhft---deaeLdsfYeteMpggvVrplLefkAaelGIGFNLG-YaelVveggvkrFNTSILVdksGkiyvkYKihlFghkeyeay
2e11 37: DLVILLHTTTS-C-Sn---eaLdk--aedmdgpTvaWlrtQaarLgAATIGS-VQLrteh---gVFNRLWMApdg-alqyYKihlF
2duy 54: eLlIFHAYSTQGlnt---akWlseeFLldVpgEtelYakACkeakVYgVFS-IMERNpdankN-PYNIAIIdqGeiIkYKihlF
2uxy 53: dLVVFLHSLQGIMy---dpaemmetAvaIpggeTeifSRAcrkanVwGVFSLT-ErheehprkaPyNTLVLdnngelVQYKihlF
2plq 53: dLVVFLHSLQGIMy---dqdemtAAAsIpggeTafIaeACkkaQTVGVFSLTGEKhedhpnkApyNTLVLdnngelVQYKihlF
2vhi 114: nIVCTQHWMTMPFACTrefk---pWceFAeaA-e-nGpTtkmleLaynMVIIHS-ILERdmehegtiWNTAVVITansgrylkhHkhhIF
<--β2--> <--α2--> <--α3--> <--β3--> <--β4--> <--β5-->

Dac521 148: AAEIIVWGGGG-STLPVFDTPYGRIGALINWENYMLPARAAAYM---GQIYIAPTADA---RETWQSTIRHIALEGRCFVLSANQYVTK
RzJ1 136: HVEASVYGGNG-SDISVYDMFARLGALEWEIFOTLTKYAMYSQ---HEQVHVASWPGMSLYQPEVPAP---GVDAQSTIRHIALEGQTFVVCVTQVVPV
BpumC1 135: VAERLIWGDGSG-SMPPVFQTEIGNLGGIMQEHQVPLDLAMNAQ---NEQVHVASWPGY---PDDEISSRYAIATQTFVLMTSSMYTE
Bpum8A3 135: VAERLIWGDGSG-SMPPVFQTEIGNLGGIMQEHQVPLDLAMNAQ---NEQVHVASWPGY---PDDEISSRYAIATQTFVLMTSSMYTE
PstuCDH 134: VAERLWGDGNG-SMPPVFQTEIGNLGGIMQEHNVPLDIAAMNSQ---NEQVHVAAWPGF---PDDEISSRYAIATQTFVLMTSSMYTE
GsorCH 133: HVEKLVYGDGSGDFEPVTEIGNLGGIMQEWNNPFLKSLAVAR---GQIHVAAPVYVPLSKQVHPDPATNADPADSLVTPAYAEITGTWVLAFFQRISV
NcraCH 133: HVEKLVYGDGAGDFMSVPTPELGRGLQNCWENMNPFLKSLAVAR---GEGIHIAAWPIYPKETILKYDPDPATNADPADSLVTPAYAEITGTWVLAFFQRISV
1j31 118: yrlkvfFepGdlg-fkVfdlg-fakVGVMTCDTfLGAELAK---gAEIHAEPALV---p-y-pramp-AlIrVTLITADrVE
1f89 141: SmetIspGek-s-TtdtkYgkFGVLC-DMrfpsLAmLSk---gAFMIYPSAsnt---vtGhlhllLars-AvngVYVMLCSpArnl
1ems 138: kvIneeEskkaGemi-pPvcTp-IgrLGLSIdvVrpsLISLWNg---gqLLSFPsAft---IntGlahWetLLe-AiNOCYVVAAGQgah
1erz 139: RpfOHLkrYFepGdlg-fpVydVd-aakMGMPfLdRwpseAWVMLg---gAEITCCGYntGthPpv-pqghdhsfHllsMgagSyqNGAWSAAGKVGM
1fo6 139: RpfOHLkrYFepGdlg-fpVydVd-aakMGMPfLdRwpseAWVMLg---gAEITCCGYntGthPpv-pqghdhsfHllsMgagSyqNGAWSAAGKVGM
1uf5 139: RpfOHLkrYFepGdlg-fpVydVd-aakMGMPfLdRwpseAWVMLg---gAEITCCGYntGthPpv-pqghdhsfHllsMgagSyqNGAWSAAGKVGM
2e11 114: -rfgnhrlYaaqr-er-1Cvewk-gWrINPC-DLrIspVcrNrdvrrpqlLDFDLQLFVANW---sarayaWktLlrs-AiNLCFVAAVNVGM
2duy 140: -ie-PWypggq-MpVceGpGgSkLAVCI-DgnypLAAACAYk---gCNVYRISGyst-gvndqWlItrsnAwhNLMYTVSVNLAGyD
2uxy 141: -ie-PWypggq-TyvseGpKkMkISLII-CDgnypLAAACAYk---gAEILVRCQGYp-akdqQymmaKamAwaNcYVAVANAGfD
2plq 141: -ie-gWypgdt-TyvtEgPkgLkISLII-CDgnypLAAACAYk---gAEILVRCQGYp-AkeQQLmAKAMAWANNYVAVANAGfD
2vhi 206: InstYmeGntg-hpVfeLefg-kLAVNIGS-nhYQNWmFGLN---gAEIVFNSAigrIs---epIwIeArnAAIahSYFTYPINRVgtE
<α4> <β6> <β7> <--α5--> <β8> <--α6--> <β9> <β10>

Dac521 233: DMYPKDLACYDELASSPEIMSRGSAIVGPLGEYVAVPVG-KEDIIIAELDMKQIAYSQDFDPVGHYARPDVFKLLVNKEKKTIEIWNK
RzJ1 232: EAHEFFCDNDBQRKLI---GRGGFARIIGDPGRDLATPLAEDEEGILYADIDLSAITLAKQAADPVGHYSRPDVLSLNFNRHTTVPNTAISTIHATHTLVQSGALDGVR
BpumC1 219: EMKEMICLTQEQRDYFE-TFKSGHTCIYGPDGEPISDMVAETEGIAYATVERVIDYKYYIDPAGHYSNQSLSMNFNQOPTPVVKHLNHQKNEVFTYEDIQYGHGILEE
Bpum8A3 219: EMKEMICLTQEQRDYFE-TFKSGHTCIYGPDGEPISDMVAETEGIAYATVERVIDYKYYIDPAGHYSNQSLSMNFNQOPTPVVKHLNHQKNEVFTYEDIQYGHGILEE
PstuCDH 218: EMKMLCETQEQRDYFN-TFKSGHTRIYGPDGEPISDMVAETEGIAYATVERVIDYKYYIDPAGHYSNQSLSMNFNQOPTPVVKHLNHQKNEVFTYEDIQYGHGILEE
GsorCH 235: EGLKRRHTPPGVEPETDA-TPYNGHARIYFRPDGSLYAKPAV-DFDGLMYVDIDLNEHSLTKALADFAGHYMRPDLIRLVLVDTRRKLVLTEVGGGNGIQSYSTMARIGLDR
NcraCH 235: EGLKNTPEGVEPETD-STYNGHARIYRDPGSLVVRPDK-DFDGLLVFDIDLNECHLTKALADFAGHYMRPDLIRLVLVDTRRKLVLTEVDRNGGIVQYSTRERLGLNTP
1j31 202: rg---lKPIgkSIITAspkaeVlsiaSete-eeIgvveIdInlArnkrdmndIfrkreeyyfr
1f89 229: qs---shayGhSIVVDPrgKivaeAqe-geetiYaelDpvesfrqavpltkq-rrf
1ems 229: np---krGyGhSMVDPwGavvaqCS---ervdMcfaeldLsyVdtIremg-pvfhrrsdlytlhineksset
1erz 240: en---cmLlghSCIVAPtGeivalTtle-deVitaavLDlrgrelrehfnfkqhrppqhygliaef
1fo6 240: eg---cmLlghSCIVAPtGeivalTtle-deVitaavLDlrgrelrehfnfkqhrppqhygliaef
1uf5 240: en---cmLlghSCIVAPtGeivalTtle-deVitaavLDlrgrelrehfnfkqhrppqhygliaef
2e11 208: gn---ghYaGDSAVIdfIqppveIre-qeqvtttIsaaaLaehrarfpaImldgdsfvlg
2duy 224: nv---fyfFEGQICnfDgttlvqghr-npweIvtgeYpKmadArIsqglenniylnghrgyvakpg-GehdagltyikdlaagkykIpedhmkI
2uxy 223: gv---ysYfGhSaIIGDgrtlIgeCve-neemqYAQLSlsqIrdarandqgnhfkIhrGysqIqasgddgrLaecepFeyrtvwtDaeakaren
2plq 225: gv---ysYfGhSaIIGDgrtlIgeCgt-eeenQYAEVYSlsQrFRKNAQSONHLFLKLRHGLYLInSesgdrGvAeCpFdfYrtVwIaeakaren
2vhi 294: qFpIYsgdgnLahkefGpFYGhSYVAAdgSRTpSLsr-dddGLLYVeLDLnrerqvkdfwg-frmtqrVpyaesFkkaeshgfkpqliket
<β11> <β12> <β13> <β14> <--α7--> <α8> <α9--> <--α10--> <--α11-->

RzJ1 341: ELNGADEQRALPSTHSDETDRATASI
BpumC1 329: KV
Bpum8A3 329: KV
PstuCDH 328: VVRSRLK
GsorCH 344: PLEEDYRQGTIDAGETEKASSNGHA
NcraCH 344: ENDKEGKK
2duy 317: kdgsiygypttggrfgk
2uxy 317: verItrsttGvaqcpvgrlpyeLEKEA
2plq 319: vekItrsttGvaCpiagipneGKTKBIVG
<-->

```

Figure 1.4 continued

Figure 1.4 Multiple alignment of protein sequences of characterised members of the nitrilase superfamily. The conserved catalytic residues (EKC) are shown in a box outline. The extra conserved E residue, which has been implicated in the nitrilase reaction mechanism (Kimani *et al.* 2007), is shown in bold and double underlined. The secondary structural elements identified in 2plq (Kimani *et al.* 2007) are indicated in the bottom line. The approximate regions of the intersubunit surfaces, namely A, C, D and E are indicated on the top line. The conserved sequence motif 'DP / FXGHY' in the tail region of the spiral forming Nases is underlined, and in which a conserved histidine residue (corresponding to H296 in the enzyme from *Pseudomonas fluorescens* EBC 191 (Kiziak *et al.* 2005)), is coloured green. The residues missing in the crystal structures are white on a black background. The alignment and legend were taken from Thuku *et al.*, (2009)

Extent of structural conservation

Despite the low sequence conservation, all structures share high structural similarities. The sequences share characteristic monomer fold of (Thuku *et al.*, 2009). A cartoon representation and topology of the structural fold for *G. pallidus* aliphatic amidase is shown in Figure 1.5. In addition, the structural folds, α -helices and β -sheets, of the aliphatic amidase of *G. pallidus* are included in the alignment (Figure 1.4, bottom line).

The monomer fold of *G. pallidus* aliphatic amidase consists of 11 α -helices and 14 β -strands, which are interconnected by external loops (Figure 1.5). There are two six stranded β -sheets which are sandwiched between the two helical layers, forming a four-layer sandwich architecture (Figure 1.5). The two outer helical layers are formed by one set of helices 1-3 and the other set of helices 4-6 (Figure 1.5). The two β -sheets are composed of β -strands 1-5 and 14 and the other sheet of β -strands 6--9, 12 and 13 (Figure 1.5).

The catalytic cysteine residue (C166 of *G. pallidus* aliphatic amidase) is located on a 3_{10} -helix. This unique conformation was proposed to be essential for the orientation of the cysteine residue within the catalytic cleft. This feature is conserved in all known structures (Kimani *et al.*, 2007).

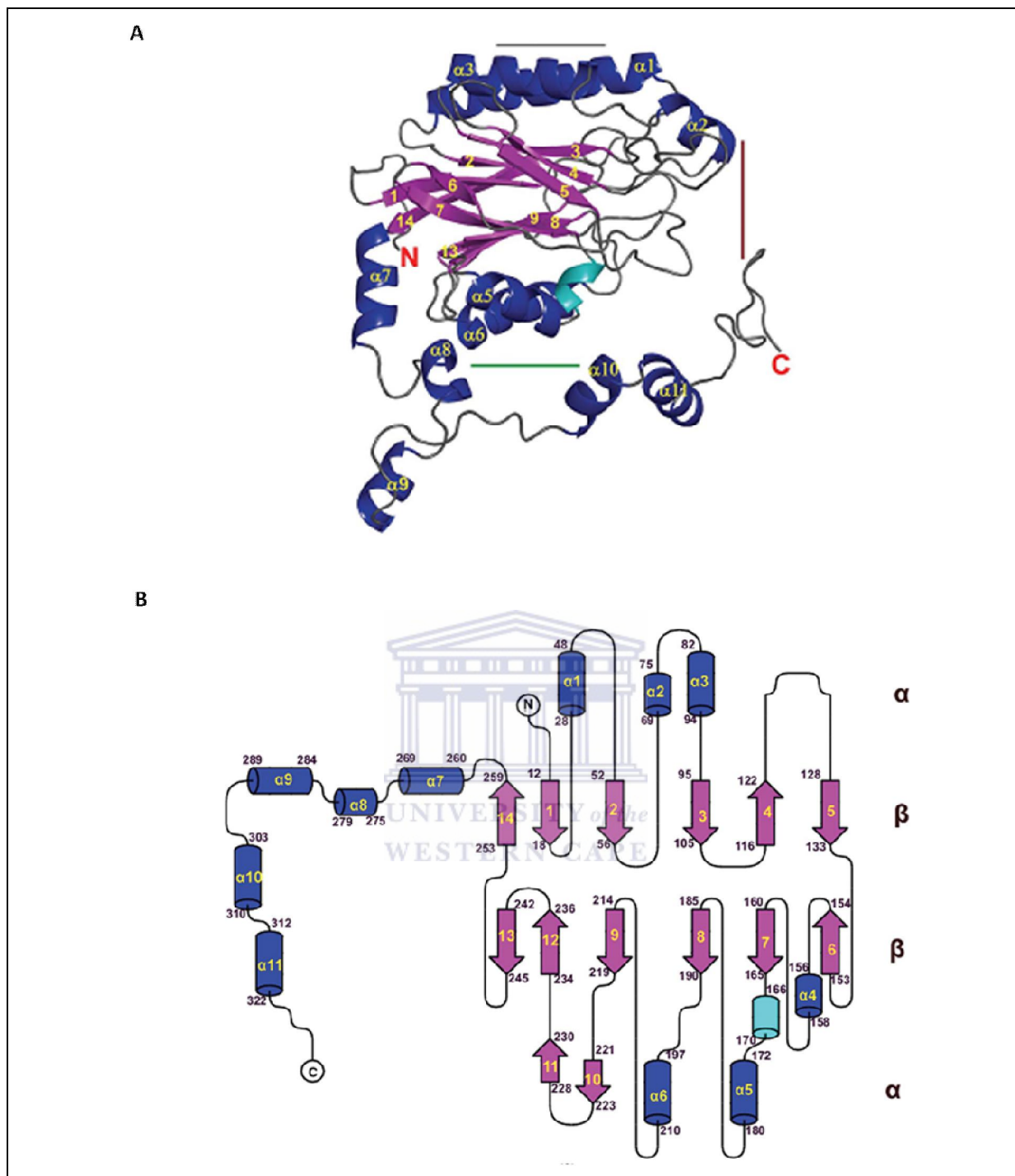


Figure 1.5 The monomer fold of *G. pallidus* aliphatic amidase. Panel A, cartoon representation of the monomer. The bars shows the following intersubunit interacting surfaces: green, 'A surface'; red, 'C surface'; grey, 'D surface'. Panel B, α -helix and β -sheet topology of the monomer. β -sheets (labelled 1–14) are shown as purple arrows, while α -helices are shown as blue cylinders. The cyan cylinder in the topology diagram is the 3_{10} -helix on which the catalytic C166 residue resides. The secondary-structure elements are numbered in sequence from the N-terminus. Images and text were taken from Kimani *et al.*, (2007).

1.7.3 Intersubunit surfaces

Six surfaces namely A, B, C, D, E, and F have been used to describe the intersubunit interactions for multimeric structures of nitrilases (Sewell *et al.*, 2005, Thuku *et al.*, 2009). Two-fold axes relate all these surfaces whereas the E-surface is asymmetric. As described earlier, the intersubunit surfaces for spiral forming Nases have largely been elucidated from a combination of negative staining electron microscopy and docking of homology models (Thuku *et al.*, 2009). The following surfaces, A, C, D, E and F have been described for Nases (Thuku *et al.*, 2009). The E and F surfaces are still hypothetical and need to be experimentally determined. *G. pallidus* aliphatic amidase, which is a hexamer, has the following A, C, and D surfaces (Kimani *et al.*, 2007).

A surface – conserved in known structures of the nitrilase superfamily

The A surface represents the interaction between two monomers that forms a sandwich (Figure 1.6). According to the structure of *G. pallidus* aliphatic amidase, the A surface is formed by the intramolecular salt bridges and hydrophobic interactions between residues of the 5, 6 helices and the C-terminal region (residues 273–340) of two monomers (Kimani *et al.*, 2007). This association between two monomers, which involve 5 and 6 and the C-terminal region, is conserved in all structures (Thuku *et al.*, 2009). The extended C-terminal of aliphatic amidases and Nases, which is involved in interlocking of two monomers, was proposed to strengthen the intersubunit interactions at the A surface (Andrade *et al.*, 2007, Kimani *et al.*, 2007).

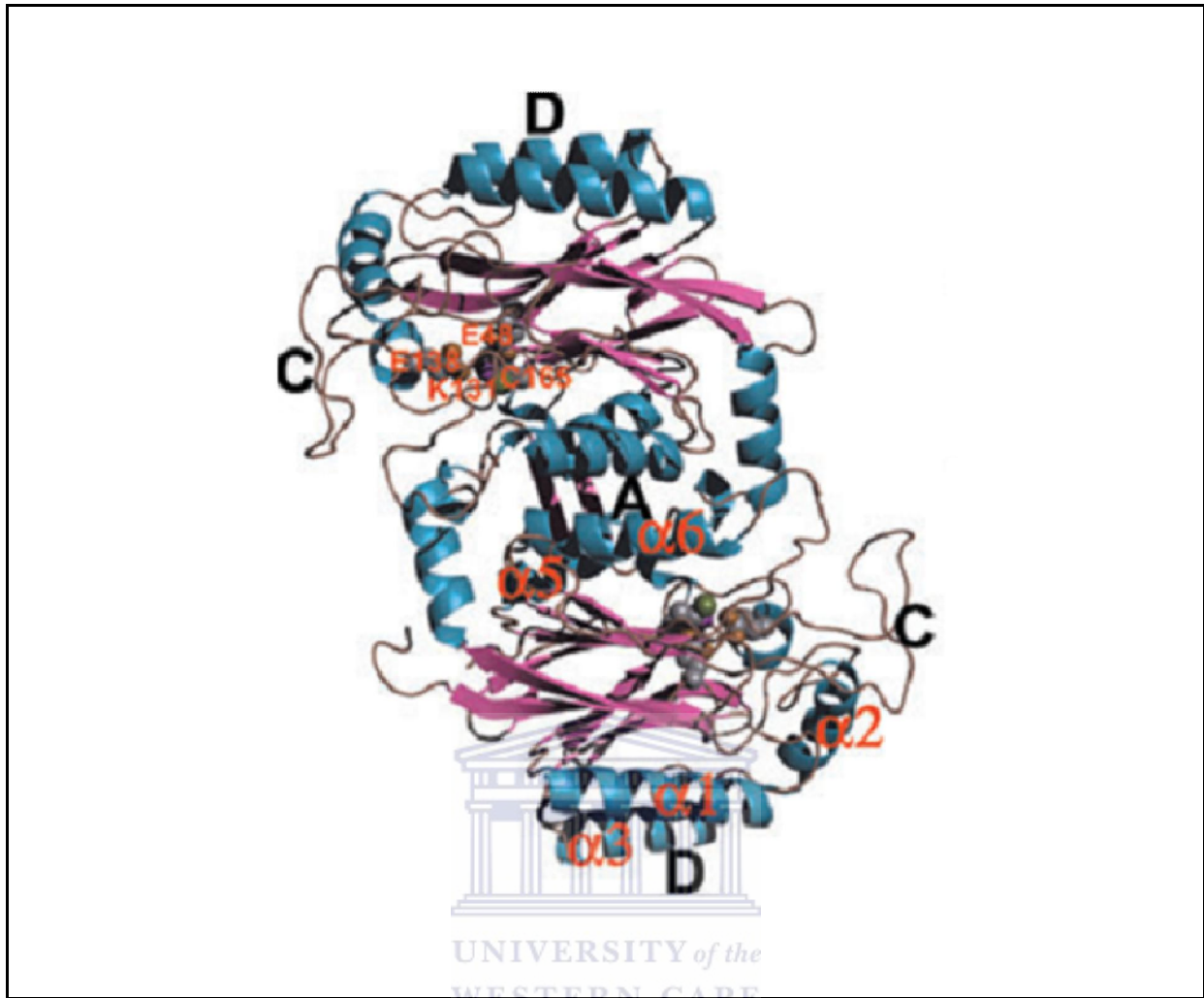


Figure 1.6 A homology model of *R. rhodochrous* J1 Nase showing the intersubunit interacting surfaces. The interacting surfaces are labelled in black. The helices (1, 3, 5 and 6) involved in the interacting surfaces are also highlighted. Image was taken from Thuku *et al.*, (2009).

B surface

The B surface is only described for the structures of NitFhit (Pace *et al.*, 2000), DCases (Nakai *et al.*, 2000) and the prokaryotic XC1258 Nit protein (Chin *et al.*, 2007). The monomers of these structures have an exposed β -sheet that allows two dimers to interact forming tetramers (Thuku *et al.*, 2009).

C surface

For spiral forming Nases, the C surface interaction occurs between adjacent dimers by associating with the A surface (Thuku *et al.*, 2009) (Figure 1.6 and 1.7). The C-surface is composed of the 12-16 residues insertion (Figure 1.4). This insertion is not conserved amongst structures of the nitrilase superfamily, possibly accounting for the lack of spiral formation (Thuku *et al.*, 2009).

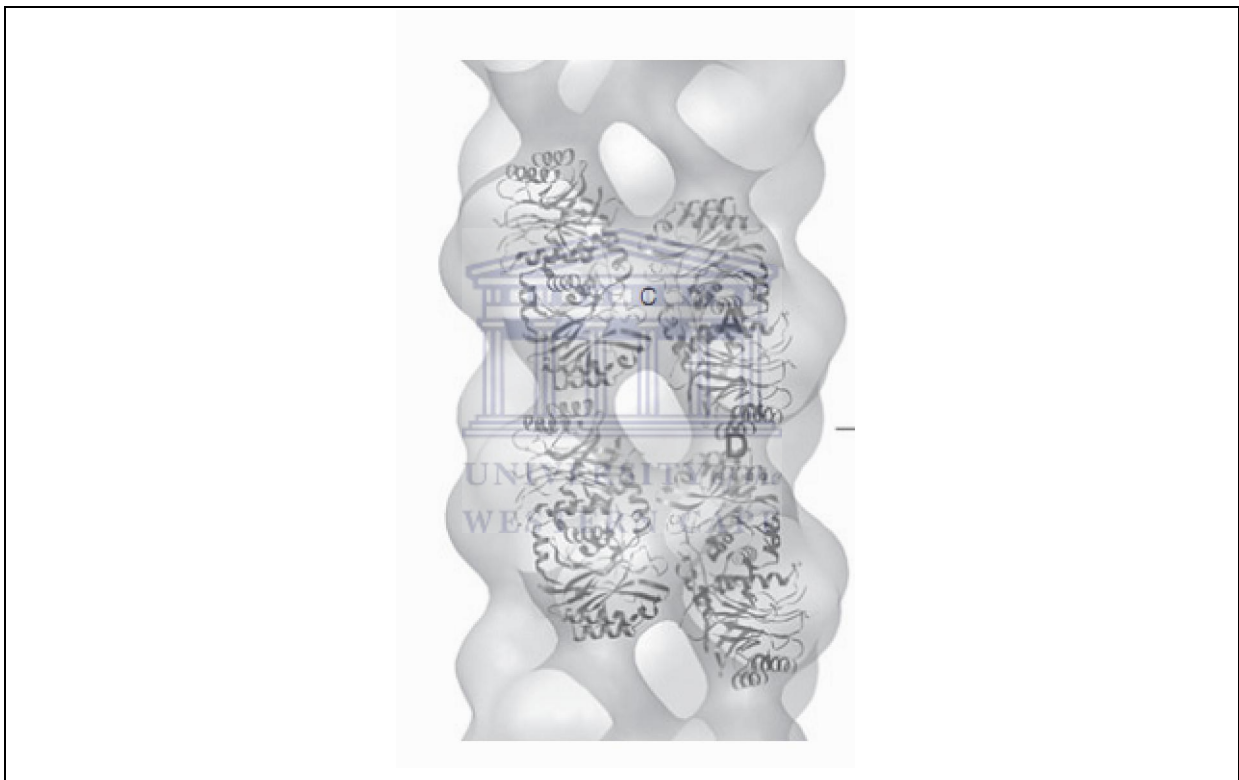


Figure 1.7 A 3D electron microscopic reconstruction of *R. rhodochrous* J1 Nase showing the A, C and D intersubunit interacting surfaces. Image was taken from Thuku *et al.*, (2009).

The interaction between the C and A surfaces was proposed to initiate spiral formation, since it is located at right angles to the A surface (Figure 1.7). Mutations of residues in these surfaces leads to inactivation of the enzyme, which provides further evidence of a connection between these interfaces and the active site (Sewell *et al.*, 2005). The histidine residue within the conserved motif

found in the C-terminal region of Nases (Kiziak *et al.*, 2007) is positioned facing the C surface. The side chain of the histidine residue was suggested to interact with the substrate on its way to the active site (Thuku *et al.*, 2009).

D-F surfaces

Both the D and F surfaces were suggested to confer stability to the helical twist of the spiral forming Nases (Figure 1.8). The E surface is asymmetrical and has been described for the terminating spiral of cyanide dihydratase from *Pseudomonas stutzeri* AK61. The asymmetry of the E surface causes the spiral to terminate after 14 subunits by preventing further addition of subunits (Thuku *et al.*, 2009) (Figure 1.8). However, the termination mechanism for other Nase spirals has not yet been described.

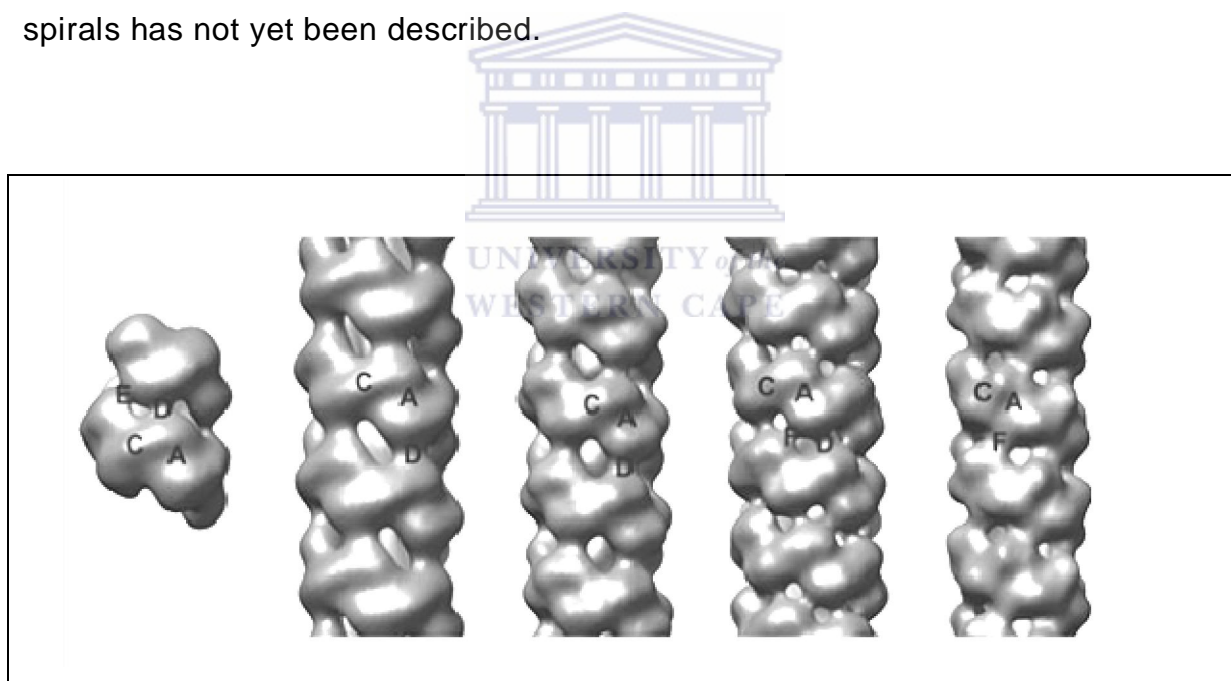


Figure 1.8 The A, C, D, E and F surfaces of spiral forming Nases. From left, terminating 14-subunit spiral of the cyanide dihydratase from *Pseudomonas stutzeri* AK61, the variable length helices of the cyanide dihydratase from *Bacillus pumilus* C1 and the C-terminal truncated nitrilase from *R. rhodochrous* J1, and the cyanide hydratases from *Neurospora crassa* and *Gloeocercospora sorghi*. The C, D and F surfaces that stabilise the spiral formation for Nases and cyanide hydratases are shown. The asymmetric E surface occurs only in the terminating spiral of cyanide dihydratase from *Pseudomonas stutzeri* AK61. Images were taken from Thuku *et al.*, (2009).

1.7.4 Catalytic cleft of nitrilase structures

The active site is located near the edge of the A surface (Kimani *et al.*, 2007). The arrangement of the side chains of the catalytic residues (EKEC), is conserved among nitrilase structures (Kimani *et al.*, 2007) (Figure 1.9).

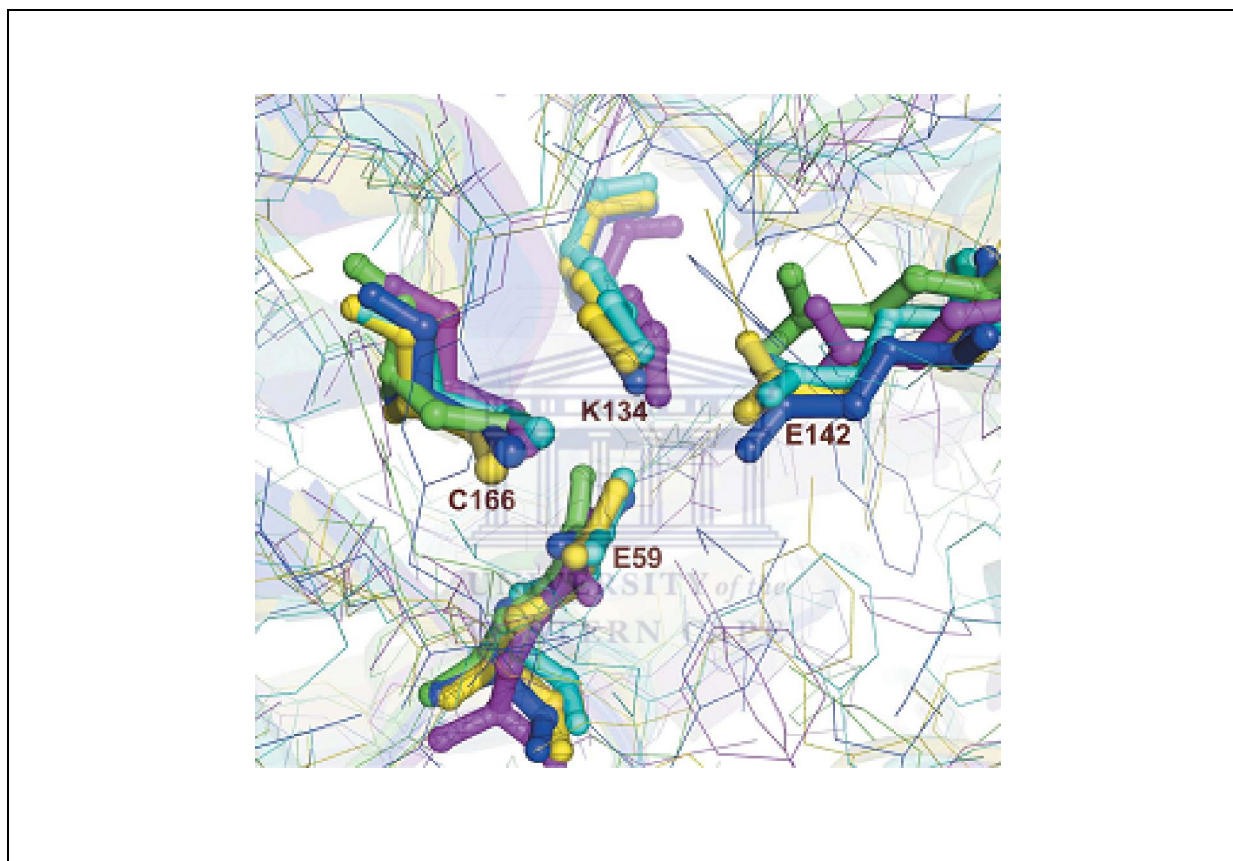


Figure 1.9 Superimposition of the catalytic residues (EKEC) of five nitrilase structures. The colour of the structures are as follows: 1j31, yellow; 1ems, green; 1erz, cyan; 1f89, magenta; 2plq, blue. The catalytic residues are in *G. pallidus* aliphatic amidase numbering. Image was taken from Kimani *et al.*, (2007).

The catalytic cleft volumes for *G. pallidus* and *P. aeruginosa* aliphatic amidases, which are 53.59 \AA^3 and 23.9 \AA^3 , respectively, were described to be smaller than those of other structures (Andrade *et al.*, 2007, Kimani *et al.*, 2007, Kumaran *et al.*, 2003, Nakai *et al.*, 2000, Sakai *et al.*, 2004). The catalytic cleft volume of the formamide hydrolysing amidase (AmiF) was described as the smallest, since it

accommodates the 1-carbon atom substrate (Skouloubris *et al.*, 2001). The catalytic cleft of DCCase (PDB code: 1fo6) has a volume of 1134.7 Å³, which is larger than the aliphatic amidases (Nakai *et al.*, 2000). The small catalytic cleft volume of the amidases may explain their preferences for short aliphatic amides (Andrade *et al.*, 2007, Makhongela *et al.*, 2007, Skouloubris *et al.*, 2001).

1.7.5 Reaction mechanism

A reaction mechanism has been proposed for the nitrilase superfamily, since all members shared four conserved catalytic residues (Thuku *et al.* 2009, Kimani, *et al.* 2007) (Figure 1.10). The roles of the four catalytic residues in *G. pallidus* amidase were proposed as follows: the cysteine (C166) acts as the nucleophile, one glutamate (E59) acts as a general base catalyst, the other glutamate, (E142) acts as a general base catalyst that enhances the nucleophilicity of the water which hydrolyses the acyl intermediate, and the lysine (K134) stabilizes the tetrahedral intermediate.

The proposed reaction mechanism, as described in Figure 1.10, is as follows: (i) E59 increases the nucleophilicity of C166, which in turn initiates a nucleophilic attack on the substrate to form a tetrahedral intermediate, which is stabilised by K134. The E59 participates in electron transfer releasing ammonia giving rise to a thioester intermediate. (ii-iii) E142 increases the nucleophilicity of a nearby water molecular, therefore causing a nucleophilic attack by water on the thioester intermediate forming a second tetrahedral intermediate. (iv) The tetrahedral intermediate then breaks down with the release of the acid product and the restoration of the enzyme.

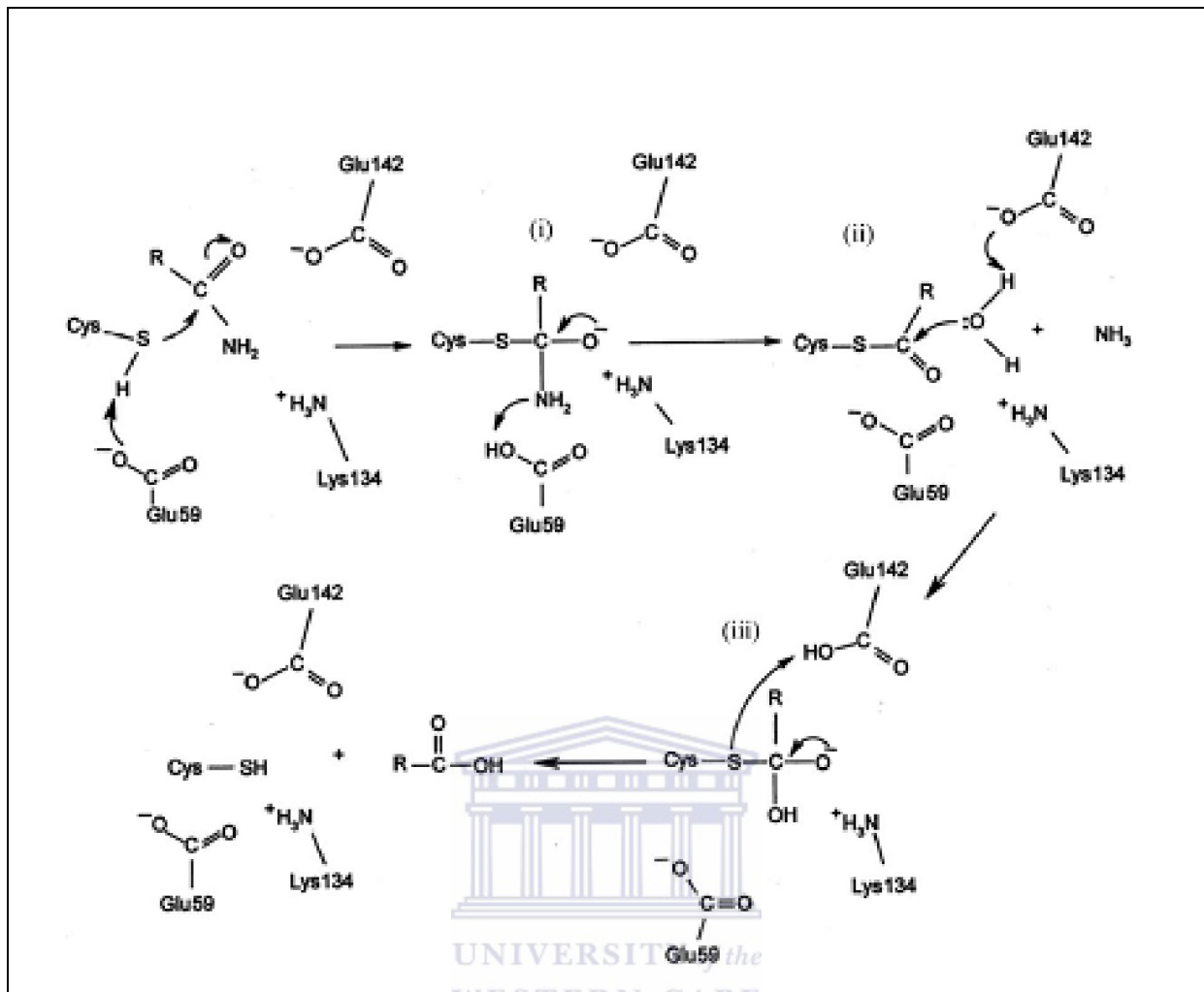


Figure 1.10 Proposed reaction mechanism for the *G. pallidus* amidase hydrolysis of amides.

Although no structures of Nases have been determined yet, these enzymes share the same conserved catalytic residues found in all structures (Thuku *et al.*, 2009). It is not known what distinguishes an enzyme having Nase activity from one having amidase activity.

1.8 Cold adapted enzymes

As shown in Table 1.1, the majority of nitrile hydrolysing microorganisms reported is of either mesophilic or thermophilic origins. Mesophiles have a minimal growth greater than 10°C, optimal growth greater than 25°C and have a maximum growth beyond 35°C. In addition, thermophiles have a minimal growth of 40°C, optimum growth at or beyond 50°C and has a maximum growth of roughly 70°C or higher.

NHases from mesophiles are not ideal for industrial applications because of their instability (Cowan *et al.*, 1998). These enzymes usually have very short activity half-lives. In particular, *Corynebacterium pseudodiphtheriticum* ZBB-41 NHase has a half life $t_{1/2} = 65$ min at 20°C (Li *et al.*, 1992), *Pseudomonas chlororaphis* B23, $t_{1/2} = 11$ min at 30°C (Nagasawa *et al.*, 1987), *R. rhodochrous* J1, $t_{1/2} = 58$ min 60°C (Nagasawa *et al.*, 1991); *Corynebacterium* sp. C5, $t_{1/2} = 7.5$ min at 45°C (Yamamoto *et al.*, 1992b). Stability has been enhanced by the addition of aliphatic acids (butyrates or valerate) (Kopf *et al.*, 1996). More recently, nitrile hydrolysing enzymes have been isolated from thermophilic bacteria such as the *Geobacillus* strains and *Pseudonocardia thermophila*, which have optimal growth between 50°C and 65°C (Table 1. 1). These enzymes were shown to have higher stabilities than mesophilic enzymes and rapid catalytic rates under sub-optimal conditions (Cowan *et al.*, 2003). For example, the NHase of *G. pallidus* has a $t_{1/2}$ of 6.8 mins at 60°C and 7 hrs at 30°C (Cowan *et al.*, 1998).

To date, no Nases, NHases or aliphatic amidases have been purified from cold-adapted microorganisms. Cold adapted bacteria are referred to as psychrophiles and psychrotrophs. Psychrophiles grow at or below 0°C and have an optimum growth temperature 15°C and an upper limit of 20°C (Morita, 1975). In comparison, psychrotrophs are capable of growth close to 0°C and have a growth optima 15°C (Morita, 1975). Cold adapted bacteria species generally produce enzymes that have high catalytic activity at low temperatures and low thermostability at elevated temperatures (Cavicchioli *et al.*, 2002). An example of an enzyme from a psychrophilic bacterium is dihydrofolate reductase purified from *Moritella profunda* (Xu *et al.*, 2003). The purified enzyme had an optimal

temperature for activity of 34°C and 19% activity at 2°C, the temperature at which the bacteria had optimal growth. The enzyme was less resistant to thermal denaturation than a mesophilic homologue from *E. coli* and much less than a thermophilic homologue from *Thermophila maritima* (Xu *et al.*, 2003).


Enzymes from cold-active organisms typically show high conformational flexibility, which contributes to their high catalytic activity at low temperatures and their increased thermolability (Cavicchioli *et al.*, 2002). Conversely, thermophilic enzymes tend to have rigid conformational structures that enable them to withstand higher temperatures.

Cavicchioli *et al.* (2002) reported a survey of cold-adapted enzymes where they were compared with their mesophilic and/or thermophilic counterparts. This survey revealed several features that promoted their increased conformational flexibility. Cold adapted enzymes generally have a reduced core hydrophobicity, decreased ionic and electrostatic interactions, increased charge of surface residues that promote increased solvent interaction, additional surface loops, substitution of proline residues by glycines in surface loops, a decreased arginine/lysine ratio, fewer interdomain and subunit interactions, and fewer aromatic interactions (Cavicchioli *et al.*, 2002).

The properties of cold adapted enzymes are attractive for both applied and basic research. The use of cold adapted enzymes as biocatalysts may preclude the requirement for expensive heating that is used to maximise catalytic activity, may minimise undesirable chemical reactions that occur at higher temperatures, and labile enzymes can be rapidly deactivated by heating when required (Gerday *et al.*, 2000, Russell, 1998). Furthermore, studies on the molecular basis of cold activity and the relationship between flexibility and catalytic efficiency address fundamental issues regarding structure-function relationships in proteins. Such issues are often approached through comparisons of homologous mesophilic and thermophilic counterparts or by the use of site-specific or random mutations (Alquati *et al.*, 2002, Narinx *et al.*, 1997, Santarossa *et al.*, 2005, Wintrode *et al.*, 2000).

1.8 Aims

Although some nitrile-hydrolysing bacterial strains, including some from the *Rhodococcus* genera (Brandao *et al.*, 2003), are known to exist ubiquitously, it is evident that no cold-adapted varieties have been isolated. The broad aim of this research was to isolate and characterise nitrile-hydrolysing bacterium from cold environment. In addition, to screen genomic DNA of the isolate for genes of nitrile hydratases or nitrilases for cloning and expression in *E. coli* as hexahistidine tag fusion proteins for Ni-chelation purification. Characterisation of the purified protein would determine its enzymic properties at low temperatures. X-ray diffractable crystals could also be produced from the purified enzyme in order to describe its high-resolution crystal structure for comparison with mesophilic and thermophilic counterparts. The four specific aims of this investigation were the following:

- 
- 1) To isolate, identify and characterise a nitrile hydrolysing bacteria from a cold environment.
 - 2) To screen the genomic DNA library prepared from an isolate for nitrile hydrolysing gene(s).
 - 3) To clone the nitrile-hydrolysing gene for expression in *E. coli* as hexahistidine tag fusion proteins for purification and subsequent enzymic characterisation.
 - 4) To produce diffraction quality crystals of the protein for X-ray diffraction for the description of the high-resolution crystal structure

Chapter 2: Isolation of a cold-adapted nitrile hydrolysing bacterium

2.1 Introduction	37
2.2 Materials and methods.....	38
2.2.1 Media	38
2.2.2 Enrichment of nitrile hydrolysing bacteria	40
2.2.3 Genomic DNA extraction.....	41
2.2.4 16S rRNA gene identification	41
2.2.5 Preliminary determination of cardinal growth temperatures	43
2.2.6 Screening of isolates for nitrile and amide hydrolysis.....	43
2.2.7 Brief characterisation of <i>Nesterenkonia</i> AN1	44
2.3 Results.....	45
2.3.1 Isolation of nitrile hydrolysing bacteria from soil samples.....	45
2.3.2 Screening of isolates for activity on nitriles and amides	48
2.3.3 Preliminary determination of isolates cardinal growth temperatures	49
2.3.4 Utilisation of nitrile(s) as sole nitrogen and/or carbon source for growth	49
2.3.5 Effect of temperature, pH and salinity on the growth of <i>Nesterenkonia</i> AN1	52
2.3.6 Comparison of AN1 with known <i>Nesterenkonia</i> strains	53
2.4 Discussion.....	56

2.1 Introduction

The most commonly used procedure to isolate nitrile hydrolysing bacteria is a trophic selection strategy where a sole nitrogen and/or carbon source supports growth on nitrogen free minimal medium (NFMM) (Cowan *et al.*, 2003). For example, enrichment using nitriles as a sole source of nitrogen and/or carbon has resulted in the isolation of a range of bacteria, including *Acinetobacter* sp. AK 226 (Yamamoto *et al.*, 1990), *Alcaligenes faecalis* JM3 (Nagasawa *et al.*, 1990), *Pseudomonas putida* (Nawaz *et al.*, 1989), *R. rhodochrous* J1 (formerly *Arthrobacter* J1) (Asano *et al.*, 1980) and *Bacillus subtilis* ZJB-063 (Zheng *et al.*, 2008b). Brandao *et al.*, (2002) reported that the highest percentage of isolations was produced with acetonitrile, a highly soluble low molecular weight compound, rather than for bulkier hydrophobic nitrile substrates like benzonitrile, succinonitrile or bromoxynil.

In this study, isolation of cold-adapted nitrile hydrolysing bacteria was carried out from soil samples collected from Miers Dry Valley, Antarctica. Miers is part of the McMurdo Dry Valleys, which is the largest ice-free region of Antarctica. The Dry Valleys have been described as the coldest, most arid deserts on earth (Cowan *et al.*, 2002, Doran *et al.*, 2002). In addition, Cowan *et al.*, (2002) reported that soil samples collected from Dry Valleys in Antarctica contain high levels of microbial biomass. For the isolation of such cold adapted bacteria, incubation should be carried out at temperatures below 20°C and characterisation of growth optima is an important determinant (Russell & Cowan, 2006). For example, although a nitrile hydrolysing *R. erythropolis* strain ANT-AN007 has been isolated at 30°C from soil samples collected from Antarctica (Brandao & Bull, 2003), it has not been determined whether this strain has psychrophilic or psychrotolerant growth.

This chapter describes the isolation of cold-adapted nitrile hydrolysing bacteria and a brief phenotypical characterisation of a novel isolate.

2.2 Materials and methods

2.2.1 Media

The following media, M9 (Pardee *et al.*, 1959, Sambrook & Russell, 2001), Castenholz (Atlas, 2005), Halophilic and Alkaline (Grant, 2006, Litchfield *et al.*, 2006, Atlas, 2005) were modified to Nitrogen Free Minimal Media (NFMM) in order to enrich for nitrile hydrolysing bacteria. The chemical composition of each medium, excluding nitrogenous compounds, is listed in Table 2.1.

Table 2.1 Chemical composition of four types of media that were modified to NFMM.

Media (abbreviation)	pH	Composition (per L) of modified NFMM
M9	7.5	MgSO ₄ 0.24 g, CaCl ₂ 0.011 g, 10% M9 salts (6.4 % Na ₂ HPO ₄ ; 1.5% KH ₂ PO ₄ ; 0.25% NaCl)
Castenholz (CAS)	7.2	0.1% FeCl ₃ solution (0.03%); CaSO ₄ · 2H ₂ O 0.06 g; MgSO ₄ · H ₂ O 0.1 g; NaCl 0.008 g; Na ₂ HPO ₄ 0.11 g; 0.1% Nitsch's Trace Elements (0.05% H ₂ SO ₄ ; 0.22% MnSO ₄ ; 0.05% ZnSO ₄ · 7H ₂ O; 0.05% H ₃ BO ₃ ; 0.0016% CuSO ₄ · 5H ₂ O; 0.0025% Na ₂ MoO ₄ · 2H ₂ O; 0.0046% CoCl ₂ · 6H ₂ O)
Halophilic (HAL)	7.2	KCl 2 g; CaCl ₂ ·2H ₂ O 0.1 g, FeSO ₄ ·7H ₂ O 0.01 g; MnCl ₂ ·4H ₂ O 0.01 g; MgCl ₂ 0.95 g
Alkaline (ALK)	10.66	KH ₂ PO ₄ 1 g; MgSO ₄ ·7H ₂ O 0.2 g; Na ₂ CO ₃ 10 g; NaCl 40 g;

Each type of medium was supplemented with additional reagents as described in Table 2.2, in order to alter the pH, the nitrogen and carbon source, and/or the salinity. Glycerol was used as the carbon source for microbial growth. In addition, the following nitriles, acetonitrile, benzonitrile and acrylonitrile, were used as the nitrogen source (Table 2.2). CoCl₃ and FeCl₃ were added to the media since cobalt is required for active Co-type NHases (Kim *et al.*, 2001, Kobayashi *et al.*, 1991a, Takashima *et al.*, 2000). Solid medium was prepared using 2-3% ultrapure agar (GE Healthcare).

Table 2.2 Variations of media used to isolate nitrile hydrolysing bacteria. Type of NFMM is described in Table 2.1. Abbreviations: Gly, % of glycerol (w/v); S/L, solid or liquid; ACE, acetonitrile; BEN, benzonitrile; ACR, acrylonitrile.

Media	NFMM	S/L	Gly (%)	pH	NaCl (%)	Na ₂ CO ₃ (%)	FeCl ₃ (μM)	CoCl ₃ (μM)	ACE (mM)	BEN (mM)	ACR (mM)
+M9 ACE	M9	S,L	0.4	7.5	-	-	0.1	0.1	10	-	-
+M9 BEN	M9	S,L	0.4	7.5	-	-	0.1	0.1	-	10	-
+M9 ACR	M9	S,L	0.4	7.5	-	-	0.1	0.1	-	-	10
M9 ACE	M9	S,L	-	7.5	-	-	0.1	0.1	10	-	-
M9 BEN	M9	S,L	-	7.5	-	-	0.1	0.1	-	10	-
M9 ACR	M9	S,L	-	7.5	-	-	0.1	0.1	-	-	10
A ACE	HAL	S,L	1	7.2	5	-	-	0.1	10	-	-
A BEN	HAL	S,L	1	7.2	5	-	-	0.1	-	10	-
A ACR	HAL	S,L	1	7.2	5	-	-	0.1	-	-	10
B ACE	HAL	S	1	7.2	10	-	-	0.1	10	-	-
B BEN	HAL	S	1	7.2	10	-	-	0.1	-	10	-
B ACR	HAL	S	1	7.2	10	-	-	0.1	-	-	10
C ACE	HAL	S	1	7.2	20	-	-	0.1	10	-	-
C BEN	HAL	S	1	7.2	20	-	-	0.1	-	10	-
C ACR	HAL	S	1	7.2	20	-	-	0.1	-	-	10
D ACE	ALK	S,L	2	10.7	-	-	0.1	0.1	10	-	-
D BEN	ALK	S,L	2	10.7	-	-	0.1	0.1	-	10	-
D ACR	ALK	S,L	2	10.7	-	-	0.1	0.1	-	-	10
E ACE	CAS	S,L	2	7.2	-	-	-	-	10	-	-
E BEN	CAS	S,L	2	7.2	-	-	-	-	-	10	-
E ACR	CAS	S,L	2	7.2	-	-	-	-	-	-	10
F ACE	CAS	S,L	2	7.2	10	-	-	-	10	-	-
F BEN	CAS	S,L	2	7.2	10	-	-	-	-	10	-
F ACR	CAS	S,L	2	7.2	10	-	-	-	-	-	10
G ACE	CAS	S	2	5.8	-	-	-	-	10	-	-
G BEN	CAS	S	2	5.8	-	-	-	-	-	10	-
G ACR	CAS	S	2	5.8	-	-	-	-	-	-	10
H ACE	CAS	S,L	2	10.7	-	1	-	-	10	-	-
H BEN	CAS	S,L	2	10.7	-	1	-	-	-	10	-
H ACR	CAS	S,L	2	10.7	-	1	-	-	-	-	10

2.2.2 Enrichment of nitrile hydrolysing bacteria

Soil samples (Table 2.3) collected during the 2006 and 2007 expeditions to Miers Dry Valley Antarctica were stored at -80°C until use for isolation trials.

Table 2.3 Description of soil samples collected from Miers Dry Valley, Antarctica.

Soil sample	Collection reference	Description of location	Date of collection
1	Bag B-MVG SUSTR 3	open soil	2006
2	Bag C –MVH 0625.1	hypolith	2006
3	DUC for SA – MV06 25.1 UIXC	open soil	2006
A	MVH3-8	hypolith	2007
B	MVH3-9	hypolith	2007
C	MVH3-10	hypolith	2007
D	MVH3-11	hypolith	2007

Enrichment of nitrile hydrolysing bacteria from the soil samples (Table 2.3) was performed as follows. Approximately 1 g of soil sample was resuspended in 10 mL of liquid medium or sterile H₂O and was mixed at 100 rpm for 30 min to 1 hr at 4°C. The soil particles within the resuspension were settled using brief centrifugation and 100 µL of the particle free resuspension was used to inoculate 5 mL of liquid media or plated onto solid media. Duplicates of inoculated solid media were prepared and incubated at 4 and 18-22°C. Inoculated liquid media were only incubated at 18-22°C with 100 rpm shaking. Inoculated media were monitored on a daily basis until growth was observed. Colonies formed on solid media were picked and re-streaked onto fresh plates. For growth in liquid media, dilutions were prepared and spread-plated onto the solid media of the same composition and incubated until colonies were observed.

Pure colonies were finally streaked on two types of nutrient rich media. In the case of colonies isolated from M9 and +M9 (-ACE, -BEN, -ACR) media, these colonies were streaked onto nutrient agar (NA) plates. For colonies isolated from A, B, C, D, E, F, G, and H, both NA and solid plates of similar composition

containing 0.1% yeast extract were used. Dense cultures of each isolate were prepared in liquid nutrient rich media for genomic DNA extraction and preparation of stocks containing 50% glycerol (w/v) for long-term storage at -80°C.

2.2.3 Genomic DNA extraction

Genomic DNA extraction was adapted from Zhou *et al.*, (1996). Cells from 5 mL of bacterial culture were harvested by centrifugation and resuspended with 675 µL of extraction buffer (1% CTAB, 100 mM Tris-HCl (pH 8.0), 100 mM NaH₂PO₄, 100 mM EDTA, 1.5 M NaCl, 0.1 mg/mL Protease K). The cell resuspension was incubated at 37°C with shaking for 30 min. 75 µL of 20% SDS was added to the mixture and further incubated at 65°C for 2 hrs. The mixtures were centrifuged at 16 000 × g and an equal volume of phenol:chloroform:isoamyl (25:24:1) was mixed with the supernatants. This mixture was centrifuged at 16 000 × g and an equal volume of chloroform was mixed with the upper aqueous phase and centrifuged. The extractions with chloroform were repeated with subsequent centrifugation until the extraction was clear. The DNA was finally precipitated with 0.6 vol of isopropanol by overnight incubation at 25°C. The pellets were collected by centrifugation at 16 000 × g for 30 min and washed twice with 70% ethanol, dried and resuspended in 50 µL of sterile H₂O. The concentration of gDNA was estimated using the Nanodrop 1000 (Thermo Scientific) or the Qubit™ Quantitation System (Invitrogen) and the purity of DNA was evaluated by separation on a 0.7% agarose gel containing 0.5 µg/mL of ethidium bromide and visualised using the Alphamager HP (Alpha Innotech) gel imaging system.

2.2.4 16S rRNA gene identification

The DNA template used for PCR was either a 1/10 or 1/100 dilution of genomic DNA prepared as described in Section 2.2.3 or a single colony of a pure isolate resuspended in 10 µL of sterile H₂O. 1 µL was used as the template DNA for PCR. The final concentrations of reagents used in the PCR were as follows: 1 ×

PCR buffer (10 mM KCl, 20 mM Tris-HCl (pH 8.8), 0.1% Triton X-100, 2 mM MgCl₂, and 10 mM (NH₄)₂SO₄, 0.2 mM of each dNTP, 25 pmol of each primer E9F (5'-GAG TTT GAT CCT GGC TCA-3') (Farrelly *et al.*, 1995) and U151OR (5'-GGT TAC CTT GTT ACG T -3') (Reysenbach & Pace, 1995) and 1 U of Taq DNA polymerase (Southern Cross Biotechnology). The PCR thermal cycling programme used was as follows: initial denaturation at 95°C for 5 min, 30 cycles of amplification consisting of denaturation at 95°C for 30 s, primer annealing at 55°C for 30 s and extension at 72°C for 1 min 30 s followed by a final extension step at 72°C for 10 min. The PCR was carried out using an Applied Biosystems thermocycler Gene Amp® 2700. PCR amplicons were analysed by separation on a 0.7% agarose gel containing 0.5 µg/mL of ethidium bromide and visualised using Alphamager HP (Alpha Innotech) gel imaging system.

For Amplified rDNA Restriction Analysis (ARDRA), approximately 5 µL of PCR of each was used. Three DNA digests using the tetranucleotide-specific restriction endonucleases, *Alu* I, *Rsa* I, and *Hae* III (Fermentas) were used, as follows: 5 µL of PCR product, 2.5 U of restriction enzyme, 2 µL restriction enzyme specific buffer in a total volume of 20 µL. After incubation at 37°C for 2 hrs, digests were analysed by separation on a 3% agarose gel. The separation pattern of bands was compared to a prepared library of 16S rRNA ARDRA of strains isolated from Antarctica.

Selected 16S rRNA amplicons were cloned using either InstAclone™ PCR cloning kits (Fermentas) or CloneJET™ PCR cloning kits (Fermentas) according to the manufacturers' instructions. Sequencing was done at the University of Stellenbosch Central DNA sequencing facility or at the University of Cape Town sequencing Facility. Sequencing primers used for the pTZ57R/T cloning vector (Fermentas) are M13F (5' – CGC CAG GGT TTT CCC AGT CAC GAC – 3') and M13R (5' – GAG CGG ATA ACA ATT TCA CAC AGG – 3'). Sequencing primers for the pJET vector of the CloneJET™ PCR cloning Kit (Fermentas) were provided with the kit.

16S rRNA sequences were compared to those stored in the NCBI (www.ncbi.nlm.nih.gov) database using the basic local alignment search tool

(BLAST) algorithm (Altschul *et al.*, 1990, Altschul *et al.*, 1997, Morgulis *et al.*, 2008).

2.2.5 Preliminary determination of cardinal growth temperatures

Isolates were streaked out on solid nutrient rich media and growth was monitored at the following temperatures: 4, 15, 20, 30 and 37°C.

2.2.6 Screening of isolates for nitrile and amide hydrolysis

Cell pellets were obtained from 10 mL confluent cultures prepared in nutrient rich media containing selected nitriles. Cell pellets were washed twice with sterile H₂O, resuspended in 1 mL of 50 mM KH₂PO₄/K₂HPO₄ (pH 7.6) and lysed using sonication on ice for a total period of 1 min with cycles of 2 sec bursts followed by 2 sec pauses. Sonicates were clarified by centrifugation at 12000 rpm for 5 min at 4°C and the supernatant was used for activity assays. A standard reaction mixture (100 µl) contained 50 mM KH₂PO₄/K₂HPO₄ (pH 7.6), 50 µl supernatant and substrates (acetonitrile, benzonitrile, acrylonitrile, acetamide, benzamide, acrylamide) at 10 and 25 mM final concentration. Assays were carried out at 25°C overnight in 96 well plates. To determine ammonia concentration, the reaction mixture was terminated by the addition of 3.5 vols of reagent A (0.59 M phenol, 1 mM sodium nitroprusside), followed by the addition of equal volumes of reagent B (2.0 M sodium hydroxide, 0.11 M sodium hypochlorite). Substrate-free controls were included. Purified preparations of NHase and amidase of *G. pallidus* recombinantly expressed from pNH14K and pN322 (Cameron, 2003)(Appendix D), respectively, in *E. coli* BL21 (DE3) pLysS (Appendix C) were used as positive controls.

2.2.7 Brief characterisation of *Nesterenkonia* AN1

Phenotypical tests for comparison with other strains of the *Nesterenkonia* genus were carried out using the API 20E system (bioMérieux) according to the manufacturer's instructions.

Nutrient rich H medium (pH 10.7) (Table 2.2) with 0.01% tryptone was used to determine the effect of temperature on the growth of *Nesterenkonia* AN1. A confluent culture of *Nesterenkonia* AN1 was used to inoculate flasks containing 1/5 vol of nutrient rich H medium to a final OD₆₀₀ of 0.1. Incubation was carried out at 16, 21, 25 and 30°C with shaking at 150 rpm. To determine the effect of pH on the growth of *Nesterenkonia* AN1, the ratios of NaHCO₃ and Na₂CO₃ (500 mM final concentration) in nutrient rich H media (Table 2.2) were altered to give a pH of 7, 8.5, 9, 9.5, 10 and 10.8. The medium was supplemented with NaCl to maintain the total Na⁺ content at 500 mM. Incubation was carried out at the optimal temperature determined above, with shaking. The effect of salinity on the growth of *Nesterenkonia* AN1 was determined at 5, 7.5, 10, 12.5, 15 and 20% w/v NaCl. Growth of *Nesterenkonia* AN1 under the different culture conditions was carried out in triplicate and was monitored spectrophotometrically at OD_{600nm}. The growth rate μ was calculated by using the following formulae; $\mu = (\ln OD_2 - \ln OD_1) / (t_2 - t_1)$. OD₁ and OD₂ represent the natural log of the OD_{600nm} reading of the cultures at the start and the end of exponential growth, respectively. t_1 and t_2 represent the time in days at the start and the end of exponential growth, respectively.

2.3 Results

2.3.1 Isolation of nitrile hydrolysing bacteria from soil samples

Table 2.4 and 2.5 shows the preliminary identification of bacterial isolates using the PCR amplification of 16S rRNA genes with universal bacteria primers E9F (Farrelly *et al.*, 1995) and U151OR (Reysenbach & Pace, 1995) (Section 2.2.4). The top two species retrieved from BLAST analysis that shared more than 99% 16S rRNA sequence identity with the isolate are shown (Table 2.4 and 2.5).

Table 2.4 16S rRNA identification of isolates obtained from NFMM containing nitrile as the sole nitrogen and/or carbon source for growth. Abbreviations: Loc, reference of soil sample (see Table 2.3); Isol (bp) length of the 16S rRNA sequence of isolate obtained.

Isolate	Loc	NFMM + nitrile	Isol (bp)	Related 16S rRNA sequences (length of sequence (bp))	Accession number
49.8	3	+M9 ACE	1487	<i>Arthrobacter</i> sp. AN16	AJ551154
3.1	1	+M9 ACR	1486	(1485 bp)	
33.3	1	+M9 ACR	1485	<i>Arthrobacter</i> sp. Nj-37	AM491456
32.2	1	+M9 BEN	1485	(1487 bp)	
50.7	3	+M9 BEN	1485		
51.1	3	+M9 ACR	1471		
43.2	3	M9 ACE	1488		
			1475		
49.6	3	+M9 ACE	1501	<i>Psychrobacter fozii</i>	AY771717
52.4	3	M9 ACE	1500	(1504 bp)	
				<i>Psychrobacter cryohalolentis</i> K5	CP000323
				(1586 bp)	
49.1	3	+M9 ACE	1478	<i>R. erythropolis</i> strain HS8	AY168586
52.5	3	M9 ACE	1478	(1534 bp)	
				<i>Rhodococcus</i> sp. AN6	AJ551145
				(1622 bp)	

Three isolates, 43.2, 52.4 and 52.5, that shared significant 16S rRNA sequence conservation with *Arthrobacter* AN16, *Psychrobacter fozii* and *R. erythropolis*, respectively, utilised acetonitrile as the sole nitrogen and carbon source for growth (Table 2.4). *Arthrobacter* AN16 was also isolated from NFMM supplemented with acrylonitrile and benzonitrile as the sole nitrogen source (Table 2.4). Isolates that shared significant 16S rRNA gene sequence conservation with *Psychrobacter fozii* also shared 99% sequence identity with *Psychrobacter cryohalolentis* K5 (Genome accession: NC 007969).

Table 2.5 shows isolates identified from other types of NFMM (see Table 2.2). Several *Arthrobacter* AN16 strains were isolated from NFMM-E (pH 7.2), containing acetonitrile as the sole nitrogen source (Table 2.5). Another strain of *Arthrobacter*, *Arthrobacter* Tibet-IX22 was isolated at 4 and 18°C on similar media plates (Table 2.5). Isolates identified as *Kocuria* 29Y1zhy, *Pseudomonas* LaGso27g and *Microbacterium* VKM were also isolated from similar plates (Table 2.5). The following isolates, D1C, D1B, H1D and H1B2, which shared 16S rRNA gene sequence conservation with *Nesterenkonia* YIM 90713 (*Nesterenkonia* AN1) were isolated from two types of NFMM, D and H (pH 10.5), containing acetonitrile as the sole nitrogen source.

No growth was observed on NFMM (pH 5.8) and plates supplemented with 20% NaCl, acrylonitrile or benzonitrile.

Table 2.5 16S rRNA identification of isolates obtained from alternative types of NFMM supplemented with nitrile as the sole nitrogen source for growth.

Isol	Loc	NFMM + nitrile	°C	Isol (bp)	Related 16S rRNA sequences (length of sequence (bp))	Accession number
D1C	C	D ACE	18	<i>c</i> ¹	<i>Nesterenkonia</i> sp YIM 90713	EF151505
D1B	B	D ACE	18	<i>c</i> ¹	(1509 bp)	AJ717365
H1D	D	H ACE	18	<i>c</i> ¹		
H1B2	B	H ACE	18	1496	<i>Nesterenkonia</i> sp AC84 (1500 bp)	
4E1C2	C	E ACE	4	<i>c</i> ¹	<i>Arthrobacter</i> sp. Tibet-IX22	DQ177488
E1C1	C	E ACE	18	1485	(1503 bp)	EF093123
F1D	D	F ACE	18	<i>c</i> ¹	<i>Arthrobacter</i> sp. VTT E-052904 (1522 bp)	
E1D1	D	E ACE	18	<i>c</i> ¹	<i>Arthrobacter</i> sp. AN16	AJ551154
E1B3	B	E ACE	18	<i>c</i> ¹	(1485 bp)	
E1B2	B	E ACE	18	1498	<i>Arthrobacter</i> sp. Nj-37 (1487 bp)	AM491456
E1A1	A	E ACE	18	1488	<i>Kocuria</i> sp. 29Y1zhy (1487 bp) <i>Kocuria rosea</i> (1487 bp)	AM418390 DQ060382
4E1B1	B	E ACE	4	1501	<i>Pseudomonas</i> sp. LaGso27g (1528 bp) <i>Pseudomonas</i> sp. VTT E-052911 (1523 bp)	EU934227 DQ465010
E1B2	B	E ACE	18	1489	<i>Microbacterium</i> sp. VKM Ac-1808	AB042075
E1D1	B	E ACE	18	<i>c</i> ¹	(1507 bp) <i>Microbacterium</i> sp. BBCT30 (1483 bp)	DQ337545

*c*¹ – 16S rRNA identity confirmed through ARDRA

2.3.2 Screening of isolates for activity on nitriles and amides

The ammonia assay was used to confirm the presence of nitrile hydrolysing activity in cell free extracts. Figure 2.1 shows the colorimetric detection of nitrile degrading activity in cell free extracts of three isolates. Only the cell free extracts of *R. erythropolis* had activity (Figure 2.1). This isolate had more activity on acrylonitrile than for acetonitrile. In addition, no activity was observed for benzonitrile and only weak activity was observed for 25 mM benzamide (Figure 2.1). As reported (Cameron, 2003), the mixture of purified *G. pallidus* NHase and amidase that were used as controls had activity on acetonitrile and acrylonitrile (Figure 2.1). No activity was observed for benzonitrile since it inhibited *G. pallidus* NHase activity (Cameron, 2003). The purified amidase was confirmed to have activity on acetamide and acrylamide as reported (Makhongela *et al.*, 2007). The amidase activity on 25 mM benzamide was unexpected. This activity could not be attributed to the background detection of amine group of the substrate since activity was not present for all wells. No background detection was observed for substrate-free controls.

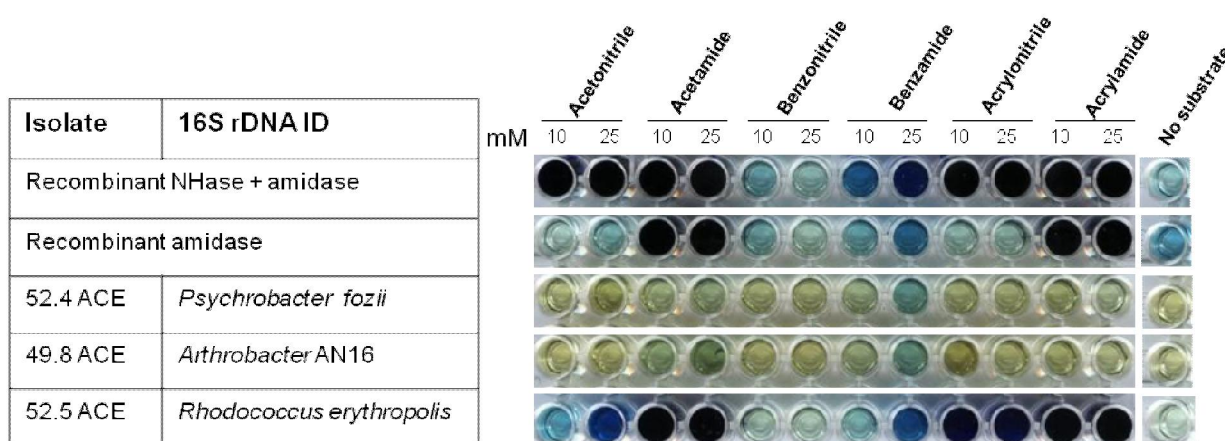
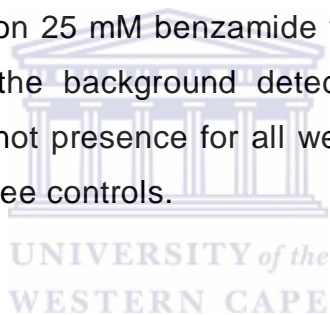


Figure 2.1 Colorimetric detection of nitrile hydrolysing activity in the cell free extracts of three isolates. A dark blue colour indicates positive nitrile/amide hydrolysing activity.

2.3.3 Preliminary determination of isolates cardinal growth temperatures

Table 2.6 shows the effect of temperature on the growth of each isolate. The cardinal growth temperatures determined for *Psychrobacter*, *Pseudomonas*, *Nesterenkonia* AN1 and the two strains of *Arthrobacter* suggested these are psychrotolerant species. These strains grew well at 20°C and had minimal or no growth at 30°C. The remaining isolates that grew well at 30°C suggested that these are either psychrotrophic with an optimal growth temperature at or above 30°C or are mesophilic strains.

Table 2.6 Effects of temperature on growth of isolates. X and XX refer to slow and rapid growth, respectively.

Isolate reference	16S rRNA identification	Temperature (°C)				
		4	15	20	30	37
49.8 ACE	<i>Arthrobacter</i> AN16		X	XX		
E1C1	<i>Arthrobacter</i> Tibet-IX22		X	XX	X	
4E1B1	<i>Pseudomonas</i> LaGso27g		X	XX	X	
E1A1	<i>Kocuria</i> 29Y1zhy		X	X	XX	XX
E1B2	<i>Microbacterium</i> VKM Ac-1808		X	X	XX	
H1B2	<i>Nesterenkonia</i> AN1		X	XX	X	
52.4 ACE	<i>Psychrobacter</i> <i>fozii</i>		X	XX	X	
52.5 ACE	<i>R. erythropolis</i>		X	XX	XX	

2.3.4 Utilisation of nitrile(s) as sole nitrogen and/or carbon source for growth

None of the isolates grew on NFMM supplemented with glycerol but not nitrile (Table 2.7), which confirmed that no exogenous nitrogen source was present. All the isolates other than *Pseudomonas* utilised acetonitrile as the sole nitrogen and carbon source for growth (Table 2.7). *Nesterenkonia* AN1 grew slowly on NFMM-H containing acetonitrile. All the isolates grew well on plates containing acetonitrile and glycerol (Table 2.7).

Table 2.7 Utilisation of acetonitrile as the sole nitrogen and/or carbon source for growth.

Isolate reference	16S rRNA identification	NFMM	Glycerol only	Nitrile only	Nitrile and glycerol
52.5	<i>R. erythropolis</i>	M9	-	XX	XX
52.4	<i>Psychrobacter fozii</i>	M9	-	XX	XX
4E1B1	<i>Pseudomonas</i> LaGso27g	E	-	-	XX
49.8	<i>Arthrobacter</i> AN16	M9	-	XX	XX
H1B2	<i>Nesterenkonia</i> AN1	H	-	X	XX

Figure 2.2 shows the growth profiles of isolates in medium containing different nitriles as the sole nitrogen source for growth. *R. erythropolis* was capable of utilising acetonitrile and benzonitrile as the sole nitrogen source for growth. In addition, the slow growth on acrylonitrile suggested this is a poorly utilised substrate. *Psychrobacter* and *Arthrobacter* AN16 utilised acetonitrile and had slow growth on benzonitrile as the sole nitrogen source (Figure 2.2).

Nesterenkonia AN1 was observed to form clumps in alkaline NFMM-H in the presence of nitriles and in medium supplemented with a non-nitrile nitrogen source, NH₄Cl. However in NFMM supplemented with acetonitrile, AN1 clump of cells increased in size with time. In addition, there was an increase in culture turbidity of AN1 cells in the presence of an additional nitrile, 3-cyanopyridine. AN1 did not grow in NFMM supplemented with benzonitrile and acrylonitrile. None of the isolates grew in NFMM lacking nitriles.

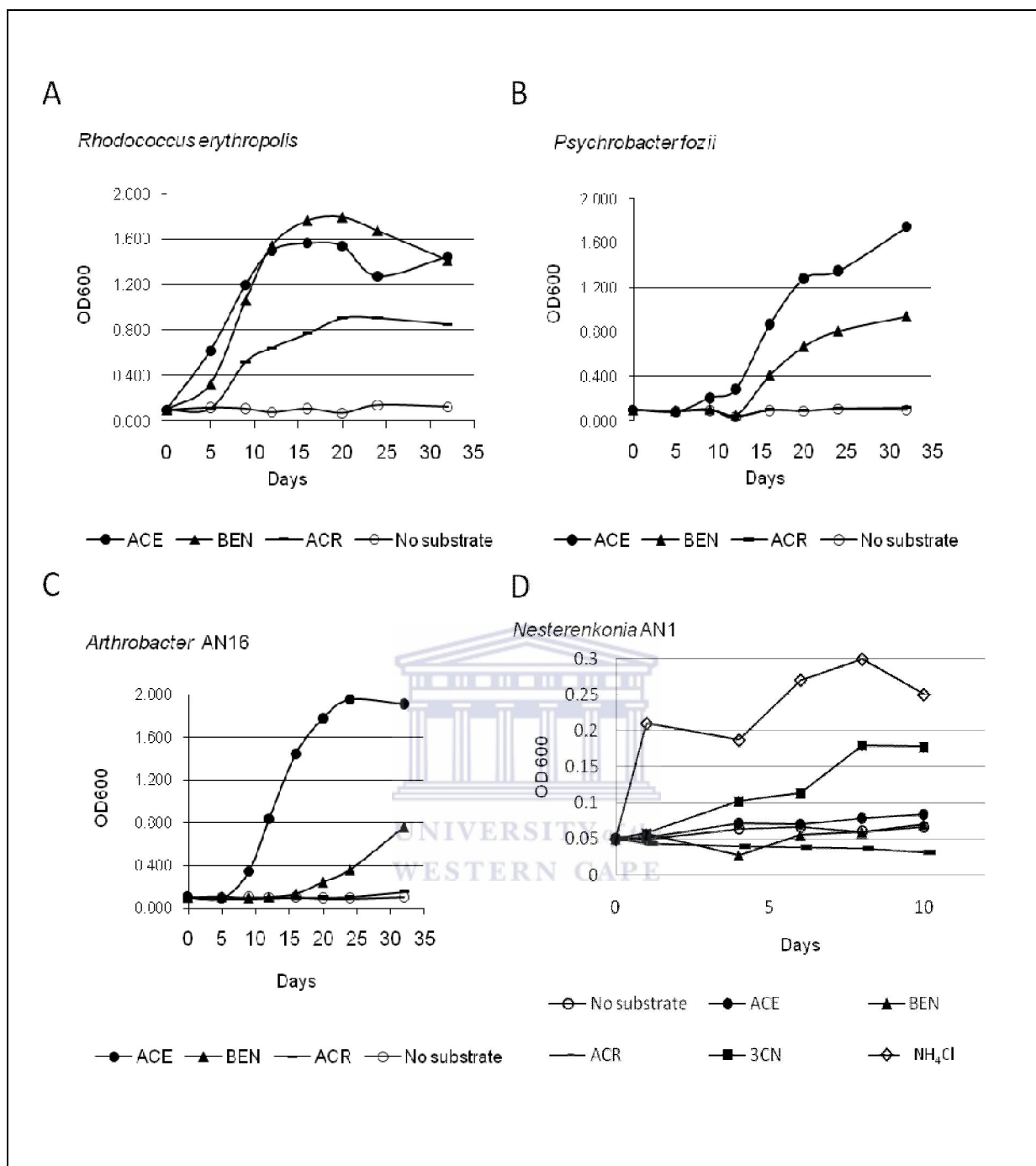


Figure 2.2 Utilisation of different nitriles as the sole source of nitrogen for growth. Abbreviations: ACE, acetonitrile; BEN, benzonitrile, ACR, acrylonitrile; 3CN, 3-cyanopyridine.

2.3.5 Effect of temperature, pH and salinity on the growth of *Nesterenkonia* AN1

The effects of temperature, pH and salinity on the growth of *Nesterenkonia* AN1 are shown in Figure 2.3. AN1 had the fastest growth rate (μ) at approximately 21°C, decreasing slightly at 15 and 25°C (Figure 2.3, panel A). Above 25°C, the growth rate decreased significantly. The growth temperature profile of AN1 suggested it is a psychrotolerant strain. Since strains of *Nesterenkonia* genera are typically halotolerant alkaliphiles, the effects of pH and salinity on the growth rate of the isolate were also determined. AN1 had an optimal growth rate at pH 9.6 (Figure 2.3, panel B) and with a very narrow pH range (pH 9 and 10), indicating that the strain is an obligate alkaliphile. AN1 was also moderately halotolerant, since it was capable of growth in media containing 15% Na⁺ (w/v). No growth was detected at 20% Na⁺ (w/v) (Figure 2.3, panel C).

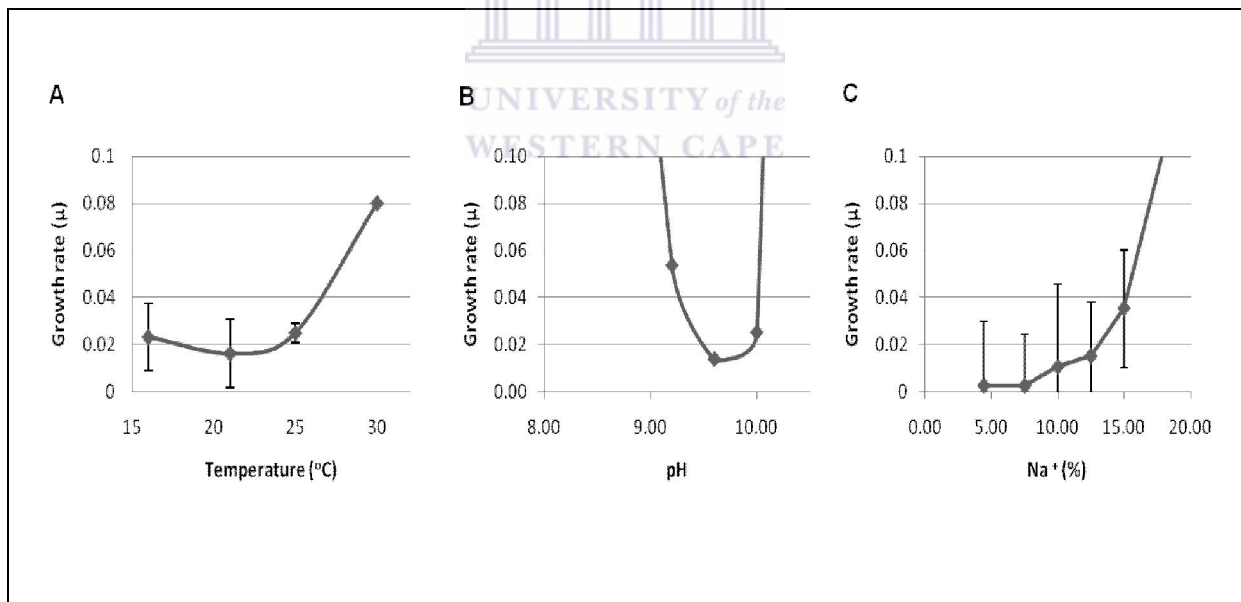


Figure 2.3 Effect of temperature, pH and salinity on the growth rate (μ) of the *Nesterenkonia* AN1.

2.3.6 Comparison of AN1 with known *Nesterenkonia* strains

Table 2.8 shows the phenotypic properties of AN1 for comparison with related strains of the *Nesterenkonia* genera.

Nesterenkonia lacusekhoensis (Collins *et al.*, 2002), which was isolated from hypersaline Ekho Lake, East Antarctica, differed phenotypically from AN1: with short rods and bright yellow colony pigmentation; *c.f.* coccoid morphology and red pigmented colonies (Table 2.8). Unlike published strains, AN1 had a narrow growth pH range and did not grow near neutrality. In addition, AN1 had the lowest optimal temperature of all *Nesterenkonia* strains. AN1 shared similar tolerance to Na⁺ with that of *Nesterenkonia lacusekhoensis*.

AN1 utilised glycerol, D-arabinose and D-glucose for growth. It had weak acid production from mannitol. It did not hydrolyse gelatine and was negative for the citrate test. It had a positive reaction for the Voges-Proskauer reaction.

Figure 2.4 shows the phylogenetic position and 16S rRNA sequence identities of AN1 with known *Nesterenkonia* strains. AN1 did not share significant 16S rRNA sequence identity with *Nesterenkonia lacusekhoensis* at 96% (Figure 2.4). It shared 99% 16S rRNA sequence identities with three coccoid strains of the *Nesterenkonia* genus: strains *halotolerans*, *sandarika*, and *jeotgali*. However, the latter strains differ phenotypically from AN1, in colony pigmentation, optimal growth temperatures, and pH range of growth (Table 2.8). The data suggested that 16S rRNA sequence identities are not a good indicator of relatedness for members of the *Nesterenkonia* genera.

Table 2.8 Comparison of phenotypic characteristics of AN1 with known strains of the genus *Nesterenkonia*. Abbreviations: ND, not determined; w, weak reaction; +, positive reaction; -, negative reaction. Table was adapted from Luo *et al.*, (2008).

Strains (Accession number)	<i>N. flava</i> (EF680886)	<i>N. aethiopica</i> (AY574575)	<i>N. xinjiangensis</i> (AY226510)	<i>N. lacusekhoensis</i> (AJ290397)	<i>N. halobia</i> (X80747)	<i>N. lutea</i> (AY588278)	<i>N. halotolerans</i> (AY226508)	<i>N. sandarakina</i> , (AY588277)	<i>N. jeotgali</i> , (AY928901)	AN1
Characteristics										
Morphology	Short rods	Short rods	Short rods	Short rods	Cocci	Cocci	Cocci	Cocci	Cocci	Cocci
Colony pigmentation	Yellow w	Yellow	Light yellow	Bright Yellow	Colourless	Light yellow	Orange-yellow	Orange-yellow	Light yellow	Red-orange
Optimal temperature	40-42	30-37	28	27-33.5	30	28	28	28	25-30	21
pH tolerance	8-12	7-11	7-12	7.5-9.5	<6-10	6.5-10	7-9	5-12	6-8.5	9-10
NaCl tolerance (%)	0-10	3-12	0-25	0-15	5-23	0-20	0-25	1-16	0-16	4-15
Citrate test	-	-	ND	W	-	ND	ND	ND	ND	-
Voges-Proskauer reaction	-	ND	ND	W	+	-	+	-	+	+
Hydrolysis of gelatin	+	+	+	-	-	-	+	+	-	-
Utilisation of										
D-glucose	+	ND	+	+	ND	w	+	+	+	+
L-arabinose	+	+	+	ND	+	w	-	w	+	+
Glycerol	ND	+	ND	W	-	w	-	ND	ND	+
Acid production from										
Mannitol	-	-	-	-	+	+	-	+	+	w

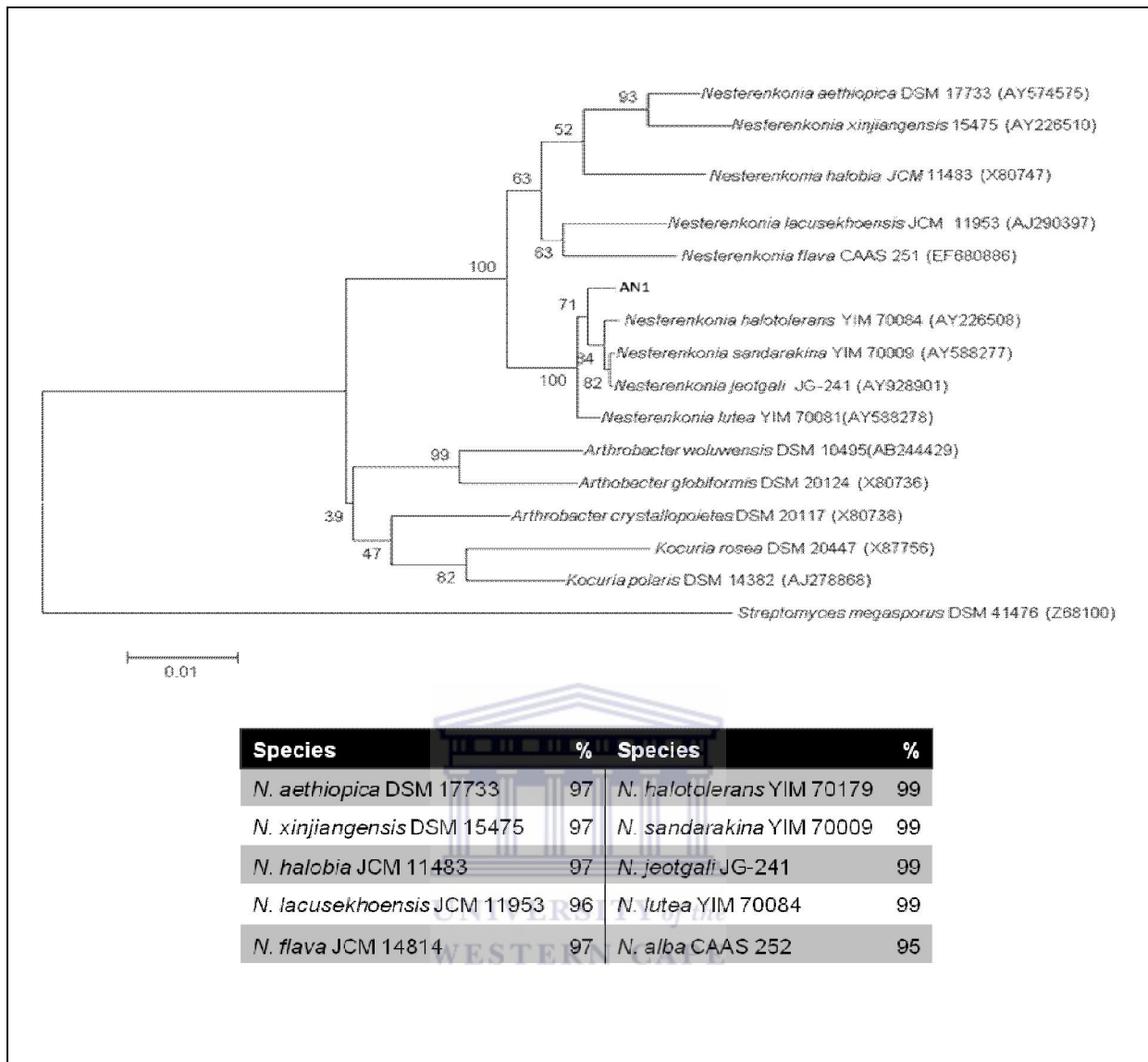


Figure 2.4 Neighbour-joining phylogenetic dendrogram and 16S rRNA percentage identities showing relationship of AN1 with known *Nesterenkonia* strains. Five other strains of the bacterial family *Micrococcaceae* are included. Bootstrap percentages (based on 1000 replications) are shown at branch points. The 16S rRNA sequence of *Streptomyces megasporus* DSM 41476T was used as the root. Bar represents 1% sequence divergence. Dendrogram parameters were reproduced from Lou *et al.*, (2008) using Mega 4 (Tamura *et al.*, 2007).

2.4 Discussion

The majority of nitrile hydrolysing strains was isolated on NFMM containing acetonitrile as the sole nitrogen and/or carbon source. This confirmed the observation of Brandao *et al.*, (2002) where the soluble nitrile yielded the most isolates. Benzonitrile and acrylonitrile were suggested to be poorly transported into bacteria cells, possibly due to their bulkiness and hydrophobicity (Brandao *et al.*, 2002). Only *Psychrobacter*, *Arthrobacter* AN16 and *R. erythropolis* had the fastest growth in the presence of acetonitrile. *R. erythropolis* was the only strain that utilised acrylonitrile. However, the nitrile hydrolysing activity detected in the cell free extracts of *R. erythropolis* showed higher activity on acrylonitrile than for acetonitrile. Whole cells might have slowed down the transport of acrylonitrile into the cytoplasm.

The ammonia assay was used to screen cell free extracts for nitrile- and amide degrading activity. Positive results were only obtained for strains related to *R. erythropolis* (data not shown). Strains of *R. erythropolis* are known to constitutively express their NHases and coupled amidases (Brandao *et al.*, 2002). This suggested that the nitrile hydrolysing activities of other isolates were probably not induced. Since the isolates were prepared from nutrient rich media containing nitriles for the activity assay, the high nitrogen background might have inhibited induction of nitrile hydrolysing activities. Although most bacteria are known to express amidases, no activities on amides were detected for the isolates. The amidases might have either been thermally deactivated by sonication or removed as membrane bound proteins during the preparation of cell free extracts.

No nitrile hydrolysing activity has previously been reported for members of the *Nesterenkonia*, *Kocuria* and *Psychrobacter* genera. The *Nesterenkonia*, *Kocuria*, and *Arthrobacter* genera share the same Order *Actinomycetales* with the *Rhodococcus* and *Microbacterium* genera. Numerous nitrile hydrolysing species have been identified within this bacterial order. However, the *Kocuria* strain was eliminated from future work since determination of its cardinal growth temperatures suggested that it was either a mesophile or a psychrotroph with a

high maximal growth temperature. *Psychrobacter* isolate shared 99% 16S rRNA sequence conservation with *Psychrobacter cryohalolentis* K5 (Genome accession: NC_007969). The two putative nitrilase genes found in the sequenced genome are described briefly in Chapter 3.

Nesterenkonia AN1 utilised acetonitrile on solid media and 3-cyanopyridine in liquid medium as the sole nitrogen source for growth. Other *Nesterenkonia* strains were reported to require nicotinic acid in the media for stimulation of growth (Collins *et al.*, 2002). This carboxylic acid is a product of the hydrolysis of 3-cyanopyridine.

Although *Nesterenkonia* AN1 shared significant 16S rRNA sequence identities with known strains of its genus, it is the only psychrotolerant strain that grew optimally at approximately 21°C. *Nesterenkonia* AN1, similar to known strains of its genus, has alkaliphilic and halotolerant growth properties. Alkaliphiles generally grow at pH values greater than 8 (Horikoshi, 1999) and halotolerant species can grow rapidly in media containing NaCl up to 15% (w/v) (Kushner, 1978). *Nesterenkonia* AN1 was phenotypically different and did not share significant 16S rRNA sequence identity with *Nesterenkonia lacusekhoensis* (Collins *et al.*, 2002), which was also isolated from Antarctica.

This is the first report of a novel nitrile hydrolysing psychrotolerant, halotolerant alkaliphilic *Nesterenkonia* strain.

Chapter 3: Gene mining and *in silico* protein characterisation of nitrile hydrolysing enzymes

3.1 Introduction	60
(i) PCR Screening	60
(ii) Library/expression screening.....	61
(iii) <i>In silico</i> gene mining.....	62
3.2 Materials and Methods.....	63
3.2.1 Design of degenerate NHase primers.....	63
3.2.2 Screening systems	64
Aminoacetonitrile screening sytem.....	64
Pyrazinecarbonitrile screening system.....	65
3-Cyanopyridine screening system	65
3.2.3 Preparation of genomic DNA library using pJET cloning vector	66
3.2.4 Screening of <i>E. coli</i> clones for nitrile hydrolysis	67
3.2.5 Genome sequencing and <i>in silico</i> gene mining	67
3.2.6 Homology modelling	68
3.3 Results.....	69
3.3.1 PCR screening of isolates for NHases.....	69
3.3.2 Development of functional screening systems	74
Aminoacetonitrile screening system	74
Pyrazinecarbonitrile screening system.....	74
3-Cyanopyridine screening system.....	75
3.3.3 <i>In silico</i> gene mining of the <i>Nesterenkonia</i> AN1 genome	76
3.3.4 Genetic maps of Nit1, Nit2 and neighbouring ORFs.....	76
3.3.5 Analysis of Nit1 and Nit2 protein sequences – sequence conservation	80

3.3.6 Alignment of Nit1 and Nit2 protein sequences with characterised members of nitrilase superfamily	82
3.3.7 Assignment of Nit1 and Nit2 to a branch of the nitrilase superfamily	84
3.3.8 Comparison of Nit1 and Nit2 homology models with known structures of the nitrilase superfamily	86
3.3.9 Description of Nit1 and Nit2 homology models.....	89
3.4 Discussion.....	93
3.4.1 Screening for nitrile hydrolysing gene(s).....	93
(i) Molecular screening of isolates for NHases	93
(ii) Genomic library screening systems	94
3.4.2 Putative nitrilases of <i>Nesterenkonia</i> AN1	95

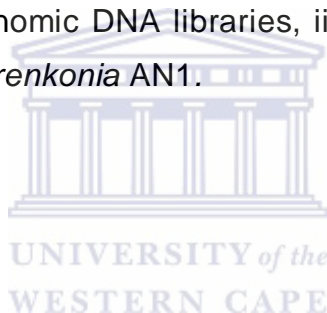


3.1 Introduction

The previous chapter described the isolation of four bacterial strains: *Arthrobacter* AN16, *Psychrobacter fozii*, *Pseudomonas* and *Nesterenkonia* AN1. These species were isolated solely for their ability to thrive on media containing nitrile as the sole nitrogen and/or carbon source for growth, which suggested the presence of nitrile-hydrolysing activity. In addition, these isolates had optimal growth at low temperatures. The purpose of the work presented in this chapter was to screen for nitrile hydrolysing gene(s) from these isolates and to characterise the function of the deduced protein sequence(s).

Several approaches were undertaken to screen the isolates for nitrile hydrolysing gene(s): i) PCR based screening of extracted genomic DNA using degenerate primers, ii) screening the genomic DNA libraries, iii) *in silico* gene mining of the sequenced genome of *Nesterenkonia* AN1.

(i) PCR Screening



PCR based screening has been reported for NHases where a consensus sequence generated from alignments of protein sequences of the highly conserved α -subunit was used for primer design (Brandao *et al.*, 2003, Liebeton & Eck, 2004, Lourenco *et al.*, 2004, Precigou *et al.*, 2001). In several cases, screening for novel NHases by PCR has induced a bias towards known NHase producing clades (Precigou *et al.*, 2001). Cloning by PCR is known to be limited, since prior knowledge of the sequence is usually based on analogous genes of previously isolated organisms. However, due to numerous metagenomic studies, a large input of protein sequences into databases has arisen and this has led to a significant increase in diversity in enzyme families (Ferrer *et al.*, 2009, Handelsman, 2004). The continued input of novel NHase sequences in such databases provides a different template for the design of unbiased degenerate primers. The use of inosine within primers and a touchdown PCR method could be used to account for two potential problems usually associated with

degenerate primers; degeneracy and target specificity, respectively. Substitution of this nucleotide analogue within degenerate primers would increase the concentration of distinct primer sequences (Martin *et al.*, 1985, Ohtsuka *et al.*, 1985, Xuan & Weber, 1992, Zheng *et al.*, 2008a). Touchdown PCR employs an initial annealing temperature above the projected melting temperature of the primer pair, then progressively transitions to a lower, more permissive annealing temperature over the course of successive cycles (Korbie & Mattick, 2008). Touchdown PCR has routinely been used to increase the specificity of primers for its target sequence.

(ii) Library/expression screening

A screening system could be used to mine a genomic DNA library of an isolate prepared in *E. coli*. Clones that are positive for the desired trait are identified through screening assays based on target functionality (Ferrer *et al.*, 2009, Handelsman, 2004, Schmeisser *et al.*, 2007). Three potential screening systems are described for the screening of the genomic DNA for functional nitrile hydrolysing genes. Two variations of complementation screening methods were developed where the growth of the screening host organism is dependent on the hydrolysis of two types of nitriles, aminoacetonitrile and 3-cyanopyridine (nicotinonitrile). Nitrile hydrolysis of aminoacetonitrile releases glycine that would complement the growth of a glycine auxotrophic *E. coli* strain. The other complementation screening system was based on the fact that amidase activity found in *E. coli* strains utilises nicotinamide as a sole nitrogen source for growth (Frothingham *et al.*, 1996). If one of the library clones expresses a functional NHase that hydrolysed 3-cyanopyridine, nicotinamide produced would be utilised by *E. coli*. The third screening assay is an adaptation of colourimetric assay for identification of mycobacteria that relies on the hydrolysis of pyrazinamide to pyrazinoic acid (Wayne, 1974). Pyrazinoic acid is detected by the formation of a red-coloured complex with ferrous ammonium sulphate. The same enzyme that hydrolyses nicotinamide has been reported to have activity on pyrazinamide in *E. coli* strains (Frothingham *et al.*, 1996). In this case, pyrazinecarbonitrile is used

as the substrate for screening genomic DNA libraries where positive clones may be detected rapidly by colourimetric detection.

(iii) *In silico* gene mining

The genome of *Nesterenkonia* AN1 was sequenced in the final year of this project using the Illumina DNA sequencing technology at the University of the Western Cape. This provided the opportunity for *in silico* gene mining for nitrile hydrolysing genes.

The PDB database (www.rcsb.org) contains over 20 crystal structures for the NHases and 10 crystal structures for members of the nitrilase superfamily. Computational methods using these structures as templates could be used to infer function and monomer fold for target protein sequences. Homology modelling is useful in the studies of uncharacterised members of the nitrilase superfamily, since these proteins shares low sequence conservation, but are highly conserved structurally. For example, the protein sequence of NitPf5 nitrilase from *Pseudomonas* Pf-5 (Kim *et al.*, 2009) was modelled using the nitrilase structure 1j31 as the template. The substrate specificity of the Nase was determined from analysis of its homology model (Kim *et al.*, 2009). A comparison of homology models with atomic structures has the potential to outline regions involved in intersubunit interactions and residues lining the catalytic site that determine substrate specificity.

3.2 Materials and Methods

General recombinant DNA techniques were carried out as described in Appendix A.

3.2.1 Design of degenerate NHase primers

The protein sequences of the α -subunits of NHases, retrieved from NCBI and EMBL (www.ebi.ac.uk/embl/), were aligned using ClustalW (Larkin *et al.*, 2007). Degenerate primers were designed using the consensus sequence of selected conserved regions. The degeneracy of the primers was reduced by the substitution of inosine (I) in positions where there was either cytosine (T) and adenine (A) (Martin *et al.*, 1985, Ohtsuka *et al.*, 1985, Xuan & Weber, 1992, Zheng *et al.*, 2008a). The Oligo Design and Analysis Tools of Integrated DNA technologies (www.idtdna.com) were used to calculate the theoretical melting temperatures and the G+C contents of the oligonucleotides. Oligonucleotides were synthesized commercially (Integrated DNA technologies). Four primers; NHg1aF, NHg1aR, NHg2aF, NHg2aR, were constructed (Table 3.1). The average size of the expected amplicon is 342 bp. Primer pairs NHFe1/2 and NHCo1/2 (Precigou *et al.*, 2001) were also used to screen the isolates for NHase genes (Table 3.1).

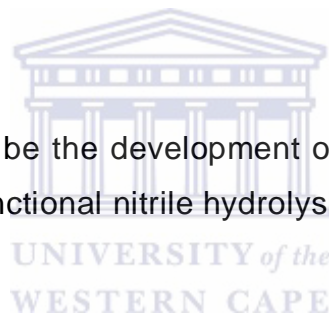
Table 3.1 Primers used for the molecular screening of NHases.

Primer	Sequence	Reference
NHg1aF	5'- TGG TCG CCA ARK CIT GGR BIG ABC C -3'	This work
NHg1aR	5'- GTI TGG GAI WSS ASI KCI GAA ATC CGC TA -3'	This work
NHg2aF	5'-TCG TBG CVC GIG CIT GGR BIG AYC C-3'	This work
NHg2aR	5'-ACC GCC GAN AIB CGC TAY GTS GTG CTG CC-3'	This work
NHFe1	5'-CCC GAC GGT TAC GTC GAG-3'	Precigou <i>et al.</i> (2001)
NHFe2	5'-CCA TGT AGC GAG TTT CGG CG-3'	Precigou <i>et al.</i> (2001)
NHCo1	5'-GTC GTG GCG AAG GCC TGG-3'	Precigou <i>et al.</i> (2001)
NHCo2	5'-GTC GCC GAT CAT CGA GTC-3'	Precigou <i>et al.</i> (2001)

The PCR reaction mixture (100 µl) contained 1 x PCR buffer (10 mM KCl, 20 mM Tris-HCl (pH 8.8), 2 mM MgCl₂, 0.1% [v/v] TritonX-100), 0.2 mM of each dNTP, 25 pmol of each primer and 1 U of Taq DNA polymerase (Southern Cross Biotechnology). PCR amplification was carried out in an Applied Biosystems thermocycler Gene Amp® 2700 thermal cycler. The optimised touchdown thermocycling conditions were: initial denaturation at 95°C for 5 min, 2 repeated 7 cycles of denaturation at 95°C for 30 secs, primer annealing at 68-62°C for 30 secs, extension at 72°C for 15 secs; then 25 cycles of denaturation at 95°C for 30 secs, primer annealing at 62°C for 30 secs, and extension at 72°C for 15 secs; followed by a final extension step at 72°C for 10 mins. Genomic DNA used for the PCR was prepared as described in Chapter 2, section 2.2.3.

3.2.2 Screening systems

The following sections describe the development of the three systems to screen genomic DNA libraries for functional nitrile hydrolysing genes.



Aminoacetonitrile screening system

Glycine auxotrophic *E. coli* strain JK84 (Parker & Fishman, 1979) (Appendix C) was used as the screening host. M63 minimal medium (Appendix B) was supplemented with 0.4% glycerol, 10 µg/ml thiamine, 0.2% arabinose, and 0.1 µM CoCl₃. In the case of *E. coli* JK84, the media was supplemented with the amino acids histidine and arginine at 50 µg/ml. Strain JK84 was maintained using 30 µg/ml of the antibiotic streptomycin in the media. Solid medium was prepared by the addition of 20% (w/v) agar. Aminoacetonitrile (10 mM) or glycine (50 µg/ml) was used for selection and as a medium control, respectively. The ORF of *Bacillus pallidus* NHase was cloned from pNH14K (Cameron *et al.*, 2005) (Appendix D) into pBAD18 (Guzman *et al.*, 1995) for expression under the control of an arabinose inducible P_{BAD} promoter. This plasmid was referred to as pAN1 (Appendix D) and was used as a control to determine the feasibility of the

aminoacetonitrile screening system. Transformed cells were harvested from an ON culture of *E. coli* JK84 or AT2681 harbouring pAN1 in LB at 37°C containing 0.2% glucose were washed twice in sterile H₂O and plated onto selective media. Cells transformed with pBAD18 were used as the negative control. Plates were incubated at room temperature until growth was visible.

Pyrazinecarbonitrile screening system

E. coli ArcticExpress (DE3) (Stratagene) (Appendix C) was used as the screening host. Gentamycin (20 µg/ml) was used to maintain the low copy plasmid (pACYC) which constitutively expresses the *Oleispira antarctica* chaperonins, Cpn10 and Cpn60 (Invitrogen). Solid and liquid LB media (Appendix B) was supplemented with 5-50 mM pyrazinecarbonitrile, 0.1 µM of CoCl₂, 0.1 µM FeCl₃ and 1 mM IPTG. Plasmid pJ1 C327 carrying the coding sequence of the *R. rhodochrous* J1 mutant J1 C327 nitrilase (Thuku *et al.*, 2007) was used to test the feasibility of the screening system. Cells harbouring the recombinant nitrilase were cultured in LB at 37°C overnight containing 30 µg/ml kanamycin and used to inoculate the screening medium. Cells containing only pET29b was used as a negative control. A modification of the test for the detection of pyrazinoic acid (Wayne, 1974) was adapted to develop the pyrazinecarbonitrile screening system. 0.1 vol of 20% FeNH₄(SO₄)₂ was added to liquid medium and for solid medium a solution of the 20% stock was poured onto the plate.

3-Cyanopyridine screening system

E. coli ArcticExpress (DE3) was used as the host. Controls were used as described above. M63 minimal medium with (NH₄)₂SO₄ omitted was supplemented with 0.1 mg/ml thiamine, 0.1 µM CoCl₃, 0.1 µM FeCl₃, 0.4% glycerol, 20% w/v ultrapure agar and 20 mM 3-cyanopyridine. Harvested cells harbouring the recombinant nitrilase, which was prepared in LB containing 30

$\mu\text{g/ml}$ kanamycin at 37°C , were washed twice in sterile H_2O and plated onto the selective medium. Plates were incubated at room temperature until growth was visible. Approximately 500 transformants were plated out per plate. In addition, approximately 50 washed transformants were used to inoculate 200 μl of M63 minimal medium containing 25 mM 3-cyanopyridine in each well of a 96 well plate.

3.2.3 Preparation of genomic DNA library using pJET cloning vector

Approximately 5 μg of *Nesterenkonia* AN1 genomic DNA was sheared in 200 μL of 100 mM Tris-HCl (pH 8.0) containing 200 μL of fine quartz sand particles. Shearing was carried out in a bead beater (Bio101 FastPrep FP120, Savant Instruments Inc. Holbrook, NY) at 4.5 m.s⁻¹ for 10 sec, followed by brief centrifugation for 5 min at 13 000 \times g. Sheared DNA was separated by gel electrophoresis on a 0.5% agarose gel containing 0.5 $\mu\text{g/ml}$ ethidium bromide. Fragments corresponding to approximately 6-14 Kbp were excised and gel purified. The sheared genomic DNA was cloned in pJET1.2/blunt following the Blunt-End Cloning Protocol according to the manufacturer's instructions of the CloneJETTM PCR cloning kit. Ligations were transformed into *E. coli* GeneHog competent cells and spread onto LB plates containing 100 $\mu\text{g/ml}$ ampicillin, 1 mM IPTG. The plates were incubated at 37°C overnight. Colonies were scraped off the plates into 1 mL of sterile H_2O . Plasmids were purified from cell pellets using the Qiagen plasmid purification kit and transformed into electrocompetent *E. coli ArcticExpress* competent cells. Transformed cells were washed twice with sterile H_2O before plating onto M63 minimal medium containing 3-cyanopyridine (25 mM). Restriction endonuclease *Bgl* II was used to excise the insert from the pJET vector.

3.2.4 Screening of *E. coli* clones for nitrile hydrolysis

Fresh overnight cultures of clones were used to inoculate 50 mL LB containing respective antibiotics, 0.1 μM CoCl_2 , 0.1 μM FeCl_3 , 1 mM IPTG. Cultures were incubated at room temperature with shaking and 10 mL samples were taken after 4 hrs, and overnight. Cell pellets of samples were harvested, washed twice with sterile H_2O and then resuspended in 1 mL of 50 mM $\text{K}_2\text{HPO}_4/\text{KH}_2\text{PO}_4$ (pH 7.6). Cell pellets were lysed using sonication on ice for a total period of 30 sec with cycles of 2 secs bursts followed by 2 sec pauses. Lysed cells were prepared by centrifugation at max speed for 5 min at 4°C and the supernatant was used for activity assays. A standard reaction mixture (100 μl) contained 50 mM $\text{K}_2\text{HPO}_4/\text{KH}_2\text{PO}_4$ (pH 7.6) and 20 μl supernatant. Acetonitrile, benzonitrile, and 3-cyanopyridine substrates were at a final concentration of 25 mM. Assays were carried out at room temperature overnight. To determine ammonia concentration, the reaction was terminated by the addition of 3.5 vols of reagent A (0.59 M phenol and 1 mM sodium nitroprusside). Colour development was by the addition of an equal volume of reagent B (2.0 M sodium hydroxide and 0.11 M sodium hypochlorite). The amount of ammonia released was measured spectrophotometrically at $\text{OD}_{600\text{nm}}$ after 5 min incubation at 55°C. For negative controls, assays were performed with no substrate, or supernatant from a negative clone (pJET containing non-nitrile hydrolysing, 967 bp insert).

3.2.5 Genome sequencing and *in silico* gene mining

The genome of *Nesterenkonia* AN1 was sequenced using Illumina DNA sequencing technology at the University of the Western Cape. The nucleotide sequences of semi-aligned contigs generated from the sequenced genome were used as the database for local BLAST. Protein sequences of the α - and β -subunits of NHases and nitrilases retrieved from NCBI were used as queries in BLAST using BLOSUM 62 matrix with a cut off expectation value greater than 0.0001. Protein sequences with significant hits were analysed using BLAST, provided by NCBI. The nucleotide sequences of contigs were retrieved from the

Nesterenkonia database. ORFs flanking the gene of interest were predicted using the Vector NTi Suite (www.invitrogen.com) and Rapid Annotation using Subsystem Technology (RAST) (Aziz *et al.*, 2008) (www.theseed.org) and analysed using BLAST.

3.2.6 Homology modelling

MetaServer (Ginalski *et al.*, 2003, Kajan & Rychlewski, 2007) was used for the threading of protein sequences for suitable structural templates for the construction of 3D homology models. The 3D-Jury scoring (Ginalski *et al.*, 2003) of MetaServer were used to analyse the threads returned from local structure and fold recognition servers such as PDB-BLAST, 3D-Jigsaw, EsyPred3D, GRDB, FFAS03, Sam-T99, INBGU, FUGUE2, 3D-PSSM, mGenTHREADER, psipred, and profsec. The comparative modelling program MODELLER (Sali & Blundell, 1993) linked with Metaserver was used to construct the 3D models by optimally satisfying spatial restraints. Subsequently, the stereochemistry of selected homology models were evaluated using RAMPAGE (Lovell *et al.*, 2003). Homology models with optimal stereochemistry were compared against structures within the Protein Bank Database using the 3D superimposition analysis server of SSM (Krissinel & Henrick, 2004).

3.3 Results

3.3.1 PCR screening of isolates for NHases

Figure 3.1 shows a portion of the ClustalW (Larkin *et al.*, 2007) alignment constructed from 180 NHase α -subunit protein sequences. These sequences included putative and experimentally determined NHases. Two conserved regions that flanked the highly conserved co-factor binding region were selected for primer design (Figure 3.1). This motif was used for identification of NHases from sequenced amplicons.

Initial PCR trials using the degenerate primers and a standard thermocycling condition (annealing temperature of 50°C) yielded multiple bands (data not shown). The application of touchdown PCR thermocycling programme greatly reduced multiple bands for most PCR analysis. The results of the PCR are tabulated in Table 3.2 for each primer combination used. In addition, PCR trials using the non degenerate primers NHFe1/2 and NHCo1/2 (Precigou *et al.*, 2001), specific for Fe-type and Co-type NHases, respectively, are shown.

Only the sequenced amplicons derived from the *R. erythropolis* and *Arthrobacter* AN16 using primer pairs NHFe1/2, NH1gF/NH2gR, and NH2gF/NH2gR were positive for Fe-type NHases. The amplicon derived using primer pair NHFe1/2 was used for further analyses, since it was 62 bp longer than that derived using the new degenerate primers. Furthermore, these sequences shared high sequence conservation (>98%) with the α -subunit of Fe-type NHases of *R. erythropolis* IND-AN014 (Accession number: AAP57643) (Brandao *et al.*, 2003), *Brevibacterium* sp. (AAA62722) (Mayaux *et al.*, 1990), *Rhodococcus* sp. R312 (PDB code: 1AHJ-A) (Huang *et al.*, 1997) and *R. erythropolis* ANT-AN007 (AAP57640) (Brandao & Bull, 2003) (Figure 3.2). The latter bacterial strain was isolated from lake sediment in Antarctica, and was reported to utilise acetonitrile and benzonitrile as the sole nitrogen source for growth (Brandao *et al.*, 2003).

Species	Accession	Ty	Len	Sequence	Co-factor binding domain
<i>Acidiphilium cryptum</i>	ABQ30292	Co	193 ...	A T L L A G L R S L L A A K S I A S A D E I A E R I R I T D G G G P A O G A R M V A K A W T D P D Y K A L M L A D G A R A A E L L	D I P M R G L P P L G V V E N T P G I H H L V V C T L C S C Y P
<i>Acinetobacter</i>	CAG68465	Fe	200 ...	G E R A W A L H K V L T N K G L I P E G F I E G L T D L L A N K F D P A N G A Q V V A K A W T D P A Y R E L L L R D G T A A C E E F	G F T G P Q G E Y I V A L E D T T D V K N V I V C S L C S C T N
<i>Agrobacterium tumefaciens</i>	CAD54074	Co	205 ...	A L R V K A L E S L L T E K G L V D P A A L D E L V D T Y E N R I G P R N G A L V V A K A W T D P A Y K Q R L L T N A T E A I A E L	G F S G V Q G E D M L V V E N S P T V H N M T V C T L C S C Y P
<i>Arthrobacter aureus</i>	ABM10675	Co	200 ...	A A R V K A L E S M L I D Q G V M T T S M V D R M A E I F E N E V G P Q L G A K V V A K A W T D P D Y K A K L L K D G T A A C K D L	G Y T G L Q G E D M K F V E N T D D V H N T I V C T L C S C Y P
<i>Aurantimonas</i>	EAS50464	Co	222 ...	T A R V M A L E T I L T E K G M V D P D A L D A I I D T Y E T K V G P R N G A S V V A K A W S D P D Y A D W L A R D A T A A I A S L	G F T G R Q G E H M Q A V F N T P E R H N L V V C T L C S C Y P
<i>Bacillus</i>	AAQ23015	Co	217 ...	E A R A K A L E S L L I E K G H L S S D A I E R V I K H Y E H E L G P M N G A K V V A K A W T D P A F K Q R L L E D S E T V L R E L	G Y Y G L Q G E H I R V V E N T D T V H N V V V C T L C S C Y P
<i>Bradyrhizobium</i>	ABQ36151	Co	211 ...	D L R V R A L E S I L T E K G Y I D P A A L D V L I E T Y E S K V G P R N G A R V V A R A W T D P A F R A R L L S D A T P A I G E L	G Y A G R Q G E H I V A V E N T P E L H N M V V C T L C S C Y P
<i>Brevibacterium</i>	AAA62722	Fe	189 ...	S D R A W A L F R A L D G K G L V P D G Y V E G W K K T F E E D F S P R R G A E L V A R A W T D P E F R Q L L L T D G T A A V A Q Y	G Y L G P Q G E Y I V A V E D T P T L K N V I V C S L C S C T A
<i>Burkholderia ambifaria</i>	EAV52923	Fe	200 ...	G E R A W A L F R V M K E K N L I P D G Y I E G L T E L M S T T W D P A N G A R I V A R A W A D P G F R E L L L K D G T A A C A Q F	G Y T G P Q G E Y I V A L E D T P T L K N V I V C S L C S C T N
<i>Burkholderia phytofirmans</i>	EAV07364	Co	223 ...	D L R V R A L E S L L V E K G Y V D P Q A L D A L V E T Y E H K V G P R N G A R V I A K A W R D P E Y K O W L L D D A T A A I A S L	G Y T G R Q G E H M I V L E N T P A T H N M V V C T L C S C Y P
<i>Comamonas testosteroni</i>	AAU87542	Co	211 ...	A L R V K A L E S L L I E K G L V D P A A M D L V V Q T Y E H K V G P R N G A K V V A K A W V D P A Y K A R L L A D G T A G I A E L	G F S G V Q G E D M V I L E N T P A V H N V V V C T L C S C Y P
<i>Dinoroseobacter shibae</i>	EAV78658	Co	204 ...	Q L T E I A L R E L L I E K G V L T P A E V T A Q V T Q M D A R S P A N G A A V V A R A W T D P A F R A R L L A D G A E A C R E M	G Y D I G T L N L I A V E N T P E V H N V I V C T L C S C Y P
<i>Mesorhizobium loti</i>	BAB48803	Co	202 ...	A A R V R A L E T I L T R K G L I D P A A I D I I V D T Y E T K I G P R N G A R V V A K A W S D P A Y A D W L K R D A T A A I E S L	S Y T G R Q G E H M Q A V F N T E E T H N L V V C T L C S C Y P
<i>Methylbacterium</i>	EDK93889	Co	212 ...	D L R V R A L E S I L V E K G Y V D P A A L D A L I D T Y E T K V G P R N G A R V V A R A W V D P A Y R A R L L D D A T A A I R E L	G I G G R G G E H M V V V A N T P E E H N L V V C T L C S C Y P
<i>Mycobacterium gilvum</i>	ABP43494	Co	207 ...	A D R V A A L E R L L I E K G V I T G O T V D K V L S Y F E S E M T P L N G K K I V V K A W T D P D F A A R V V V D T P A A I A E L D L P E	G M A G A E G E H L O A V A N E P G V H N L V I C T L C S C Y P
<i>Nocardia</i>	AAN71593	Co	204 ...	E A R T K A I E T L L Y E R G L I T P A A V D R V V S Y Y E N E I G P M G G A K V V A K S W V D P E Y R K W L E E D A T A A M A S L	G Y A G E Q A H Q I S A V F N D S Q T H H V V V C T L C S C Y P
<i>Oceanicola batsensis</i>	EAQ01756	Co	202 ...	T A R V M A L E K L L I D K G L V D P A A L D R I L E T Y E T E I G P R N G A Q V V A R A W T D P A F A Q A L R D D A T A A I H G M	G F G G R Q G E H L T A V F N A P E T H N M V V C T L C S C Y P
<i>Pseudomonas chlororaphis</i>	BAA14245	Fe	201 ...	G E R A W A L F Q V L K S K E L I P E G Y I E Q L T Q L M A H D W S P E N G A R V V A K A W V D P Q F R A L L L T D G T A A C A Q F	G Y T G P Q G E Y I V A L E D T P G V K N V I V C S L C S C T N
<i>Pseudomonas putida</i>	ABQ78862	Fe	194 ...	G E R A R A L F A V L K R K D L I P E G Y I E Q L T Q L M E H G W S P E N G A R I V A K A W V D P Q F R E L L L K D G T A A C A Q F	G F T G P Q G E Y I V A L E D T P Q L K N V I V C S L C S C T N
<i>Rhizobium leguminosarum</i> bv. <i>vici</i>	CAK08726	Co	218 ...	Q A R V K A L E T L L T E K G L I D P A A I D A I V E T Y E T K V G P R N G A H V V A K A W S D A D F A D W L R R D A T A A I N S L	G Y T G R Q G E H M R A V F N T A E T H N L V V C T L C S C Y P
<i>Rhodobacteriales bacterium</i>	EBA03728	Co	217 ...	Q T M E I A M R E L L I E K E I T T A A E I T A R I E E M D R R S P A D G A A V I A R A W V D P E Y K A H L L A D G S A A C K A M	G F E P G V L R L I A V E N T A D V H N V V V C T L C S C Y P
<i>Rhodococcus</i>	ABG92196	Fe	208 ...	S D R A W A L F R A L D G K G L V P E G Y T E G W K K T F E E D F S P K R G A E L V A R A W T D P E F R D L L L T D G T A A V D Q Y	G Y L G P Q G E Y I V A L E D T P T L K N V I V C S L C S C T A
<i>Rhodococcus erythropolis</i>	AAP57658	Fe	208 ...	S D R A W A L F R A L D G K G L V P D G Y V E G W K K T F E E D F S P R R G A E L V A R A W T D P E F R Q L L L T D G T A A V A Q Y	G Y L G P Q G E Y I V A V E D T P T L K N V I V C S L C S C T A
<i>Rhodococcus rhodochrous</i>	CAA45712	Co	208 ...	A A R V K A M E A I L V D K G L I S T D A I D H M S S V Y E N E V G P Q L G A K I V A R A W V D P E F K Q R L L T D A T S A C R E M	G V G G M Q G E E M V V L E N T G T V H N M V V C T L C S C Y P
<i>Rhodopseudomonas palustris</i>	ABD88296	Co	210 ...	E L R V R A L E T I L I E K G Y V D P K A L D L L I E T Y E T K V G P R N G A R V V A R A W S D P A Y H A R L M E N A S A A I A E L	G Y Q G R Q G E H L V V V E N T P T L H N M V V C T L C S C Y P
<i>Roseobacter denitrificans</i>	ABG31518	Co	211 ...	A L R I K A L E T L L T R K G L I D P Q A L D A I I D T Y E N R I G P R N G A H V V V K A W T D P A F R A A L L E D A T K V V S E L	G Y Y G R Q G E H M V A V E N T D S V H N M V V C T L C S C Y P
<i>Roseovarius</i>	EAQ25715	Co	219 ...	Q R M E I A V R E L L V E K S H L I P A O I A T Q I E V M D A R S P A N G A A V V A R A W I D P D F K A R L L A D A S A A S R E M	G F D I G P L N L I A V E N T A D A H N L I V C T L C S C Y P
<i>Rubrobacter xylanophilus</i>	ABG05244	Co	208 ...	L R I R A I E S L L V E K G V L T E A E I Q D Q I E Y M D S R S P A N G A R L V A R A W V D P E F R R R L L A D T K A A A L E L	G I D A S G P V E F V V V E N T P E V H N L I V C T L C S C Y P
<i>Silicibacter pomeroyi</i>	AAV94603	Co	205 ...	A L R V K A L E T I L T R K G L I D P A A L D E I I D T Y Q N R I G P Q N G A R V V A R A W A D P A F K A A L L A D A M P L L T E L	G Y Y G R Q G E H M V V V E N T P E T H N M V V C T L C S C Y P
<i>Sinorhizobium meliloti</i>	CAC46686	Co	214 ...	E A R V K A L E T V L T E K G L I D P A A I D A I V D A Y E T K V G P R N G A R V V A K A W S D P G F A D W L K R D A T A A I A S L	G F T G R Q G E H M R A V F N T S E T H N L I V C T L C S C Y P
<i>Stappia aggregata</i>	EAV46030	Co	214 ...	E L R V R A L E T L L T E K G Y I D P P A L D E L I E T Y E T K I G P R N G A L V V A K A W T D P D Y R E R L M K D A T A A I A E L	G F T G R Q G E H M V A V E N T D D I H N M V V C T L C S C Y P
<i>Sulfobacter</i>	EAP83682	Co	209 ...	E A R V R A L E S L L S A K G Y I D S A A V D R I I Q T Y E T K I G P R N G A H V V A K S W V E P E F E A W L R R D S S A A I H S L	G Y H S R Q G E H I E A V F N S D E V H H V V C T L C S C Y P
<i>uncultured bacterium</i>	CAC83632	Co	204 ...	E A R T K A I E T L L Y E R G L I T P A A V D R V V S Y Y E N E I G P M G G A K V V A K S W V D P E Y R K W L E E D A T A A M A S L	G Y A G E Q A H Q I S A V F N D S Q T H H V V V C T L C S C Y P
<i>uncultured bacterium</i>	CAC83635	Co	180 ...	E R T K A V E T L L Y E R G L I T P A A V D R V V S Y Y E N E I G P M G G A K V V A K S W V D P E Y R K W L E E D A T A A M A S L	G Y A G E Q A H H V V V C T L C S C Y P

Figure 3.1 continued.

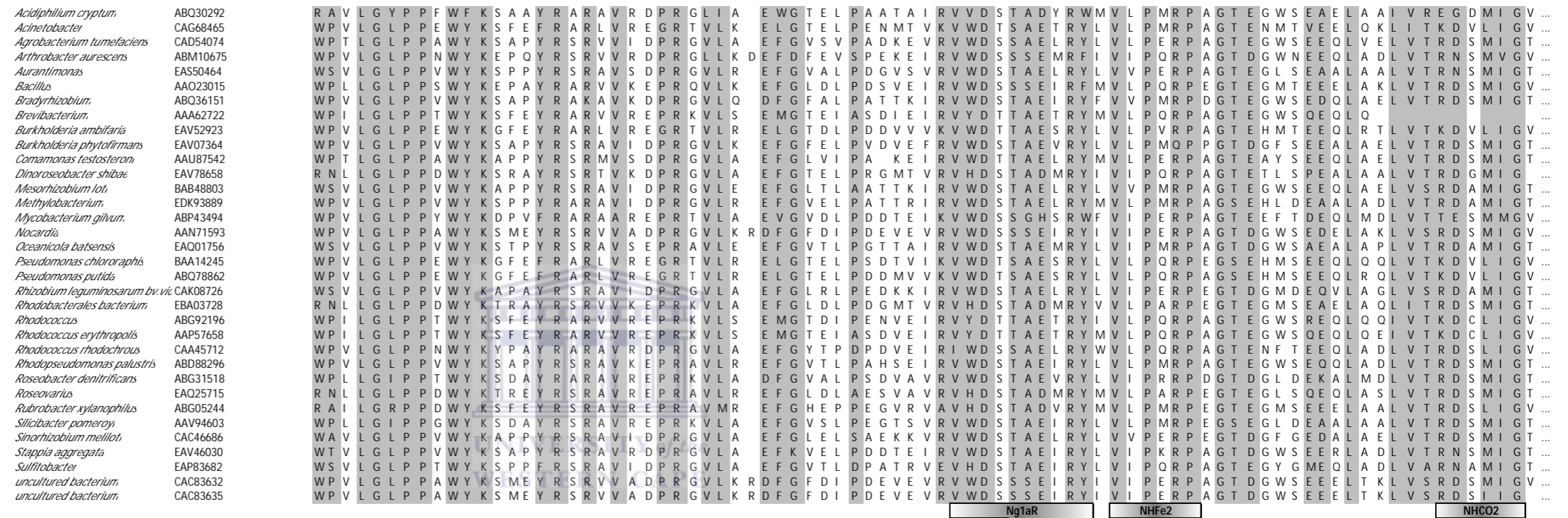


Figure 3.1 ClustalW alignment of NHase α -subunit protein sequences used for primer design. Position of primer pairs, Ng1aF/R, Ng2aF/R, NHCo1/2, and NHFe1/2, are shown below the alignment. Light grey shading represent residues that are 50% conserved. Dark grey shading represent residues of the highly conserved co-factor binding domain. Abbreviations: Ty, Co- or Fe-Type NHases; Len, length of α -subunit protein sequence.

Table 3.2 Results of PCR trials using the degenerate primers. Abbreviations: ND, not determined; -, no reaction; +, positive reaction.

Isolate	16S rRNA	NHFe1 NHFe2	NHCo1 NHCo2	NH1gF NH1gR	NH1gF NH2gR	NH2gF NH2gR	NH2gF NH1gR
49.6	<i>Psychrobacter fozii</i>	-	-	-	-	-	-
H1B2	<i>Nesterenkonia</i> AN1	ND	ND	-	+	+	-
49.1	<i>R. erythropolis</i>	+	-	-	+	+	-
49.8	<i>Arthrobacter</i> AN 16	+	-	-	+	+	-
4E1B1	<i>Pseudomonas</i>	ND	ND	-	-	+	-
<i>E. coli</i> gDNA		-	-	-	-	-	-
pNH14K		-	-	-	-	-	+

Although amplicons of ~350 bp were obtained for the *Nesterenkonia* AN1 and *Pseudomonas* (Table 3.2), no significant sequence relatedness to NHases was found. This amplification is probably due to the non-specific binding of the degenerate primers. No amplification was obtained for *Psychrobacter* and the negative control, *E. coli* (Table 3.2). A closely related *Psychrobacter* genome has been fully sequenced, and shows no NHase-related ORFs. The gene of *G. pallidus* Co-type NHase in plasmid pNH14K only amplified with the NH2gF/NH1gR combination. No amplification was obtained with NHCo1/2 primers, which are specific for Co-type NHases.

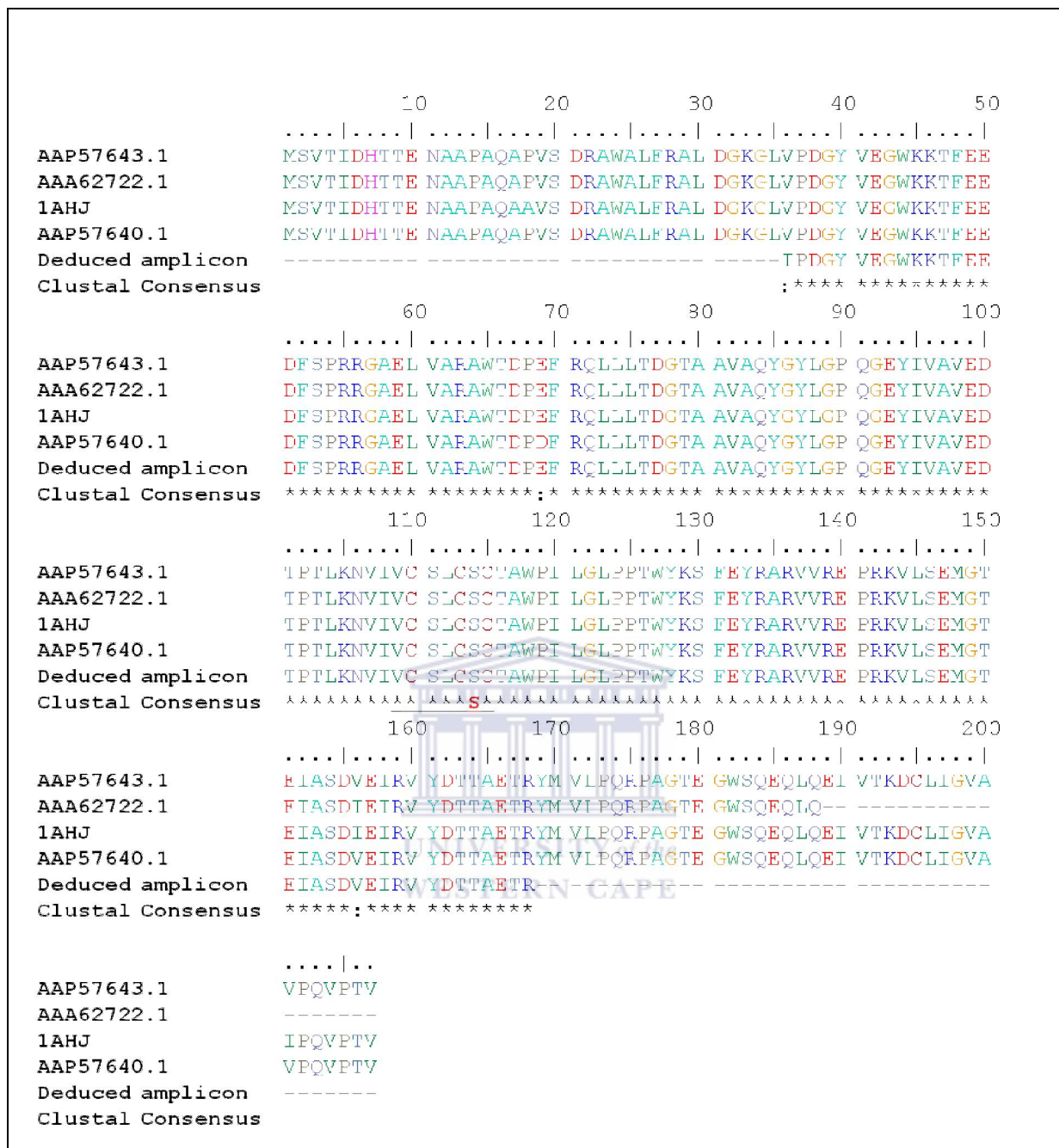


Figure 3.2 ClustalW alignment showing the conservation of the deduced protein sequence of *R. erythropolis* amplicon with known NHase -subunits. The co-factor binding domain is underlined. The serine (S) residue that denotes Fe-type NHases is marked in red. The accession numbers AAP57643, AAA62722, 1AHJ-A and AAP57640 refer to the Fe-type NHase -subunits of *R. erythropolis* IND-AN014, *Brevibacterium* sp., *Rhodococcus* sp. R312, *R. erythropolis* ANT-AN007, respectively.

3.3.2 Development of functional screening systems

Aminoacetonitrile screening system

The glycine auxotroph *E. coli* JK81 strain did not grow on M63 minimal medium lacking glycine. The strain grew on media supplemented with aminoacetonitrile and glycine, which confirmed that the nitrile was not toxic to the host strain. Cell free extracts of arabinose-induced *E. coli* JK81 harbouring pAN1 were shown to have activity on aminoacetonitrile and acetonitrile in the presence of purified amidase (data not shown). However, no growth was observed for cells harbouring pAN1 on M63 minimal medium containing aminoacetonitrile as the sole nitrogen source. The data suggests that *E. coli* JK81 lacks an amidase capable of converting aminoacetamide to ammonia and glycine. The co-expression of an aminoacetamide degrading amidase is required, in addition to NHase for this complementation assay to function successfully.

Pyrazinecarbonitrile screening system

A faint brown colour was observed for *E. coli* colonies harbouring pJ1 C327 on LB plates containing pyrazinecarbonitrile, which were soaked in 20% $\text{FeNH}_4(\text{SO}_4)_2$ solution. No distinction could be made between colonies harbouring pJ1 C327 and pET29b possibly due to the diffusion of pyrazinoic acid in the agar plates. To improve the detection of pyrazinoic acid, cells harbouring pJ1 C327 were inoculated into liquid LB medium containing pyrazinecarbonitrile. Pyrazinoic acid could be detected for cells harbouring pJ1 C327 at 20-50 mM pyrazinecarbonitrile (Figure 3.3). No colour was present at 0 mM pyrazinecarbonitrile and for cells harbouring pET29b (Figure 3.3). However, the cell density of cultures was observed to decrease at concentration of the nitrile greater than 30 mM, possibly due to the toxicity of pyrazinecarbonitrile. This screening system is suitable if performed in liquid media in the presence of 10- 30 mM pyrazinecarbonitrile.

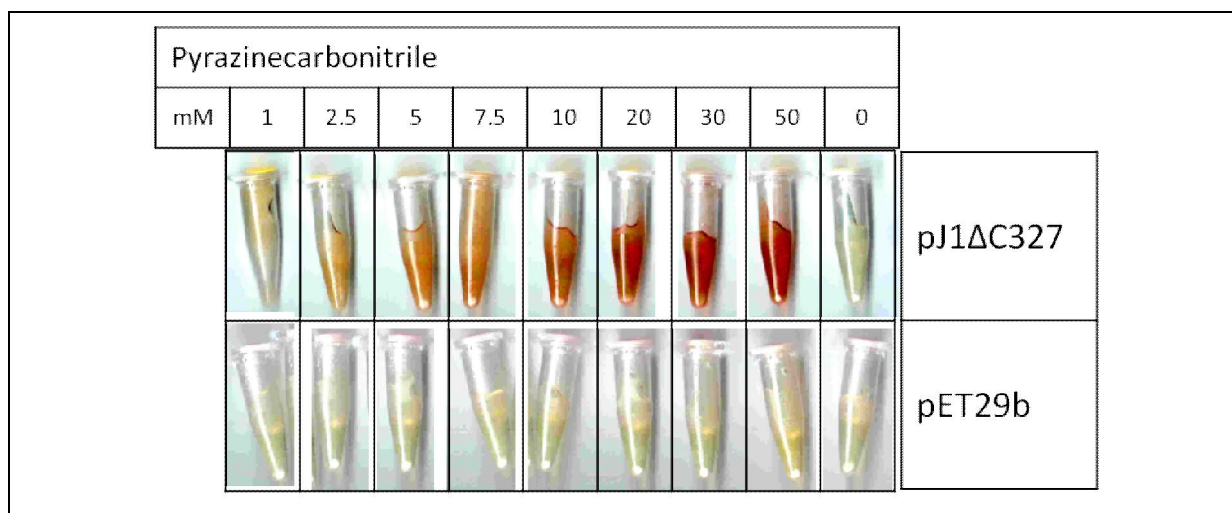


Figure 3.3 Colorimetric detection of cultures for activity on pyrazinecarbonitrile.

3-Cyanopyridine screening system

E. coli ArcticExpress cells harbouring the pNit plasmid grew on M63 minimal medium supplemented with 25 mM 3-cyanopyridine as the nitrogen source. Cells harbouring the negative control plasmid pET29b, did not grow on this medium. Since *Nesterenkonia* AN1 utilised 3-cyanopyridine as a sole source of nitrogen for growth, this screening system was used.

Several transformed *E. coli* ArcticExpress colonies were observed on the selective plates after a week of incubation. These colonies were re-streaked onto fresh selective plates and re-incubated. Colonies that did not grow after the second re-streaking suggested that the initial growth was due to the presence of residual nitrogen, either from the transformation mixture or from dead cells. One clone, pD1, had strong activity on benzonitrile and acetonitrile. No activity was obtained for a crude extract that was boiled for 5 mins or for crude extracts of cells harbouring the control plasmid (data not shown). Analysis of a *Bgl* II digest of pD1 DNA showed that the 2974 bp vector backbone was not present. It could not be established with several pJET vector specific restriction endonucleases whether pD1 could be a contaminating vector. The same analysis was performed on plasmids extracted from several other colonies also revealed no vector backbone. A possible reason is that since *E. coli* ArcticExpress is a rec⁺ strain,

the insert or vector might have contained a repeated sequence or secondary structures that underwent rearrangement (Bi *et al.*, 1995), or recombination might have occurred between the plasmid and the genome of *E. coli* ArcticExpress or its low copy pACYC plasmid.

With the availability of the sequenced genome of *Nesterenkonia* AN1, no further attempts were made to optimise the screening systems.

3.3.3 *In silico* gene mining of the *Nesterenkonia* AN1 genome

Computational analysis of the partially sequenced *Nesterenkonia* AN1 genome did not identify protein sequences with significant similarity to the α - or β -subunits of NHases. In addition, no sequence similarities were found for the cluster of proteins associated with NHases, such as the activator (enhancer) protein (Cowan *et al.*, 2003).

Two protein sequences (276 and 264 amino acids, referred to as Nit1 and Nit2, respectively) had significant similarity to nitrilases in the local BLAST database. BLAST of Nit1 and Nit2 against the NCBI protein database detected conserved domains, pfam00795, (Bork & Koonin, 1994) identified as non-peptide carbon-nitrogen hydrolases of the nitrilase superfamily. The full nucleotide and deduced protein sequences of Nit1 and Nit2 are shown in Appendix F.

3.3.4 Genetic maps of Nit1, Nit2 and neighbouring ORFs

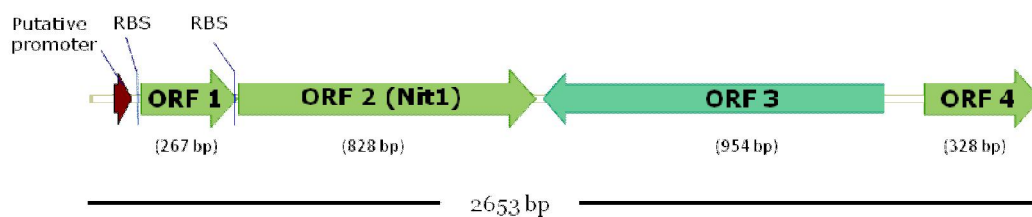
Genetic maps of the Nit1 and Nit2 ORFs, including the neighbouring ORFs, were generated and are illustrated in Tables 3.3 and 3.4. ORF2 is the 828 bp Nit1 gene (Table 3.3). A ribosome binding site (5'-agagg-3') was sited 8bp upstream of the initiation start (ATG) of the Nit1 gene and an amber stop codon (TAG) terminated the ORF. Nit1 shared 56-57% identity with putative amidohydrolases, nitrilases, cyanide hydratases or apolipoprotein N-acyltransferases of

Arthrobacter strains (Table 3.3). These are all members of the nitrilase superfamily.

Upstream of the Nit1 gene, ORF1 (267 bp, 89 aa) shared 51% identity with the hypothetical protein RSal33209_1001 (Accession ABY22741.1) of *Renibacterium salmoninarum* ATCC 33209 (Table 3.3). Downstream of Nit1, the 964 bp ORF3 encodes a 318 aa polypeptide that had 56% identity to aminotransferase class IV of *Arthrobacter chlorophenolicus* A6 (Table 3.3). Aminotransferases are 4-amino-4-deoxychorismate lyase protein members of the fold-type IV of PLP dependent enzymes that convert 4-amino-4-deoxychorismate (ADC) to p-aminobenzoate and pyruvate. The fourth ORF was truncated but the partial sequence had significant identity to cardiolipin synthetase of *Arthrobacter* sp. F24 (Table 3.3).

Nit2 and the adjacent ORFs are shown in Table 3.4. Nit2 (ORF4) was calculated to be 1107 bp and had a ribosome binding site (5'-agggg-3') 10 bp upstream of its start codon (ATG). This ORF terminated with an amber stop codon overlapped with ORF5 by 203 bp (data not shown). The deduced protein sequence for ORF 5 shares 72% identity with the amine oxidase of *Arthrobacter chlorophenolicus* A6. Further analysis of the genome sequence revealed that Nit2 ORF was inconsistent at position 791 bp: sequenced PCR amplicons of Nit2 showed a T at position 791, while a G was present in the genome assemblies (described further in Chapter 4, Section 4.3.1). This was an error within the assemblies of the genome. Due to the error, an amber stop codon terminated Nit2 ORF at 790 bp. Nit2 shared 47-45% identity with putative nitrilases, cyanide hydratases or apolipoprotein N-acyltransferases of *Arthrobacter* strains (Table 3.4). ORF1 had 49% identity to a hypothetical membrane protein of *Kocuria rhizophila* (Table 3.4). In addition, ORF2 had 54% identity to the major facilitator serine transporter protein of the same species. The deduced protein sequence of ORF3 had high sequence conservation (57% identity) with the sodium: sulphate symporter transmembrane component of *Erythrobacter* sp. NAP1 (Table 3.4).

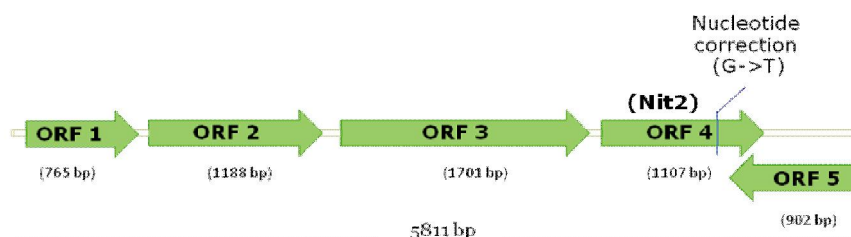
Table 3.3 Genetic map of Nit1 and its neighbouring ORFs. The top three results retrieved from BLAST analysis of ORFs are shown.



ORF	Predicted protein length (aa)	Similarity: X/Y = X% identity / Y% homology	Protein Length (aa)	General protein information (Accession)	Organism (Accession of sequence genome)
ORF 1	89	51/63	86	hypothetical protein RSal332 09_1001 (ABY22741.1)	<i>Renibacterium salmoninarum</i> ATCC 33209 (CP000910.1)
		36/62	87	hypothetical protein Achl_3654 (ACL41609.1)	<i>Arthrobacter chlorophenolicus</i> A6 (CP001341.1)
		40/57	87	hypothetical protein Arth_3867 (ABK05242.1)	<i>Arthrobacter</i> sp. FB24 (CP000454.1)
ORF 2	276	57/68	264	putative amidohydrolase (CAR47877.1)	<i>Arthrobacter</i> sp. PY22
		56/68	264	predicted amidohydrolase (ABR66996.1)	<i>Arthrobacter</i> sp. AK-1
		56/68	264	Nitrilase/cyanide hydratase and apolipoprotein N-acyltransferase (ACL41203.1)	<i>Arthrobacter chlorophenolicus</i> A6 (CP001341.1)
ORF 3	318	56/68	309	aminotransferase class IV (ACL41593.1)	<i>Arthrobacter chlorophenolicus</i> A6 (CP001341.1)
		54/66	306	4-amino-4-deoxychorismate lyase (ABK05225.1)	<i>Arthrobacter</i> sp. FB24 (CP000454.1)
		52/65	313	4-amino-4-deoxychorismate lyase (ABM06859.1)	<i>Arthrobacter aureescens</i> TC1 (CP000474.1)
ORF 4*	109	44/65	491	cardiolipin synthetase 2 (ABK05224.1)	<i>Arthrobacter</i> sp. FB24 (CP000454.1)
		43/66	479	phospholipase D/Transphosphatidylase (ACL41592.1)	<i>Arthrobacter chlorophenolicus</i> A6 (CP001341.1)
		46/67	489	putative phospholipase, cardiolipin synthetase (CAN02888.1)	<i>Clavibacter michiganensis</i> subsp. <i>michiganensis</i> NCPPB 382 (AM711867.1)

* ORF4 truncated by 1150 bp

Table 3.4 Genetic map of Nit2 and its neighbouring ORFs.



ORF	Predicted protein length (aa)	Similarity: X/Y = X% identity / Y% homology	Protein Length (aa)	General protein information (Accession)	Organism (Accession of sequence genome)
ORF 1	255	49/65	249	hypothetical membrane (BAG30374.1)	<i>Kocuria rhizophila</i> DC2201 (AP009152.1)
		41/65	253	hypothetical protein (CAQ05111.1)	<i>Corynebacterium urealyticum</i> DSM 7109 (AM942444.1)
		41/65	249	Putative domain of unknown function (EEB63541.1)	<i>Corynebacterium amycolatum</i>
ORF 2	396	54/69	433	MFS transporter (BAG30345.1)	<i>Kocuria rhizophila</i> DC2201 (AP009152.1)
		53/67	399	major facilitator family protein transporter (ABK71320.1)	<i>Mycobacterium smegatis</i> str. MC2 155 (CP000480.1)
		55/66	376	major facilitator superfamily (EDT57186.1)	<i>Micrococcus luteus</i> (NCTC2665)
ORF 3	567	57/71	508	Sodium:sulfate symporter transmembrane component (EAQ27847.1)	<i>Erythrobacter</i> sp. NAP1
		49/63	569	DASS family transporter (BAG30405.1)	<i>Kocuria rhizophila</i> DC2201 (AP009152.1)
		52/88	566	anion transporter (EDT57225.1)	<i>Micrococcus luteus</i> (NCTC 2665)
ORF4 *	264	46/62	292	Nitrilase/cyanide hydratase and apolipoprotein N-acyltransferase (ABK025001.1)	<i>Arthrobacter</i> sp. FB24 (CP000454.1)
		47/62	267	Nitrilase/cyanide hydratase and apolipoprotein N-acyltransferase (ACL39174.1)	<i>Arthrobacter chlorophenolicus</i> A6 (CP001341.1)
		45/61	267	carbon-nitrogen family hydrolase (ABM10070.1)	<i>Arthrobacter aurescens</i> (CP000474.1)
ORF5 *	540	72/80	578	amine oxidase (ACL39177.1)	<i>Arthrobacter chlorophenolicus</i> A6 (CP0001341.1)
		71/80	543	putative tryptophan 2-monooxygenase (ABM08490.1)	<i>Arthrobacter aurescens</i> TC1 (CP000474.1)
		71/81	576	amine oxidase (ABK02504.1)	<i>Arthrobacter</i> sp. FB24 (CP000454.1)

* ORF4 & ORF5 –due to an error within the sequencing of the genome, the 264 bp nucleotide sequence of ORF4 was used.

Most of the deduced protein sequences of *Nesterenkonia* ORFs shared significant conservation with proteins found in *Arthrobacter*, *Kocuria* and *Micrococcus* strains. The latter three genera shared the same family, *Micrococcaceae*, as *Nesterenkonia*. The genomes of several of these strains, as shown in Tables 3.3 and 3.4, have been fully sequenced. The arrangement of Nit1, Nit2 and the neighbouring ORFs was not conserved in other organisms.

3.3.5 Analysis of Nit1 and Nit2 protein sequences – sequence conservation

Nit1 and Nit2 showed an overall protein sequence conservation of 56 and 62% with putative nitrilases in *Arthrobacter* strains. In order to determine the enzyme function of Nit1 and Nit2, a comparison of protein sequence conservation with known members of the nitrilase superfamily was made (Table 3.5). In addition, the putative nitrilases from sequenced genomes of *Arthrobacter* strains and *Psychrobacter cryohalolentis* K5 were included.

There was low sequence conservation (25% sequence identity) between the protein sequences of Nit1 and Nit2 (Table 3.5). Of the three putative nitrilases in *Arthrobacter* sp. FB24, Nit1 shared significant sequence conservation (58 and 48%) with ABK04917 and ABK830230, respectively (Table 3.5). Nit2 only shared 42% sequence identity with the third putative nitrilase, ABK02500 (Table 3.5). No significant sequence conservation was found between Nit1 and Nit2 and the putative nitrilases found in *Psychrobacter cryohalolentis* K5 genome and with characterised members of the nitrilase superfamily. Overall, Nit1 and Nit2 were most similar to the putative nitrilase/cyanide hydratase and apolipoprotein N-acyltransferase proteins of the *Arthrobacter* strains, the functions of which have not been experimentally determined.

Table 3.5 Protein sequence conservation (percentage identity) of Nit1 and Nit2 with putative and characterised members of the nitrilase superfamily. Abbreviation: ApoL, apolipoprotein N-acyltransferase.

Enzyme	Accession /PDB number	Organism	Nit1	Nit2
Nit1	NA	<i>Nesterenkonia</i> (this work)		25%
Nit2				
Putative nitrilases				
Nase/cyanide hydratase/ApoL	ABK04917.1	<i>Arthrobacter</i> sp. FB24	58%	26%
Nase/cyanide hydratase/ApoL	AB830230.1	<i>Arthrobacter</i> sp. FB24	48%	22%
Nase/cyanide hydratase/ApoL	ABK02500.1	<i>Arthrobacter</i> sp. FB24	22%	42%
Nase/cyanide hydratase/ApoL	ACL39174.1	<i>Arthrobacter chlorophenolicus</i> A6	25%	45%
Nase/cyanide hydratase/ApoL	ACL41203.1	<i>Arthrobacter chlorophenolicus</i> A6	57%	25%
Nase/cyanide hydratase/ApoL	ABE74006.1	<i>Psychrobacter cryohalolentis</i> K5	19%	15%
Nase/cyanide hydratase/ApoL	ABE74190.1	<i>Psychrobacter cryohalolentis</i> K5	7%	8%
Characterised members of the nitrilase superfamily				
Nitrilase	ABH04285	<i>G. pallidus</i> DAC521	14%	13%
Nitrilase	BAA01994.1	<i>R. rhodochrous</i> J1	10%	12%
NitFhit fusion protein	1ems	<i>Caenorhabditis elegans</i>	21%	22%
AmiF formamidase	2dyu	<i>Helicobacter pylori</i>	13%	12%
Prokaryotic Nit protein	2e11	<i>Xanthomonas campestris</i>	15%	20%
Aliphatic amidase	2plq	<i>G. pallidus</i>	12%	16%
Aliphatic amidase	2uxy	<i>P. aeruginosa</i>	14%	16%
-alanine synthetase	2vhh	<i>Drosophila melanogaster</i>	10%	12%
Putative CN hydrolase	1f89	<i>Saccharomyces cerevisiae</i>	22%	19%
DCase	1uf5	<i>Agrobacterium radiobacter</i>	17%	15%
DCase	1erz	<i>Agrobacterium</i> sp. Strain KNK712	18%	15%
Hypothetical protein PH0642	1j31	<i>Pyrococcus horikoshii</i>	18%	22%
Predicted amidohydrolase	2w1v	<i>Mus musculus</i>	22%	20%

3.3.6 Alignment of Nit1 and Nit2 protein sequences with characterised members of nitrilase superfamily

An alignment of the Nit1 and Nit2 protein sequences with those of known nitrilases (kindly constructed by Dr Robert Thuku, Electron Microscope Unit, University of Cape Town) is shown in Figure 3.4. The predicted fold of α -helices and β -sheets for Nit1 and Nit2 are highlighted in the alignment. The secondary structural fold of *G. pallidus* aliphatic amidase (Kimani *et al.*, 2007) was included for comparison.

Nit1 and Nit2 conserved the catalytic residues (EKEC) and the four glycine residues (Figure 3.4). In addition, the predicted folds of Nit1 and Nit2 superimposed on the monomer fold of *G. pallidus* aliphatic amidase. These features of Nit1 and Nit2 are conserved in known members of the nitrilase superfamily. It could be determined from the alignment that Nit1 and Nit2 are not Nases or aliphatic amidases (Figure 3.4). The putative nitrilases did not have the significant insertions of 12-16 amino acids that correspond to the “C” surface nor the conserved sequence motif “DP/FXGHY” of spiral forming Nases (Figure 3.4). In addition, these putative nitrilases did not possess an extended C-terminal region associated with Nases and aliphatic amidases (Figure 3.4).

Furthermore, no significant similarities could be found between Nit1 and Nit2 and other members of the nitrilase superfamily. Nit1 and Nit2 did not possess an extended N-terminal region as reported for α -alanine synthetase nor did these protein sequences share similar amino acid insertions with other members of the nitrilase superfamily (Figure 3.4).

The data suggested Nit1 and Nit2 are related to the nitrilase superfamily and could be novel Nases.

```

Nit1 1: MRFAAAQI--T-TGPF-----DPDANLEL
Nit2 1: RTAIAW--TARPL-----DPQHNDL
Dac521 1: MEGKNMSNRAQKVKVAVIQA-SSVIM-----DRDATTKK
RrcJ1 1: MVEYTNTEFKVAAVAQA-QPVWF-----DAAKTVDK
1j31 1: mvkVGYIQm-e-Pkil-----eldkNysk
1f89 1: saakiLsqkIkVALVQL-sGssp-----dkmaNLqr
1Ems 10: matgrhfIAVCGQM-tS-dn-----dleKNFga
1Krz 1: trqmiLAVGQQg-pIara-----etreqVVvr
1uf5 1: trqmiLAVGQQg-pIara-----etreqVVvr
2K11 1: mhdLrISLVQQG-s-Trwh-----dpagNrdy
2dyu 1: MGSIGSMGKPIEGFLVAATQFpVpIvns---rkdldhNtes
2usy 1: mthgdIsSsdhTVGVAVVNYKMprlht---aaeVldnArk
2plq 1: mthgdIsSsdhTVGVAVVNYKMprlht---kaeVlenAkk
2vhh 1: MSAFfelknlnDcLehlpdpdelkevKrilYgveedqtleLptsAkdIaeqngPdIkGyrftAreeqtrkrriVrVGAIQNSivipTtapikeQreaIwnk
<--b1--> <--b1-->

<-----C-----> <-----D---/-E> <C>
Nit1 21: IREYTRAAACAGAR--VVVPEAAQRAFQHP-----LPPVVAEPVTEAWAPAVRGLAREFQIVIVAGMFTPGVPSADGRPRVVNT
Nit2 22: IDDAARASECQAQ--LILTPLELFGFG-YVP-----SQICAQVSAEQVDAARSRLRGIARDGIALVWS-LPGPE-----GPEQRGIT
Dac521 34: AVSLIHQAEEKGAK--IVVFPFAFIPA-YPRGLSFGTTLGSRSAEGRKDWYRWSNVAVPDEITFEQ-LGFAARKAGVYLVIG-VTERDNEPFGG-TLYCS
RrcJ1 29: TVSIIAEARNGCE--LVAFPEVFIPIG-YPHYIWDSDS---PLAGMAKFAVRYHENSIMDSPHVQLLDAARDHNIAVVVG-I-SERDGG-----SLYMT
1j31 23: AekLIkeAskegAk--LVVLPPLFDIG-ynFe-----sreeVfdvAqgIpegeTTLfLmeLareIglYIvAGTAEKsg-----nyLyNS
1f89 31: AatfIerAmkeqpdPkLVVLPFCFNSp-ys-----tdqFrkySeViNpkepstSVqfLsnLankfXILLVGGTIPeLdpktdk-IYNT
1Ems 26: AkmIerAGekKce--MVFLPEPEPI-GI-----nkeqidLamaPdceymekYreLARKhnIwLSIGLlhhkdpS--daahpwnT
1Krz 27: LldMLtkAasrgAn--FIVFPELALTFPPRwhft-----deaeIdsfYeteMpgpvVrpLfeKAAeIlgIFNIGYAElvve--ggykrFNT
1uf5 27: LldMLtkAasrgAn--FIVFPELALTFPPRwhft-----deaeIdsfYeteMpgpvVrpLfeKAAeIlgIFNIGYAElvve--ggykrFNT
2K11 25: YgalLepla--gq-SDLVILPEPTSG-fSn-----eaidk--aedmdgpTVawIrtQAARLgAAIPG3VQLrt-----ehgVfNR
2dyu 39: IartLhaTKagypgVeLIIFFPYSTPGIntakWL-----seePLldVpgkTeIYakACkeakYyGVFSIMERnp--dsnknPYNT
2usy 38: IeamIvgmkqglpgkLlvvFPYSLGIMy-----dpaeemetaVavIpgeeTeiFSAACRkanVGVFSLTGErhe-ehprkaPYNT
2plq 38: IeamVvgmkqglpgkLlvvFPYSLGIMy-----dgdemfaTAAAsIpgeETaiFaeACKkAdTGVFSLTGEkke-dhpnkAPYNT
2vhh 101: VktMIKAaaAgCn--IVCTQEAWTMPfafCTrekf-----pWceF--AeeAengpTtkmLaelAkaynMVIHSHIIErdm--ehgetIwnT
á1-----> <-b2-> <--á2--> <-----á3-----> <-b3--> <-b4

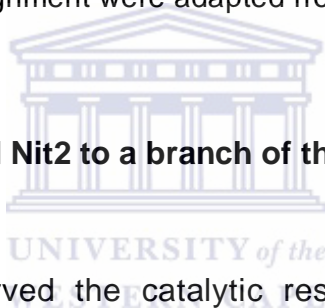
# # <-----A----->
Nit1 98: LIAVGFAGAGGAAEIDVAYDKIHLDYDAFG-----FKESDGVQGRS--PAHFVDDITFGLATYDIRFENLFTAHAARS-----GAQVTLVPSWVG
Nit2 96: AELADEHG--EVLASYQKVLQLYGP-----EKAAAFVGEQPP--FVLSWGVRLSLLVGVDFEFPEMVRAAAAR-----GAQLVLVPTALA
Dac521 28: VLFDFSDG--QLLGKRRKLPKPT-----AARIVWGEEDGSTLPVDFDTPYGRIGALICWENYMLLARAAMYAQ-----GIQIYIAPTADA
RrcJ1 116: QLVIDADG--QLVARRRKLKPT-----HVRSRYGEGNGSDISVYDMPEFARLGAALNCEHFQTLTKYAMYSM-----HEQVHVASWPGM
1j31 99: AVVVGprg--yigkYrkKihLf-----yrkvrFepGdl-gfkVfdIgfAkVGVMICTDWFfpeSartLalk-----gaeIIAHPANLp
1f89 112: SIIFnedG--klidkHrkvhLFDVDPNGIS--fhsetlspGeks--TtIdtkYgkFVGVIcyDMrfpelAmLsark-----gAFAMILYPSAFA
1Ems 103: HLIIdsdG--vt.raeYnkKihLfdleipg--kvrImsefkskaGtemi--pPvdTfPGrLGLSICyDvrFpeLSlWnrkr-----gAgLLSFP3Aft
1Krz 111: SILVdksG--kivgkYrkKihLpghkEyaeyRfQhLkryFepGdl-gfpVydVdaAKMGFIChdRrwrpeAWrvMGLr-----gaeIICGGYNTp
1uf5 111: SILVdksG--kivgkYrkKihLpghkEyaeyRfQhLkryFepGdl-gfpVydVdaAKMGFIChdRrwrpeAWrvMGLr-----gaeIICGGYNTp
2K11 95: LIAATpdga--lqyYdkKihLlrfg-----nKhLrYaag-r-erLCVewkgWrlNPQVcyDLrFpfvCnRfDverpgqLDFDLQLFVANWp
2dyu 118: AIIIdpgG--eiIlkYrkKlFpwp--iEPWy--pgdLgmpVceGpGg3kLAVCIChDnIpeLareAAy-----gCNVYIRISGys
2usy 119: LYLIdnng--eivQKrkKiiPwcp--iEGWy--pqqgT-yvseGpkMkISLIIICDGNypeiWrdCamk-----gaeLIVRCQGYM
2plq 119: LVLInnkG--eivQKrkKiiPwcp--iEGWy--PgdTl-yvteGpkLkISLIVCDDGNYPEIWRDCAMk-----gaeLIVRCQGYM
2vhh 182: AVVIIsng--rylgkHRKhhpvrvgd--fnRstYmeGatghpV-feTefgkLAVNIcyGRhhpqnWmPGLn-----gaeIVFNP3Aati
--> <-b5-> <á4> <b6> <b7> <--á5--> <-b8->

<-----A-----> <-----C-----> # #
Nit1 182: AG-----EGKLEQWRLLAQARALLSTQYIILACQADPTAAGVEAVQGAP-----TCLGHSMIVSPLGVPLSEAGS--APPELLI
Nit2 173: GD-----ETSVPGLILPARAVEENGLITLAYANHCGP-EGGLVET-----GGSVVVGPAGCPLGELGV--EPGLLV
Dac521205: RETWQSTIRHIALEGRCFVLSANQY-----VTKDMYPKDLACYDELASSPEIMSRGSAIYVGLGEYVAEPVFG-KEDIII
RrcJ1 193: SILYQPEVPAP--GVDAQLTATRMVALEGGQFFVVTQV-----VPEAHEFFPCDNDQQRKLI--GRGGGFARIILGPDGRDLATPLAEDEGILLY
1j31 174: mpyAprampirAleNcVYITADRV--geerg-----lKfIGkSLIASPkaevLSiAset-eeEigv
1f89 196: tv--tGplhwhllArsrAvdnqYVVMCLC3pAmIqssyha-----yGhSIVVDPPrGkivaEAge-geeIiy
1Ems 188: IntGlahWetLlraRAieNcYVVAAGTgahHpkrg3y-----GhSMVVDpGavvaqC3e-rvMcf
1Krz 199: thnPpv--pqhdhltshhllsmqagSyqGAWSAAGKV--gmEen-----CmlLGHSCIVAPTGeivaIpttl-edeVIt
1uf5 199: thnPpv--pqhdhltshhllsmqagSyqGAWSAAGKA--gmEen-----CmlLGHSCIVAPTGeivaIpttl-edeVIt
2K11 177: psarayaWkTLlraRAieNcFVAAVNR--VgVdngq-----lhYaGDSAVIdfLgqqveire-geqvvt
2dyu 194: tqv--ndqWiltnrSNAwhNIMYTVSVNLACydnvfy-----yFEGQICnfdGttlvqghr-npweiVt
2usy 194: Yp-----akdqVmmAkamAwaNnCYVAVANA--AgfDgv-----ysYFGH3aIIGfdgrtlgeCge-eeemgiQY
2plq 194: YP-----AkeQQimMAkAMANNNTYVAVANA--TgfDgv-----YSYFGH3aIIGFDGrTLgeCgT-eeemGIQY
2vhh 262: grls-----eplWsieArNAaIANSYFTVPINR--VgtEqfpeYtsgdgnkahkeFpGfyG3SYVAAPdgSRTPsLsr-dkdGLLV
<-----á6-----> <-b9-> <b10> <b11> <b12> <b13> <-b

<C> <-A-->
Nit1 253: AELDPELVSRTRIVFLRNARQL
Nit2 234: VDLPDQSQDAGSDSADYLDQRRAELEHNRNI
Dac521280: AELDMKQIAYSQFDFDPVGHYARPDPVKLLVNVKEKKTIEWKN
RrcJ1 278: ADIDLSAITLARQAADPVGHYSRPDLVLSLNFNRQHTTPVNTAISTIHATHTLVPSQSGALDGVREINGADEQRALPSTHSDETDRATASI
1j31 233: veidlnlArnkrlndmndifkdrreeyyfr
1f89 259: aeLdpevIesfrqavpltkqrrf
1Ems 251: aeIdLsyVdtlremq-pvfshrcsdlytIhineksset
1Krz 271: aaVdLdrcrcleRehiFnfkhrqpqhygliae1
1uf5 271: aaVdLdrcrcleRehiFnfkhrqpqhygliae1
2K11 239: ttIsaanLaehrarfpamldgdsfvlg
2dyu 256: geIyPkmAdnArIswglenniynlghrgyvakpg-GehdagltyikdlaagkyklpWedhmkikdgsiyypttgrgfrgk
2usy 256: AQLSlsqIrdRknaQSQMHLFKLLHRGYtGlinSgegdRGAecPFdfYrtvwtDaekarenverItrsttGvaqcpvgrlpyegLEKEA
2plq 256: AEF81sQIrdRknaQSQMHLFKLLHRGYtGlinSgegdRGAecPFdfYrtvwtDaekarenVekiTrsttVGTaeCpiqgIpnegKTKELGV
2vhh 341: VeLDLnlcrqvkdfwgrmtqrVplyaesfkakegfrpqiiKetQFPFGDDDDKHHHHHHHSG
14-><-á7-----> <á8> <-á9-> <-á10-><-á11-----> \

```

Figure 3.4 Multiple alignment of Nit1 and Nit2 protein sequences with known members of the nitrilase superfamily. The protein sequences of Nases of *G. pallidus* DAC521 (Dac521, accession no ABH04285) and *R. rhodochrous* J1 (RrJ1, Accession no BAA01994), and the 10 members of the nitrilase superfamily for which structural information is available (see Table 1.3). The predicted secondary structure of Nit1 and Nit2 is included in their sequences with α -sheets (blue) and α -helices (red). The secondary structural elements identified for 2plq (Kimani *et al.* 2007) are indicated in the bottom line. The conserved catalytic residues (CEK) are shown in a box outline. The additional glutamate catalytic residue is in bold and double underlined. # indicates the locations of the catalytic residues and four glycine residues that are conserved in all members of the nitrilase superfamily. The conserved sequence motif 'DP / FXGHY' in the tail region of the spiral forming Nases is in bold and underlined. The approximate regions of the interacting surfaces of Nases, namely 'A', 'C', 'D' and 'E' are indicated on the top line. The alignment was kindly provided by Dr. Robert Thuku (University of Cape Town). Other features in the alignment were adapted from Thuku *et al.*, (2008).



3.3.7 Assignment of Nit1 and Nit2 to a branch of the nitrilase superfamily

While Nit1 and Nit2 conserved the catalytic residues and the characteristic structural folds of known members of the nitrilase superfamily, it could not be established to which of the 13 branches of the nitrilase superfamily these enzymes belonged.

Pace and Brenner (2001) developed two methods by which members of the nitrilase superfamily could be assigned to a branch. The first method uses BLAST and an E-value cut-off of 1×10^{-25} . Thirteen local BLAST databases were created using the recommended representative nitrilase of each branch as described in the supplementary data of Pace and Brenner (2001). Nit1 and Nit2 were used as protein queries for the BLAST databases and hits with E value smaller than 1×10^{-25} were indicated with a plus sign (+) (Table 3.6). Although Nit1 and Nit2 had positive hits for Branch 10, their E-value was just bordering the E-cut off score (Table 3.6). Nit2 also had positive hits of similar magnitude with branches 6 and 11. In general this was a rapid method to assign the two

unknown nitrilases to one of the branches of the nitrilase superfamily, the local BLAST database lacked sufficient characterised sequences.

The second method was to compare the signature sequence that flanked the catalytic triad (EKC), which are conserved in each branch of the nitrilase superfamily (Pace & Brenner, 2001). A scoring system was created to calculate the percentage match of the signature sequence surrounding the catalytic residues with those of Nit1 and Nit2. The residues surrounding the Nit1 catalytic triad had the high percentage match to branch 13 (92%), followed by branch 10 (79%) and branch 9 (78%). Nit2 also had match to branch 13 (92%), followed by branch 9 (78%).

Table 3.6 Alignment of conserved signature sequences of branches of the nitrilase superfamily with Nit1 and Nit2. Table was adapted from Pace and Brenner (2001).

Branches	38-42				116-122				152-160				Nit1		Nit2	
	F	P	E	A	Y	D	K	I	A	T	C	Y	Sequence BLAST	Signature sequence conservation	Sequence BLAST	Signature sequence conservation
Nit1	F	P	E	A	Y	D	K	I	A	T	C	Y	-	59%	-	45%
Nit2	T	P	E	L	Y	Q	K	V	L	V	C	Y	-	62%	-	51%
1 Nitrilase	f	p	e	a	h	r	k	i	l	v	c	w	-	63%	-	56%
2 Aliphatic Amidase	F	P	E	Y	Y	R	K	I	i	I	C	d	-	77%	-	68%
3 N-terminal Amidase	F	P	E	.	Y	r	K	.	.	I	C	M	-	37%	-	26%
4 Biotinidase	F	P	E	D	Y	r	K	.	F	t	C	F	-	68%	+	45%
5 Beta-ureidopropionase	.	Q	E	A	.	R	K	N	N	I	C	Y	-	71%	-	53%
6 Carbamylase	F	p	E	L	Y	R	K	I	f	I	C	N	-	78%	-	78%
7 Pro. NAD+ Synthetase	f	P	E	L	.	.	K	.	.	I	C	E	-	79%	+	64%
8 Euk. NAD+Synthetase	G	P	E	L	R	p	K	M	E	i	C	E	-	71%	+	71%
9 ALP N-acyltransferase	w	p	E	.	.	.	K	.	.	i	C	y	-	67%	-	59%
10 Nit and NitFhit	L	P	E	.	y	r	K	.	.	i	C	Y	+	92%	+	92%
11 NB11	.	q	E	L	Y	R	K	.	.	i	C	w	-	71%	+	71%
12 NB12	F	P	E	I	Q	y	K	I	q	I	C	Y	-	67%	-	59%
13 Non-fused Outliers	I	P	E	.	y	r	K	.	.	i	C	y	92%		92%	

However, according to this method of analysis no enzymic function could be attributed to the two putative nitrilases. Branch 13 consisted of mainly uncharacterised enzymes that did not fit into any of the 12 branches assigned (Pace & Brenner, 2001). Branch 10 enzymes are represented by the Nit domain of the NitFhit fusion protein, but no enzyme function has been assigned to this domain (Brenner, 2002, Pace *et al.*, 2000). Apolipoprotein N-acyltransferase

proteins form the branch 9 enzymes, but these have a hydrophobic N-terminal domain and their protein sequences were an average of 510 residues (Pace & Brenner, 2001).

The data presented re-affirmed the suggestion that Nit1 and Nit2 could be novel Nases of the nitrilase superfamily.

3.3.8 Comparison of Nit1 and Nit2 homology models with known structures of the nitrilase superfamily

Since Nit1 and Nit2 shared the same conserved structural folds, the atomic structures of nitrilases could be used as templates to build putative 3D models of these two proteins. Such 3D models could be used for comparison with known structures and to infer functional information.

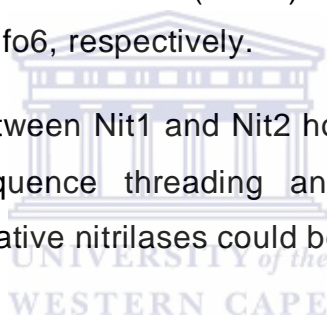
Meta Server (Kajan & Rychlewski, 2007) threading of Nit1 and Nit2 protein sequences only retrieved structures of members of the nitrilase superfamily to be used as templates. The 3D-Jury score (Ginalski *et al.*, 2003, Kajan & Rychlewski, 2007) of Meta Server indicated that 1fo6 was the best template to build Nit1 homology model using MODELLER (Sali & Blundell, 1993). In addition, 1uf5 was the most suitable template for Nit2.

Nit1 homology model was evaluated using RAMPAGE (Lovell *et al.*, 2003) that plots the stereochemistry of residues on a Ramachandran plot (Figure 3.5). The percentage of the residues of Nit1 homology model in the favoured, allowed and outlier region were 92.3, 5.8 and 1.8%, respectively (Figure 3.5, Nit1). In addition, the generated Ramachandran plot values for Nit2 were 96.6, 2.3 and 1.1%, respectively (Figure 3.5, Nit2). The validation of Nit1 and Nit2 final homology models indicated that these were suitable for 3D comparative analyses. Residues falling within the outlier region of Nit1 (P177, D212, A224 and P12) and of Nit2 (P165, E175 and S247) were all located on the N-terminal, external loops and C-terminal regions. Since known structures of the nitrilase superfamily are highly conserved, it was unlikely that the side chains of these outlier residues did not disturb the basic topology of the protein. The

Ramachandron plots for 1uf5 and 1fo6 were obtained for comparison with the Nit1 and Nit2 homology models (Figure 3.5). The plots of Nit1 and 1uf5A showed that the majority of the residues were in favourable regions, similar to those observed for the crystal structure (Figure 3.5). However, there was a difference in residues in the region of the α -helix fold (region 20,-50: -135,-45). These differences could be possibly due to errors in the alignment, improper orientation of side chains and variability in the loop regions, which leads to poor fit and consequently, poor stereochemistry in the model. The same results were observed between Nit2 and 1fo6 (Figure 3.5).

3D comparative analysis of Nit1 and Nit2 homology models with structure Protein Data Bank (PDB) were searched using SSM. Nit1 and Nit2 shared significant 3D similarity scores with only structures of DCases. The homology models of Nit1 and Nit2 shared low sequence identities (<25%) and a deviation of C_α rmsd of 1.1 and 1.2 Å with 1uf5 and 1fo6, respectively.

Despite the high C_α rmsd between Nit1 and Nit2 homology models and DCases, the data from protein sequence threading and 3D comparative analysis suggested that these two putative nitrilases could be unique DCases.



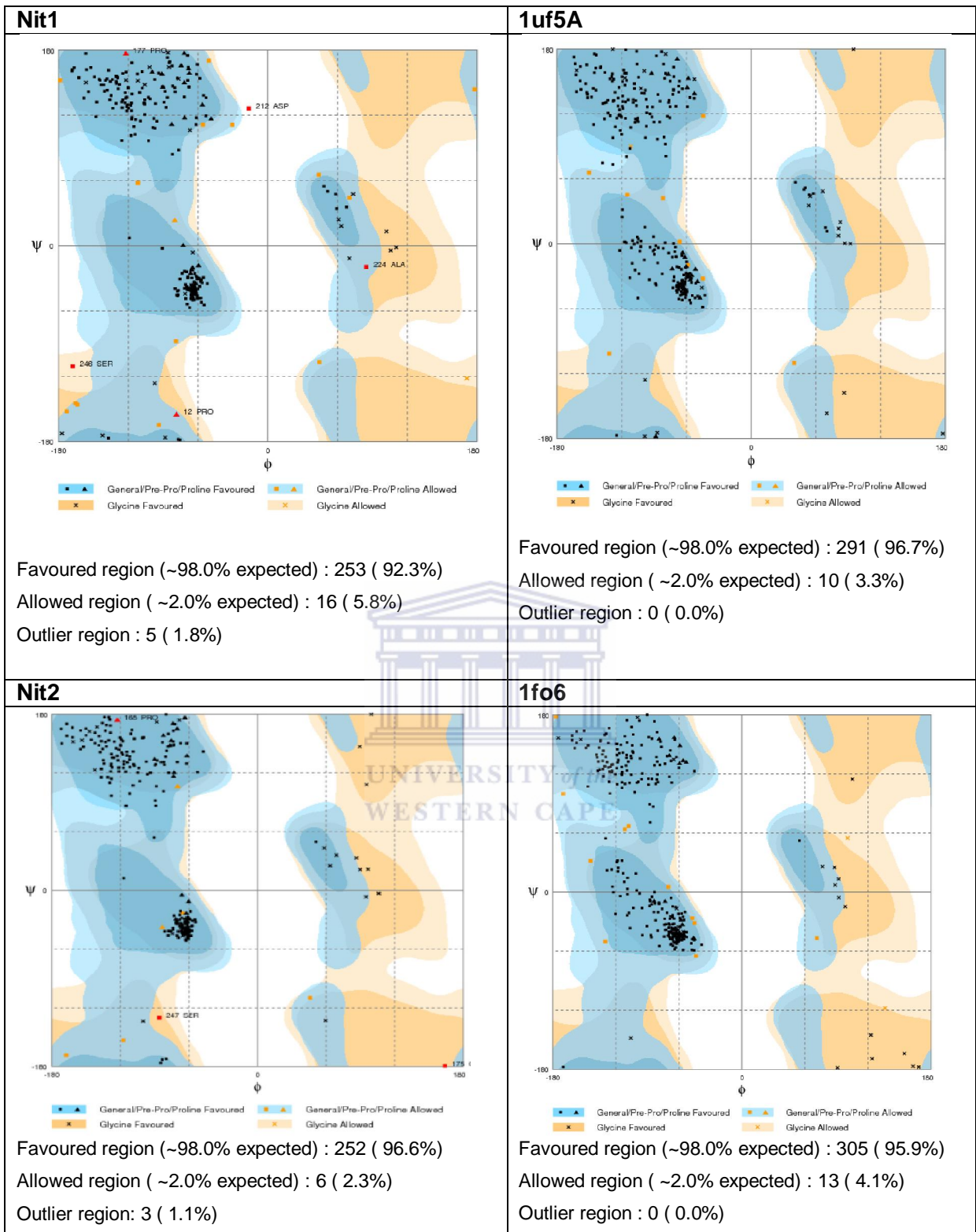


Figure 3.5 Ramachandran plots for the Nit1 and Nit2 homology models and their structurally similar DCases.

3.3.9 Description of Nit1 and Nit2 homology models

Since the homology models of Nit1 and Nit2 shared structural similarity with all DCase structures, the detailed structure of 1fo6 (Wang *et al.*, 2001) was used for comparison with both Nit1 and Nit2.

Figure 3.6 panel A and B shows Nit1 and Nit2 respectively superimposed on 1fo6. The superimposition of Nit1 homology model showed that this protein had a truncated C-terminal region (Figure 3.6 A, panel A, top figure). 1fo6 had 303 aa while Nit1 had 276 aa. The 263 aa Nit2 homology model superimposed on the C-terminal region of 1fo6, but did not share similar α -helices in this region (Figure 3.6 panel B, top figure).

The monomers of 1fo6 form a tight dimer along the A surface with mostly hydrophobic interactions occurring between residues located on the α 5 and α 6 helices and the C-terminal region (Wang *et al.*, 2001). Nit1 and Nit2, despite their low sequence identities, shared a similar hydrophobic A surface with 1fo6 (Figure 3.6, panel A and B). The side chains of Nit2 homology model residues A248, A256, L263, W262 that superimpose with I286, P295, L300, I301 1fo6 are all hydrophobic (Figure 3.6, panel B, C-terminal). The C-terminal region of Nit1 homology model was truncated with only two hydrophobic residues V267 and L270 superimposing I286 and F287 of 1fo6 (Figure 3.6, panel A, C-terminal figure). Similar results were found for the superimposed reported side chains of residues lining the α 5 and α 6 helices of 1fo6 with those of Nit1 and Nit2 (Figure 3.6, panel A and B, H5 and H6 panels).

Although Nit1 and Nit2 shared low sequence identity with 1fo6, they were structurally superimposable and although the side chains were generally different, they shared many of the same side chain properties. The similar A surface between Nit1, Nit2 and 1fo6 confirmed that the two putative nitrilases monomers would interact forming dimers, a characteristic found in all known structures of the nitrilase superfamily.

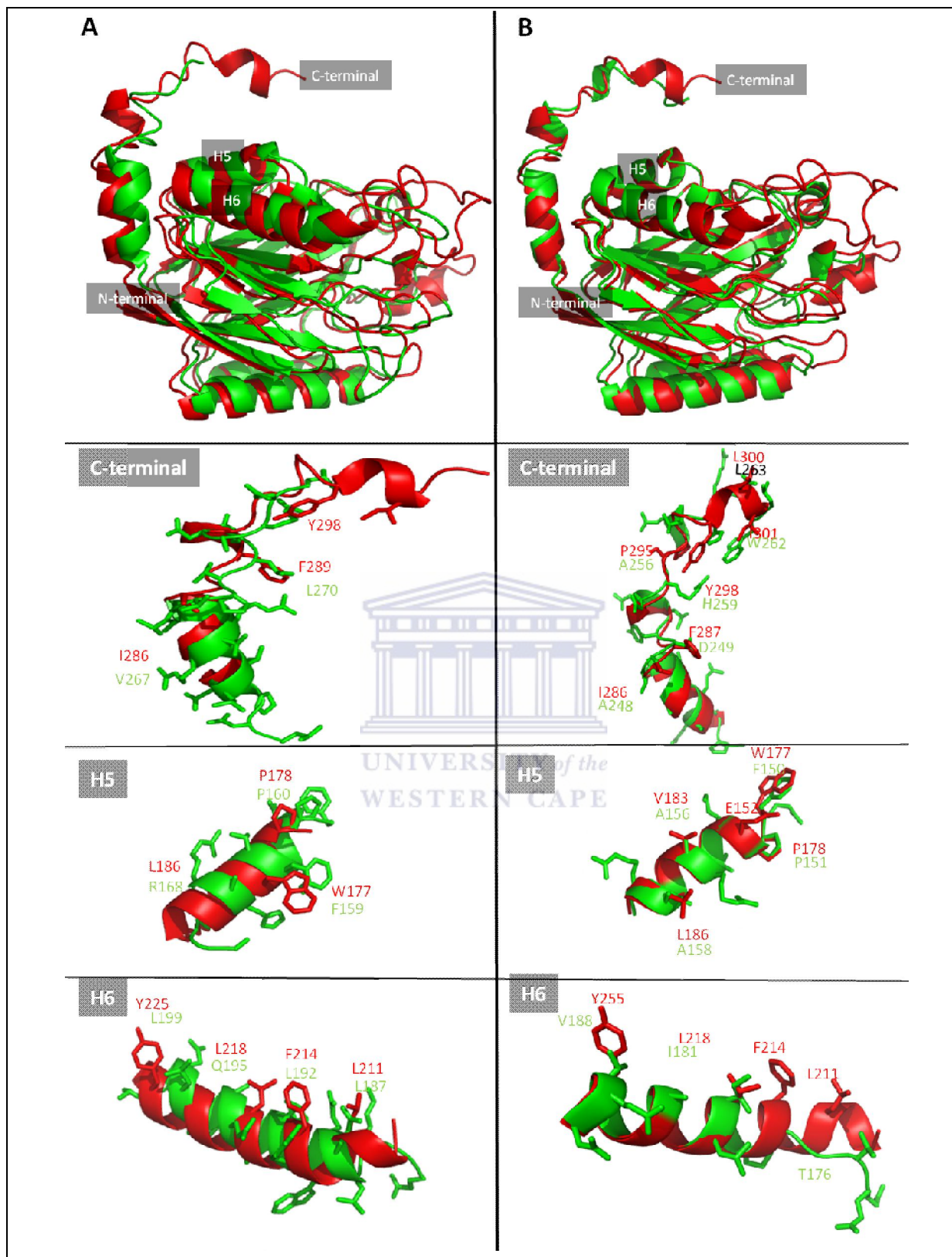


Figure 3.6 Superimposition of Nit1 and Nit2 homology models on 1fo6. The structure and residues labels are shown in green for Nit1 and Nit2 homology models and in red for 1fo6. Only the side chains of 1fo6 that were implicated in intersubunit interactions along the A surface as described in Wang *et al.*, (2001) are shown.

The catalytic residues of 1fo6 (E47,C172,K127) were located deep inside a cleft, which was lined with mostly polar residues (F53, P131, H144, N173, R175, R176, N197, T198, P199, and N202) (Wang *et al.*, 2001) (Figure 3.7 panel B, 1fo6). These residues lining the cavity provided a suitable environment for the docking of substrates, in particular carbamoyl compounds for DCases (Wang *et al.*, 2001). A molecular surface representation for 1fo6, Nit1 and Nit2 is shown in panel A of Figure 3.7. The catalytic site of 1fo6 was described as small and deep (Wang *et al.*, 2001) and it appeared that the active site of Nit1 was of similar dimensions (Figure 3.7, panel A, compare 1fo6 with Nit1). Nit2 had a large oblong catalytic site (Figure 3.7, panel A, compare Nit2 with 1fo6 and Nit1), which appeared much larger than that of Nit1 and 1fo6.

The residues lining the cavity of Nit1 were selected for their superimposition on 1fo6. Since the side chains lining the catalytic site for Nit2 were found not to superimpose on those of 1fo6, the residues lining the cavity were predicted from the model. Residues lining the cavity for Nit1 were F46, L121, F127, Y155, R158, S179, W180, E184, A1825, and T198 (Figure 3.7, panel B, Nit1) and for Nit2 they were Y46, Y115, P117, E118, Y146, T169, A170, L171, A172 and E175 (Figure 3.7, panel B, Nit2). Of these 11 residues, 82% are polar for 1fo6, 45% for Nit1 and 64% for Nit2. The differences in polar residues along the dimer interface might suggest a weaker interaction between two monomers of Nit1 and Nit2.

Most importantly, the three histidine residues (H129, H144, H215 for 1fo6) that are conserved in DCases and have been implicated for the catalysis of carbamoyls (Wang *et al.*, 2001) were different for the two putative nitrilases. Only H120 and H129 of Nit1 and 1fo6 superimpose, respectively. Other residues of Nit1 (except for H120) and Nit2 superimposed the three histidine residues of 1fo6 (data not shown). The data suggested that Nit1 and Nit2 could be unique types of DCases that had preferences for different types of carbamoyl substrates, or the putative nitrilases were not DCases.

Since the location of the four catalytic residues are conserved in structures of the nitrilase superfamily (Kimani *et al.*, 2007), the distances between three catalytic residues of Nit1 and Nit2 homology models were measured for comparison with 1fo6 (Figure 3.6, panel C). The total sum of distances amongst three residues of

1fo6, Nit1, and Nit2 were 14.03, 15.18 and 30.73 Å, respectively. The large distances obtained between the catalytic residues of Nit2 suggested that the active site of the homology model might be incorrectly constructed.

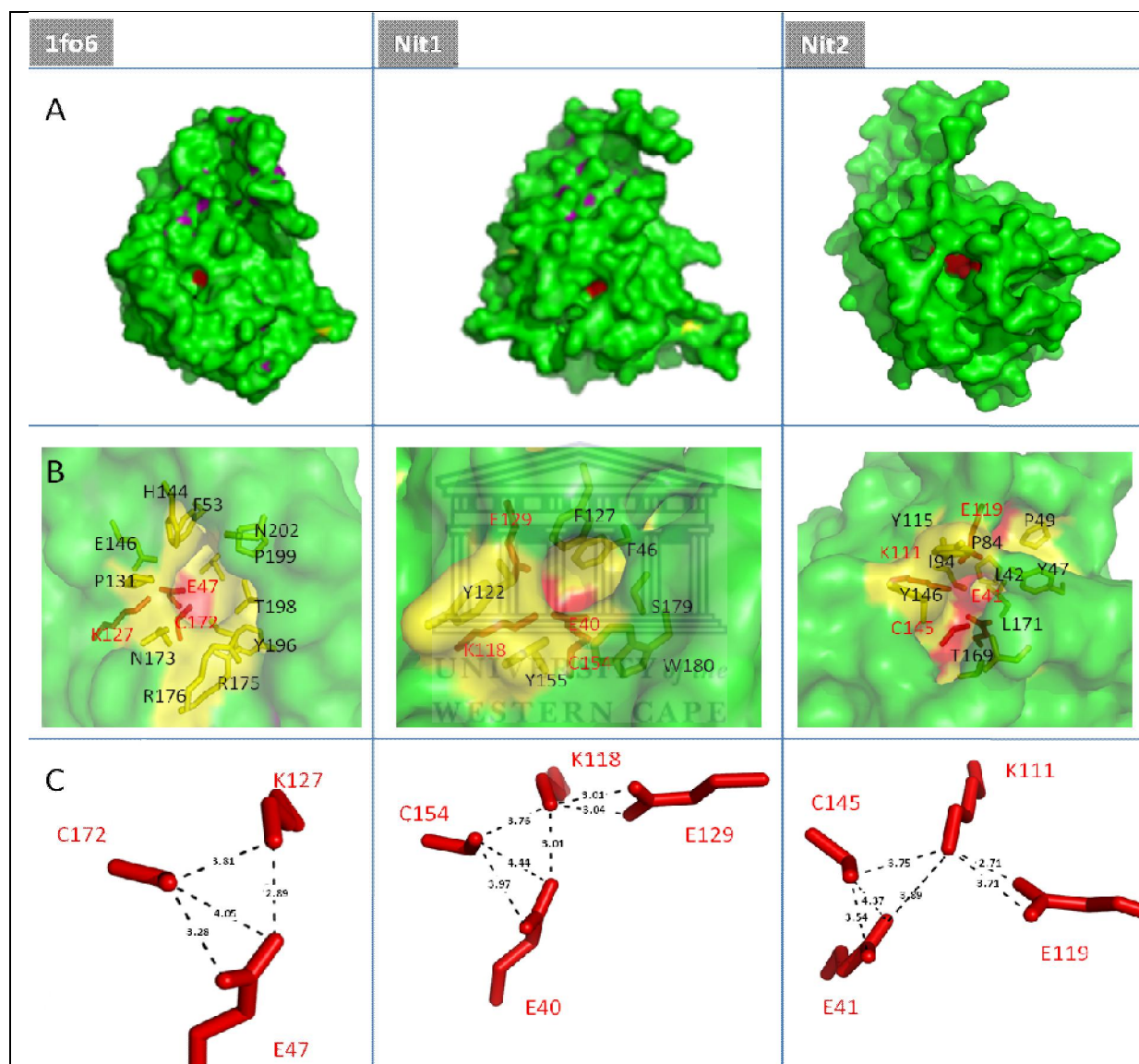


Figure 3.6 Catalytic cleft of 1fo6 and homology models of Nit1 and Nit2. Panel A, surface representation 1fo6, Nit1, Nit2 in green with the catalytic site in red. Panel B, residues lining the catalytic site of 1fo6, Nit1 and Nit2. Catalytic residues (EKEC) are shown in red. Panel C, represents the residues of the catalytic residues of 1fo6, Nit1 and Nit2 with distances between side chains measure in Å. Only three catalytic residues are shown for 1fo6 (Wang *et al.*, 2001).

3.4 Discussion

The objectives of the work described in this chapter were to identify the gene(s) and characterise the deduced protein sequence(s) that were responsible for the nitrile hydrolysing activity of *Arthrobacter* AN6, *Psychrobacter fozii*, *Pseudomonas* and *Nesterenkonia* AN1.

3.4.1 Screening for nitrile hydrolysing gene(s)

(i) Molecular screening of isolates for NHases

Primers designed were optimised in three ways for the PCR amplification of NHases: (i) The consensus sequence of a ClustalW alignment was generated from the latest databases of NHase α -subunit protein sequences; (ii) Two pairs of degenerate primers were designed; (iii) Inosine was used to decrease the degeneracy of the primers. Although the touchdown PCR methodology successfully increased the specificity of the primers in PCR trials, there was amplification of non-specific bands of the expected size, especially for the *Nesterenkonia* AN1.

In future, to verify cloned amplicons before sequencing, an extra PCR step should be carried out. This PCR could use non-degenerate primers specific for either the Fe or Co-type binding domain of NHase α -subunits in conjunction with the both the cloning vector primers. Only the clones with positive amplicons would be sequenced.

The psychrotolerant *Arthrobacter* AN6 was the only isolate that had a Fe-type NHase. The translated protein sequence was identical to that of *R. erythropolis*, which was used as a control. *R. erythropolis* strains are known Fe-type NHase producing strains (Brandao *et al.*, 2003). The deduced protein sequences of the amplicons for both isolates were identical to that of *R. erythropolis* ANT-AN0007 (Accession number AAP57640), which was isolated from lake sediment in

Antarctica (Brandao *et al.*, 2003). This strain was reported to utilise acetonitrile and benzonitrile as the sole nitrogen source for growth (Brandao *et al.*, 2003). It was suggested that horizontal gene transfer (O'Mahony *et al.*, 2005) might have occurred between the two species, which might account for the sequence identity.

(ii) Genomic library screening systems

Three screening systems were developed to screen genomic DNA libraries for nitrile hydrolysing genes.

Aminoacetonitrile screening system

It was shown that the transformation of a recombinant NHase in *E. coli* JK81 cells was insufficient for the strain to grow on minimal medium containing aminoacetonitrile. This suggested that *E. coli* JK81 lacks an amidase capable of converting aminoacetamide to release glycine for this complementation assay to function successfully. The co-expression of an aminoacetamide hydrolysing amidase with the NHase or the expression of a nitrilase was suggested as alternative controls.

Two additional screening systems were developed, based on the capability of *E. coli* strains to utilise nicotinamide as a sole nitrogen source and to hydrolyse pyrazinamide to a readily detectable product (Frothingham *et al.*, 1996).

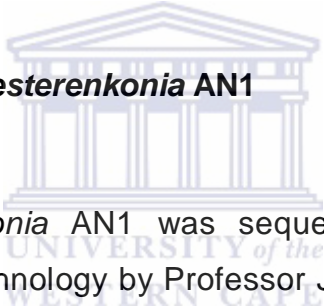
Pyrazinecarbonitrile assay

It was shown that the colourimetric detection assay was best suited for liquid cultures. Only the liquid cultures of cells expressing an active Nase had a detectable colour reaction. To screen a genomic DNA library in liquid LB supplemented with pyrazinecarbonitrile, a 96-well plate could be used with multiple *E. coli* transformants inoculated into each well. Cultures that are positive for pyrazinecarbonitrile hydrolysis could be plated out and further screening of single colonies for pyrazinoic production could be carried out.

3-Cyanopyridine screening system

This complementation screening system was used to screen the genomic DNA library of *Nesterenkonia* AN1, since this strain utilises 3-cyanopyridine as the sole nitrogen source for growth. Several *E. coli* clones grew on minimal media supplemented with the nitrile, suggesting that a functional nitrile hydrolysing gene was present. Although one clone was confirmed to have activity on benzonitrile and acetonitrile, no plasmid that resembled the cloning vector could be extracted. It could not be determined whether these were contaminating plasmids or whether the *rec* activity associated with *E. coli* ArcticExpress strain might have caused plasmid instability (Bi *et al.*, 1995). Other *rec* negative strains of *E. coli* are available and should be explored for compatibility with this screening system.

3.4.2 Putative nitrilases of *Nesterenkonia* AN1



The genome of *Nesterenkonia* AN1 was sequenced and assembled using Illumina DNA sequencing technology by Professor Jasper Rees, University of the Western Cape. Two ORFs of 828 bp and 789 bp, coding for putative Nases (Nit1 and Nit2) were detected. The protein sequences of Nit1 and Nit2 had significant sequence conservation (~50% identity) only with proteins found in *Arthrobacter*, *Kocuria*, and *Micrococcus* species, which belong to the same family, *Micrococcaceae*. Several genomes have been sequenced for members of this bacterial family. However, there was no conservation of ORFs flanking the two nitrilases genes within the other genomes. The nitrilases found in *Arthrobacter* strains have been annotated as nitrilase/ cyanide hydratase and apolipoprotein N-acyltransferase (see accession numbers in Table 3.5).

An alignment of Nit1 and Nit2 protein sequences with characterised members of the nitrilase superfamily was used to determine their relatedness. Despite the low sequence conservation (<25% identity) between Nit1 and Nit2 and members of the nitrilase superfamily, these putative proteins conserved the catalytic residues (EKEC) and the four glycine residues (Thuku *et al.*, 2009). In addition,

the predicted secondary structures of Nit1 and Nit2 monomers have the fold that is characteristic of the nitrilase superfamily. However, it could not be determined from this alignment to which branch of the nitrilase superfamily these enzymes belonged. For example, Nit1 and Nit2 did not share the extended C-terminal region associated with spiral forming Nases and the aliphatic amidases. The assignment of Nit1 and Nit2 to a specific branch of the nitrilase superfamily could not be determined using the two methods described by Pace and Brenner (2001). Alternatively, threading and modelling of Nit1 and Nit2 protein sequences suggested that they were most similar to structures of the DCases.

The A surface and the catalytic cleft of 1fo6 (DCase from *Agrobacterium radiobacter* (Wang *et al.*, 2001)) were compared by superimposition on Nit1 and Nit2 homology models. The homology models of Nit1 and Nit2 shared a similar A surface comprising of hydrophobic residues located on the 5 and 6 helices and the C-terminal region. The data suggested the monomers of the Nit1 and Nit2 associate along the A surface to form a sandwich. This sandwich architecture is conserved in known structures of the nitrilase superfamily.

Of the two homology models, the Nit1 catalytic site was the most similar to that of 1fo6. In addition, the location of the four catalytic residues was similar between the two structures, which are conserved in known structures of the nitrilase superfamily (Kimani *et al.*, 2007). The large distance obtained between the four catalytic residues of Nit2 homology model suggested that the area of the catalytic cleft region was not modelled correctly. Most importantly, the structural models of Nit1 and Nit2 did not conserve the three histidine residues that were implicated in the DCase hydrolysis of carbamoyls (Wang *et al.*, 2001).

Although the Nit1 and Nit2 homology models shared overall structural similarities with DCases, the differences in their catalytic sites suggested that these two putative nitrilases might either be novel DCases that have different carbamoyl substrate preferences or could belong to a different branch of the nitrilase superfamily. This could only be confirmed by expression and characterisation of the two nitrilases *in vitro*.

Chapter 4: Expression and characterisation of the two putative nitrilase proteins, Nit1 and Nit2

4.1 Introduction	98
4.2 Materials and methods.....	99
4.2.1 Cloning procedures.....	99
4.2.2 Heterologous expression	100
4.2.3 Ni-chelation chromatography	100
4.2.4 Analytical methods for recombinant expressed His-tag fused proteins	101
4.2.5 Nitrile hydrolysing activity assay.....	102
4.2.6 Determination of optimal temperature and thermoactivity.....	103
4.2.7 Determination of optimal pH.....	103
4.2.8 Substrate specificity.....	103
4.2.9 Determination of kinetic constants.....	104
4.2.10 Acyl transfer activity assay.....	104
4.3 Results.....	105
4.3.1 Truncation of the Nit2 ORF	105
4.3.2 Expression, purification and characterisation of His-tagged Nit1 and Nit2 proteins.....	106
4.3.3 Determination of substrate range for ChNit1 and NhNit2.....	109
4.3.4 Determination of initial rate for NhNit2 using acetamide.....	111
4.3.5 Determination of optimal temperature.....	112
4.3.6 Determination of thermostability	112
4.3.7 Determination of optimal pH.....	114
4.3.8 Determination of different amide compounds on NhNit2 activity.....	115
4.3.9 Kinetic behaviour of NhNit2 on acetamide and propionamide.....	117
4.3.10 Determination of acyl transfer activity in NhNit2.....	117
4.4 Discussion.....	118

4.1 Introduction

Two ORFs were detected in the sequenced genome of *Nesterenkonia* AN1, coding for putative nitrilases of 276 and 263 aa and referred to as Nit1 and Nit2, respectively (Chapter 3 section 3.3.3). Nit1 and Nit2 belonged to the nitrilase superfamily since they shared the characteristic monomer fold and conserved catalytic residues (EKEC). Homology models of Nit1 and Nit2 shared similarities with structures of 1fo6, a DCCase. From the structural comparison of the homology models with 1fo6, it was proposed that monomers of Nit1 and Nit2 might form dimers since they shared a similar A surface composed of two α -helices and a C-terminal region. However, both Nit1 and Nit2 homology models did not conserve the three histidine residues in their catalytic cleft that were implicated in the DCCase decarbamylation of carbamoyls (Wang *et al.*, 2001).

Since it could only be inferred from *in silico* predictions that the two putative nitrilases formed dimers and had catalytic clefts that distinguished them from DCases, the characterisation of the recombinantly expressed *in vitro* was essential to clarify their identities.

Numerous nitrilases have been purified through direct cloning and heterologous expression in *E. coli*. Ni-chelation chromatography purification of an active hexahistidine tagged fusion protein recombinantly expressed in *E. coli* had been reported for different members of the nitrilase superfamily: C-terminal hexahistidine tagged purification has been used for the nitrilase from *Synechocystis* sp. (Heinemann *et al.*, 2003), DCCase from *Agrobacterium radiobacter* (Chen *et al.*, 2005); and N-terminal hexahistidine tagged purification has been reported for four fungal cyanide hydratases from *Neurospora crassa*, *Aspergillus nidulans*, *Gibberella zeae* and *Gloeocercospora sorghi* (Basile *et al.*, 2008).

This chapter describes the cloning, expression and purification of the two nitrilase proteins and their subsequent characterisation.

4.2 Materials and methods

4.2.1 Cloning procedures

General recombinant DNA techniques were carried out as described in Appendix A. The following expression vectors, pET21a(+) and pET28a(+) (Novagen), were used for the construction of C-terminal and N-terminal His-tag fused proteins, respectively. For the PCR amplification of Nit1 ORF, the primer pairs Nit1F & Nit1R and Nit1F & Nit128R were used for cloning into pET21a(+) and pET28a(+), respectively. In addition, primer pairs Nit2F & Nit2R and Nit2F and Nit228R, were used for the cloning of Nit2 ORF into pET21a(+) and pET28a(+), respectively.

Table 4.1 Primers for the cloning of Nit1 and Nit2 ORFs from *Nesterenkonia* AN1 into pET21a(+) and pET28a(+). *Nde* I and *Xho* I recognition sites are underlined and double underlined, respectively. Amber stop codons are shown in bold.

Primer	Recipient vector(s)	Sequence
Nit1F	pET21 & pET28	5'- <u>CAT ATG CGC</u> ATT GCT GCC GCT CAG ATC ACC AC-3'
Nit1R	pET21	5'- <u>CTC GAG CTG</u> GCG GGC GTT GCG CAG CAC-3'
Nit128R	pET28	5'- <u>CTC GAG CTA</u> GAG CTG GCG GGC GTT GCG CAG C-3'
Nit2F	pET21 & pET28	5'- <u>CAT ATG CGA</u> ATC GCG CTG ATG CAG CAC ACC G-3'
Nit2R	pET21	5'- <u>CTC GAG CCA</u> GGA GCG GCT CTT CGG GCA CTT CG-3'
Nit228R	pET28	5'- <u>CTC GAG CTA</u> CCA GGA GCG GCT CTT CGG GCA CTT CG-3'

PCR amplification was performed using the Phusion™ High-Fidelity PCR kit (New England Biolabs) under the conditions described by the manufacturer. *Nesterenkonia* gDNA was prepared as described in Chapter 2, Section 2.2.3. The thermocycling conditions used for amplification were as follows: denaturation at 95°C for 30 sec followed by 2 repeated 7 cycles of denaturation at 98°C for 10 sec, 72-65°C for 15 sec, 72°C for 40 sec, 25 cycles of 98°C for 10 sec, 65°C for 15 sec and 72°C for 40 sec, and a final step of 72°C for 10 mins.

Amplicons were cloned into pJET1.2/blunt vector of the CloneJET™ PCR Cloning Kit (Fementas). pJET plasmids containing the insert were digested with *Nde* I and *Xho* I and the excised fragments of 834 bp and 1116 bp for Nit1 and Nit2, respectively, were ligated between the *Nde* I and *Xho* I sites of pET21a(+) and pET28a(+). The following plasmids generated were pET21-Nit1, pET21-Nit2, pET28-Nit1 and pET28-Nit2 (Appendix D).

4.2.2 Heterologous expression

E. coli BL21 (DE3) pLysS (Appendix C) harbouring the constructed vectors as described in section 4.2.1 was grown overnight at 37°C in 5 ml LB (Appendix B) containing 100 µg/ml ampicillin for pET21 vectors or 30 µg/ml kanamycin for pET28 vectors. Chloramphenicol was added to the cultures at a final concentration of 34 µg/ml to maintain the pLysS plasmid in *E. coli* BL21 (DE3). The overnight cultures were used to inoculate 1 litre volumes of LB containing antibiotics excluding chloramphenicol and were incubated at 37°C with shaking until the culture reached mid-log phase (OD_{600nm} of 0.5). 1 mM IPTG final concentration was added to the cultures and induction was carried out at room temperature with shaking for 4 hrs. The cells were harvested by centrifugation and were stored at -20°C.

4.2.3 Ni-chelation chromatography

The His•Bind Resin and Buffer Kit (Novagen) was used for the Ni-chelation chromatography purification of His-tag fusion proteins. Cell lysates were prepared using BugBuster® Protein Extraction Reagent plus benzonuclease (Novagen) according to the manufacturer's instructions, or by sonication. Cells were lysed at room temperature with gentle mixing for 20 mins. Lysates were centrifuged at 20 000 × g for 10 mins and the supernatant (clarified extract) was directly applied to a Ni-chelation column. For preparation of cell lysates using

sonication, cells were resuspended in 20 mM Tris-HCl (pH 8.0) and sonicated on ice in cycles of 10 secs pulse and 10 sec pause for 5 mins. Purification was followed according to the manufacturer's instructions with the exception of the elution step. Elution buffer was optimised to contain 500 mM imidazole, 500 mM NaCl and 20 mM Tris-HCl (pH 7.9). Elution of bound protein was carried out using 4 columns of elution buffer. The eluate was diluted to 5 ml with elution buffer containing a final concentration of 10% glycerol and 2 mM DTT. The eluate was dialysed overnight in a 5 mL Slide-A-Lyzer Dialysis Cassette (Thermo Fisher Scientific) in a ratio of 1:400 against 50 mM $\text{KH}_2\text{PO}_4/\text{K}_2\text{HPO}_4$ (pH 7.6), 150 mM NaCl, 10% glycerol, 2 mM DTT. The purified protein was stored at 4°C. Fractions of each step of Ni-chelation chromatography were analysed by SDS-PAGE.

4.2.4 Analytical methods for recombinant expressed His-tag fused proteins

ProtParam software from ExPASy Proteomics Server (www.us.expasy.org/) was used to calculate the molecular mass of the fusion proteins based on their amino acid sequences.

An adaptation of the SDS-PAGE (Laemmli, 1970) protocol is described in Appendix E. SDS-PAGE was used to confirm expression of recombinant His-tag fusion proteins. For SDS-PAGE analyses of expressed cells (whole cell fractions), 0.1 ml of cells were harvested and resuspended in an equal volume of gel loading buffer (Appendix E). Cells were sonicated on ice in cycles of 2 sec pulse and 2 sec pause for 1 min using a Bandelin Sonoplus HD2070 sonicator. The cell lysate was then centrifuged at 4°C for 10 mins at $10\,000 \times g$. The supernatant was mixed with an equal volume of gel loading buffer. The pellet was resuspended in 1 ml of 20 mM Tris-HCl (pH 8.0) and an equal volume of gel loading buffer added. The protein molecular weight was determined using standard protein molecular weight markers (Fermentas). Protein bands were detected using Coomassie Brilliant Blue R-250 as described in Appendix E.

Protein concentration was determined using bovine serum albumin (BSA) as a standard (Bradford, 1976). The Bradford reagent was purchased commercially

from Sigma and protein concentration estimation was carried out according to the manufacturers' instructions.

The molecular masses of the purified recombinant proteins were determined by size exclusion chromatography on a TSK-gel G4000 PW_{XL} (Tosoh BioScience) column. The column was equilibrated with 50 mM KH₂PO₄/K₂HPO₄ (pH 7.6) containing 10% glycerol and 2 mM DTT. Protein standards used for molecular mass determination were thyroglobulin (670 kDa), γ -globulin (158 kDa), ovalbumin (44 kDa), myoglobin (17 kDa), and vitamin B12 (1.35 kDa) (Sigma-Aldrich). Tobacco mosaic virus (TMV) and acetone were included in the calibration standards to determine the void volume and the geometric bed volume of the column, respectively. The mass of the native protein was calculated from its retention time based on the calculated standard curve of K_{av} versus log of molecular weights of standards. A flow rate of 0.5 ml/min was used with 0.2 ml fractions collected using a Gilson FC203B fraction collector. Protein absorbance at OD_{280nm} was measured using a Gilson UV/VIS 151 detector. The chromatographic procedure was controlled via Unicorn software (Version 3.4). Fractions with maximum protein absorbance were analysed on SDS-PAGE.

UNIVERSITY of the
WESTERN CAPE

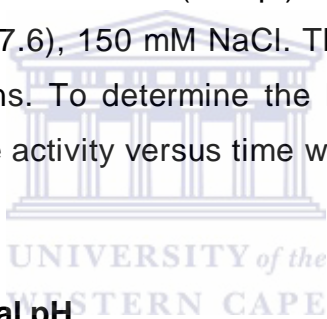
4.2.5 Nitrile hydrolysing activity assay

Enzyme activity was determined by the release of ammonia using the phenol-hypochlorite ammonia detection method (Weatherburn, 1967). A standard reaction mixture (100 μ l) contained 50 mM KH₂PO₄/K₂HPO₄ (pH 7.6), 150 mM NaCl, 2-500 mM substrate and 5 μ l of enzyme. The reaction was terminated by the addition of 3.5 vols of reagent A (0.59 M phenol and 1 mM sodium nitroprusside). Colour was developed by the addition of equal volume of reagent B (2.0 M sodium hydroxide and 0.11 M sodium hypochlorite). Ammonia release was measured spectrophotometrically at OD_{600nm} after 5 min incubation at 55°C. Control reactions were carried out without enzyme. Standards were prepared using ammonium chloride (Appendix G). One unit of enzyme activity was defined as the amount of enzyme that catalyzed the release of 1 μ mol of NH₃ per minute under standard assay conditions. All assays were repeated in triplicate.

4.2.6 Determination of optimal temperature and thermoactivity

To determine optimal temperature, reactions were carried out at the following temperatures: 4, 10, 20, 30, 40, 50 and 60°C. Aliquots of standard reaction mixture (100 µl) containing 100 mM acetamide substrate, 50 mM $\text{KH}_2\text{PO}_4/\text{K}_2\text{HPO}_4$ (pH 7.6), and 150 mM NaCl were incubated at the specified temperature for 5 min before the addition of the enzyme. Reactions were carried out for 30 mins.

To determine thermoactivity, aliquots of the enzyme were assayed after incubation at the specified temperature for 10, 20, 30 and 60 mins. The assay was carried out using a reaction mixture (100 µl) containing 100 mM acetamide, 50 mM $\text{KH}_2\text{PO}_4/\text{K}_2\text{HPO}_4$ (pH 7.6), 150 mM NaCl. The reaction was carried out at room temperature for 30 mins. To determine the half-life of enzyme activity, a plot of the logarithmic relative activity versus time was used.



4.2.7 Determination of optimal pH

To determine optimal pH, CH_3COOHNa , MES, $\text{KH}_2\text{PO}_4/\text{K}_2\text{HPO}_4$, $\text{Na}_2\text{B}_4\text{O}_7/\text{H}_3\text{BO}_3$, NaOH/glycine and $\text{Na}_2\text{CO}_3/\text{NaHCO}_3$ buffers were used for pH values of 4.5, 5.5-6.5, 6.5-8, 8-9, 9-9.5 and 9.5-11, respectively. Standard reaction mixtures (100 µl) containing 100 mM of the respective buffer (90 mM in the case of borate buffer), 150 mM NaCl, and 100 mM acetamide. Reactions were initiated by the addition of 5 µl enzyme and were incubated at 25°C for 30 mins.

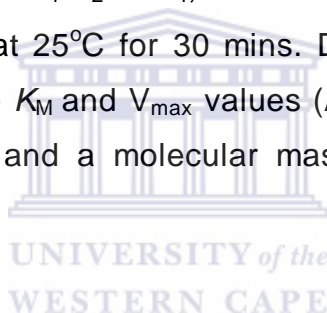
4.2.8 Substrate specificity

1M stocks of nitriles and amides were prepared in distilled water, except for L-alaninamide hydrochloride (prepared in 29% (w/v) NaOH), and hexanoamide

(prepared in 50% (v/v) ethanol). Stock solutions of L-glutamine, L-asparagine, N-carbamoyl DL-alanine, and N-carbamoyl-DL- -amino *n*-butyric acid were prepared in 50 mM $\text{KH}_2\text{PO}_4/\text{K}_2\text{HPO}_4$ (pH 7.6) to their maximum solubility (171 mM, 133 mM, 76 mM, and 68 mM, respectively). Reaction mixture (100 μl) contained 100 mM substrate (50 mM in the case of carbamoyl substrates), 50 mM $\text{KH}_2\text{PO}_4/\text{K}_2\text{HPO}_4$ (pH 7.6) and 5 μl of enzyme.

4.2.9 Determination of kinetic constants

Apparent K_M values were determined for acetamide and propionamide using the standard reaction assay (100 μl) containing various substrate concentrations (2.5- 500 mM), 50 mM $\text{KH}_2\text{PO}_4/\text{K}_2\text{HPO}_4$, 150 mM NaCl and 5 μl of enzyme. Reactions were carried out at 25°C for 30 mins. Direct plots (Cornish-Bowden, 1995) were used to calculate K_M and V_{max} values (Appendix G). k_{cat} values were calculated using ProtParam and a molecular mass of xx kDa, assuming one active site per monomer.



4.2.10 Acyl transfer activity assay

Acyl transfer reactions were performed using a modification of the method determined by Fournand *et al.*, (1998) method. A reaction mixture (300 μl) contained 100 mM substrate and 500 mM hydroxylamine in 50 mM potassium $\text{KH}_2\text{PO}_4/\text{K}_2\text{HPO}_4$ (pH 7.6). The reaction was initiated by the addition of 5 μl of enzyme and was carried out at 25°C for 2 hrs. At 30 mins, 1 hr and 2 hrs, 100 μl aliquots of the reaction mixture was mixed with 1 ml of acidic FeCl_3 (0.133 M in 0.68 M HCl). Colour development was recorded at $\text{OD}_{500 \text{ nm}}$. *G. pallidus* amidase was used as a positive control, at 55°C. Enzyme-free controls were included. All assays were performed in triplicate.

4.3 Results

For clarity, the C-terminal hexahistidine tag fused Nit1 and Nit2 proteins expressed from plasmids pET21-Nit1 and pET21-Nit2 are referred to as ChNit1 and ChNit2, respectively. Likewise, the N-terminal hexahistidine terminal tag fused Nit1 and Nit2 proteins from constructs pET28-Nit1 and pET28-Nit2 are referred to as NhNit1 and NhNit2, respectively.

4.3.1 Truncation of the Nit2 ORF

The nucleotide sequences of the Nit2 ORF inserts in plasmids pET21-Nit2 and pET28-Nit2 showed that there was a stop codon 790 bp downstream from the first base pair of the initiation codon. At position 791 bp of the insert nucleotide sequence, a T was identified rather than the G present in the sequence from the *Nesterenkonia* genome. This changes the codon of the GAG triplet that codes for the amino acid glutamate (E) to an amber termination codon (TAG). This mutation was not a sequencing error or a PCR amplification error. The error was due to the lack of overlapping contigs in the alignment for the assembly of the *Nesterenkonia* genome sequence. This truncated the Nit2 ORF to 789 bp, coding for a 263 amino acid protein. The pET28-Nit2 construct was therefore only used to express Nit2 ORF as a NhNit2 fusion protein.

4.3.2 Expression, purification and characterisation of His-tagged Nit1 and Nit2 proteins

Figure 4.1 shows the SDS-PAGE analysis of expressed ChNit1 and NhNit2 fusion proteins in *E. coli* BL21 (DE3) pLysS cells. A band migrating at ~30 kDa was visible in the induced fraction, and absent in the uninduced fraction (Figure 4.1, panel A, compare lanes I with U, respectively). In addition, a ~30 kDa band probably the NhNit2 fusion protein was also visible (Figure 4.1, panel B, compare lanes I with U). The molecular masses of the two putative fusion proteins are in close approximation to the calculated values using ProtParam; 29.9 kDa for ChNit1 and 30.1 kDa for NhNit2.

To determine that the fusion proteins were soluble, SDS-PAGE analysis was used to compare the presence of the ~30 kDa fusion protein bands in the soluble/supernatant and the insoluble/pellet fractions (Figure 4.1, panel A and B, compare lanes S with P). Both fusion proteins were present in the soluble fraction.

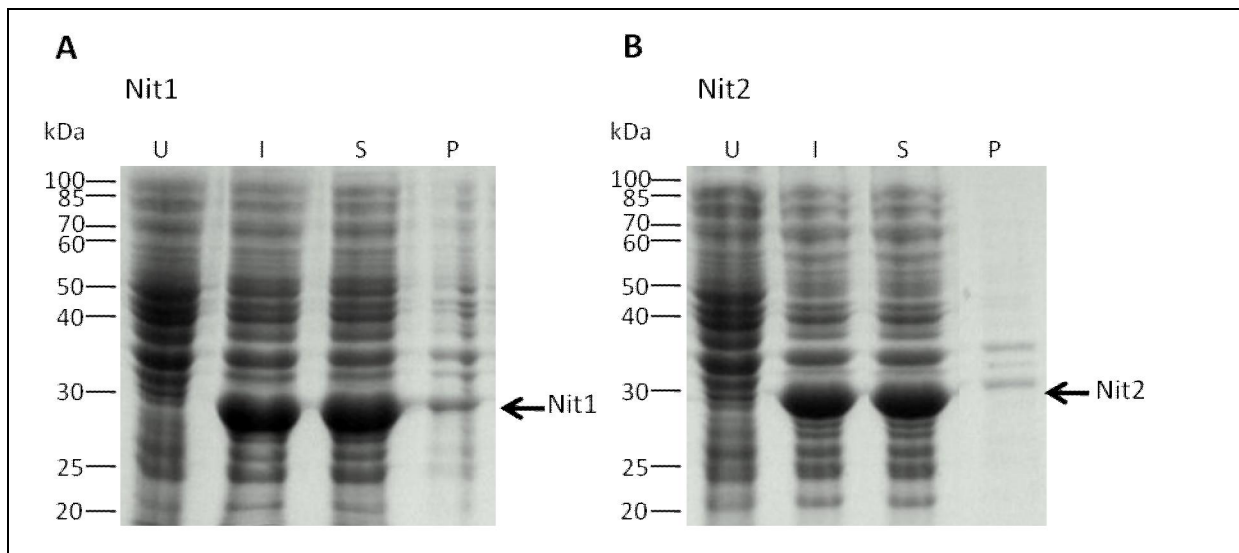
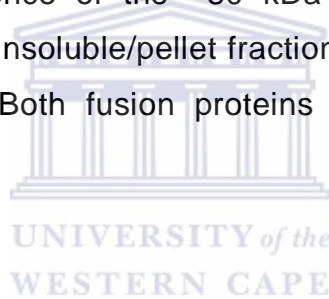


Figure 4.1 Expression of Nit1 and Nit2 in *E. coli* BL21 pLysS cells. Lanes: U, uninduced cells; P, induced cells; S, supernatant; P, pellets. The sizes (kDa) of the protein molecular weight markers, Nit1 (ChNit1) and Nit2 (NhNit2) proteins are indicated.

Cell lysates were prepared using the BugBuster Extraction Reagent (Novagen) for Ni-chelation chromatography. However, both N- and C-terminal hexahistidine tagged fusion proteins were insoluble when using this method (data not shown). Since the chemical composition of the cell lysis solution is not reported, the cause of insoluble proteins was not established. Sonication was used only for the preparation of cells expressing ChNit1. Figure 4.2 represents SDS-PAGE analysis of ChNit1 and NhNit2 purified by Ni-chelation chromatography. Both His-tagged fusion proteins bound to the Ni-chelation column with high affinity, since little expressed protein was present in the run-through fraction obtained while loading the column (Figure 4.2, panel A and B, lanes 1 and 3, respectively). *E. coli* proteins were removed using two consecutive washes containing 8 mM and 60 mM imidazole (Figure 4.2, panel A and B, lanes 2,3 and 4,5, respectively). ChNit1 and NhNit2 were eluted with high purity using an elution buffer containing 500 mM imidazole (Figure 4.2, panel A and B, lanes 4 and 6 or 7, respectively).

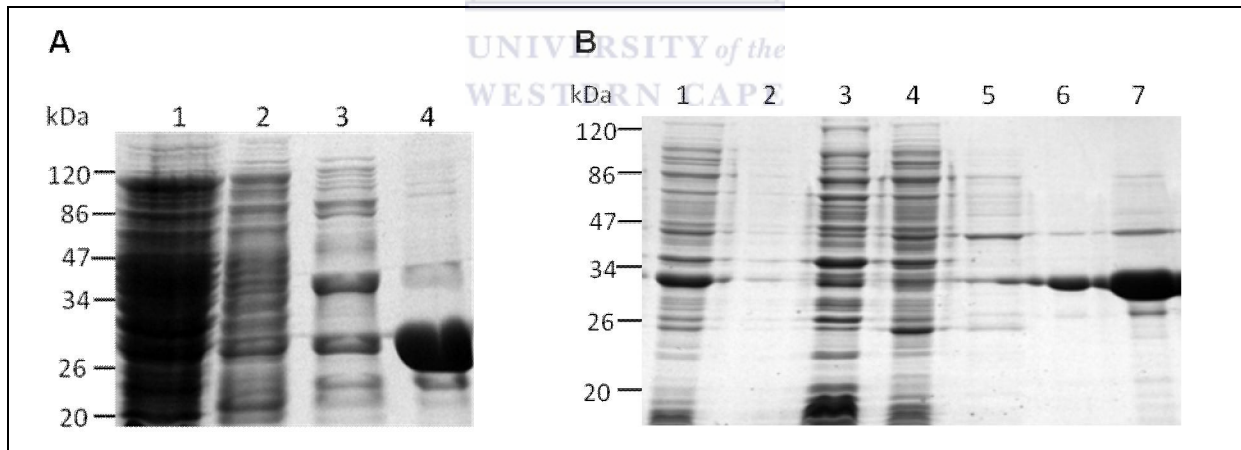


Figure 4.2 Ni-chelation purification of the His-tagged Nit1 and Nit2 (panel A and B, respectively). Panel A, Lanes: 1, cell extract after column loading; 2, 8 mM imidazole wash; 3, 60 mM imidazole wash; 4, eluted ChNit1. Panel B, lanes: 1 soluble fraction; 2, pellet fraction; 3, cell extract after column loading; 4, 8 mM imidazole wash; 5, 60 mM imidazole wash; 6, eluted NhNit2 (1 µl loaded); 7, eluted NhNit2 (2.5 µl loaded).

The relative molecular masses of ChNit1 and NhNit2 proteins were determined by gel filtration on a TSK-gel G4000 PW_{XL} column. The elution profile of ChNit1 had a single peak with a retention time corresponding to 34 kDa (Figure 4.3), similar to the values from SDS-PAGE analysis and calculated using Protparam.

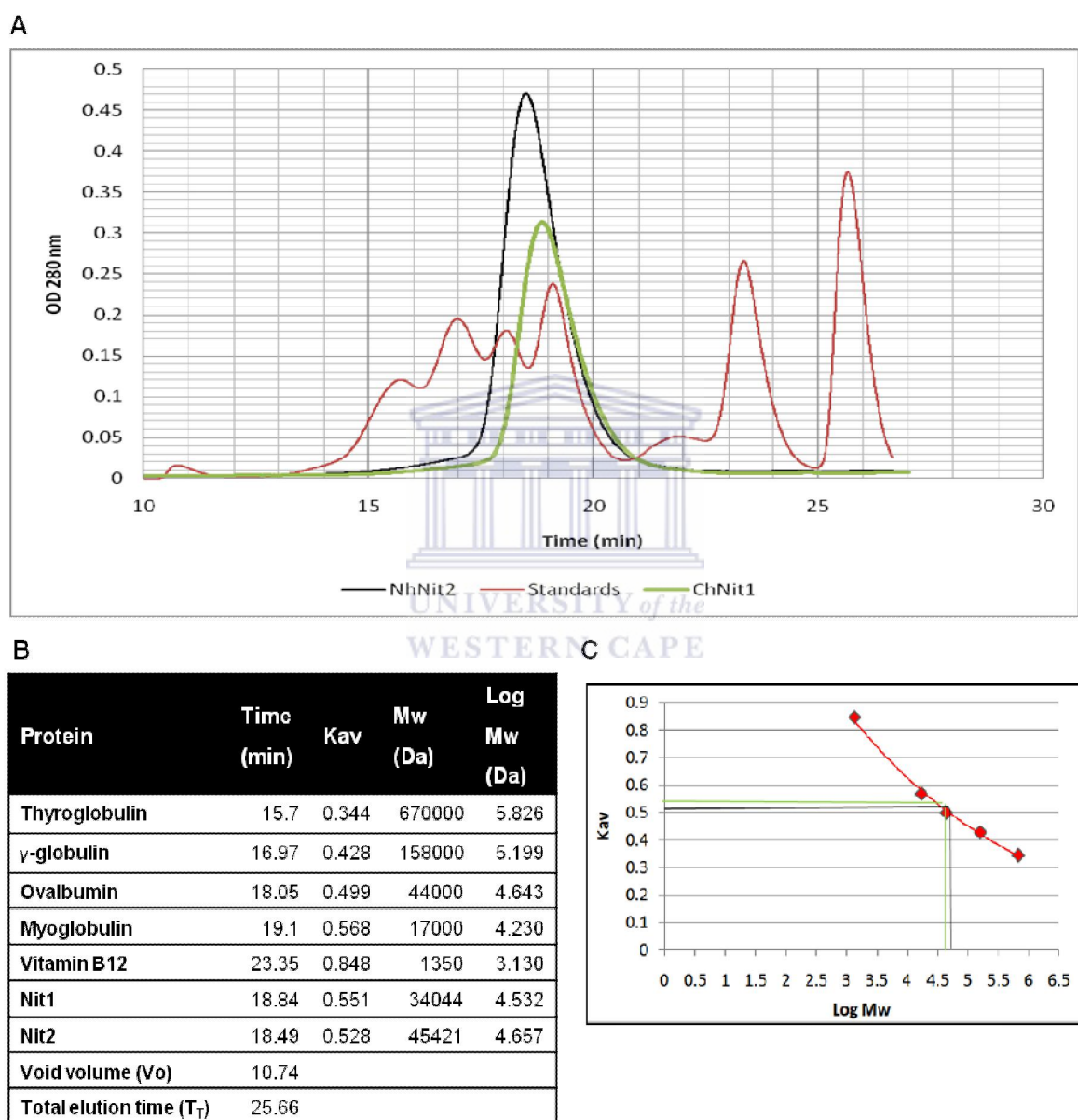


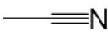
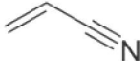
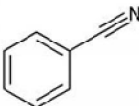
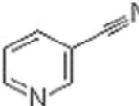
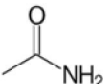
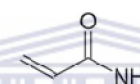
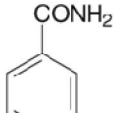
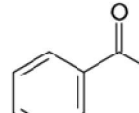
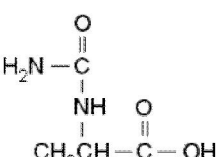
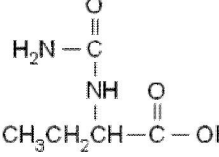
Figure 4.3 Calculation of ChNit1 and NhNit2 native molecular masses. Panel A, elution profile of ChNit1 (green), NhNit2 (black) and standards (red). Panel B, calculation of molecular weight for ChNit1 and NhNit2 using the formula $K_{av} = (x - V_0) / (t_1 - V_0)$, where x is the retention time of protein. Panel C, plot of K_{av} versus Log M_w .

The data suggested that ChNit1 exists as a monomeric protein. NhNit2 had a single elution peak (Figure 4.3), corresponded to a molecular mass of 45.4 kDa. SDS-PAGE analysis of fractions from the NhNit2 peak confirmed the presence of 30 kDa bands (data not shown). In addition, the same molecular mass for NhNit2 has been re-confirmed on a S300 column (Chapter 5, section 5.3.1). Although the molecular mass for an expected dimer for both putative nitrilases would be ~60 kDa, the data suggest that NhNit2 could be either a loosely folded monomeric protein or a highly compact dimer protein, which would affect its elution within the column.

4.3.3 Determination of substrate range for ChNit1 and NhNit2

A range of nitrile, amide and carbamoyl substrates were investigated in order to establish substrate specificity. Initial results showed that NhNit2 had maximal activity on acetamide followed by acrylamide (48% relative activity) and nicotinamide (28%) (Table 4.2). No activity for NhNit2 was obtained for nitriles or carbamoyls substrates. No detectable activity was observed for ChNit1. Consequently, NhNit2 was selected for further investigations.

Table 4.2 Determination of the substrate range of NhNit2. Activities are expressed as percentage relative to the maximum activity of acetamide (100%).

Nitriles				
Substrate	Acetonitrile	Acrylonitrile	Benzonitrile	3-Cyanopyridine
Relative activity	0%	0%	0%	0%
Structure				
Amides				
Substrate	Acetamide	Acrylamide	Benzamide	Nicotinamide
Relative activity	100%	48%	0%	28%
Structure				
Carbamoyls				
Substrate	N-carbamoyl DL alanine		N-Carbamoyl-DL-α-amino-n-butyric acid	
Relative activity	0%		0%	
Structure				

4.3.4 Determination of initial rate for NhNit2 using acetamide

The initial rate of NhNit2 activity at different enzyme loadings was determined using 100 mM acetamide as the substrate (Figure 4.4, panel A). The plot of absorbance versus amount of enzyme was linear between 2.5 and 20 μg . In addition, a plot using 5 μg of enzyme versus time was linear (Figure 4.4, panel B). All kinetic data were performed using 5 μg of enzyme over 30 mins.

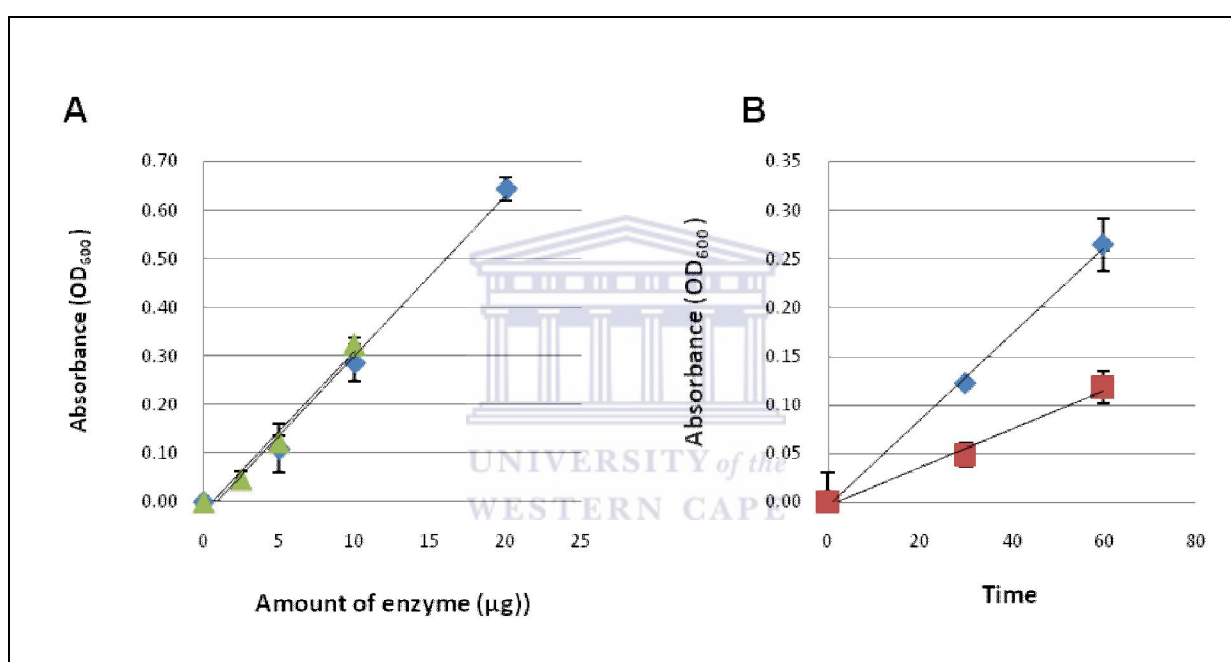


Figure 4.4 Determination of the initial rate for NhNit2 using 100 mM acetamide. Panel A, determination of initial rate using 5, 10 and 20 μg (diamonds) and 2.5, 10, 20 μg (triangles) over a reaction period of 20 mins. Panel B, determination of the initial rate over period of 30 and 60 mins using 5 μg (diamonds) and 2.5 μg (squares) of enzyme.

4.3.5 Determination of optimal temperature

Nit2 activity was investigated across a range of temperatures from 4 to 60°C (Figure 4.5). The apparent optimal temperature (T_{opt}) of NhNit2 activity is 30°C (Figure 4.5). NhNit2 retains 35% activity at 4°C, which increases gradually to 30°C (Figure 4.5). The gradual increase of activity suggests a small amount of thermal inactivation of the enzyme might be occurring. Beyond 30°C the activity decreased, suggesting susceptibility to thermal inactivation. NhNit2 is inactive beyond 50°C. The thermal activity profile is compatible with its low temperature origins.

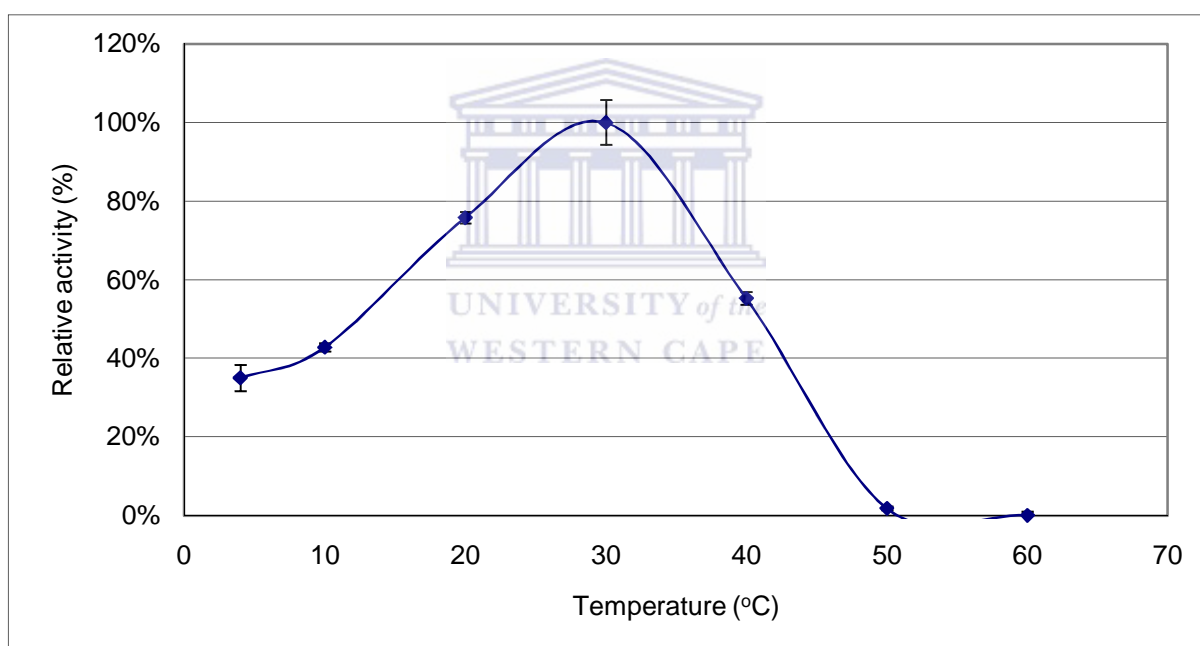


Figure 4.5 Effect of temperature on NhNit2 activity. Activities are expressed as percentages relative to the maximum activity at 30°C (100%).

4.3.6 Determination of thermostability

To determine the thermostability of NhNit2, the enzyme was incubated at 30, 40, 50 and 60°C over a period of 1 hr. Aliquots taken at 10, 20, 30 and 50 mins intervals were assayed under standard conditions (Figure 4.6, panel A). In order

to ensure that inactivation was irreversible, aliquots incubated at each temperature for 60 mins were further incubated on ice for 30 mins. Incubation of the deactivated enzyme on ice might reverse its activity by refolding at low temperatures.

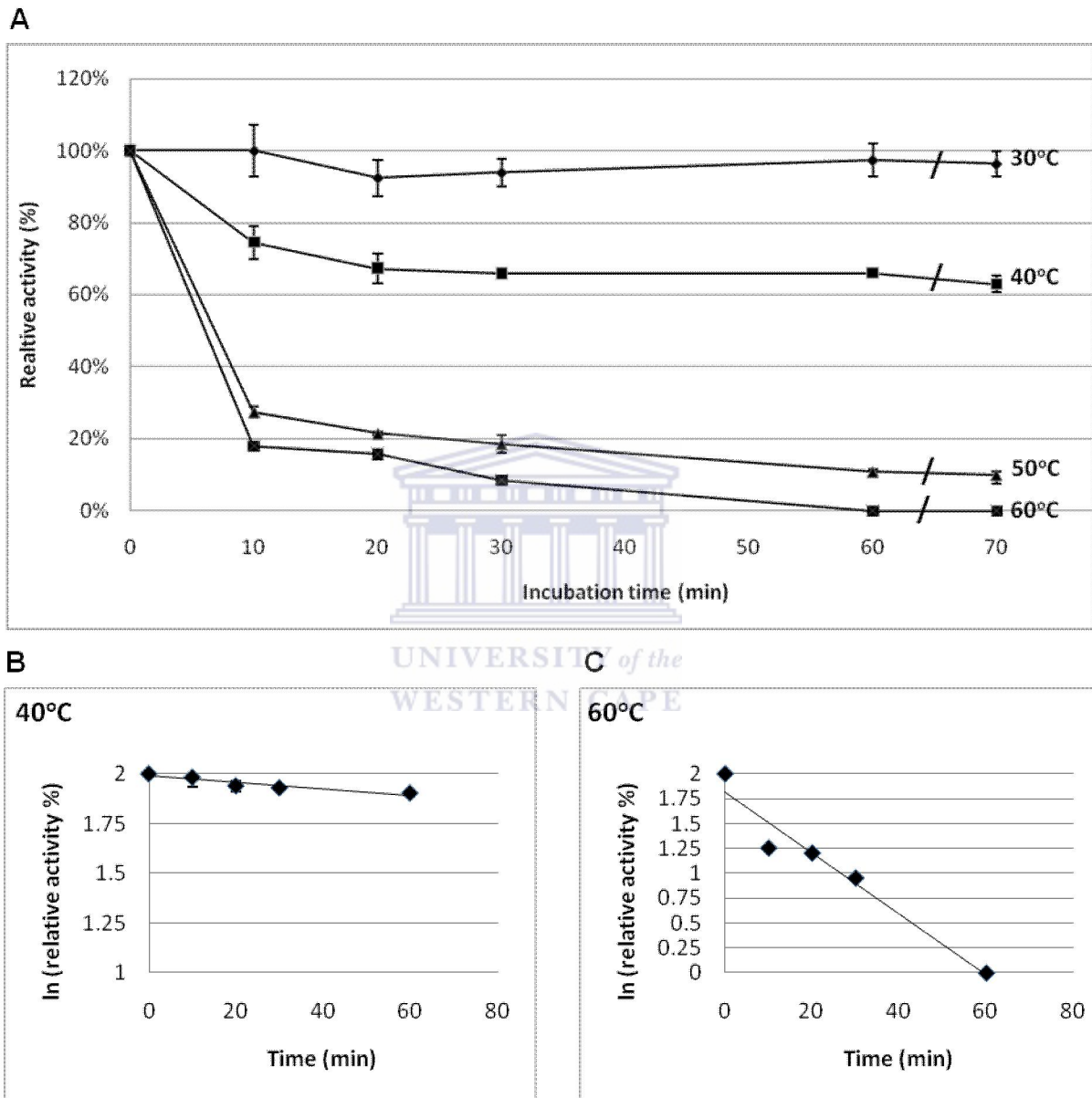


Figure 4.6 Effect of temperature on the stability of NhNit2 activity (panel A). Panels B and C, semi-log plots of activity versus time for NhNit2 at 40°C and 60°C, respectively. Activities are expressed as percentage relative to the maximum activity of NhNit2 (100%). The symbol / in panel A shows the activity of samples re-assayed after 30 mins on ice.

NhNit2 maintained maximum activity and showed no significant decrease in activity, at 30°C over 60 mins (Figure 4.6). This disagreed with the suggestion that thermal inactivation was taking place at temperatures above 20°C. At 40°C there was a 40% decrease in NhNit2 over 1 hr, while less than 10% residual activity at 50 and 60°C was obtained (Figure 4.6, panel A). The semi-log plots of activity versus time for 40 and 60°C (Figure 4.6 panel A and B, respectively), were linear, suggesting that inactivation followed first order rates that are typical of thermal inactivation and aggregation. From these semi-log plots a half life of 23 mins at 60°C was calculated. However, the value is anomaly high compared to the value, $t_{1/2}$ 7 mins, extracted from Figure 4.6, panel A. The anomaly is derived from the fact that the denaturation profile is not a logarithmic curve, and appears to be biphasic. The half life value calculated for 40°C was 7.2 hrs. NhNit2 enzyme incubated at denaturing temperatures did not regain activity (Figure 4.6, panel A).



4.3.7 Determination of optimal pH

The effect of pH on NhNit2 activity was determined over a range of pH values from 4.5 to 11 (Figure 4.7). Tris-HCl and CAPS buffers, used for the pH 8-11 ranges were found to inhibit NhNit2 activity. In several, NhNit2 activity was inhibited by an average of 10-20% for buffers used (Section 4.2.7)

NhNit2 has optimal activity between pH 6.5 and 7.5 and retained 50% activity between a broad range of pH 6 to 9 (Figure 4.7). At pH 4.5, NhNit2 has ~20% maximal activity (Figure 4.7). At higher pH values, NhNit2 activity gradually decreases from 80% at pH 8.5 to 18% at pH 10.

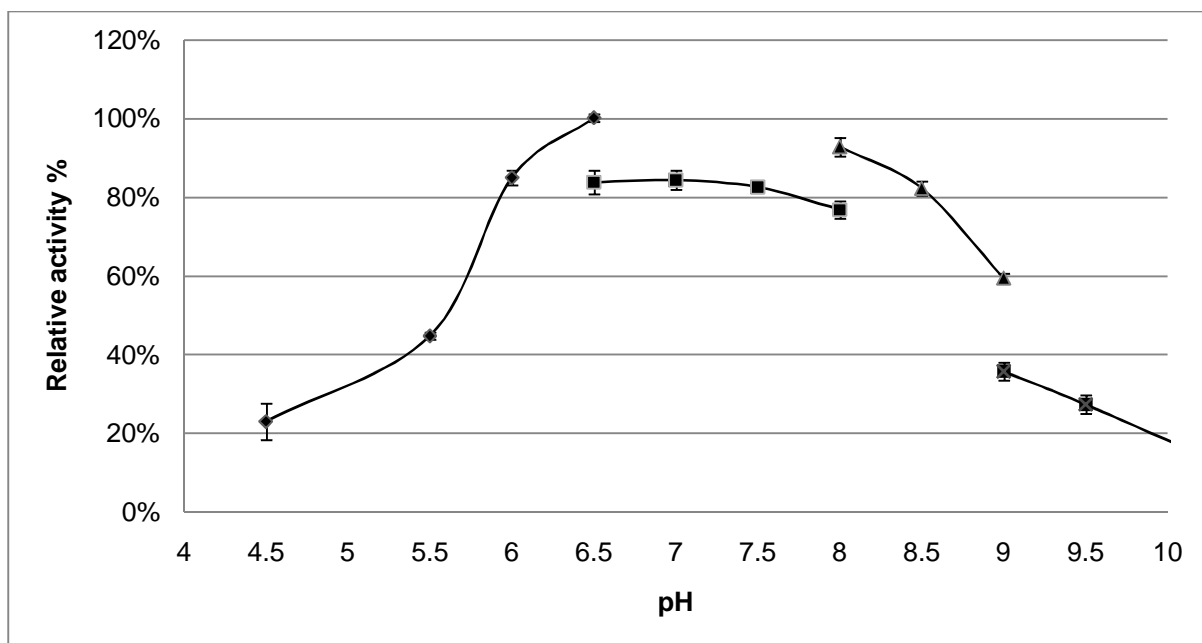
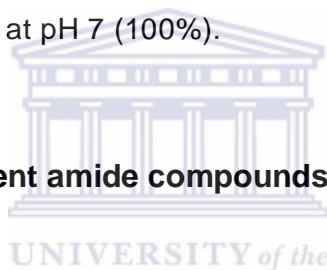


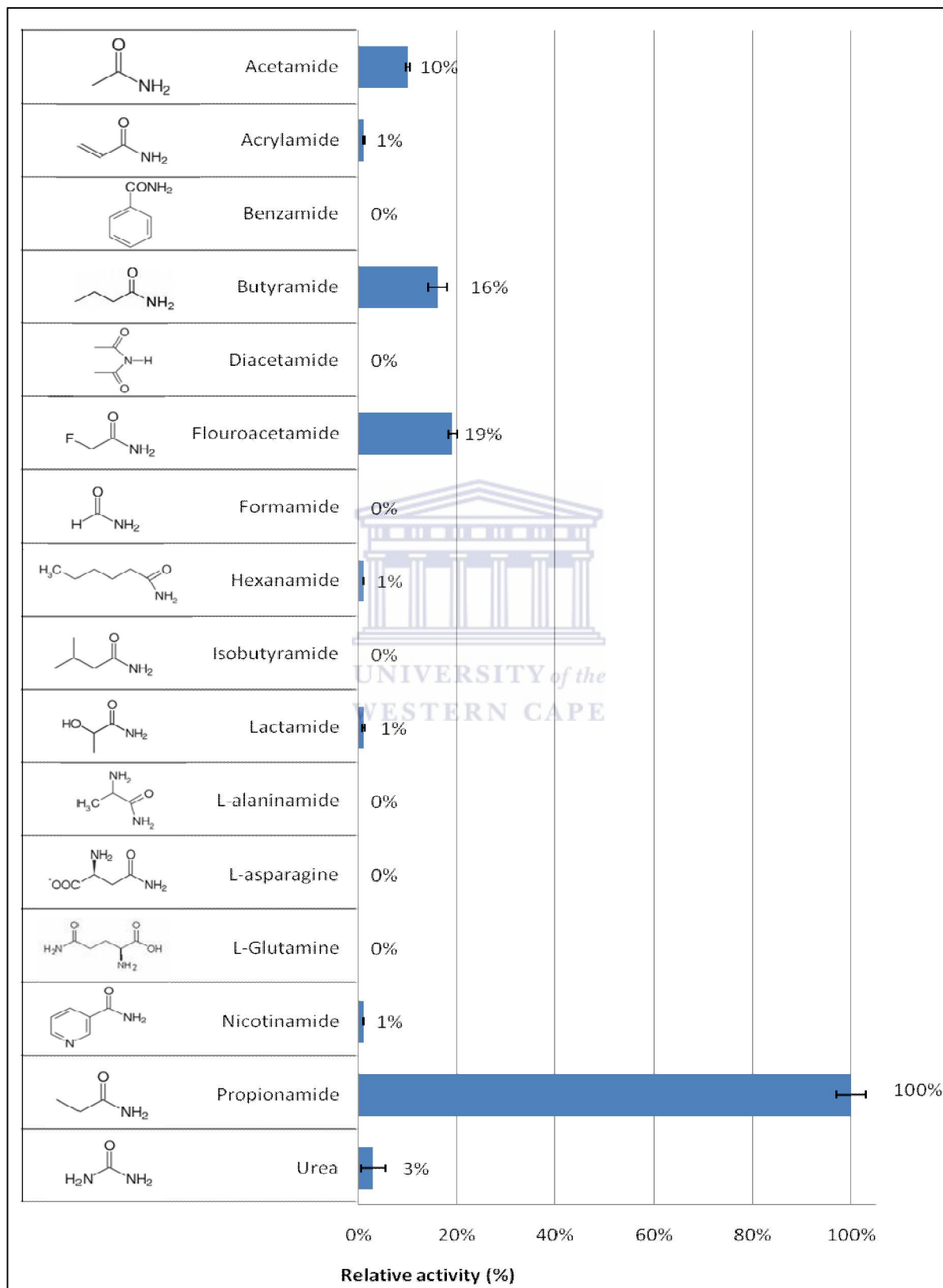
Figure 4.7 Effect of pH on the activity of NhNit2. Activities are expressed as percentage relative to the maximum activity at pH 7 (100%).



4.3.8 Determination of different amide compounds on NhNit2 activity

Various amides (100 mM) were tested as substrates under standard reaction conditions. Reactions were carried out at 25°C for 30 mins. The data (Table 4.3) indicate that NhNit2 has the most activity on aliphatic amide substrates of 2 to 4 carbon atoms, with a maximum relative activity on the 3 carbon amide (propionamide) (Table 4.3). Little activity was obtained on another 3 carbon amide, acrylamide, which has an alkene bond. Only ~19% activity was observed on fluoracetamide that has a smaller atomic length than propionamide (Table 4.3) due to its fluoride substituting a terminal methyl group.

Table 4.3 Activity of NhNit2 activity on different amide compounds. Activities are expressed as percentage relative to the maximum activity of propionamide (100%).



4.3.9 Kinetic behaviour of NhNit2 on acetamide and propionamide

The kinetic parameters for NhNit2 on acetamide and propionamide (Table 4.4) were determined using direct linear plots of V_i versus substrate concentration. NhNit2 has a higher affinity ($K_M = 38.6$ mM) for propionamide (C3) than for the acetamide (C2) ($K_M = 137.73$ mM) (Table 4.3). In addition, the relative value of k_{cat} , specific activity and enzyme specificity (k_{cat}/K_M : $\text{mM}^{-1}\text{s}^{-1}$) clearly demonstrate that propionamide is favoured as a substrate. The high K_M and low K_{cat}/K_M ratio obtained for acetamide and propionamide suggest these are not particularly good substrates.

Table 4.4 Kinetic parameters for NhNit2 on acetamide and propionamide

Substrate	K_M (mM)	Specific activity (U mg^{-1})	k_{cat} (s^{-1})	k_{cat}/K_M ($\text{mM}^{-1}\text{s}^{-1}$)
Acetamide	137.73 ± 1.89	3.67 ± 0.34	1.71	0.012
Propionamide	38.6 ± 1.24	8.53 ± 0.27	3.97	0.103

4.3.10 Determination of acyl transfer activity in NhNit2

It has been reported that amidases of the nitrilase superfamily exhibit acyl transfer activity in the presence of hydroxylamine (Andrade *et al.*, 2007, Makhongela *et al.*, 2007). NhNit2 was therefore screened for this activity using acetamide, butyramide and propionamide in the presence of hydroxylamine. The purified amidase from *G. pallidus*, which exhibits acyl transfer activity was used as a positive control (Makhongela *et al.*, 2007). No acyl transfer activity was observed for NhNit2 under standard assay conditions over incubation periods of up to 2 hrs.

4.4 Discussion

This is the first report of the cloning, expression, purification and characterisation of an aliphatic amidase (Nit2) of the nitrilase superfamily from a psychrotrophic, halotolerant alkaliphilic bacteria.

The N-terminal hexahistidine tagged Nit2 protein was actively expressed in soluble form in *E. coli* at 25°C was purified to near homogeneity using Ni-chelation chromatography. Since SDS-PAGE analysis of NhNit2 showed a 30 kDa band, it was expected that the native molecular mass would be a 60 kDa dimer on the basis that all structures of the nitrilase superfamily associate along the A surface to form an α -sandwich (Thuku *et al.*, 2009). In addition, the superimposition of the homology model of NhNit2 with 1fo6, the structure of DCase from *Agrobacterium radiobacter* (Wang *et al.*, 2001), showed evidence of a hydrophobic interface at the A surface of the enzyme. However, the intermediate value of 45.5 kDa for NhNit2, might be attributed to the presence of loosely folded monomer or a highly compact dimer that could have affected the elution time of the enzyme within the column. The latter form is the most favoured option due to the structural evidence, but further investigations are required to verify this.

Since NhNit2 had activity on amides, a comparison with aliphatic amidases (branch 2 enzymes) is appropriate. The protein sequence of Nit2 was approximately 85 amino acids shorter than the aliphatic amidases of *G. pallidus* (Kimani *et al.*, 2007) and *P. aeruginosa* (Andrade *et al.*, 2007), comprising 348 and 346 aa, respectively, with longer N-terminal sequences than Nit2. Although the native molecular weight of NhNit2 still requires further investigations, a monomeric or dimeric quaternary structure is unique for aliphatic amidases. Those amidases where the quaternary structures have been determined include tetramers (*Helicobacter pylori* (Skouloubris *et al.*, 2001); *R. erythropolis* R312 (Soubrier *et al.*, 1992) formerly *Brevibacterium* sp. R312 (Duran, 1998)), hexamers (*P. aeruginosa* (Ambler *et al.*, 1987); *G. pallidus* (Makhongela *et al.*, 2007)), octomers (*Rhodococcus* sp. J1 (Asano *et al.*, 1982)).

Aliphatic amidases are known to rapidly hydrolyse short chain aliphatic amides (Fournand & Arnaud, 2001). In addition, these amidases have higher specificities constants for acetamide (2C) than for propionamide (3C). Conversely, NhNit2 had a higher specificity constant for propionamide than for acetamide, 38.6 mM and 137.8 mM, respectively. The K_M (mM) values of known aliphatic amidases are listed as acetamide/propionamide as follows: 3.9/20, for *Helicobacter pylori* (Skouloubris *et al.*, 2001); 1/21, for *P. aeruginosa* (Asano *et al.*, 1982); 0.97/8.05, for *Rhodococcus* sp. J1 (Asano *et al.*, 1982). *G. pallidus* aliphatic amidase has 100% relative activity on acetamide and 67% on propionamide (Makhongela *et al.*, 2007). These amidases have little to no activity for linear amides containing less than 2 (formamide) and greater than 4 (butyramide, hexanamide) carbon atoms. All these amidases were assayed using the acyl transfer assay for which bioconversion rates are usually much higher (Fournand *et al.*, 1998). No acyl transfer activity was found for NhNit2, which suggested that the assay conditions used might have inhibited the enzymic activity.

Cold adapted enzymes typically exhibit low affinity for their substrates and have high catalytic velocity (Xu *et al.*, 2003). It has been proposed that these enzymes might trade off substrate affinity for catalytic velocity (Xu *et al.*, 2003). However, NhNit2 has both high K_M values and low catalytic rates on the tested amides, suggested that these are possibly not the natural substrates.

The preference for short chain amides suggested that the NhNit2 cavity cleft is smaller than predicted in the homology model. It could be inferred from the NhNit2 activity profile on different amides that the catalytic cleft is selective for substrates based on size and polarity. No activity was obtained for acrylamide, which was possibly due to the bulky pi cloud of the alkene structure. There was low NhNit2 activity on acetamide, flouracetamide and butyramide possibly due to their difference atomic lengths. A high resolution atomic structure of NhNit2 possibly would describe the catalytic cleft relationship with its substrate preference.

NhNit2 showed optimal activity between pH 6.5 and 7.5 and 50 % relative activity limits at pH 6 and 9. The optimal pH of the enzyme is lower than the optimal pH growth of *Nesterenkonia* (pH 9.6), which suggests that the intracellular pH is

maintained nearer neutrality. Known aliphatic amidases, except for *Rhodococcus* J1, typically have pH optima around 7 and less than 50% activity at pH 9 (Asano *et al.*, 1982, Cheong & Oriel, 2000, Fournand *et al.*, 1998, Makhongela *et al.*, 2007, Skouloubris *et al.*, 2001). *Rhodococcus* J1 amidase has an optimal at pH of 8 (Asano *et al.*, 1982) and, like Nit2, retains more than 50% activity at pH 9.

The optimal temperature for activity of NhNit2 was 30°C, some 10°C above the optimal growth temperature of the psychrotrophic *Nesterenkonia* sp. (~21°C). A temperature optimum of 55°C was reported for the thermophilic *G. pallidus* and the mesophilic *Rhodococcus* J1 aliphatic amidases (Asano *et al.*, 1982, Makhongela *et al.*, 2007). The half-life of Nit2 at 40°C was 7.2 hrs and activity was rapidly lost at 60°C. Semi-log plots confirmed a linear rate inactivation profile typical of thermal inactivation and aggregation. Activity was not restored after thermal inactivation.

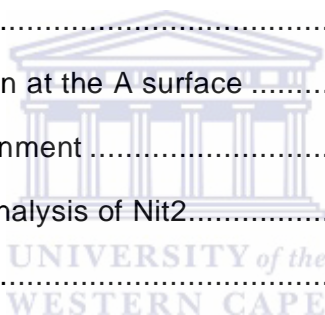
Although ChNit1 was purified to near homogeneity, no activity was detected on any of the substrates tested. The enzyme was confirmed to have a molecular weight of 30 kDa and the appearance of a monomer using size exclusion chromatography suggests the native form of the enzyme is monomeric. However, the fusion of a polar C-terminal hexahistidine tag on Nit1 might prevent dimerisation from occurring. Evidence from the superimposition of the Nit1 homology model with 1fo6 (Wang *et al.*, 2001) showed that Nit1 had similar hydrophobic residues in the 5 and 6 helices and C-terminal region which were implicated in intersubunit contacts between two monomers. The C-terminal regions of several structures of the nitrilase superfamily has been proposed to provide stability to the interaction at the A surface interface required for oligomerisation and activity (Thuku *et al.*, 2009). The deletion of 28 and 55 residues in the extended C-terminal region of *Bacillus pumilis* and *R. rhodochrous* J1 cyanide hydratase and Nase, respectively, (Jandhyala *et al.*, 2003, Thuku *et al.*, 2007), led to the loss of enzyme activity. In addition, the Nase failed to oligomerise into spirals. Although active Nase, cyanide hydratase and a DCase have been purified using a C-terminal hexahistidine tag (Chen *et al.*, 2005, Heinemann *et al.*, 2003, Jandhyala *et al.*, 2003), Nit1 has approximately 85 and 25 aa shorter C-terminal region than Nases and DCase (1fo6), respectively. The polar tag fused to Nit1 possibly was more exposed at the hydrophobic A

interface thus disrupting the interaction between two monomers. The expression, purification and characterisation of N-terminal hexahistidine tagged Nit1 fusion protein should therefore be undertaken.



Chapter 5: Crystal structure of Nit2

5.1 Introduction	123
5.2 Materials and Methods.....	123
5.2.1 Alternate purification method for NhNit2 protein	123
5.2.2 Protein crystallisation.....	124
5.2.3 Data collection, model building and refinement.....	125
5.3 Results & discussion	126
5.3.1 Evidence of high molecular weight Nit2 protein.....	126
5.3.2 Crystallisation of Nit2	128
5.3.3 Structure of Nit2	130
5.3.4 Evidence of interaction at the A surface	134
5.3.5 The active site environment	135
5.3.6 3D superimposition analysis of Nit2.....	137
5.3.7 Thermolability of Nit2.....	140




5.1 Introduction

Nit2 is similar to characterised aliphatic amidases of the nitrilase superfamily due to its preference for small aliphatic amides. However, this enzyme is distinct from known aliphatic amidases: the enzyme did not possess an extended C-terminal region; is active in monomeric or dimeric form; has high substrate affinity for 3C amides rather than 2C amides and has a low overall catalytic rate.

This chapter describes the crystallisation of Nit2 and the determination of its structure. A brief discussion of the crystal structure of Nit2 and comparisons with known homologues in the nitrilase superfamily are included.

5.2 Materials and Methods

5.2.1 Alternate purification method for NhNit2 protein

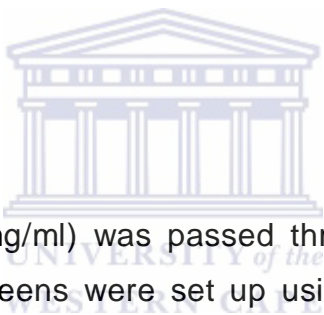


The expression of the N-terminal hexahistidine tagged Nit2 fusion protein in *E. coli* BL21 (DE3) pLysS and the preparation of cell free extracts were carried out as described in sections 4.2.2 and 4.2.3, respectively. The protein was purified using immobilized nickel ion adsorption chromatography employing a 5 ml HisTrap™ HP Column (GE Healthcare) on a Delta prep 3000 preparative chromatography (Waters). Protein absorbance was obtained at OD_{280nm} using a Water 484 Tunable absorbance detector (Waters). The column was charged with 1 column volume of 50 mM NiSO₄ followed by a 1 column volume of binding buffer (500 mM NaCl; 20 mM Tris-HCl (pH 7.9); 5 mM imidazole). The clarified extract was passed through the column followed by 10 column volumes of binding buffer and 6 column volumes of wash buffer (500 mM NaCl; 60 mM imidazole; 20 mM Tris-HCl (pH 7.9)). The bound proteins were eluted with a linear gradient of increasing imidazole concentration. The gradient was prepared by mixing elution buffer (500 mM NaCl; 20 mM Tris-HCl (pH 7.9); 1 M imidazole) in a two chamber gradient mixer. A flow rate of 1 ml/min was used with 0.5 ml fractions collected using a Gilson FC204 collector.

Fractions with significant protein absorbance at OD_{280nm} were analysed by SDS-PAGE. Fractions containing the N-terminal hexahistidine tagged Nit2 fusion protein that eluted as a 45 kDa protein were pooled and concentrated using Vivaspin, 10,000 MWCO PES. The concentrated protein was injected into a S-300 HR size exclusion chromatography column (GE-Healthcare) equilibrated with protein buffer (50 mM K₂HPO₄/KH₂PO₄ (pH 7.6); 150 mM NaCl; 2 mM DTT; 10% Glycerol). Collected fractions were analysed by SDS-PAGE. Fractions containing purified protein were pooled and concentrated to 10 mg/ml (Vivaspin 10,000 MWCO PES).

Negative staining of protein samples and electron microscopy were kindly carried out by Dr Brandon Weber at the Electron Microscopy Unit, University of Cape Town.

5.2.2 Protein crystallisation



Concentrated protein (~10 mg/ml) was passed through a 0.2 µm filter prior to crystallisation screening. Screens were set up using Hampton Crystal Screens HR2-110 and PEG/Ion screen (Hampton Research) in 96-well vapour diffusion plates with 3 sitting drop positions (Greiner Bio-One) according to the manufacturer's instructions. The screens were incubated at room temperature and monitored daily using a LEICA stereo microscope. Protein crystals were identified by the absorption of methylene blue dye. Seeding was carried out using 24-well Linbro plates using the hanging drop vapor diffusion crystallisation method (Fitzgerald & Madsen, 1986, Hampel *et al.*, 1968). Prior to seeding, equal mixtures of protein and crystallisation solution were incubated at room temperature for an hour for saturation to occur. Crystallisation was optimised by varying protein concentration in each condition that yielded a positive result.

5.2.3 Data collection, model building and refinement

Collection of diffraction data for Nit2 crystals, subsequent model building and refinements were carried out by Professor Trevor Sewell at the Electron Microscope Unit, University of Cape Town. Diffraction data were collected at beamline ID14 using single axes oscillation photography at the European Synchrotron Radiation Facility, Grenoble, France. Data frames were collected at one degree oscillates spanning a range of 180°.

The data were integrated using d*TREK (Pflugrath, 1999) and the spacegroup was determined using dtcell. The structure was solved using Phaser (McCoy *et al.*, 2007) with an ensemble comprising the aligned polyglycine backbones of 2plq, 1f89 and 1j31. This produced a unique solution, but the resultant map was uninterpretable. An interpretable map was produced using 1f89, which was positioned correctly, as a phasing model. The model was improved through three cycles of automatic building using Phenix (Terwilliger *et al.*, 2008) followed by manual inspection and re-interpretation using coot (Emsley & Cowtan, 2004) and O (Jones *et al.*, 1991). After ten cycles of refinement using Refmac5 (Vagin *et al.*, 2004) and manual inspection and re-interpretations using coot, a satisfactory Rfactor of 0.18 was obtained.

All molecular graphics operations were performed using PyMOL (DeLano, 2002) or Chimera (Pettersen *et al.*, 2004). 3D superposition analysis was carried out using SSM (Krissinel & Henrick, 2004).

5.3 Results & discussion

5.3.1 Evidence of high molecular weight Nit2 protein

An initial attempt to crystallise Nit2 protein prepared as described in section 4.2.3 produced no protein crystals. Protein precipitates were present in over 50% of the range of crystallisation conditions, possibly due to the presence of impurities in the protein preparation. A combination of Ni-chelation and size-exclusion chromatography techniques was used to purify Nit2. However, the elution profile of Nit2 was different (Figure 5.1, panel A). A shoulder peak adjoining the ~45 kDa Nit2 peak indicated the presence of high molecular weight proteins (Figure 5.1, panel A). SDS-PAGE analysis of fractions containing protein confirmed the presence of 30 kDa bands (Figure 5.1, panel B). These high molecular weight particles could be observed using electron microscopy and were shown to decrease in size with increasing retention time (Figure 5.1, panel C, compare panels 1 with 3). The highest molecular weight (110 mins) was calculated to be ~130 kDa. Although the native ~45.5 kDa Nit2 protein was suggested to be of either a monomer or a dimer, the 130 kDa protein could be of a trimer or a hexamer. The latter form is the most accepted form, since a trimer would possibly consists of one monomer with an exposed A surface. The high molecular weight protein was confirmed to have activity on propionamide.

Since there was a small amount of the high molecular weight protein, it could be suggested that these are weakly bonded multimeric structures and are easily disrupted by force. It is likely that Nit2 could be multimeric protein, which is true for known aliphatic amidases which are tetramers, hexamers and octomers (Ambler *et al.*, 1987, Asano *et al.*, 1982, Makhongela *et al.*, 2007, Skouloubris *et al.*, 2001, Soubrier *et al.*, 1992). One possible reason for a weakly bonded multimeric structure of Nit2 could be attributed to the fused 20 residues N-terminal hexahistidine tag. It is possible that the three dimers of Nit2 are weakly bonded, but are being repelled apart due to the polar hexahistidine tags fused to each monomer. An alternative purification of Nit2 with no fused tag should be attempted in order to characterise the true quaternary structure of the enzyme.

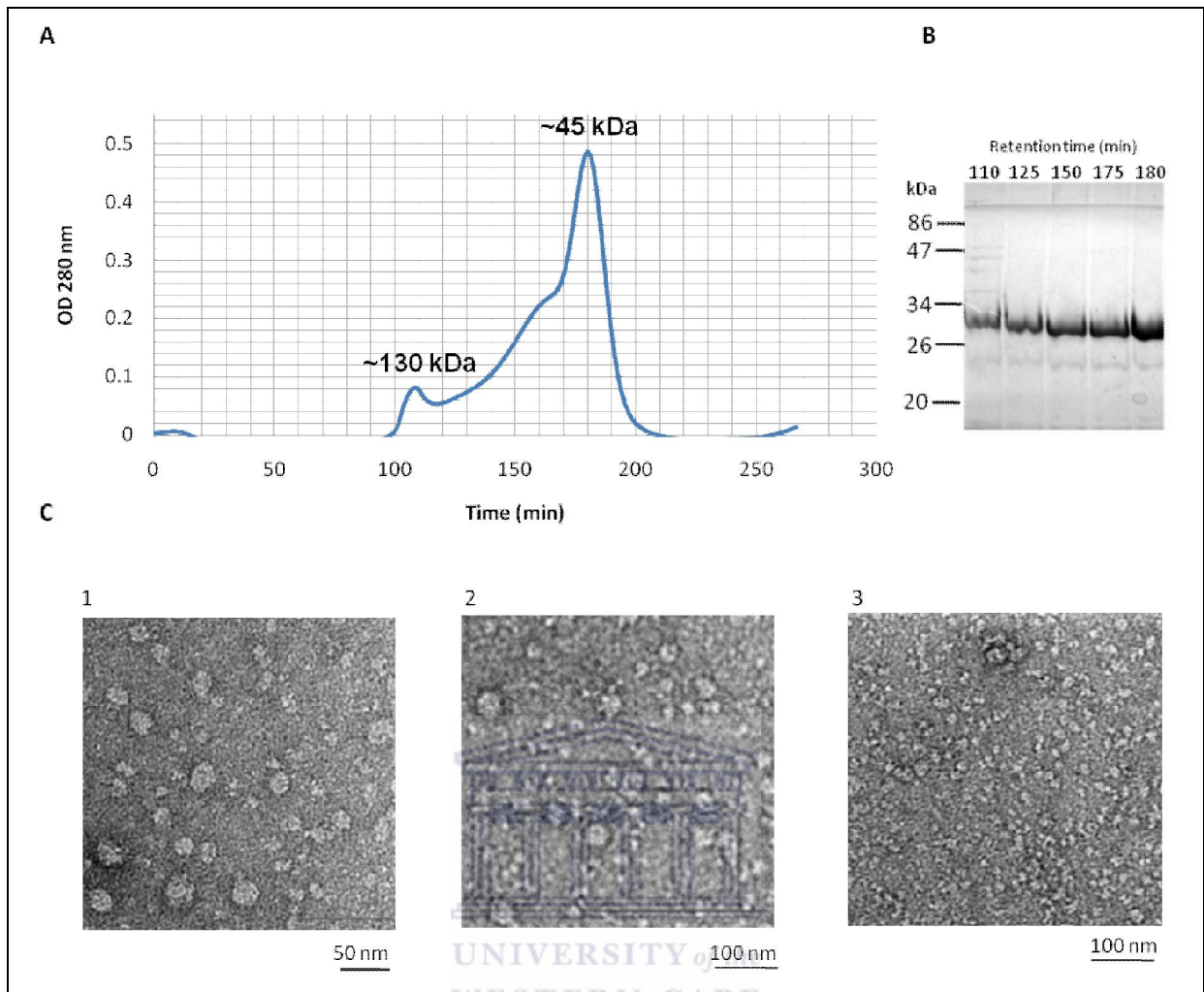


Figure 5.1 Evidence of high molecular weight Nit2 protein. Panel A, elution profile of Nit2 from the S300 size exclusion chromatography. Panel B, SDS-PAGE analysis of fractions collected. Panel C, electron micrograph of high molecular weight protein particles observed in fractions 110 mins (panel 1 & 2) and 150 mins (panel 3).

5.3.2 Crystallisation of Nit2

Figure 5.2 shows crystals that formed after two days incubation under two different crystallisation conditions (Figure 5.2, panel A and B). These crystals had 0.1 mm width. The flat rectangular crystals were considered good candidates for X-ray diffraction (Figure 5.2, panel B). Further optimisations were carried out using these as seeds in order to prepare thicker crystals in the presence of varying concentration of ammonium sulphate and Nit2 protein. No crystals were found for wells containing protein from the high molecular weight elution peak.

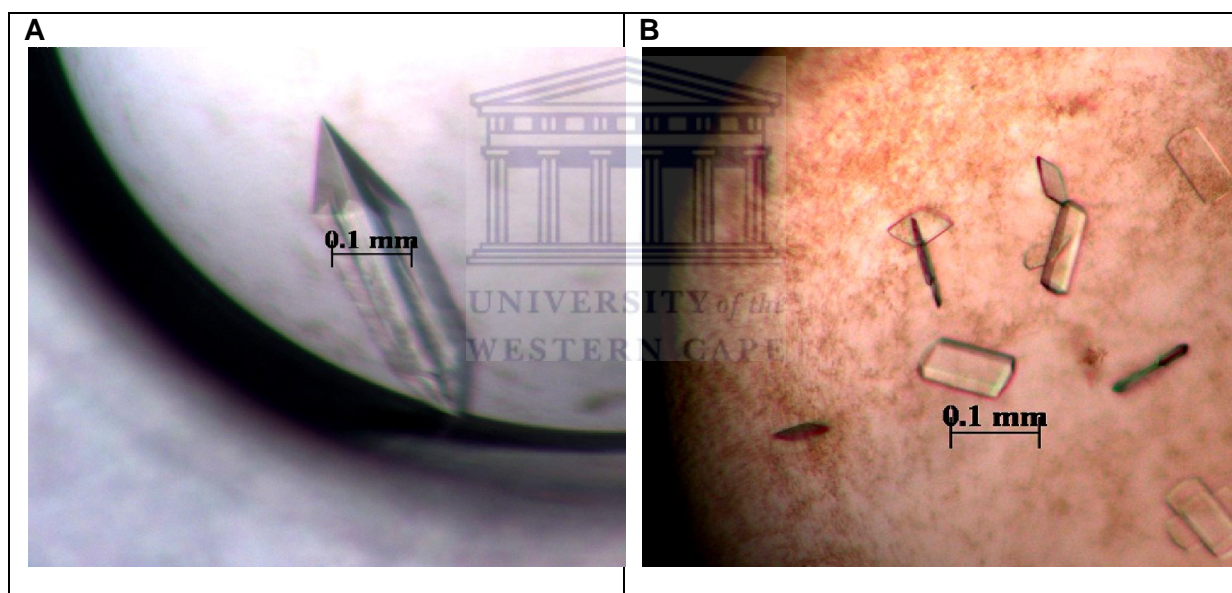


Figure 5.2 Crystals of Nit2 in initial crystallisation screens. The crystallisation conditions were for panel A, 0.2 M ammonium sulphate, 0.1 M sodium cacodylate trihydrate (pH 6.5) and 30% (w/v) polyethylene glycol 8000 and panel B, 2 M ammonium sulphate.

Seeded crystals failed to grow in ammonium sulphate concentrations lower than 1.95 M and greater than 2 M (data not shown). In addition, varying concentration of Nit2 protein had no effect on the growth of the crystals, except for reduction of protein precipitate. However between 1.95-2 M ammonium sulphate, seeded

crystals grew rapidly and reached a thin ultimate size within 2 hrs (Figure 5.3). These crystals comprised multiple stacked layers, which separated easily, while others were apparently single crystals (Figure 5.3).



Figure 5.3 Single and stacked layers crystals of Nit2 that were produced from seeds in 2 M ammonium sulphate.

Good quality hexagonal crystals were also found after approximately 3 weeks of incubation in 0.1 M sodium acetate trihydrate (pH 4.6) and 2 M ammonium sulphate (Figure 5.4). The low pH of the crystallisation condition might have slowed down the growth of these crystals, thus producing uniform width and length growth with no visible stacked layers (Figure 5.4). Preliminary X-ray diffraction of crystals from both conditions (Figure 5.3 and 5.4) had the same space group, $C222_1$, and both were suitable for data collection.

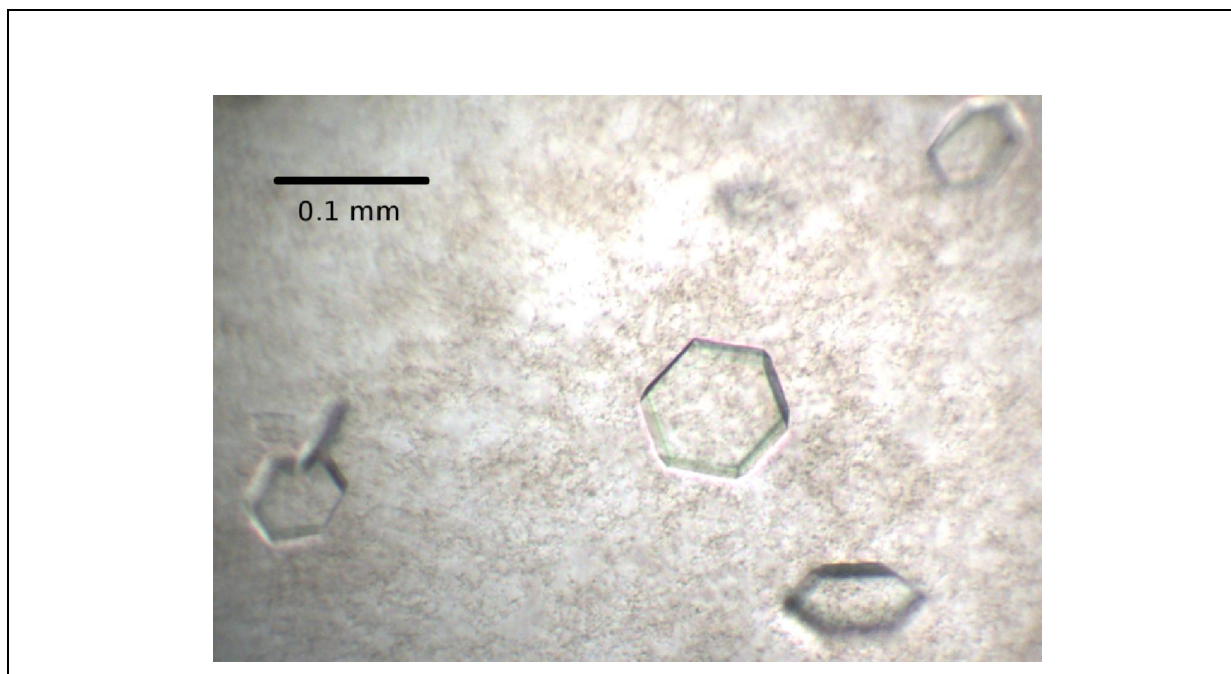


Figure 5.4 Hexagonal crystals of Nit2.



5.3.3 Structure of Nit2

The Nit2 hexahistidine tag fusion protein contained 284 residues. The 1.65 Å resolution map allowed for an unambiguous determination of the location of residues 10-259 and 269-284 where the start of Nit2 sequence is M20 (refer Table 5.1 for further data statistics). No interpretable density was found for the first 10 residues of the 20-residue N-terminal tag and 10 residues located on the C-terminal region. A physical reason for the absence of residues 259-269 could be interaction of side chains of H19 of the N-terminal hexahistidine tag and N259 of the C-terminal region, which possibly destabilises this region (data not shown).

The structure of Nit2 showed two identical monomers associated in a twofold symmetry along the A surface (Figure 5.5, panel A). This structural evidence confirmed that the ~45.5 kDa Nit2 protein obtained from size exclusion chromatography is of a dimer composed of two tightly bound 30 kDa monomers.

Table 5.1 Crystallographic data for Nit2

Data set	N-terminal hexahistidine tagged Nit2
Data Collection Statistics	
Wave length (Å)	0.979
Space group	C222 ₁
Unit cell Parameters	a = 76.00 b = 115.64 c = 65.32 = = = 90.00°
Unit cell volume (Å ³)	574074
Mosaicity	1.45
Resolution Range (Å) (outer shell)	38.00 - 1.66 (1.72 - 1.66)
Total observations	240821
Total observations (unique)	34232
Completeness (%) (outer shell)	99.6 (98.9)
Redundancy (outer shell)	7.03 (6.92)
Signal-to-noise ratio (I/ (I)) (outer shell)	15.6 (4.2)
R _{merge} (outer shell)	0.046 (0.366)
Reduced ChiSquared	0.94 (1.33)
Wilson plot average B-factor (Å ²)	24.53
Matthew's coefficient	2.21
Solvent content	45.0
Refinement statistics	
Number of Amino Acids	A12-A258, A269-283
Protein Molecular mass (Da)	30085.86 (Average isotopic composition of entire expressed peptide)
Number of non-hydrogen atoms	1980
Number of water atoms	196
Number of reflections	
Working set	32495
Test set (%)	5.05
R-factor§ (%) (overall)	18.64
R-free# (%) (overall)	21.88
Overall figure of merit	0.8589
Rms deviations from ideality	
Bond lengths (Å)	0.0220
Bond angles (°)	1.802
Average B value (Å ²)	26.37

The monomer fold of Nit2 consisted of 12 α -sheets and 9 α -helices which are interconnected by external loops (Figure 5.5, panel B). Nit2, similar to the monomer fold of *G. pallidus* aliphatic amidase (Kimani *et al.*, 2007), had two six-stranded α -sheets sandwiched between two layers of α 1-4 and α 6-9 helices (Figure 5.5, panel B).

The α 6, α 7 helices and C-terminal region of the two monomers are close to each other and forms the A surface (Figure 5.5, panel A & B). The two monomers associate along the A surface forming a β - α sandwich architecture (Figure 5.5, panel A). The monomer fold, the A surface and the β - α sandwich architecture of Nit2 are conserved in known structures of the nitrilase superfamily.



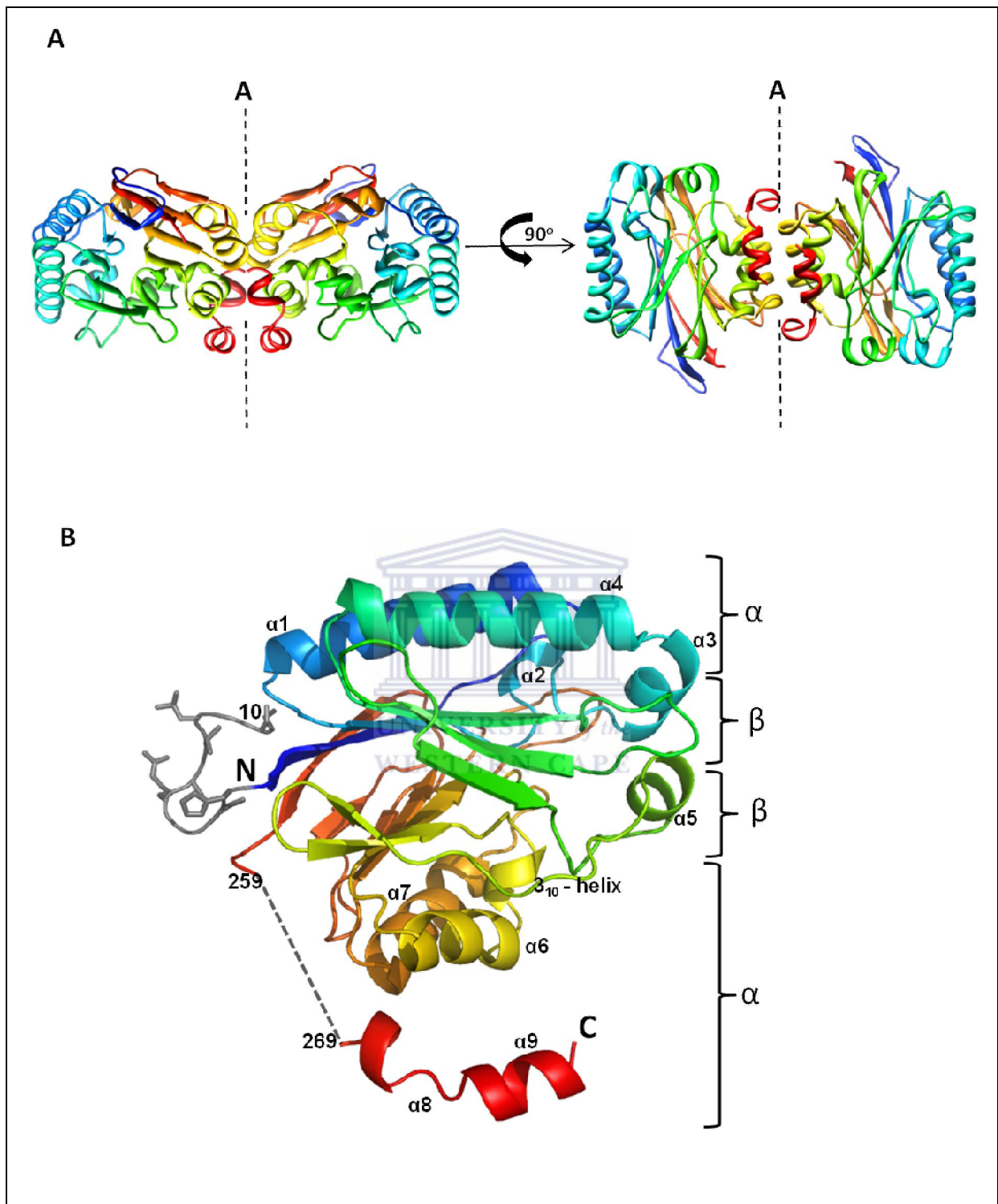


Figure 5.5 Structure of Nit2 dimer and monomer fold. Panel A, schematic representation of two perpendicular views of the Nit2 dimer. The A surface that represent the intersubunit interaction region between two associated monomers is shown. Panel B, schematic representation Nit2 monomer fold with α and β sheet topology shown. The monomers are coloured from blue (N-terminal) to red (C-terminal).

5.3.4 Evidence of interaction at the A surface

Figure 5.6 shows four intersubunit interactions occurring at the A surface. These residues are located on the 6 (E172 and R175) and 7 (R206 and E209) helices. Salt bridges are formed between residues E172 and R172 and between E209 and R206 and *vice versa*, linking the two monomers (Figure 5.6).

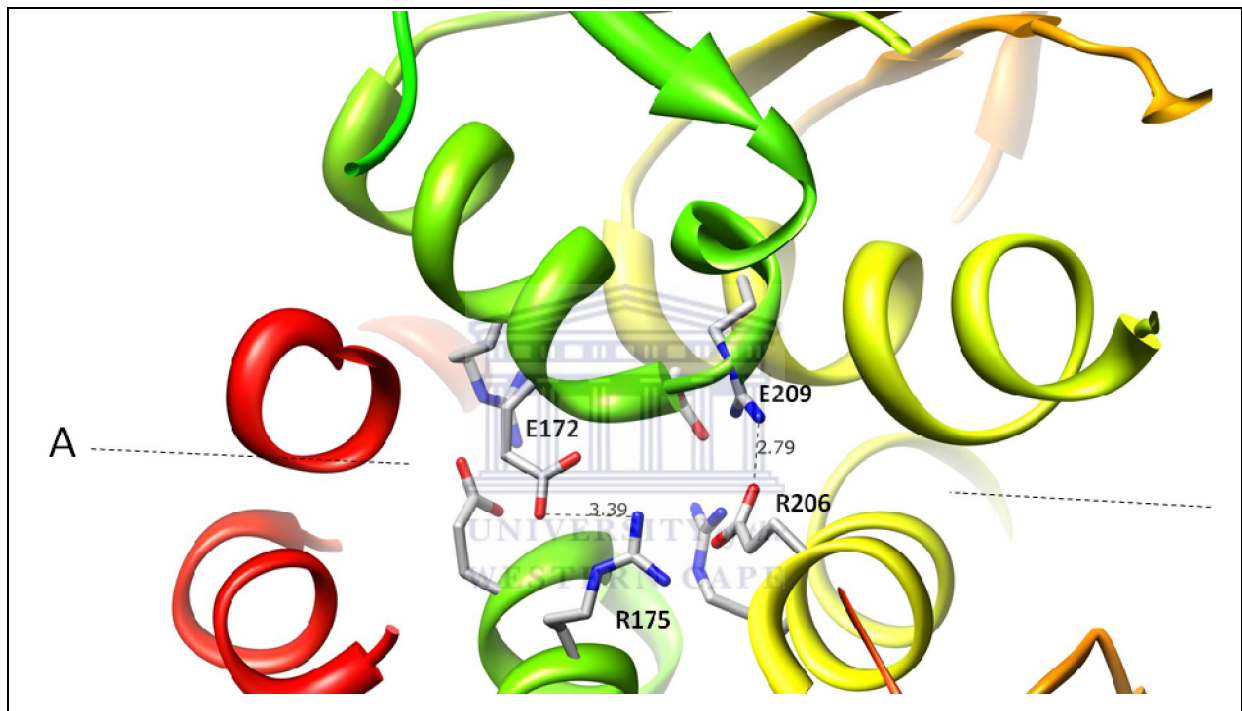


Figure 5.6 Details of the interaction at the A interface.

5.3.5 The active site environment

Another conserved motif in the nitrilase superfamily consists of catalytic residues (EKEC) (Kimani *et al.*, 2007, Thuku *et al.*, 2009). The conserved catalytic residues of Nit2 are E61, K131, C165 and E139 (Figure 5.7, panel A). The side chains of Nit2 catalytic residues superimposes on those of *G. pallidus* aliphatic amidase (Kimani *et al.*, 2007), which was reported to be conserved amongst crystalline structures of the nitrilase superfamily. In addition, the 3_{10} -helix that was implicated in the orientation of the active site cysteine residue in *G. pallidus* aliphatic amidase superimposed on Nit2 (Figure 5.7, panel A).

The Nit2 catalytic cleft is described as shallow and slightly elongated (Figure 5.7, panel B). The elongated dimension of the catalytic cleft possibly fits the docking of 3C aliphatic amides (propionamide). Residues lining the catalytic cleft are mostly polar (E169, Y166, Y135, Y67). These polar residues may repel long chain amides (>4C), which are more hydrophobic than propionamide. Small amides (<2C) probably do not interact well with the active site residues since the substrate might be out of range of stabilising residues lining the catalytic cleft. This may explain Nit2 low affinity for small amides and >4C amides.

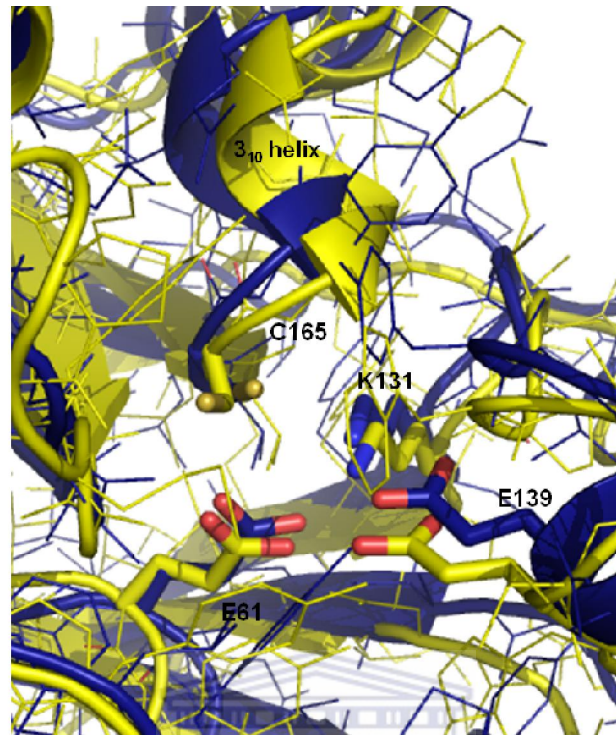
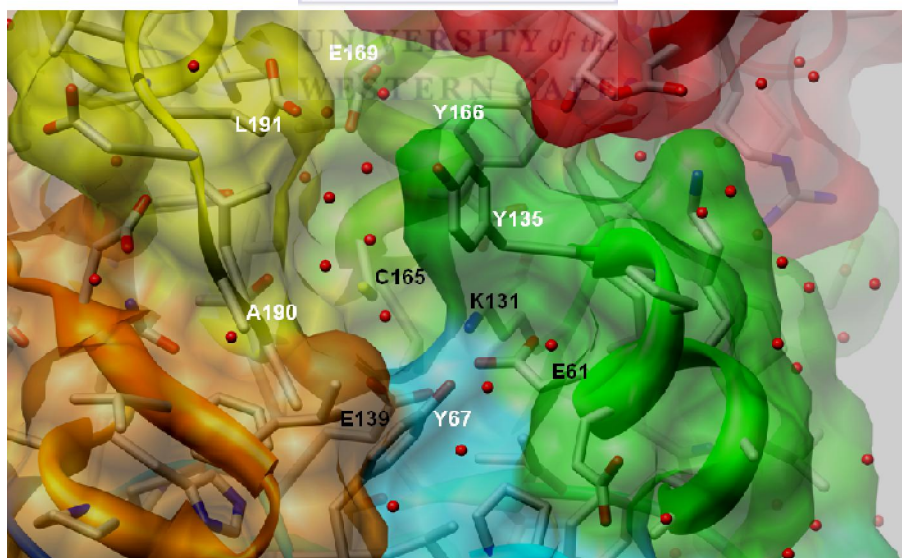
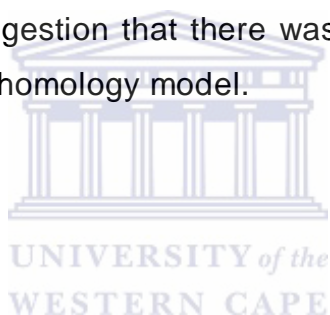
A**B**

Figure 5.7 Arrangement of the four catalytic residues (EKEC) of Nit2 compared with *G. pallidus* aliphatic amidase (2plq) panel A, Nit2 (blue) 2plq (yellow). Panel B, surface shading of Nit2 catalytic cleft. Catalytic residues are labelled in black and residues lining the catalytic cleft in white.

5.3.6 3D superimposition analysis of Nit2

Figure 5.8 shows the comparison between the Nit2 structure and its homology model (Chapter 3, section 3.3.8-9). There is a clear difference in the highlighted catalytic area between the structure and homology model (Figure 5.8, panel A). It has been shown that the catalytic site of the homology model was not build properly (section 3.3.9). There were large distances between the catalytic residues, which deviated from the known fact that the catalytic residues of nitrilase structures are superimposable (Kimani *et al.*, 2007). The superimposition of Nit2 on the homology model showed that there were deviations within the 4 helix and a 3 helix was missing (Figure 5.8, panel B). The results of SSM 3D comparison of the Nit2 structure with the homology model showed that there was a poor rmsd of 1.52 for over 243 C atoms (Table 5.2). The data re-affirmed the suggestion that there was a lack of suitable structures for the construction of a Nit2 homology model.



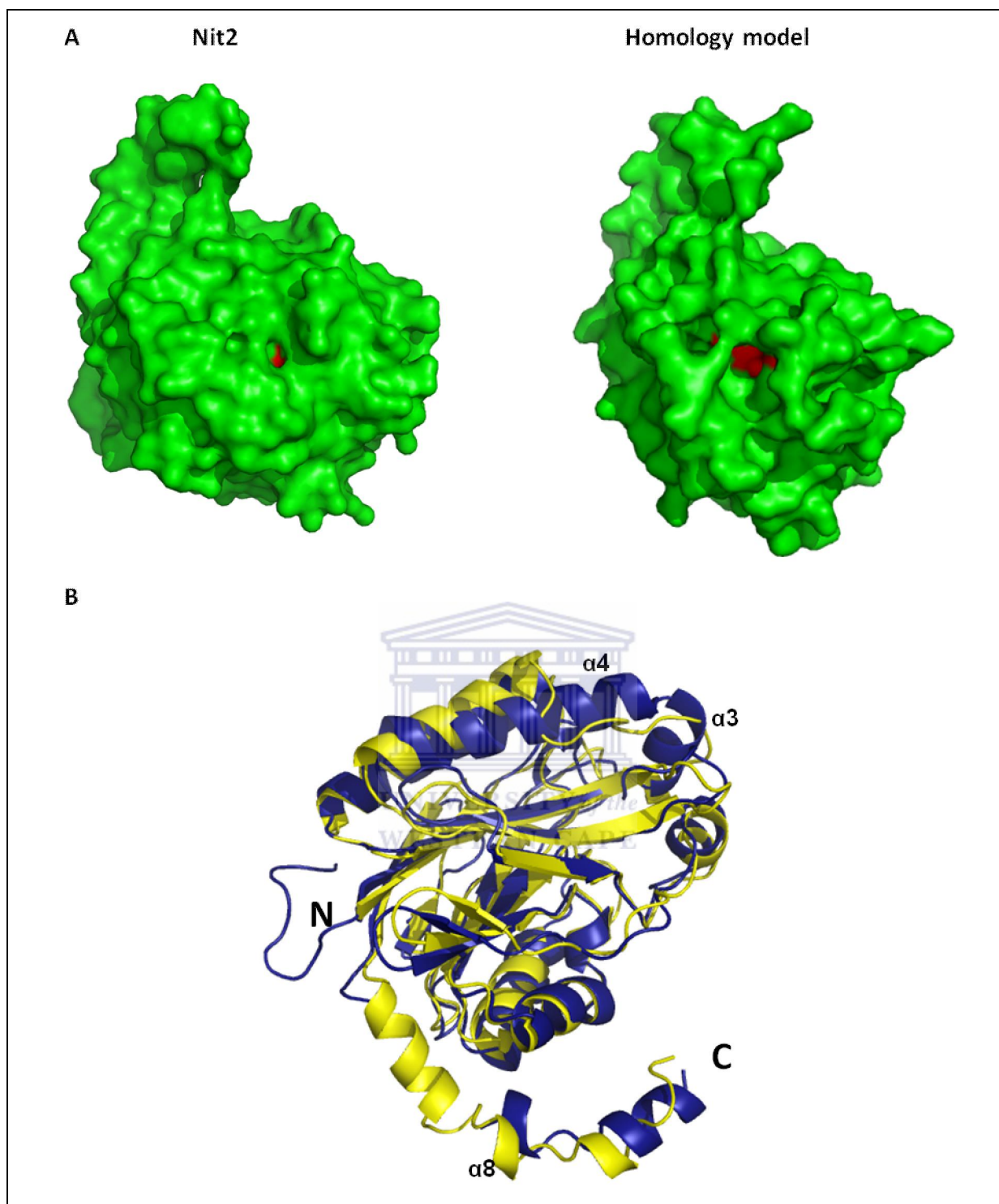


Figure 5.8 Comparison of Nit2 with its homology model. Panel A, surface representation of the two models with catalytic cleft shown in red. Panel B, superimposition of Nit2 (blue) and homology model (yellow).

The SSM 3D superimposition analysis (Krissinel & Henrick, 2004) of Nit2 with known structures of the nitrilase superfamily is shown in Table 5.2. Although the 3D similarity between *G. pallidus* and *P. aeruginosa* aliphatic amidases was reported to share a C rmsd of 0.26 Å over 335 atoms (Kimani *et al.*, 2007), the result returned from SSM server showed a C rmsd of 0.33 Å. The latter comparison value was used as a reference for Nit2 3D superimposition analyses.

SSM 3D superimposition analysis of Nit2 only returned structures related to the nitrilase superfamily. The closest superimposable structure for Nit2 was 1j31, the hypothetical protein PH0642 from *Pyrococcus horikoshii* (Sakai *et al.*, 2004). Nit2 shared poor rmsd values with known aliphatic amidases 2uxy, 2plq and DCase 1fo6 (Table 5.2).

Table 5.2 3D superposition analysis of Nit2 with known structures of the nitrilase superfamily. The total number of residues are indicated in parenthesis below the PDB codes. Abbreviations: N_{alg}, number of 3D homologous C positions to a 3.5-Å cut-off; (%), sequence identity calculated identical residues from structural alignments; rmsd, root mean square distances between 3D C .

		Nit2 (263)	1j31 (262)	2e11 (265)	1f89 (271)	2wlv (274)	1fo6 (302)	2uxy (341)	2plq (340)
Nit2	N _{alg} /(%)	243(96)	236(28)	229(24)	236(24)	233(27)	232(22)	242(24)	238(25)
	rmsd	1.52	1.61	1.65	1.83	1.71	1.95	1.77	1.94
2plq	N _{alg} /(%)	-	250(25)	-	239(22)	-	-	335(81)	-
	rmsd	-	1.76	-	1.64	-	-	0.33	-

Figure 5.9, panel A and B, show the superimposition of Nit2 on 1j31 and 2plq, respectively. For both 1j31 and 2plq, the 3 and 4 helices were different for Nit2 (Figure 5.9), which confirmed there was a lack of suitable structures for the building of the homology model. In addition, Nit2 had an extra 5 helix and did not possess an extended C-terminal region found in known aliphatic amidases.

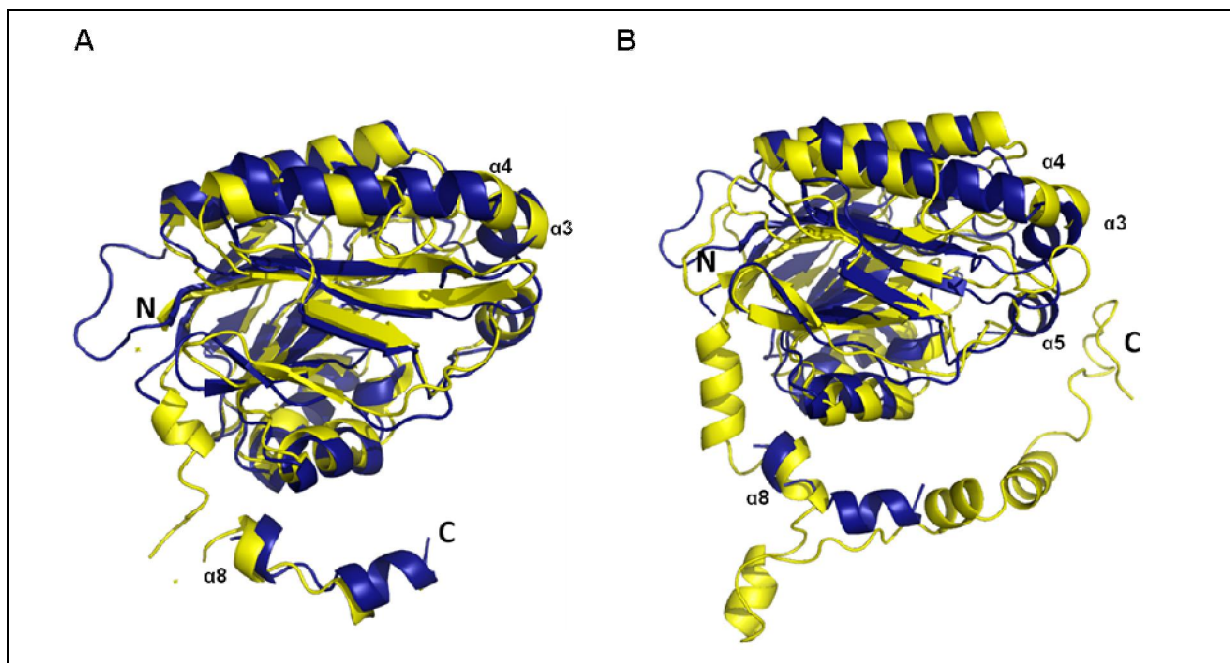


Figure 5.9 Superimposition of Nit2 on 1j31 and 2plq (panel A and B, respectively). Nit2 is in blue and the structures of 1j31 and 2plq are in yellow.

5.3.7 Thermolability of Nit2

Figure 5.10, panel A, shows a recent image of Nit2 dimer that has residues 259-270 modelled (prior to the $\alpha 8$ helix) to make up for the missing 10 residues within the C-terminal region. This unresolved region of Nit2 was predicted to be a α -helix, which is conserved in all structures of the nitrilase superfamily.

The C-terminal region of Nit2 is similar to all structural homologues where this region from opposite monomers, wrap around each other (Figure 5.10, panel A). The role of this region was proposed to stabilise the interaction across the A surface (Thuku *et al.*, 2009). The short C-terminal region of Nit2 is interesting since it may contribute to the low stability of the enzyme at elevated temperatures. This theory was drawn from the proposed role of the extended C-terminal region of *P. aeruginosa* aliphatic amidase (Andrade *et al.*, 2007). Although *P. aeruginosa* is a mesophilic bacterium with optimal growth at 37°C, its hexameric aliphatic amidase is thermostable at 55°C. The authors could not find any stabilising factors within the aliphatic amidase that contributed to thermostability such as intermolecular disulfide bridges (Andrade *et al.*, 2007). It

was suggested that the long C-terminal arm that wraps around opposite monomers forming tight bonds might promote the thermostability of the amidase (Andrade *et al.*, 2007) (Figure 5.9, panel B). This unique feature is also present in the thermophilic *G. pallidus* aliphatic amidase (Kimani *et al.*, 2007).

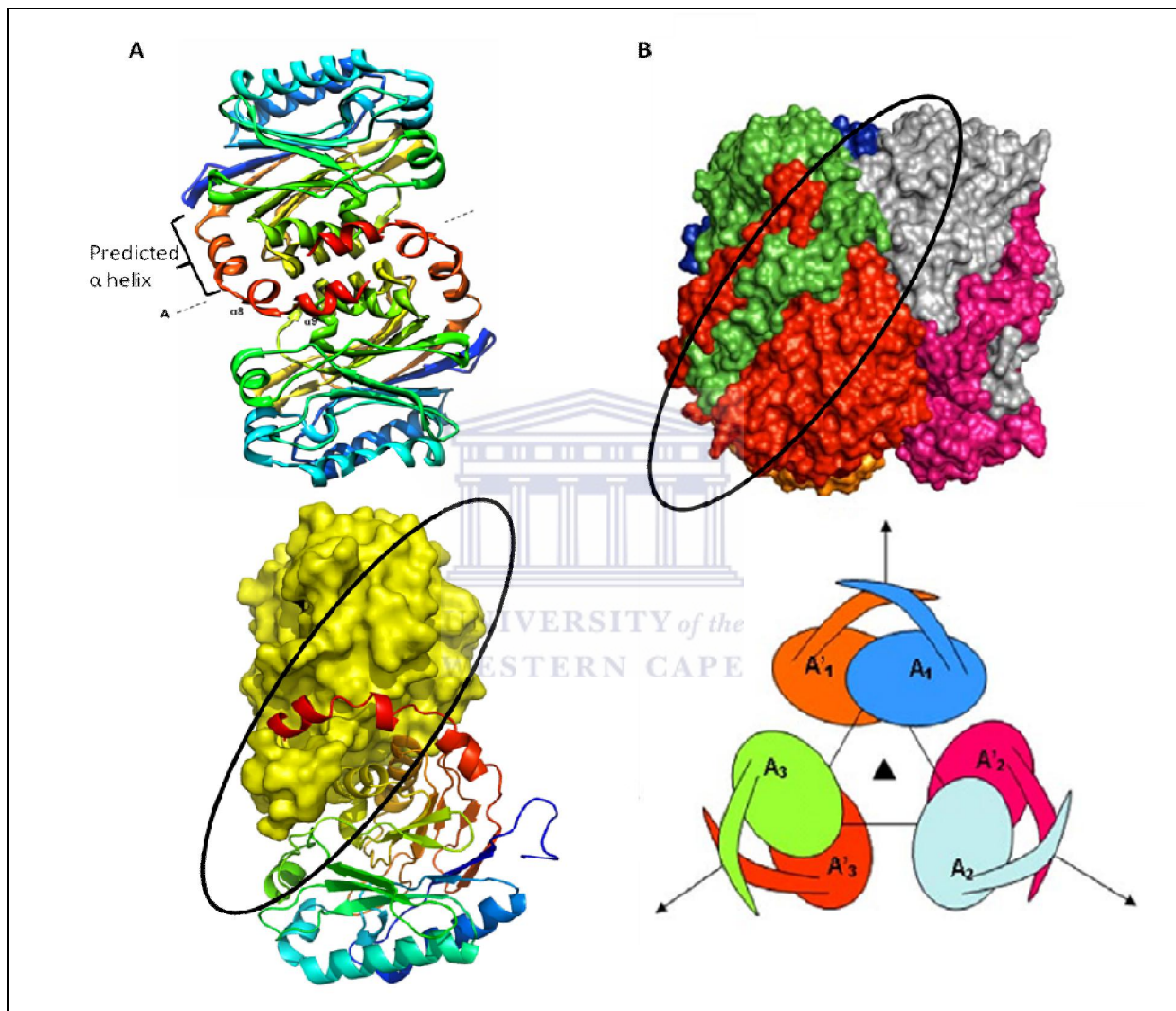


Figure 5.10 The C-terminal region of Nit2 and *P. aeruginosa* aliphatic amidases. The interactions between the C-terminal regions of two monomers are circled. Panel A, top image, structure of Nit2 with continuance of the C-terminal region. Bottom image, A cartoon representation of Nit2 structure showing the C-terminal region (red) overlapping a shaded monomer. Panel B, surface shading of the hexameric aliphatic amidase (top) with a schematic representation of the monomers (below). The A surface between the interacting monomers is indicated with arrows. Images of *P. aeruginosa* aliphatic amidase were taken from Andrade *et al.*, (2007).

This is the first report of the determination of an aliphatic amidase structure from a psychrotolerant bacterial strain. In addition, the remarkable rapid crystallisation property of Nit2 provides an excellent model for future studies on the nitrilase superfamily.



Chapter 6: General discussion and future implications

A novel psychrotrophic nitrile hydrolysing strain, *Nesterenkonia* AN1, was isolated. In addition, the *in silico* mining of its partially sequenced genome led to the identification and the *in vitro* characterisation of two putative nitrilases, referred to as Nit1 and Nit2.

Nit1 and Nit2 of *Nesterenkonia* AN1 belonged to the nitrilase superfamily since their protein sequences conserved the catalytic residues (EKEC), four glycines and had a predicted monomer fold (Thuku *et al.*, 2009). Based on homology models of Nit1 and Nit2, it was also predicted that their monomers might associate along the conserved A surface forming a characteristic sandwich. This prediction was based on the presence of two conserved helices and a C-terminal region that contributed to intersubunit interactions along the A surface (Thuku *et al.*, 2009). These predicted features were confirmed in the crystal structure of Nit2.

Although Nit2 was characterised *in vitro* as an aliphatic amidase, the assignment of Nit1 and Nit2 to a branch of the nitrilase superfamily could not be determined based on the *in silico* analyses of their protein sequences. The failure of these analyses was due to a limited range of characterised sequences and structures. As an alternative *in silico* method for analysis of putative nitrilases, a dendrogram of characterised and related putative protein sequences of the nitrilase superfamily was compiled (Figure 6.1). The 12 branches of the nitrilase superfamily divide into four branching groups: one group of nitrile/cyanide hydrolysing enzymes, two groups of enzymes related by amidase activities, of which one has both amidase and amide condensation activities and a fourth group of uncharacterised enzymes (Figure 6.1). This dendrogram was used to assign the possible enzyme function for Nit1 and to show whether Nit2 is related to known aliphatic amidases.

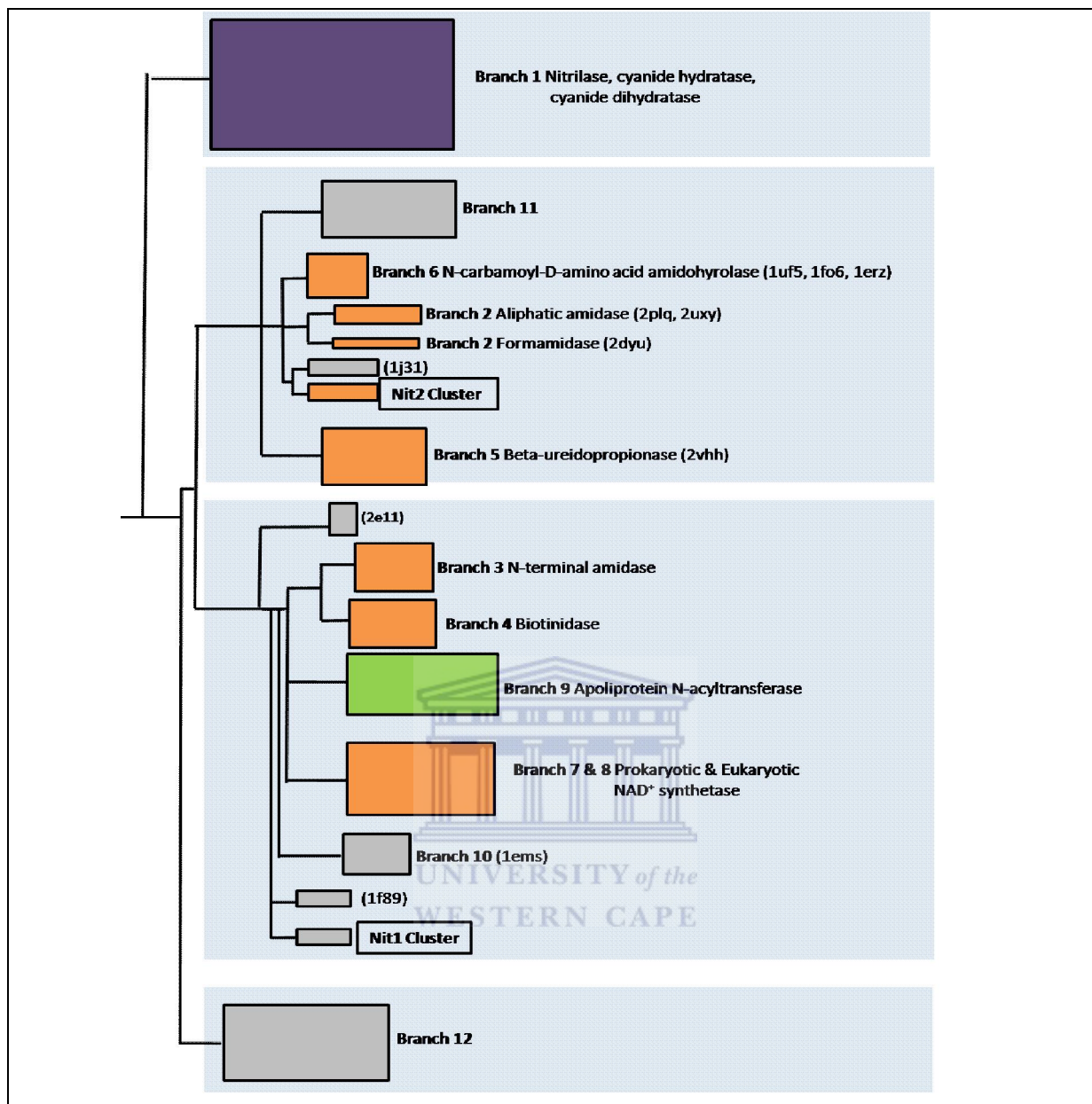


Figure 6.1 Schematic dendrogram of protein sequences of the nitrilase superfamily. The four main branching of enzymes are highlighted in pale blue. Clusters of related enzymes are grouped as blocks and are coloured according to known enzyme functions: purple, nitrile hydrolysing activity; orange, amidase activity; green, amide condensation activity; grey, unknown or putative function. BLAST (NCBI) was used to retrieve similar sequences using characterised members of the nitrilase superfamily including Nit1 and Nit2. ClustalW (Larkin *et al.*, 2007) was used for generating the alignment. The dendrogram was constructed using the Neighbour-Joining method (Saitou & Nei, 1987). Phylogenetic analyses were conducted in MEGA4 (Tamura *et al.*, 2007) and the dendrogram was viewed using A Tree Viewer (ATV) (www.phylosoft.org/atv).

Nit1 falls within a cluster of related putative nitrilases mainly from the bacterial family, *Micrococcaceae* (Figure 6.1). The Nit1 cluster shared the same branch with the putative CN-hydrolase from *Saccharomyces cerevisiae*, the structure (1f89) of which has been determined (Kumaran *et al.*, 2003). This agrees with the finding that this putative CN-hydrolase was the only member of the nitrilase superfamily that had 22% sequence identity, the highest score, with Nit1. The Nit1 cluster also shared the same grouping of protein sequences with branches 3, 4, and 7- 10 of the nitrilase superfamily (Figure 6.1). These branches contained a nitrilase related sequence that is fused to an additional protein domain (Pace and Brenner, 2001). For example, the NAD⁺ synthetase (branch 7) of *Mycobacterium tuberculosis* is composed of a nitrilase related sequence fused to NAD⁺ synthetase domain (Bellinzoni *et al.*, 2005). The nitrilase hydrolyses glutamine releasing ammonia for the synthesis of NADH. It is possible that Nit1 could have similar enzyme function to the amidases of branch 3, 4, 7 or amide condensation nitrilases of branch 9 as a non-fused protein.

An attempt to characterise Nit1 *in vitro* led to the appearance of a purified ~30 kDa monomer. Despite the attempts to determine the substrate range for Nit1, it was concluded that the expressed enzyme was inactive. This assumption was based on characterised enzymes of the nitrilase superfamily that are typically active as multimers (Thuku *et al.*, 2009). For example, spiral forming Nases are known to exist as inactive dimers in solution, but self associate to form active multimers (Thuku *et al.* 2009). The quaternary structure of the closely related putative CN-hydrolase 1f89 is a tetramer (Kumaran *et al.*, 2003). It was proposed that the C-terminal hexahistidine tag fused to Nit1 for Ni-chelation chromatography purification might have prevented the enzyme from forming multimers. To illustrate this, Figure 6.2 shows homology models of Nit1 C-terminal hexahistidine tag fusion protein superimposed on the dimer form of 1f89 (Figure 6.2). The two hexahistidine tags of Nit1 are in proximity to each other and are located at the conserved A surface (Figure 6.2). These polar tags of Nit1 fusion protein might have disrupted intersubunit interactions from occurring between two monomers. The purification of an N-terminal hexahistidine tag fusion Nit1 protein was suggested as an alternative approach for the characterisation of this enzyme.

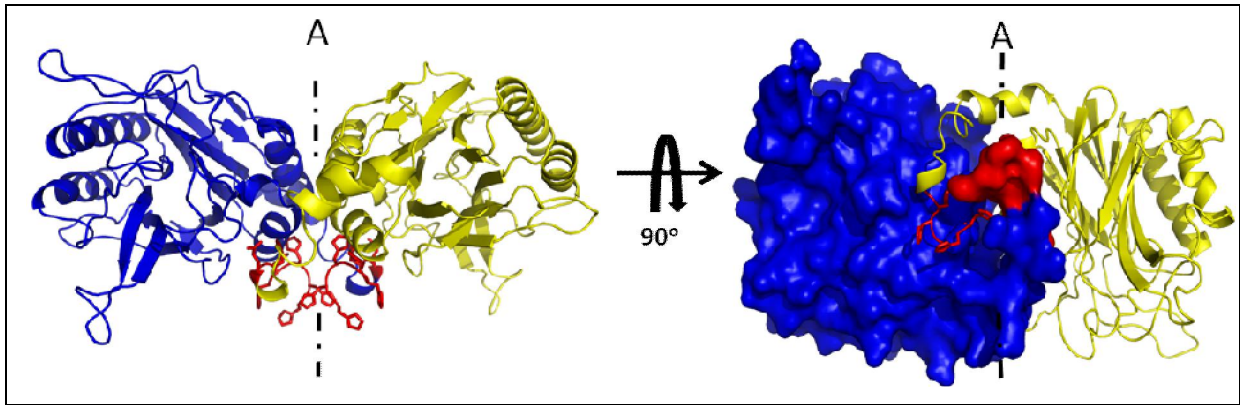


Figure 6.2 Homology model of C-terminal hexahistidine tagged Nit1 in dimer form. The two monomers that interact at the A surface are shown in blue and yellow. The C-terminal tag (8 residues), which contains the hexahistidine residues, is shown in red. The structure of 1f89 dimer form (not shown) was used for the superimposition of Nit1 homology models.

Nit2 was characterised as an aliphatic amidase due to its preference for small amides. However, Nit2 was structurally different from known aliphatic amidases since the enzyme did not possess an extended C-terminal region and was active as a ~45.5 kDa dimer.

As for Nit1, Nit2 fell in a cluster of related putative nitrilases from the bacterial family *Micrococcaceae* (Figure 6.1). Nit2 shared branching with known enzymes that have amidase activities, including branch 2 aliphatic amidases (Figure 6.1). Although they shared the same branching, the distance between Nit2 and aliphatic amidases agreed with the suggestion that these are two distinct groups of enzymes, primarily due to the differences in their C-terminal regions (Figure 6.1). The differences in the C-terminal region might confirm why the *in silico* analysis of Nit2 homology model suggested that the enzyme was a DCase. DCases do not possess an extended C-terminal region (Wang *et al.*, 2001, Thuku *et al.*, 2009) and share the same branching with Nit2 and branch 2 enzymes (Figure 6.1). The grouping of Nit2 with aliphatic amidases showed that this alternative *in silico* analytical method is useful for the assignment of putative protein sequences to branches of the nitrilase superfamily.

Nit2 is unique amongst aliphatic amidases since it is active in dimeric form. Known aliphatic amidases are active as tetramers, hexamers and octamers

(Ambler *et al.*, 1987, Asano *et al.*, 1982, Makhongela *et al.*, 2007, Skouloubris *et al.*, 2001, Soubrier *et al.*, 1992). It has been determined through mutational analysis on *P. aeruginosa* aliphatic amidase that the hexameric form is the active enzyme, which assembles from inactive dimers (Karmali *et al.*, 2001, Novo *et al.*, 2002). The putative CN-hydrolase of *Pyrococcus horikoshi*, the structure (1j31) of which is known (Sakai *et al.*, 2004), shared the same branching and has 22% protein sequence identity with Nit2. The quaternary structure of this CN-hydrolase is of a tetramer (Sakai *et al.*, 2004). Nit2 might exist as a hexamer due to the appearance of a small amount of active ~130 kDa protein eluted during size exclusion chromatography. It is possible that the N-terminal hexahistidine tag fused to Nit2 for Ni-chelation purification might have interfered with inter-dimer assembly. The crystal structure of Nit2 showed a possible interaction between H19 of the 20 residue N-terminal hexahistidine tag and N259 of the C-terminal region. This interaction was suggested to contribute toward the destabilisation of C-terminal region residues 259-260, which are absent in the crystal structure. The effects of hexahistidine tag fusions have not been determined for known aliphatic amidases, since these enzymes have been purified and characterised directly from the native organisms and/or from *E. coli* using a series of affinity and size exclusion chromatography techniques (Andrade *et al.*, 2007, Makhongela *et al.*, 2007, Skouloubris *et al.*, 2001). To illustrate the possible interference of an N-terminal hexahistidine tag on inter-dimer interaction, Figure 6.3 shows the *G. pallidus* (2plq) hexamer structure with the 20 residue tag fused to the N-terminus of two monomers. The 20 residues tag of the two monomers are in proximity and are located across the two fold symmetrical surface occurring between two interacting dimers (Figure 6.3). This inter-dimer interaction is formed by the N-terminal region and α 7 helix of monomers as observed in the structure of *G. pallidus* aliphatic amidase (Kimani *et al.*, 2007). The α 7 helix of *G. pallidus* aliphatic amidase superimposes the missing residues observed in Nit2 crystal structure (not shown). A purification of tag free Nit2 should be attempted in order to characterise its quaternary structure.

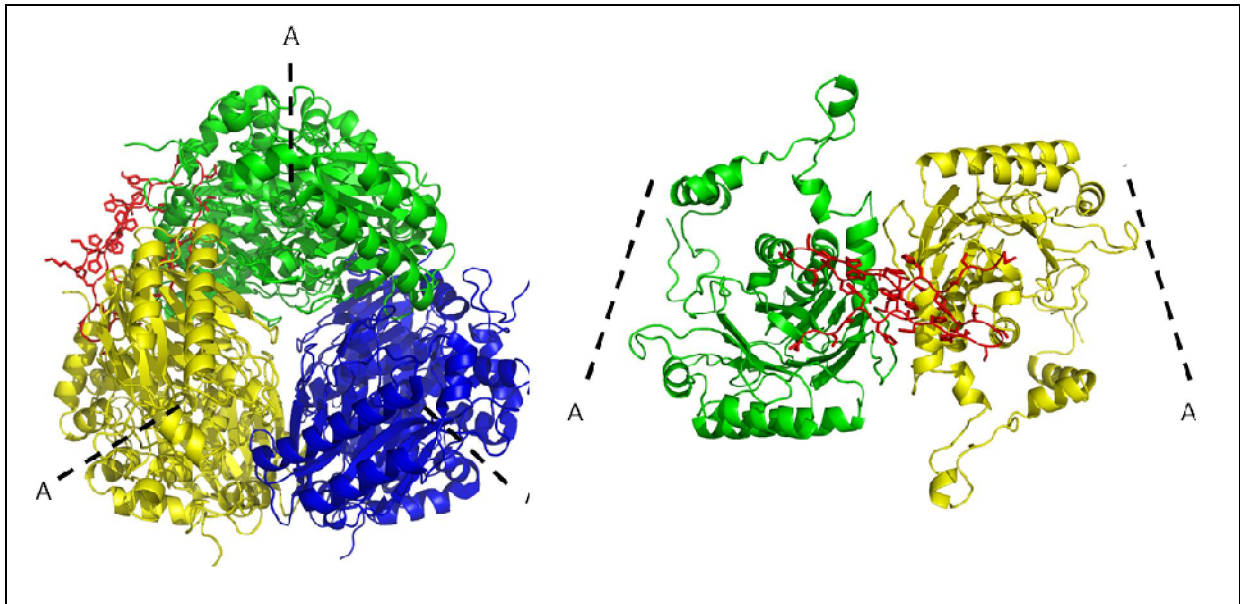


Figure 6.3 Structure of *G. pallidus* aliphatic amidase (2uxy) showing the position of the N-terminal hexahistidine tag fused to two monomers. Left image, view of hexamer. Right image, view of the interaction between two monomers of opposite dimers. The 20-residue N-terminal tag containing the hexahistidine residues is shown in red. Individual dimers are coloured separately. The A surface that occurs between interacting monomers within a dimer is shown.

UNIVERSITY of the
WESTERN CAPE

The short C-terminal region of Nit2 was proposed to contribute towards its thermostability. This assumption was drawn from the high thermostability (55°C) of the mesophilic *P. aeruginosa* aliphatic amidase, which was attributed to the extended C-terminal regions of their monomers (Andrade *et al.*, 2007). However, there are mesophilic spiral forming Nases that also have extended C-terminal regions but are not thermostable (Thuku *et al.*, 2007). Unlike Nases, the tight hexameric form of *P. aeruginosa* aliphatic amidase was also suggested as a possible thermostabilising factor (Andrade *et al.*, 2007). This suggests that both the dimer form and short C-terminal region of Nit2 may contribute to its thermostability. The thermostability of the possible Nit2 hexamer form should be determined for comparison with *P. aeruginosa* aliphatic amidase. A hexameric form of Nit2 might have higher stability at elevated temperatures than the dimer form.

It was suggested that aliphatic amides were probably not the natural substrates for Nit2, due to the low affinity and catalytic rate. No comparison could be made for the catalytic rate with known aliphatic amidases, since kinetic parameters for these enzymes were obtained using the acyl transfer assay in the presence of hydroxylamine (Makhongela *et al.*, 2007, Skouloubris *et al.*, 2001). Amidases typically have higher catalytic rates in this assay, since hydroxylamine is a better acyl acceptor than water (Fournand *et al.*, 1998). No detectable activity was obtained for Nit2 under the reported assay conditions used for other amidases. The lack of activity for Nit2 using the acyl transfer assay was probably due to the conditions used, which require further optimisation. Despite the low catalytic rate of Nit2, the low affinity of the enzyme for amides was also suggested to be attributed to its cold-adapted origins. It has been proposed that cold-adapted enzymes exhibit low affinity for their substrates in order to achieve high catalytic rates at low temperatures (Xu *et al.*, 2003). It is possible that there are several subgroups of aliphatic amidases with distinct preferences for different lengths of aliphatic amides. This was because Nit2 had higher K_M for propionamide (3C) than for acetamide (2C). Conversely, all known aliphatic amidases have the highest K_M for 2C amides (Kotlova *et al.*, 1999, Skouloubris *et al.*, 2001). In addition, the AmiF of *Helicobacter pylori* exclusively hydrolyses formamide (1C) (Skouloubris *et al.*, 2001). The structure of Nit2 provides an ideal model for the identification of residues lining the catalytic site that may determine its substrate range. The substitution of W138 residue with a neutral amino acid in *P. aeruginosa* aliphatic amidase increased the catalytic volume of the enzyme to include aromatic amides (Karmali *et al.* 2001).

The simple dimeric form of Nit2 and the ease of expression, purification and crystallisation of the enzyme, are attractive features for further studies of the nitrilase superfamily. For example, the determination of the role that the extra catalytic glutamate residue plays in the nitrilase reaction mechanism could be researched. This extra glutamate residue (E142) according to the structure of *G. pallidus* aliphatic amidase was implicated in the nitrilase reaction mechanism (Kimani *et al.*, 2007, Thuku *et al.*, 2009), since its side-chain is in proximity to water and is in a suitable position to act as the general base catalyst. Further possible studies would be to identify residues that are involved in the enzymic

conformational transitions, which enable a continued reaction cycle where the enzyme binds to the substrate and releases the product (Andrade *et al.*, 2007). Another study could be to identify residues other than the conserved catalytic residues (EKEC) that distinguish an enzyme member of the nitrilase superfamily from having either amide or nitrile hydrolysing activity (Thuku *et al.*, 2009).



Appendix

A. General recombinant DNA techniques

The *E. coli* strains used for plasmid maintenance are: DH5 (Hanahan, 1983); GeneHog (Smith *et al.*, 1990) as a host for recombinant plasmids. These strains were grown at 37°C in LB or on LB agar plates supplemented with the antibiotic to which the recombinant plasmid conferred resistance. The preparation of *E. coli* chemical competent cells and the transformation protocols were taken from Hanahan *et al.*, (1995) and Sambrook & Russel (2001). Electrocompetent cells were prepared and transformed using a GenePulser (Biorad) according to the protocols supplied by the manufacturer (available online). Cultures of transformants were stored at -80°C in 50% (v/v) glycerol.

Routine isolation of recombinant plasmid DNA from *E. coli* strains was performed using the easy plasmid preparation protocol of Berghammer and Auer (1993). DNA used for sequencing, storage, was isolated using the High Pure Plasmid Isolation Kit (Roche) or the Quantum Prep® Plasmid Kit (BioRad). DNA was stored at -20°C or at -80°C.

The resultant restriction fragments of DNA restriction analysis were separated by electrophoresis using Tris-acetate-EDTA buffer (20x stock solution (2 M Tris-HCl (pH 8.3); 25 mM EDTA) on 0.5-4% agarose gel containing 0.5 µg/ml ethidium bromide and visualised using the Alphaimager imaging system (BioRad). Excision of resultant fragments of DNA were carried out using the illustra™ GFX™ PCR DNA and Gel Band Purification Kit (GE Healthcare). DNA concentration estimation was carried out using the Nanodrop (ThermoScientific) or by fluorescent analysis using the Qubit® Quantitation Platform (Invitrogen).

Sequencing was carried out at University of Cape Town or University of Stellenbosch sequencing centers that have ABI prism automated sequencers (AppliedBiosystems) using the Big Dye terminal dideoxy chain termination method.

B. Media

Luria Bertrani (LB)	Luria Bertrani Agar	M63
10 g Bacto-tryptone	1 L LB	3 g KH ₂ PO ₄
5 g yeast extract.	15 g Bacteriological agar	7 g K ₂ HPO ₄
10 g NaCl		* 2 g (NH ₄) ₂ SO ₄
Make up to 1 L with H ₂ O		0.5 ml 1mg/ml FeSO ₄
		2 ml 0.5M MgSO ₄
		20 ml 1.5M Glycerol
		Make up to 1 L H ₂ O

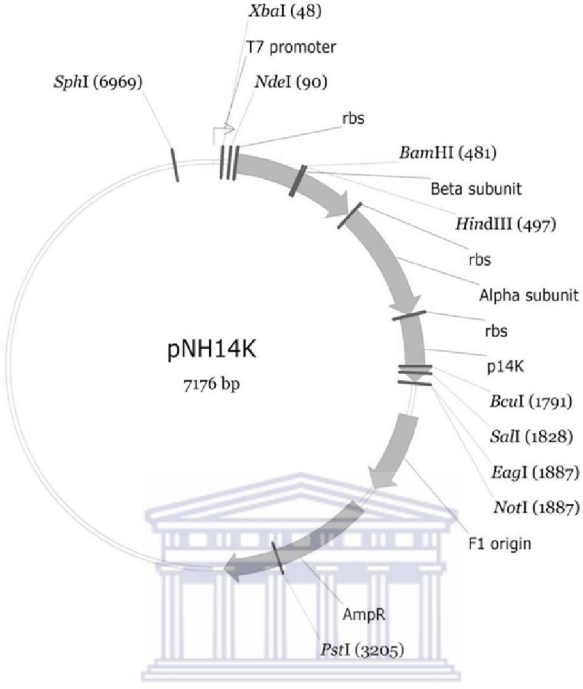
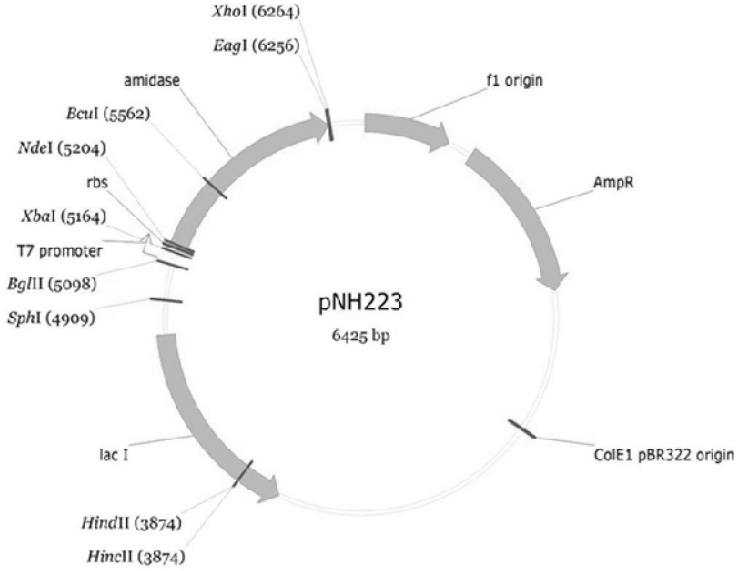
* left out for the preparation of nitrogen free minimal medium

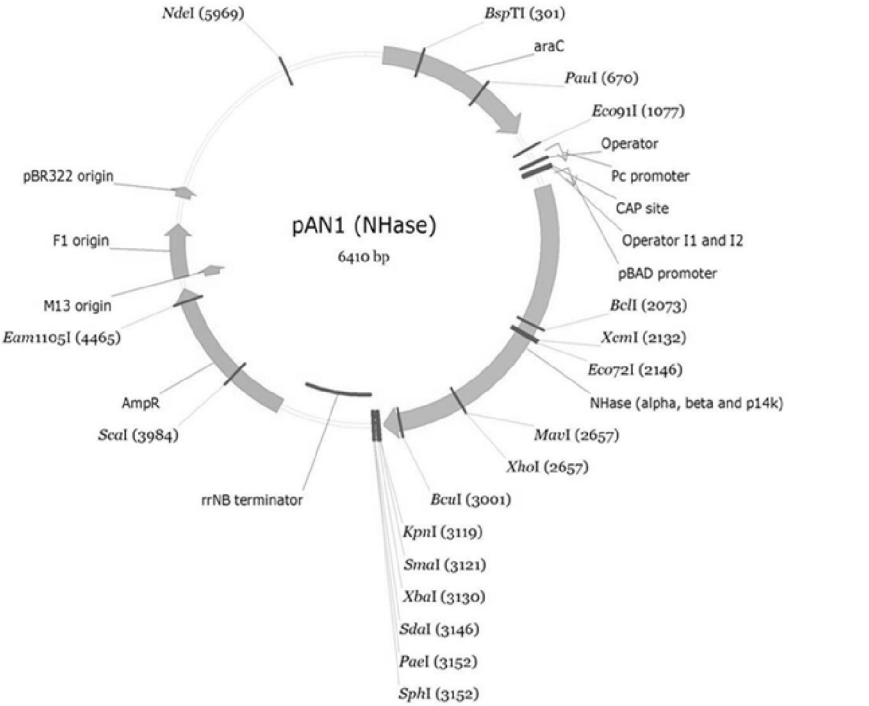
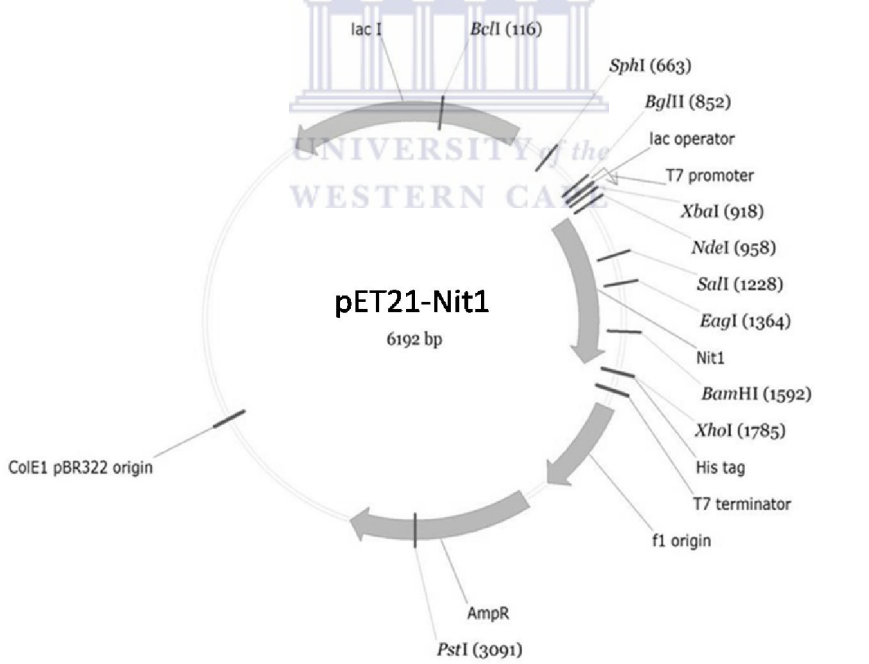
C. *E. coli* strains

<i>E. coli</i> strain	Genotype	Reference
ArcticExpress	F ⁻ <i>ompT hsdS</i> (r _B m _B) <i>dcm</i> ⁺ Tet ^r <i>gal</i> <i>endA</i> Hte [<i>cpn10 cpn60</i> Gent ^r]	Stratagene
BL21(DE3) pLysS	F ⁻ , <i>ompT</i> , <i>hsdS</i> _B (r _B ⁻ , m _B ⁻), <i>dcm</i> , <i>gal</i> , (DE3), pLysS (Cm ^r)	Davanloo, 1984, Studier & Moffatt, 1986
DH5	80 <i>lacZ</i> M15, <i>recA1</i> , <i>endA1</i> , <i>gyrAB</i> , <i>thi-1</i> , <i>hsdR17</i> (r _K ⁻ , m _K ⁺), <i>supE44</i> , <i>relA1</i> , <i>deoR</i> , (<i>lacZYA-argF</i>) U169, <i>phoA</i>	Hanahan, 1983
GeneHog	F ⁻ <i>mcrA</i> (<i>mrr-hsdRMS-mcrBC</i>) 80 <i>lacZ</i> M15 <i>lacX74</i> <i>recA1</i> <i>araD139</i> (<i>ara-leu</i>)7697 <i>galU</i> <i>galK</i> <i>rpsL</i> (Str ^R) <i>endA1</i> <i>nupG</i> <i>thiA::IS2</i> (confers phage T1 resistance)	Smith <i>et al.</i> , 1990
JK84	<i>lacY1</i> or <i>lacZ4</i> <i>glnV44</i> (AS) LAM- <i>hisS210</i> (ts) <i>glyA6</i> <i>relA1</i> <i>rpsL8</i> or <i>rplL9</i> (L?) <i>rpsL14</i> <i>xyl-7</i> <i>mtlA2</i> <i>argH1</i> <i>thi-1</i>	Parker & Fishman, 1979

D. Plasmids

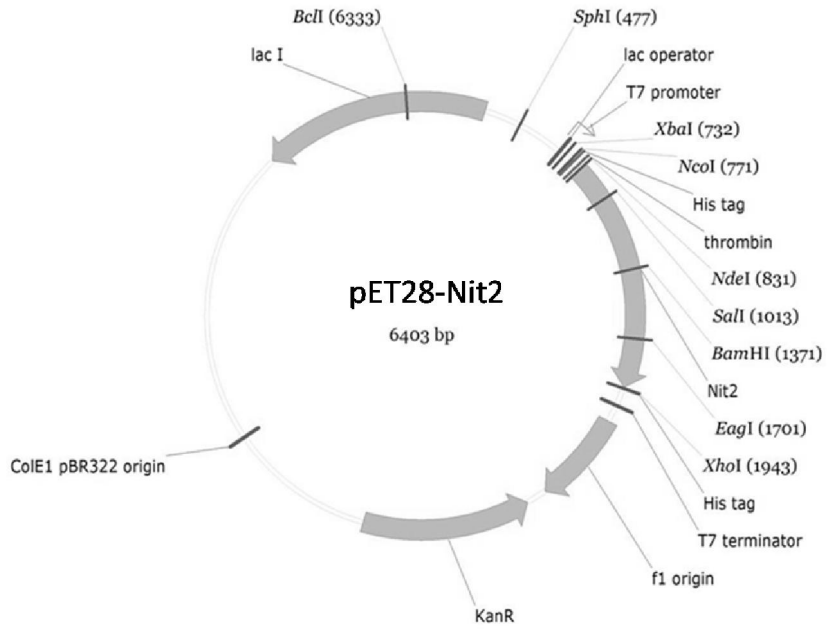
Only unique restriction sites are shown.

Plasmid	Map	Reference
pNH14K	 <p data-bbox="331 1160 1241 1240"><i>G. pallidus</i> RAPc8 NHase (, and P14K) under the control of T7 promoter; AmpR, confers ampicillin resistance</p>	Cameron, 2003
pNH233	 <p data-bbox="331 1854 1241 1926"><i>G. pallidus</i> RAPc8 aliphatic amidase under the control of T7 promoter; AmpR, confers ampicillin resistance</p>	Cameron, 2003

<p>pAN1</p>	 <p style="text-align: center;">pAN1 (NHase) 6410 bp</p>	<p>This work</p>
<p>pET21-Nit1</p>	 <p style="text-align: center;">pET21-Nit1 6192 bp</p> <p><i>Nesterenkonia</i> AN1 Nit1 fused to C-terminal hexahistidine tag under the control of T7 promoter; AmpR , ampicillin resistance</p>	<p>This work</p>

<p>pET21-Nit2</p>		<p>This work</p>
<p>pET28-Nit1</p>	<p><i>Nesterenkonia</i> AN1 Nit1 fused to N-terminal hexahistidine tag under the control of T7 promoter; KanR, confers kanamycin resistance</p>	<p>This work</p>

pET28-Nit2



This work

Nesterenkonia AN1 Nit1 fused to N-terminal hexahistidine tag under the control of T7 promoter; KanR , confers kanamycin resistance



E. SDS-PAGE

SDS-PAGE was carried out on a Hoefer SE 250 minigel electrophoresis unit. For SDS-PAGE, samples were mixed with gel loading buffer and boiled 5 mins prior to loading. Gels were electrophoresed at a constant current of 50 mA in electrode running buffer. Gels were stained with staining solution. Gels were then destained as follows: solution 1 for half an hr, solution 2 overnight and solution 3 for 2 hrs.

Recipes for a 12% resolving gel and 5.2% stacking gel

Reagents	Stock solution	Resolving gel (12%)	Stacking gel (5.2%)
Acrylamide stock	40% (w/v)	8 ml	0.85
H ₂ O	-	6.6 ml	2.8
Tris-HCl (pH 8.7)	1.5 M	5 ml	-
Tris-HCl (pH 6.8)	0.5 M	-	1.25
SDS	20% (w/v)	0.2 ml	0.05 ml
(NH ₄) ₂ S ₂ O ₈	10% (w/v)	0.2 ml	0.05 ml
TEMED	-	0.02 ml	0.01 ml

Acrylamide stock

30% (w/v) acrylamide
0.8 (w/v) bis-acrylamide

Electrode running buffer (10 ×)

2 M glycine
0.25 M Tris-HCl (pH 8.3)
1 % (w/v) SDS

Gel-loading buffer (×2)

100 mM Tris-HCl (pH 6.8)
4% (w/v) SDS
0.2 % (w/v) bromophenol blue
20% (v/v) glycerol
200 mM DTT

Commassie Stain

2 g Coomassie brilliant blue R250
200 ml Destain solution I

Destaining solutions

Solution 1 (1/2 hrs)

50% (v/v) Methanol
10% (v/v) Glacial acetic acid

Solution 2 (overnight)

5% (v/v) Methanol
7% (v/v) Glacial acetic acid

Solution 3 (2 hrs)

5% (v/v) Methanol
7% (v/v) Glacial acetic acid
3% (v/v) glycerol

F. Nit1 and Nit2 - nucleotide and protein sequences

(Only unique restriction site are shown)

Nit1

```

+1 M R I A A A Q I T T G P D P D A N L E L I R E Y T A R A A Q A G A R
1  ATGGCAATG CTGCCCTCA GATCACCACC GGGCCGGACC CCGATGCCAA CTTGGAGCTG ATCCGGGGAT ACACCCGGCG TGGCGGGCAG GCCGGGGCCG
TAGCCCTAAC GACCGGAGT CTACTGCTGG CCGGGCCCTGG GGTACTCGTT GACCTTCGAC TASSCCCTTA TGTGGGCGC ACGGCGGCTC GGGCCCGCGG
+1 R V V V F P E A A Q R A F G H P L P P V A E P V T G A W A E A V R G
101 GGTTCCTGCT CTTCCCGAG GCGCCDAG GCGCCTCGG GCACCCCTTG CCGCCCTGG CCGAACCGT CACCGCTGC TGGGCCGAGG CCGTCCGTGG
CCAGCACCA GAAGGCTC CAGCGCTG CCGGAAAGCC CGTGGGAAAC GCGGGCAC ACCGCTGGCA GTGGCCACGG ACCCGCTCC GGCAGGCACC
+1 G L A R E F Q I V I V A G M F T P G V P S A D G R P R V V N T L I A
201 CCTGGCGGG GAGTTCAGA TCGTATGCT CCGCGGATG TTACCCCGG GGTTCOCAG CGTGGACGT GACCCCGCG TGGTCACAC GGTGATGGC
GGACCGCCCC CTCRAGTCT AGCCTAGCA GCGGCCCTAC AAGTGGGGC CCCAAGGTC GCGACTGCA GCTGGGGCC ACCAGTTGT GCACTAGCGG
+1 V G P A S A G A A E I D V A Y D K I H L Y D A F G F K E S D G V Q
301 GTGGGCCCG CCGGCCCGG GAGTGGAG TCGCTTGA TCGATCCAC CTCATGAGC CTTTCGGTT CAAGGATCC GACGGGCTCC
CACCCGGGC GCGCGGGCC CTTAGCTGC AGCGATGCT GTTCTAGTG SAGTACTGC GGAAGCGAA GTTCTCTAGG GTGCCGAGG CTGCCGAGG
+1 Q P G R S P A H F V L D D T F G L A T C Y D I R F P N L F T A H A
401 AGCCCGCGG AAGCCGGCG CATTCTCC TCGACGACT CACTTCGG CTGGCACCT CTACGACAT CCGCTTCCG AACCTTCA CCGCCCATGC
TCGGCCCGC TTCGGCCCG GAAAGCAG AGCTCTGTA GTGGAGCC GACCGTGA CAGTCTGA GCGAAGGC TTGCACAGT GCGGGTACG
+1 A R S G A Q V T L V P A S W G A G E G K L E Q W R L L A Q A R A L D
501 CCGATCTGC GCACAGTA CCTGGTGC GCGCTCTGG GGTGGGGG AGGCAAGCT GAGCAGTGG CCGCTCTCG CCCAGGCCAG GCGCTGGAT
GGCTAGACG CTTGTCCACT GGGACCCAG CCGGAGGACC CCAGCCGCC TCCCGTTCG CCTGTCACC GCGCAGGRC GGTCCCGGTC CCGGACCTA
+1 S T Q Y I L A C G Q A D P T A A G V E A V Q G A P T G I G H S M I V
601 TCCAGCGAT ACATCCTGC CTGGCCAG GCGGATCCA CCGCCCGCG AGTGGAGCG STACAGGAG CCGCCACCG GATCGGTGAT TCGATGATCG
AGTGGGICA TGTAGACCG GACCCGGTC CCGCTAGGT GGGGGCGCC TCACCTCCG CATCTCCCTC GGGGGTGGC CTAGCCAGTA AGCTACTAGC
+1 V S P L G V P L S E A G S A P E L L I A E L D P E L V S R T R E L V
701 TGTCCCCCT GGGGTCCCG CTCAGGAG CCGGATGCG CCGCAGTGC CTGATGCGG AGCTGGACC CCACTGGTC ACCCGGACC GGGAGCTGGT
ACAGGGGGA CCCGCGGC GATTCGTTC GCGCTCAG CCGCTCGAC GAGCTGGGC GACTAGGCG CTTAGCCAG GCTTGGCCG CCTCGACCA
+1 V F V L R N A R Q L
801 CCGGTGCTG GCRACGCC GCGCTCTA G
GGCCACGAC GGTTCGGG CCGTCCGAT C

```

```

+1 M R I A L M Q H T A R P L D P Q H N L D L I D D A A A R A S E Q G A
1 ATCGGATCG CCGTGTGCA GCACACGGC CGTCCGTTGG ACCCGGAGCA CAACCTGGAC CTGATCGAGC AGCCCGGGC TCGGGGAGC GAGCAGGGG
IADCTTAGC GCGACTACGT CGTGTGGCCG GCGGCGAAC TGGCCCTCGT GTGGACCIG GACTAGCTGC TCGGGGGCCG AGCCCGCTCG CIGCTCCCCC

HircII
~~~~~
Sall
~~~~~
HircII
~~~~~
+1 A Q L L L T P E L F G F G Y V P S C I I C A Q V S A E Q V D A A R S R
101 CCAGCTGCT GGTACDCCG GAGTCTTGG GCTCGGCTA GATCTGTG CCGAGGICAG GCGGACACG GTCGACGGC GAGGTCCAG
GGTCCAGCA CAGTGGGGC CTCGGAGAC CAGAGCCGAI GAGGSCAGT GICTAGCAC GGTCCAGTC GGCCTTGTG CAGTGGCCG GTCOCASGTC

R L R G I A R D R G I A L V W S L P G P E Q R G I T A E L A D
201 ACTGCCGCT ATGCCCGGG ACCCGGGAT CGGCTGGTG TGGTGCCTC CGGCCCTGA GGGCCCGAG CAGCCCGGA TCACCCCGA GCTGGCCGAT
IGAGCGGCA TGGCGGCC TGGCGCCCTA GCGGACAC ACCAGGAG GGCCTGACT CCGCCGGCTC GTCCGGCTC AGTGGCGCT CGAGCGGCTA

+1 E H G E V L A S Y Q K V Q L Y G P E E K A A F V P G E Q P P P V L S
301 GAACAGGAG AAGGCTTGC CAGTACCAG AAGTCCAGC TCTACGAGC GAGGAGAG GCGCCCTTC TCCCGGGCA GACCGGGC GCGGTGCTCA
CTGTGCTTC TCACGACG GTCGATGGT TCCAGGTC AGATGCTTG GCTCCTTC GCGGGAAG AGGCCGCTC GTCGGCGGC GGCACGAGT

+1 S W G G R Q L S L L V C Y D V E F P E M V R A A A R G A Q L V L V
401 GCTGGGGGG ACGGACCTG AGCTGCTGG TCTGCTAGA CGTGGATTC CCGAGATGG TCGCGCCGC GCGAGCCGC GCGCCCCAGC TGGTCTGCT
CGACCCGSC TCGCGTGCAC TCGGAGADC AGAGATGCI GCACCTCAG GGGTCTACC AGGCGCGGG GGTGGGGC GCGGGGGTGG ACCACGACCA

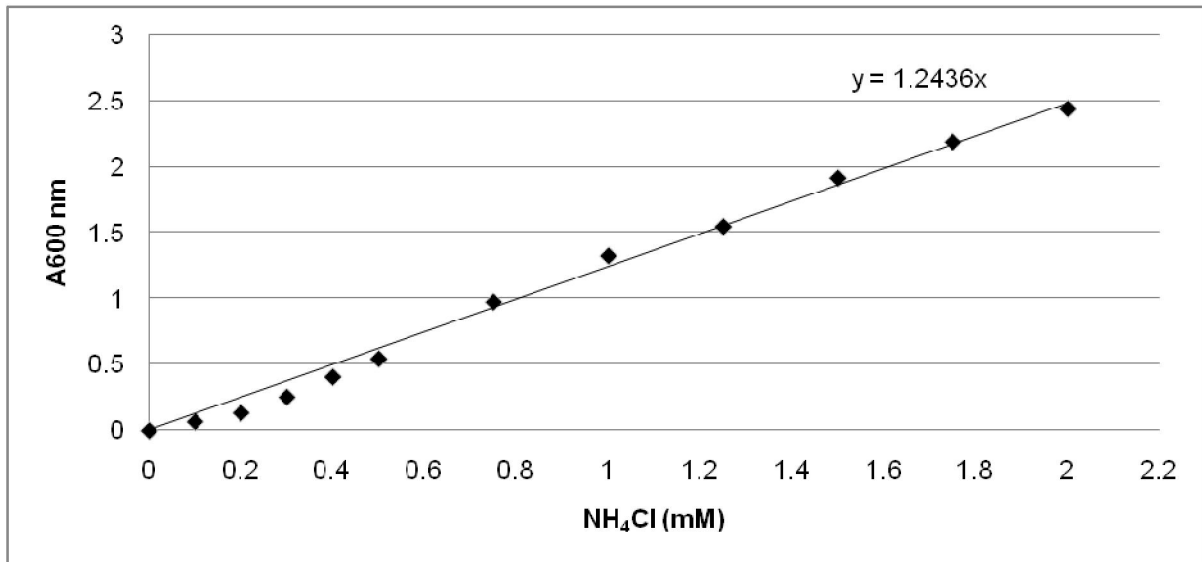
BamHI
~~~~~
+1 V P T A L A G D E T S V P G I L L P A R A V E N G I T L A Y A N H C
501 GCGCACCTT CTGGCGGG ACGACCTC GGTCCCGGG ATCTGCTGC CCGCGCGC CTGGAGAC GGGATCACCC TGGCTATGC CACCCACTGC
CGGTGGGA GACCGGCC TGCCTGGAG CCGGGGCC TAGGAGAC GCGCGCGC GACCTCTTG CCTAGTGG ACCGATAG GTGGTGAAG

+1 G P E G L V F D G G S V V G P A G Q P L G E L G V E P G L L V V
601 GGGCCGAGG GCGGGCTGG CTTCGACGG GAGAGCTCG TCGTGGCC GCGAGGCAG CCGCTGGGG AGTGGGTGI GGAACCGGT TGGTGGTGG
CCGGCCCTCC CCGCCGACCA GAAGCTGDC CCGTGGAGC ACCAGCGGG CCGTCCGIC GCGGACCCCC TCGACACACA CCTTGGCCCA AACGACCCAG

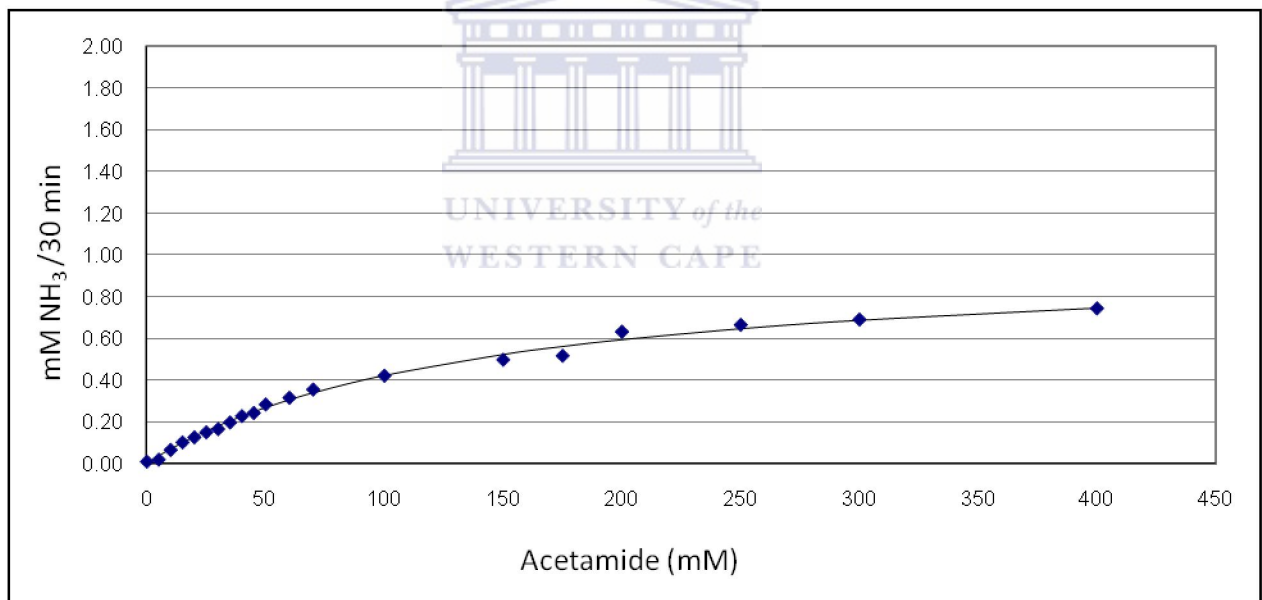
+1 V D L P D Q S Q D A G S D S A D Y L Q D R R A E L H R N W L
701 TGAACCTGCC GACACAGC CAGGACGAG GTTCGGACG GCGGACTAC CTCAGGAC GCGCGCGGA GCTCCACCG AACTGGCTGT AG
ACCTGGAGG CCGTGTCTCG GTCCTGGTC CAAGCTCC GCGCCGATG GAATCCTAG CCGCGCGCTC CGAGTGGCC TTGACCGACA TC

```

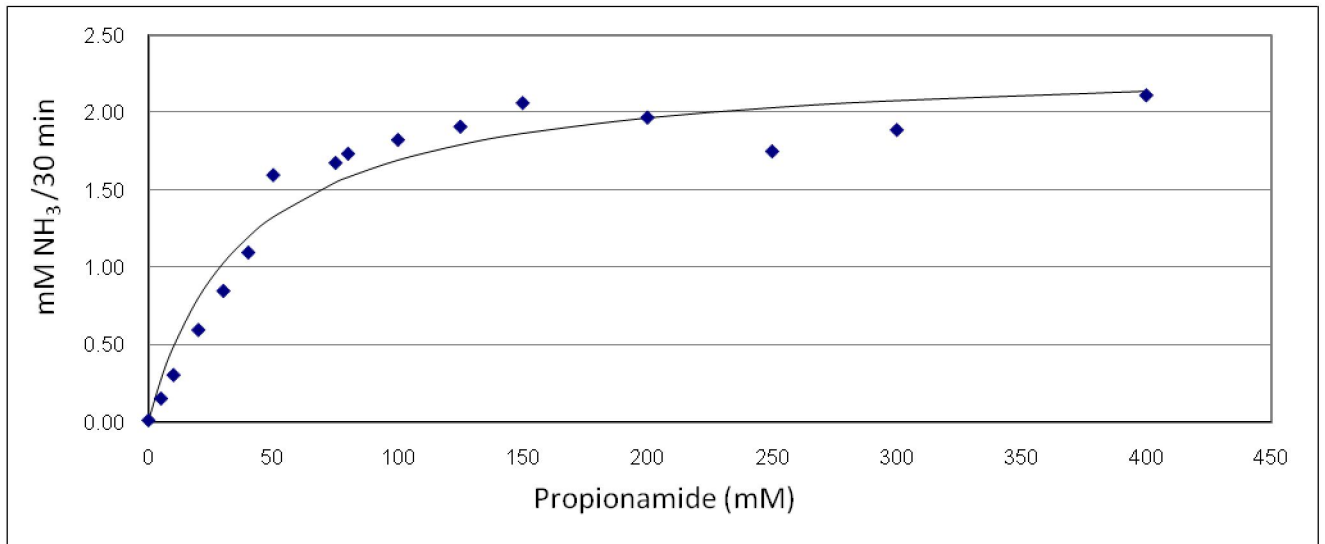

G. Kinetic data



Ammonia assay standard curve



Michaelis Menten (direct plots): Acetamide ($K_M = 137.73 \text{ mM}$; $V_{\text{max}} = 1 \text{ mM NH}_3/30 \text{ min}$)



Michaelis Menten (direct plots): Propionamide ($K_M = 38.53$ mM; $V_{max} = 2.3$ NH₃/30 min)



References

- Almatawah, Q. A., Cramp, R. & Cowan, D. A. (1999). Characterisation of an inducible nitrilase from a thermophilic *Bacillus*. *Extremophiles* **3**, 283-91
- Alquati, C., De Gioia, L., Santarossa, G., Alberghina, L., Fantucci, P. & Lotti, M. (2002). The cold-active lipase of *Pseudomonas fragi*. Heterologous expression, biochemical characterisation and molecular modelling. *European Journal of Biochemistry* **269**, 3321-8.
- Altschul, S. F., Gish, W., Miller, W., Myers, E. W. & Lipman, D. J. (1990). Basic local alignment search tool. *Journal of Molecular Biology* **215**, 403-10.
- Altschul, S. F., Madden, T. L., Schaffer, A. A., Zhang, J., Zhang, Z., Miller, W. & Lipman, D. J. (1997). Gapped BLAST and PSI-BLAST: a new generation of protein database search programs. *Nucleic Acids Research* **25**, 3389-402.
- Amann, R. I., Ludwig, W. & Schleifer, K. H. (1995). Phylogenetic identification and *in situ* detection of individual microbial cells without cultivation. *Microbiology Reviews* **59**, 143-69.
- Amarant, T., Vered, Y. & Bohak, Z. (1989). Substrate and inhibitors of the nitrile hydratase and amidase of *Corynebacterium nitrilophilus*. *Biotechnology and Applied Biochemistry* **11**, 49-59.
- Ambler, R. P., Auffret, A. D. & Clarke, P. H. (1987). The amino acid sequence of the aliphatic amidase from *Pseudomonas aeruginosa*. *Federation of European Biochemical Societies Letters* **215**, 285-90.
- Andrade, J., Karmali, A., Carrondo, M. A. & Frazao, C. (2007). Structure of amidase from *Pseudomonas aeruginosa* showing a trapped acyl transfer reaction intermediate state. *Journal of Biological Chemistry* **282**, 19598-605.
- Artaud, I., Chatel, S., Chauvin, A. S., Bonnet, D., Kopf, M. A. & Leduc, P. (1999). Nitrile hydratase and related non-heme iron sulfur complexes. *Coordination Chemistry Reviews* **190**, 577-86.
- Asano, Y., Tachibana, M., Tani, Y. & Yamada, H. (1982). Purification and characterisation of amidase which participates in nitrile degradation. *Agricultural and Biological Chemistry* **46**, 1175-81.
- Asano, Y., Tani, Y. & Yamada, H. (1980). A new enzyme "nitrile hydratase" which degrades acetonitrile in combination with amidase. *Agricultural Biology and Chemistry* **44**, 2251-52.

- Atlas, R. M. (2005). *Handbook of media for environmental microbiology* (2nd edition) CRC Press. USA
- Aziz, R. K., Bartels, D., Best, A. A., DeJongh, M., Disz, T., Edwards, R. A., Formsma, K., Gerdes, S., Glass, E. M., Kubal, M., Meyer, F., Olsen, G. J., Olson, R., Osterman, A. L., Overbeek, R. A., McNeil, L. K., Paarmann, D., Paczian, T., Parrello, B., Pusch, G. D., Reich, C., Stevens, R., Vassieva, O., Vonstein, V., Wilke, A. & Zagnitko, O. (2008). The RAST Server: rapid annotations using subsystems technology. *BioMed Central Genomics* **9**, 75.
- Bandyopadhyay, A. K., Nagasawa, T., Asano, Y., Fujishiro, K., Tani, Y. & Yamada, H. (1986). Purification and characterisation of benzonitrilases from *Arthrobacter* sp. Strain J-1. *Applied and Environmental Microbiology* **51**, 302-6.
- Banerjee, A., Kaul, P. & Banerjee, U. C. (2006). Purification and characterisation of an enantioselective arylacetone nitrilase from *Pseudomonas putida*. *Archives of Microbiology* **184**, 407-18.
- Banerjee, A., Sharma, R. & Banerjee, U. C. (2002). The nitrile-degrading enzymes: current status and future prospects. *Applied Microbiology and Biotechnology* **60**, 33-44.
- Barglow, K. T., Saikatendu, K. S., Bracey, M. H., Huey, R., Morris, G. M., Olson, A. J., Stevens, R. C. & Cravatt, B. F. (2008). Functional proteomic and structural insights into molecular recognition in the nitrilase family enzymes. *Biochemistry* **47**, 13514-23.
- Basile, L., Willson, R., Sewell, B. & Benedik, M. (2008). Genome mining of cyanide-degrading nitrilases from filamentous fungi. *Applied Microbiology and Biotechnology* **80**, 427-35.
- Battistel, E., Bernardi, A. & Maestri, P. (1997). Enzymatic decontamination of aqueous polymer emulsions containing acrylonitrile. *Biotechnology Letters* **19**, 131-4.
- Bauer, R., Hirrlinger, B., Layh, N., Stolz, A. & Knackmuss, H. J. (1994). Enantioselective hydrolysis of racemic 2-phenylpropionitrile and other (R,S)-2 arylpropionitriles by a new bacterial isolate, *Agrobacterium tumefaciens* strain d3. *Applied Microbiology and Biotechnology* **15**, 297-306.
- Beard, T. M. & Page, M. I. (1998). Enantioselective biotransformations using *rhodococci*. *Antonie van Leeuwenhoek, International Journal of General and Molecular Microbiology* **74**, 99-106.
- Bellinzoni, M., Buroni, S., Pasca, M. R., Guglierame, P., Arcesi, F., De Rossi, E. & Riccardi, G. (2005). Glutamine amidotransferase activity of NAD⁺

- synthetase from *Mycobacterium tuberculosis* depends on an amino-terminal nitrilase domain. *Research in Microbiology* **156**, 173-7.
- Betz, J. L. & Clarke, P. H. (1972). Selective evolution of phenylacetamide-utilizing strains of *Pseudomonas aeruginosa*. *Journal of General Microbiology* **73**, 161-74.
- Bhalla, T. C., Aoshima, M., Misawa, S., Muramatsu, R. & Furuhashi, K. (1995). The molecular cloning and sequencing of the nitrilase gene of *Rhodococcus rhodochrous* PA-34. *Acta Biotechnologica* **15**, 297-306.
- Bi, X., Lyu, Y. L. & Leroy, F. L. (1995). Specific stimulation of *recA*-independent plasmid recombination by a DNA sequence at a distance. *Journal of Molecular Biology* **247**, 890-902.
- Bigey, F., Chebrou, H., Fournand, D. & Arnaud, A. (1999). Transcriptional analysis of the nitrile-degrading operon from *Rhodococcus* sp. ACV2 and high level production of recombinant amidase with an *Escherichia coli*-T7 expression system. *Journal of Applied Microbiology* **86**, 752-60.
- Bonnet, D., Artaud, I., Moali, C., Pétré, D. & Mansuy, D. (1997). Highly efficient control of iron-containing nitrile hydratases by stoichiometric amounts of nitric oxide and light. *Federation of European Biochemical Societies Letters* **409**, 216-20.
- Bork, P. & Koonin, E. V. (1994). A new family of carbon-nitrogen hydrolases. *Protein Science* **3**, 1344-46.
- Bracey, M., Hanson, M., Masuda, K., Stevens, R. & Cravatt, B. (2002). Structural adaptations in a membran enzyme that terminastes endocannabinoid signaling. *Science* **298**, 1793-96.
- Brady, D., Beeton, A., Zeevaart, J., Kgaje, C., Van Rantwijk, F. & Sheldon, R. A. (2004). Characterisation of nitrilase and nitrile hydratase biocatalytic systems. *Applied Microbiology and Biotechnology* **64**, 76-85.
- Brandao, P. F. & Bull, A. T. (2003). Nitrile hydrolysing activities of deep-sea and terrestrial mycolate actinomycetes. *Antonie Van Leeuwenhoek* **84**, 89-98.
- Brandao, P. F., Clapp, J. P. & Bull, A. T. (2002). Discrimination and taxonomy of geographically diverse strains of nitrile-metabolizing actinomycetes using chemometric and molecular sequencing techniques. *Environmental Microbiology* **4**, 262-76.
- Brandao, P. F., Clapp, J. P. & Bull, A. T. (2003). Diversity of nitrile hydratase and amidase enzyme genes in *Rhodococcus erythropolis* recovered from geographically distinct habitats. *Applied Environmental Microbiology* **69**, 5754-66.

- Brenner, C. (2002). Catalysis in the nitrilase superfamily. *Current Opinion in Structural Biology* **12**, 775-82.
- Brown, J. E., Brown, P. R. & Clarke, P. H. (1969). Butyramide-utilizing mutants of *Pseudomonas aeruginosa* 8602 which produce an amidase with altered substrate specificity. *Journal of General Microbiology* **57**, 273-85.
- Brown, J. E. & Clarke, P. H. (1970). Mutations in a regulator gene allowing *Pseudomonas aeruginosa* 8602 to grow on butyramide. *Journal of General Microbiology* **64**, 329-42
- Brown, P. R. & Clarke, P. H. (1972). Amino acid substitution in an amidase produced by an acetanilide-utilizing mutant of *Pseudomonas aeruginosa*. *Journal of General Microbiology* **70**, 287-98.
- Bunch, A. W. (1998). Biotransformation of nitriles by *rhodococci*. *Antonie van Leeuwenhoek, International Journal of General and Molecular Microbiology* **74**, 89-97.
- Cameron, R. A. (2003). Nitrile degrading enzymes from extreme environments. *PhD thesis* University of London.
- Cameron, R. A., Sayed, M. & Cowan, D. A. (2005). Molecular analysis of the nitrile catabolism operon of the thermophile *Bacillus pallidus* RAPc8. *Biochimica et Biophysica Acta - General Subjects* **1725**, 35-46.
- Cantarella, M., Cantarella, L., Gallifuoco, A., Frezzini, R., Spera, A. & Alfani, F. (2004). A study in UF-membrane reactor on activity and stability of nitrile hydratase from *Microbacterium imperiale* CBS 498-74 resting cells for propionamide production. *Journal of Molecular Catalysis B: Enzymatic* **29**, 105-13.
- Cavicchioli, R., Siddiqui, K. S., Andrews, D. & Sowers, K. R. (2002). Low-temperature extremophiles and their applications. *Current Opinion in Biotechnology* **13**, 253-61.
- Chauhan, S., Wu, S., Blumerman, S., Fallon, R. D., Gavagan, J. E., DiCosimo, R. & Payne, M. S. (2003). Purification, cloning, sequencing and over-expression in *Escherichia coli* of a regioselective aliphatic nitrilase from *Acidovorax facilis* 72W. *Applied Microbiology and Biotechnology* **61**, 118-22.
- Chebrou, H., Bigey, F., Arnaud, A. & Galzy, P. (1996). Study of the amidase signature group. *Biochimica et Biophysica Acta - Protein Structure and Molecular Enzymology* **1298**, 285-93.
- Chen, H. M., Lin, K. Y. & Lu, C. H. (2005). Refolding and activation of recombinant N-carbamoyl-d-amino acid amidohydrolase from *Escherichia coli* inclusion bodies. *Process Biochemistry* **40**, 2135-41.

- Cheong, T. K. & Oriel, P. J. (2000). Cloning of a wide-spectrum amidase from *Bacillus stearothermophilus* BR388 in *Escherichia coli* and marked enhancement of amidase expression using directed evolution. *Enzyme and Microbial Technology* **26**, 152-8.
- Chin, K.H., Tsai, Y.D., Chan, N.L., Huang, K.F., Wang, A. H.J. & Chou, S.H. (2007). The crystal structure of XC1258 from *Xanthomonas campestris*: A putative procaryotic Nit protein with an arsenic adduct in the active site. *Proteins: Structure, Function and Genetics* **69**, 665-71.
- Cilia, E., Fabbri, A., Uriani, M., Scialdone, G. G. & Ammendola, S. (2005). The signature amidase from *Sulfolobus solfataricus* belongs to the CX3C subgroup of enzymes cleaving both amides and nitriles. Ser195 and Cys145 are predicted to be the active site nucleophiles. *Federation of European Biochemical Societies Letters* **272**, 4716-24.
- Collins, M. D., Lawson, P. A., Labrenz, M., Tindall, B. J., Weiss, N. & Hirsch, P. (2002). *Nesterenkonia lacusekhoensis* sp. nov., isolated from hypersaline Ekho Lake, East Antarctica, and emended description of the genus *Nesterenkonia*. *International Journal of Systematic and Evolutionary Microbiology*. **52**, 1145-50.
- Cowan, D., Cramp, R., Graham, R. P. D. & Almatawah, Q. (1998). Biochemistry and biotechnology of mesophilic and thermophilic nitrile metabolizing enzymes. *Extremophiles* **2**, 207-16.
- Cowan, D. A., Cameron, R. A. & Tsekoa, T. L. (2003). Comparative biology of mesophilic and thermophilic nitrile hydratases. In *Advances in Applied Microbiology*, (A. I. Laskin, J. W. Bennett & G. M. Gadd, eds). pp. 123-58 Academic Press. St. Louis, Missouri, USA
- Cowan, D. A., Russell, N. J., Mamais, A. & Sheppard, D. M. (2002). Antarctic Dry Valley mineral soils contain unexpectedly high levels of microbial biomass. *Extremophiles* **6**, 431-6.
- Cornish-Bowden, A. (1995) Fundamentals of enzyme kinetics. Portland Press Limited, London. ISBN-10: 1855780720
- Cramp, R., Gilmour, M. & Cowan, D. A. (1997). Novel thermophilic bacteria producing nitrile-degrading enzymes. *Microbiology* **143**, 2313-20.
- Cramp, R. A. & Cowan, D. A. (1999). Molecular characterisation of a novel thermophilic nitrile hydratase. *Biochimica et Biophysica Acta* **1431**, 249-60.
- Crosby, J., Moilliet, J., Parratt, J. S. & Turner, N. J. (1994). Regioselective hydrolysis of aromatic dinitriles using a whole-cell catalyst. *Journal of the Chemical Society Perkin Transactions* **1**, 1679-87.

- Curtis, T. P. & Sloan, W. T. (2004). Prokaryotic diversity and its limits: microbial community structure in nature and implications for microbial ecology. *Current Opinion in Microbiology* **7**, 221-6.
- Dadd, M. R., Claridge, T. D., Walton, R., Pettman, A. J. & Knowles, C. J. (2001). Regioselective biotransformation of the dinitrile compounds 2-, 3- and 4-(cyanomethyl) benzonitrile by the soil bacterium *Rhodococcus rhodochrous* LL100-21. *Enzyme and Microbial Technology* **29**, 20-7.
- Davanloo, P., Rosenberg, A.H., Dun, J.J. & Studier, F.W. (1984). Cloning and expression of the gene for bacteriophage T7 RNA polymerase. *Proceedings of the National Academy of Sciences USA* **81**, 2035-9.
- DeLano, W. L. (2002). The PyMOL Molecular Graphics System., 0.99rc6. edn. Palo Alto, CA, USA: DeLano Scientific, <http://www.pymol.org>.
- Dent, K. C., Weber, B. W., Benedik, M. J. & Sewell, B. T. (2008). The cyanide hydratase from *Neurospora crassa* forms a helix which has a dimeric repeat. *Applied Microbiology and Biotechnology* doi: 10.1007 / s00253-008-1735-4.
- Dhillon, J., Chhatre, S., Shanker, R. & Shivaraman, N. (1999). Transformation of aliphatic and aromatic nitriles by a nitrilase from *Pseudomonas* sp. *Canadian Journal of Microbiology* **45**, 811-5.
- Doran, P. T., McKay, C. P., Clow, G. D., Dana, G. L., Fountain, A. G., Nylen, T. & Lyons, W. B. (2002). Valley floor climate observations from the McMurdo Dry Valleys, Antarctica 1986–2000. *Journal of Geophysical Research Atmospheres* **107**, 4772.
- Duran, R. (1998). New shuttle vectors for *Rhodococcus* sp. R312 (formerly *Brevibacterium* sp. R312), a nitrile hydratase producing strain. *Journal of Basic Microbiology* **38**, 101-6.
- Duran, R., Chion, C. K., Bigey, F., Arnaud, A. & Galzy, P. (1992). The N-terminal amino acid sequences of *Brevibacterium* sp. R312 nitrile hydratase. *Journal of Basic Microbiology* **32**, 13-9.
- Duran, R., Nishiyama, M., Horinouchi, S. & Beppu, T. (1993). Characterisation of nitrile hydratase genes cloned by DNA screening from *Rhodococcus erythropolis*. *Bioscience Biotechnology & Biochemistry* **57**, 1323-8.
- Emsley, P. & Cowtan, K. (2004). Coot: model-building tools for molecular graphics. *Acta Crystallographica Section D* **60**, 2126-32.
- Endo, T. & Watanabe, I. (1989). Nitrile hydratase of *Rhodococcus* sp. N-774. Purification and amino acid sequences. *Federation of European Biochemical Societies Letters* **243**, 61-4.

- Fallon, R. D., Turner, I. M., & Stieglitz, B. (1997). A *Pseudomonas putida* capable of stereoselective hydrolysis of nitriles. *Applied Microbiology and Biotechnology* **47**, 156-61.
- Farrelly, V., Rainey, F. & Stackebrandt, E. (1995). Effect of genome size and *rrn* gene copy number on PCR amplification of 16S rRNA genes from a mixture of bacterial species. *Applied Environmental Microbiology* **61**, 2798-801.
- Feng, Y. S., Chen, P. C., Wen, F. S., Hsiao, W. Y. & Lee, C. M. (2008a). Nitrile hydratase from *Mesorhizobium* sp. F28 and its potential for nitrile biotransformation. *Process Biochemistry* **43**, 1391-7.
- Feng, Y. S., Lee, C. M. & Wang, C. C. (2008b). Methods for increasing nitrile biotransformation into amides using *Mesorhizobium* sp. *Prikl Biokhim Mikrobiol* **44**, 304-7.
- Ferrer, M., Beloqui, A., Timmis, K. N. & Golyshin, P. N. (2009). Metagenomics for mining new genetic resources of microbial communities. *Journal of Molecular Microbiology and Biotechnology* **16**, 109-23.
- Fitzgerald, P. M. D. & Madsen, N. B. (1986). Improvement of limit of diffraction and useful X-ray lifetime of crystals of glycogen debranching enzyme. *Journal of Crystal Growth* **76**, 600-6.
- Fournand, D. & Arnaud, A. (2001). Aliphatic and enantioselective amidases: from hydrolysis to acyl transfer activity. *Journal of Applied Microbiology* **91**, 381-93.
- Fournand, D., Arnaud, A. & Galzy, P. (1998). Study of the acyl transfer activity of a recombinant amidase overproduced in an *Escherichia coli* strain. Application for short-chain hydroxamic acid and acid hydrazide synthesis *Journal of Molecular Catalysis B: Enzymatic* **4**, 77-90.
- Frothingham, R., Meeker-O'Connell, W. A., Talbot, E. A., George, J. W. & Kreuzer, K. N. (1996). Identification, cloning, and expression of the *Escherichia coli* pyrazinamidase and nicotinamidase gene, *pncA*. *Antimicrobial Agents and Chemotherapy* **40**, 1426-31.
- Gavagan, J. E., DiCosimo, R., Eisenberg, A., Fager, S. K., Folsom, P. W., Hann, E. C., Schneider, K. J. & Fallon, R. D. (1999). A gram-negative bacterium producing a heat-stable nitrilase highly active on aliphatic dinitriles. *Applied Microbiology and Biotechnology* **52**, 654-9.
- Gerday, C., Aittaleb, M., Bentahir, M., Chessa, J. P., Claverie, P., Collins, T., D'Amico, S., Dumont, J., Garsoux, G., Georgette, D., Hoyoux, A., Lonhienne, T., Meuwis, M. A. & Feller, G. (2000). Cold-adapted enzymes: from fundamentals to biotechnology. *Trends in Biotechnology* **18**, 103-7.

- Gilligan, T., Yamada, H. & Nagasawa, T. (1993). Production of S-(+)-2-phenylpropionic acid from (R,S)-2-phenylpropionitrile by the combination of nitrile hydratase and stereoselective amidase in *Rhodococcus equi* TG328. *Applied Microbiology and Biotechnology* **39**, 720-5.
- Ginalski, K., Elofsson, A., Fischer, D. & Rychlewski, L. (2003). 3D-Jury: A simple approach to improve protein structure predictions. *Bioinformatics* **19**, 1015-18.
- Grant, W.D. (2006) Cultivation of aerobic alkaliphiles. In *Extremophiles* (F.A. Rainey & Owen, A., eds) pp. 439-50. Academic Press. St. Louis, Missouri, USA.
- Guranda, D. T., Shapovalova, I. V. & Shviadas, V. K. (2004). [A new N-acyl derivative of (S)-cysteine for quantitative determination of enantiomers of amino compounds by HPLC method with a precolumn modification with o-phthalaldehyde]. *Bioorg Khim* **30**, 451-7.
- Guzman, L., Belin, D., Carson, M. J. & Beckwith, J. (1995). Tight regulation, modulation, and high-level expression by vectors containing the arabinose P_{BAD} promoter. *Journal of Bacteriology* **177**, 4121-30.
- Hampel, A., Labanauskas, M., Connors, P., Kirkegard, L., Rajbhandary, U. L., Sigler, P. B. & Bock, R. M. (1968). Single crystals of transfer RNA from formylmethionine and phenylalanine transfer RNAs. *Science* **162**, 1384-87.
- Hanahan, D. (1983). Studies on the transformation of *Escherichia coli* with plasmids. *Journal of Molecular Biology* **166**, 557-80.
- Handelsman, J. (2004). Metagenomics: application of genomics to uncultured microorganisms. *Microbiology and Molecular Biology Reviews* **68**, 669-85.
- Hann, E. C., Sigmund, A. E., Fager, S. K., Cooling, F. B., Gavagan, J. E., Bramucci, M. G., Chauhan, S., Payne, M. S. & DiCosimo, R. (2004). Regioselective biocatalytic hydrolysis of (E,Z)-2-methyl-2-butenenitrile for production of (E)-2-methyl-2-butenic acid. *Tetrahedron* **60**, 577-81.
- Harper, D. B. (1976). Purification and properties of an unusual nitrilase from *Nocardia* N.C.I.B. 11216. *Biochemical Society Transactions* **4**, 502-4.
- Harper, D. B. (1977). Microbial metabolism of aromatic nitriles. Enzymology of C-N cleavage by *Nocardia* sp. (*Rhodochrous* group) N.C.I.B. 11216. *Biochemical Journal* **165**, 309-19.
- Harper, D. B. (1985). Characterisation of a nitrilase from *Nocardia* sp. (*Rhodochrous* group) N.C.I.B. 11215, Using p-hydroxybenzonitrile as sole carbon source. *International Journal of Biochemistry* **17**, 677-83.

- Hashimoto, H., Aoki, M., Shimizu, T., Naikai, T., Morikawa, H., Ikenaka, Y., Takahashi, S. & Sato, M. (2004). Crystal structure of C171A/V236A mutant of N-carbamyl-D-amino acid amidohydrolase. *RCSB Protein Data Bank* (**1uf5**).
- Heald, S. C., Brandao, P. F., Hardicre, R. & Bull, A. T. (2001). Physiology, biochemistry and taxonomy of deep-sea nitrile metabolising *Rhodococcus* strains. *Antonie Van Leeuwenhoek* **80**, 169-83.
- Heinemann, U., Engels, D., Bärger, S., Kiziak, C., Mattes, R. & Stolz, A. (2003). Cloning of a nitrilase gene from the cyanobacterium *Synechocystis* sp. strain PCC6803 and heterologous expression and characterisation of the encoded protein. *Applied Environmental Microbiology* **69**, 4359-66.
- Hook, R. H. & Robinson, W. G. (1964). Ricinine Nitrilase. II. Purification and properties. *Journal of Biological Chemistry* **239**, 4263-7.
- Horikoshi, K. (1999). Alkaliphiles: some applications of their products for biotechnology. *Microbiology and Molecular Biology Reviews* **63**, 735-50
- Hoyle, A. J., Bunch, A. W. & Knowles, C. J. (1998). The nitrilases of *Rhodococcus rhodochrous* NCIMB 11216. *Enzyme and Microbial Technology* **23**, 475-82.
- Huang, W., Jia, J., Cummings, J., Nelson, M., Schneider, G. & Lindqvist, Y. (1997). Crystal structure of nitrile hydratase reveals a novel iron centre in a novel fold. *Structure* **5**, 691-9.
- Hughes, J., Armitage, Y. C. & Symes, K. C. (1998). Application of whole cell rhodococcal biocatalysts in acrylic polymer manufacture. *Antonie van Leeuwenhoek, International Journal of General and Molecular Microbiology* **74**, 107-18.
- Hung, C. L., Liu, J. H., Chiu, W. C., Huang, S. W., Hwang, J. K. & Wang, W. C. (2007). Crystal structure of *Helicobacter pylori* formamidase AmiF reveals a cysteine-glutamate-lysine catalytic triad. *Journal of Biological Chemistry* **282**, 12220-9.
- Ikehata, O., Nishiyama, M., Horinouchi, S. & Beppu, T. (1989). Primary structure of nitrile hydratase deduced from the nucleotide sequence of a *Rhodococcus* species and its expression in *Escherichia coli*. *European Journal of Biochemistry* **181**, 563-70.
- Jandhyala, D., Berman, M., Meyers, P. R., Sewell, B. T., Willson, R. C. & Benedik, M. J. (2003). CynD, the cyanide dihydratase from *Bacillus pumilus*: Gene cloning and structural studies. *Applied and Environmental Microbiology* **69**, 4794-805.
- Jones, T. A., Zou, J.Y., Cowan, S. W. & Kjeldgaard, M. (1991). Improved methods for the building of protein models in electron density maps and

- the location of errors in these models. *Acta Crystallographica Section A* **47**, 110-19.
- Kajan, L. & Rychlewski, L. (2007). Evaluation of 3D-Jury on CASP7 models. *Biomed Central Bioinformatics* **8**, 304.
- Karmali, A., Pacheco, R., Tata, R. & Brown, P. (2001). Substitutions of Thr-103-Ile and Trp-138-Gly in amidase from *Pseudomonas aeruginosa* are responsible for altered kinetic properties and enzyme instability. *Molecular Biotechnology* **17**, 201-12.
- Kato, Y., Nakamura, K., Sakiyama, H., Mayhew, S. G. & Asano, Y. (2000). Novel heme-containing lyase, phenylacetaldoxime dehydratase from *Bacillus* sp. strain OxB-1: Purification, characterisation, and molecular cloning of the gene. *Biochemistry* **39**, 800-9.
- Kato, Y., Ooi, R. & Asano, Y. (1998). Isolation and characterisation of a bacterium possessing a novel aldoxime-dehydration activity and nitrile-degrading enzymes. *Archives of Microbiology* **170**, 85-90.
- Kato, Y., Tsuda, T. & Asano, Y. (1999). Nitrile hydratase involved in aldoxime metabolism from *Rhodococcus* sp. strain YH3-3 purification and characterisation. *European Journal of Biochemistry* **263**, 662-70.
- Kato, Y., Yoshida, S., Xie, S. X. & Asano, Y. (2004). Aldoxime dehydratase co-existing with nitrile hydratase and amidase in the iron-type nitrile hydratase-producer *Rhodococcus* sp. N-771. *Journal of Bioscience and Bioengineering* **97**, 250-9.
- Kelly, M. & Clarke, P. H. (1962). An inducible amidase produced by a strain of *Pseudomonas aeruginosa*. *Journal of General Microbiology* **27**, 305-16.
- Kim, J. S., Tiwari, M. K., Moon, H. J., Jeya, M., Ramu, T., Oh, D. K., Kim, I. W. & Lee, J. K. (2009). Identification and characterisation of a novel nitrilase from *Pseudomonas fluorescens* Pf-5. *Applied Microbiology and Biotechnology*. **83**, 273-83
- Kim, S. H. & Oriel, P. (2000). Cloning and expression of the nitrile hydratase and amidase genes from *Bacillus* sp. BR449 into *Escherichia coli*. *Enzyme and Microbial Technology* **27**, 492-501.
- Kim, S. H., Padmakumar, R. & Oriel, P. (2001). Cobalt activation of *Bacillus* BR449 thermostable nitrile hydratase expressed in *Escherichia coli*. *Biotechnology and Applied Biochemistry* **91-93**, 597-603.
- Kimani, S. W., Agarkar, V. B., Cowan, D. A., Sayed, M. F.-R. & Sewell, B. T. (2007). Structure of an aliphatic amidase from *Geobacillus pallidus* RAPc8. *Acta Crystallographica Section D: Biological Crystallography* **63**, 1048-58.

- Kiziak, C., Conradt, D., Stolz, A., Mattes, R. & Klein, J. (2005). Nitrilase from *Pseudomonas fluorescens* EBC191: Cloning and heterologous expression of the gene and biochemical characterisation of the recombinant enzyme. *Microbiology* **151**, 3639-48.
- Kiziak, C., Klein, J. & Stolz, A. (2007). Influence of different carboxy-terminal mutations on the substrate-, reaction- and enantiospecificity of the arylacetonitrilase from *Pseudomonas fluorescens* EBC191. *Protein Engineering, Design and Selection* **20**, 385-96.
- Kobayashi, M., Goda, M. & Shimizu, S. (1998). The catalytic mechanism of amidase also involves nitrile hydrolysis. *Federation of European Biochemical Societies Letters* **439**, 325-28.
- Kobayashi, M., Izui, H., Nagasawa, T. & Yamada, H. (1993a). Nitrilase in biosynthesis of the plant hormone indole-3-acetic acid from indole-3-acetonitrile: Cloning of the *Alcaligenes* gene and site-directed mutagenesis of cysteine residues. *Proceedings of the National Academy of Sciences of the United States of America* **90**, 247-51.
- Kobayashi, M., Komeda, H., Nagasawa, T., Nishiyama, M., Horinouchi, S., Beppu, T., Yamada, H. & Shimizu, S. (1993b). Amidase coupled with low-molecular-mass nitrile hydratase from *Rhodococcus rhodochrous* J1. Sequencing and expression of the gene and purification and characterisation of the gene product. *European Journal of Biochemistry* **217**, 327-36.
- Kobayashi, M., Komeda, H., Yanaka, N., Nagasawa, T. & Yamada, H. (1992a). Nitrilase from *Rhodococcus rhodochrous* J1. Sequencing and overexpression of the gene and identification of an essential cysteine residue. *Journal of Biological Chemistry* **267**, 20746-751.
- Kobayashi, M., Nagasawa, T. & Yamada, H. (1989). Nitrilase of *Rhodococcus rhodochrous* J1. Purification and characterisation. *European Journal of Biochemistry* **182**, 349-56.
- Kobayashi, M., Nagasawa, T. & Yamada, H. (1992b). Enzymatic synthesis of acrylamide: a success story not yet over. *Trends in Biotechnology* **10**, 402-8.
- Kobayashi, M., Nishiyama, M., Nagasawa, T., Horinouchi, S., Beppu, T. & Yamada, H. (1991). Cloning, nucleotide sequence and expression in *Escherichia coli* of two cobalt-containing nitrile hydratase genes from *Rhodococcus rhodochrous* J1. *Biochimica et Biophysica Acta - Gene Structure and Expression* **1129**, 23-33.
- Kobayashi, M. & Shimizu, S. (1998). Metalloenzyme nitrile hydratase: structure, regulation, and application to biotechnology. *Nature Biotechnology* **16**, 733-6.

- Kobayashi, M. & Shimizu, S. (1999). [Nitrile hydratase and cobalt]. *Tanpakushitsu Kakusan Koso* **44**, 42-50.
- Kobayashi, M., Yanaka, N., Nagasawa, T. & Yamada, H. (1991c). Hyperinduction of an aliphatic nitrilase by *Rhodococcus rhodochrous* K22. *Federation of European Microbiological societies Microbiology Letters* **77**, 121-3.
- Kobayashi, M., Yanaka, N., Nagasawa, T. & Yamada, H. (1992c). Primary structure of an aliphatic nitrile-degrading enzyme, aliphatic nitrilase, from *Rhodococcus rhodochrous* K22 and expression of its gene and identification of its active site residue. *Biochemistry* **31**, 9000-7.
- Komeda, H., Hori, Y., Kobayashi, M. & Shimizu, S. (1996a). Transcriptional regulation of the *Rhodococcus rhodochrous* J1 nitA gene encoding a nitrilase. *Proceedings of the National Academy of Sciences of the United States of America* **93**, 10572-7.
- Komeda, H., Kobayashi, M. & Shimizu, S. (1996b). Characterisation of the gene cluster of high-molecular-mass nitrile hydratase (H-NHase) induced by its reaction product in *Rhodococcus rhodochrous* J1. *Proceedings of the National Academy of Sciences USA* **93**, 4267-72.
- Komeda, H., Kobayashi, M. & Shimizu, S. (1996c). A novel gene cluster including the *Rhodococcus rhodochrous* J1 nhIBA genes encoding a low molecular mass nitrile hydratase (L-NHase) induced by its reaction product. *Journal of Biological Chemistry* **271**, 15796-802.
- Kopf, M. A., Bonnet, D., Artaud, I., Petre, D. & Mansuy, D. (1996). Key role of alkanolic acids on the spectral properties, activity, and active-site stability of iron-containing nitrile hydratase from *Brevibacterium* R312. *European Journal of Biochemistry* **240**, 239-44.
- Korbie, D. J. & Mattick, J. S. (2008). Touchdown PCR for increased specificity and sensitivity in PCR amplification. *Nature Protocols* **3**, 1452-6.
- Kotlova, E. K., Chestukhina, G. G., Astaurova, O. B., Leonova, T. E., Yanenko, A. S. & Debabov, V. G. (1999). Isolation and primary characterisation of an amidase from *Rhodococcus rhodochrous*. *Biokhimiya/Biochemistry (Moscow)* **64**, 459-65.
- Krissinel, E. & Henrick, K. (2004). Secondary-structure matching (SSM), a new tool for fast protein structure alignment in three dimensions. *Acta Crystallographica Section D: Biological Crystallography* **60**, 2256-68.
- Kumaran, D., Eswaramoorthy, S., Gerchman, S. E., Kycia, H., Studier, F. W. & Swaminathan, S. (2003). Crystal structure of a putative CN hydrolase from yeast. *Proteins: Structure, Function and Genetics* **52**, 283-91.

- Kushner, D. J. (1978). Life in high salt and solute concentrations: halophilic bacteria. In *Microbial life in extreme environments*. (D. J., Kushner, eds), pp. 317-68. Academic Press, London.
- Laemmli, U.K. (1970) Cleavage of structural proteins during the assembly of the head of bacteriophage T4. *Nature* **15**, 680-5
- Larkin, M. A., Blackshields, G., Brown, N. P., Chenna, R., McGettigan, P. A., McWilliam, H., Valentin, F., Wallace, I. M., Wilm, A., Lopez, R., Thompson, J. D., Gibson, T. J. & Higgins, D. G. (2007). Clustal W and Clustal X version 2.0. *Bioinformatics* **23**, 2947-8.
- Layh, N., Parratt, J. & Willetts, A. (1998). Characterisation and partial purification of an enantioselective arylacetonitrilase from *Pseudomonas fluorescens* DSM 7155. *Journal of Molecular Catalysis - B Enzymatic* **5**, 467-74.
- Lévy-Schil, S., Soubrier, F., Coq, A.-M. C.-L., Faucher, D., Crouzet, J. & Pétré, D. (1995). Aliphatic nitrilase from a soil-isolated *Comamonas testosteroni* sp.: gene cloning and overexpression, purification and primary structure. *Gene* **161**, 15-20.
- Li, W. Z., Zhang, Y. Q. & Yang, H. F. (1992). Formation and purification of nitrile hydratase from *Corynebacterium pseudodiphtheriticum* ZBB-41. *Biotechnology and Applied Biochemistry* **36**, 171-81.
- Liebeton, K. & Eck, J. (2004). Identification and expression in *E. coli* of novel nitrile hydratases from the metagenome. *Engineering in Life Sciences* **4**, 557-62.
- Litchfield, C.D., Sikaroodi, M., Gillevet, P.M. (2006) Characterisation of natural communities of halophilic microorganisms. In *Extremophiles* (F.A. Rainey & Owen, A., eds) pp. 439-50. Academic Press. St. Louis, Missouri, USA.
- Lourenco, P. M., Almeida, T., Mendonca, D., Simoes, F. & Novo, C. (2004). Searching for nitrile hydratase using the consensus-degenerate hybrid oligonucleotide primers strategy. *Journal of Basic Microbiology* **44**, 203-14.
- Lovell, S. C., Davis, I. W., Arendall, W. B., 3rd, de Bakker, P. I., Word, J. M., Prisant, M. G., Richardson, J. S. & Richardson, D. C. (2003). Structure validation by C geometry: phi, psi and C deviation. *Proteins* **50**, 437-50.
- Lundgren, S., Lohkamp, B., Andersen, B., Piskur, J. & Dobritzsch, D. (2008). The Crystal structure of α -Alanine synthase from *Drosophila melanogaster* reveals a homooctameric helical turn-like assembly. *Journal of Molecular Biology* **377**, 1544-59.
- Luo, H. Y., Miao, L. H., Fang, C., Yang, P. L., Wang, Y. R., Shi, P. J., Yao, B. & Fan, Y. L. (2008). *Nesterenkonia flava* sp. nov., isolated from paper-mill effluent. *International Journal of Systematic and Evolutionary Microbiology* **58**, 1927-30.

- Madhavan, N. K., Roopesh, K., Chacko, S. & Pandey, A. (2005). Comparative study of amidase production by free and immobilised *Escherichia coli* cells. *Biotechnology and Applied Biochemistry* **120**, 97-108.
- Maestracci, M., Thiery, A., Bui, K., Arnaud, A. & Galzy, P. (1984). Activity and regulation of an amidase, acylamide amidohydrolase EC 3.5.1.4, with a wide substrate spectrum from a *Brevibacterium* sp. *Archives of Microbiology* **138**, 315-20.
- Makhongela, H. S., Glowacka, A. E., Agarkar, V. B., Sewell, B. T., Weber, B., Cameron, R. A., Cowan, D. A. & Burton, S. G. (2007). A novel thermostable nitrilase superfamily amidase from *Geobacillus pallidus* showing acyl transfer activity. *Applied Microbiology and Biotechnology* **75**, 801-11.
- Martin, F. H., Castro, M. M., Aboul-ela, F. & Tinoco, I., Jr. (1985). Base pairing involving deoxyinosine: implications for probe design. *Nucleic Acids Research* **13**, 8927-38.
- Martínková, L. & Kren, V. (2002). Nitrile- and amide-converting microbial enzymes: stereo-, regio- and chemoselectivity. *Biocatalysis and Biotransformation* **20**, 73-93.
- Martínková, L., Uhnáková, B., Pátek, M., Nesvera, J. & Kren, V. (2009). Biodegradation potential of the genus *Rhodococcus*. *Environment International* **35**, 162-77.
- Martínková, L., Vejvoda, V. & Kren, V. (2008). Selection and screening for enzymes of nitrile metabolism. *Journal of Biotechnology* **133**, 318-26.
- Mascharak, P. K. (2002). Structural and functional models of nitrile hydratase. *Coordination Chemistry Reviews* **225**, 201-14.
- Mayaux, J. F., Cerebelaud, E., Soubrier, F., Yeh, P., Blanche, F. & Petre, D. (1991). Purification, cloning, and primary structure of a new enantiomer-selective amidase from a *Rhodococcus* strain: structural evidence for a conserved genetic coupling with nitrile hydratase. *Journal of Bacteriology* **173**, 6694-704.
- Mayaux, J. F., Cerebelaud, E., Soubrier, F., Faucher, D. & Petre, D. (1990). Purification, cloning, and primary structure of an enantiomer-selective amidase from *Brevibacterium* sp. strain R312: structural evidence for genetic coupling with nitrile hydratase. *Journal of Bacteriology* **172**, 6764-73.
- McCoy, A. J., Grosse-Kunstleve, R. W., Adams, P. D., Winn, M. D., Storoni, L. C. & Read, R. J. (2007). Phaser crystallographic software. *Journal of Applied Crystallography* **40**.

- Miyanaga, A., Fushinobu, S., Ito, K. & Wakagi, T. (2001). Crystal structure of cobalt-containing nitrile hydratase. *Biochemical and Biophysical Research Communications* **288**, 1169-74.
- Morgulis, A., Coulouris, G., Raytselis, Y., Madden, T. L., Agarwala, R. & Schaffer, A. A. (2008). Database indexing for production MegaBLAST searches. *Bioinformatics* **24**, 1757-64.
- Morita, R. Y. (1975). Psychrophilic bacteria. *Bacteriological Reviews* **39**, 144-67.
- Nagamune, T., Kurata, H., Hirata, M., Honda, J., Koike, H., Ikeuchi, M., Inoue, Y., Hirata, A. & Endo, I. (1990). Purification of inactivated photoresponsive nitrile hydratase. *Biochemical and Biophysical Research Communications* **168**, 437-42.
- Nagasawa, T., Mauger, J. & Yamada, H. (1990). A novel nitrilase, arylacetone nitrilase, of *Alcaligenes faecalis* JM3. Purification and characterisation. *European Journal of Biochemistry* **194**, 765-72.
- Nagasawa, T., Nanba, H., Ryuno, K., Takeuchi, K. & Yamada, H. (1987). Nitrile hydratase of *Pseudomonas chlororaphis* B23. Purification and characterisation. *European Journal of Biochemistry* **162**, 691-8.
- Nagasawa, T., Ryuno, K. & Yamada, H. (1986). Nitrile hydratase of *Brevibacterium* R312--purification and characterisation. *Biochemical and Biophysical Research Communications* **139**, 1305-12.
- Nagasawa, T., Takeuchi, K. & Yamada, H. (1991). Characterisation of a new cobalt-containing nitrile hydratase purified from urea-induced cells of *Rhodococcus rhodochrous* J1. *European Journal of Biochemistry* **196**, 581-9.
- Nagasawa, T., Wieser, M., Nakamura, T., Iwahara, H., Yoshida, T. & Gekko, K. (2000). Nitrilase of *Rhodococcus rhodochrous* J1: Conversion into the active form by subunit association. *European Journal of Biochemistry* **267**, 138-44.
- Nagashima, S., Nakasako, M., Dohmae, N., Tsujimura, M., Takio, K., Odaka, M., Yohda, M., Kamiya, N. & Endo, I. (1998). Novel non-heme iron center of nitrile hydratase with a claw setting of oxygen atoms. *Nature Structural & Molecular Biology* **5**, 347-51.
- Nakai, T., Hasegawa, T., Yamashita, E., Yamamoto, M., Kumasaka, T., Ueki, T., Nanba, H., Ikenaka, Y., Takahashi, S. & Sato, M. (2000). Crystal structure of N-carbamyl-D-amino acid amidohydrolase with a novel catalytic framework common to amidohydrolases. *Structure with Folding & Design* **8**, 729-38.
- Nakasako, M., Odaka, M., Yohda, M., Dohmae, N., Takio, K., Kamiya, N. & Endo, I. (1999). Tertiary and quaternary structures of photoreactive Fe-

type nitrile hydratase from *Rhodococcus* sp. N-771: roles of hydration water molecules in stabilizing the structures and the structural origin of the substrate specificity of the enzyme. *Biochemistry* **38**, 9887-98.

Narinx, E., Baise, E. & Gerday, C. (1997). Subtilisin from psychrophilic antarctic bacteria: characterisation and site-directed mutagenesis of residues possibly involved in the adaptation to cold. *Protein Engineering* **10**, 1271-9.

Nawaz, M. S., Chapatwala, K. D. & Wolfram, J. H. (1989). Degradation of acetonitrile by *Pseudomonas putida*. *Applied Environmental Microbiology* **55**, 2267-74.

Neumann, S., Granzin, J., Kula, M.-R. & Labahn, J. (2002). Crystallisation and preliminary X-ray data of the recombinant peptide amidase from *Stenotrophomonas maltophilia*. *Acta Crystallographica Section D: Biological Crystallography* **58**, 333-5.

Nishiyama, M., Horinouchi, S., Kobayashi, M., Nagasawa, T., Yamada, H. & Beppu, T. (1991). Cloning and characterisation of genes responsible for metabolism of nitrile compounds from *Pseudomonas chlororaphis* B23. *Journal of Bacteriology* **173**, 2465-72.

Nojiri, M., Yohda, M., Odaka, M., Matsushita, Y., Tsujimura, M., Yoshida, T., Dohmae, N., Takio, K. & Endo, I. (1999). Functional expression of nitrile hydratase in *Escherichia coli*: requirement of a nitrile hydratase activator and post-translational modification of a ligand cysteine. *Journal of Biochemistry* **125**, 696-704.

O'Mahony, R., Doran, J., Coffey, L., Cahill, O. J., Black, G. W. & O'Reilly, C. (2005). Characterisation of the nitrile hydratase gene clusters of *Rhodococcus erythropolis* strains AJ270 and AJ300 and *Microbacterium* sp. AJ115 indicates horizontal gene transfer and reveals an insertion of IS1166. *Antonie Van Leeuwenhoek* **87**, 221-32.

O'Reilly, C. & Turner, P. D. (2003). The nitrilase family of CN hydrolysing enzymes - A comparative study. *Journal of Applied Microbiology* **95**, 1161-74.

Ohtsuka, E., Matsuki, S., Ikehara, M., Takahashi, Y. & Matsubara, K. (1985). An alternative approach to deoxyoligonucleotides as hybridization probes by insertion of deoxyinosine at ambiguous codon positions. *Journal of Biological Chemistry* **260**, 2605-8.

Pace, H. C. & Brenner, C. (2001). The nitrilase superfamily: classification, structure and function. *Genome Biology* **2**, reviews0001.1 - 1.9

Pace, H. C., Hodawadekar, S. C., Draganescu, A., Huang, J., Bieganowski, P., Pekarsky, Y., Croce, C. M. & Brenner, C. (2000). Crystal structure of the

worm NitFhit Rosetta Stone protein reveals a Nit tetramer binding two Fhit dimers. *Current Biology* **10**, 907-17.

- Pacheco, R., Karmali, A., Serralheiro, M. L. & Haris, P. I. (2005). Application of Fourier transform infrared spectroscopy for monitoring hydrolysis and synthesis reactions catalyzed by a recombinant amidase. *Analytical Biochemistry* **346**, 49-58.
- Padmakumar, R. & Oriol, P. (1999). Bioconversion of acrylonitrile to acrylamide using a thermostable nitrile hydratase. *Biotechnology and Applied Biochemistry* **77-79**, 671-9.
- Pardee, A. B., Jacob, F. & Monod, J. (1959). The genetic control and cytoplasmic expression of "inducibility" in the synthesis of β -galactosidase in *E. coli*. *Journal of Molecular Biology* **1**, 165-78..
- Parker, J. & Fishman, S. (1979). Mapping hisS, the structural gene for histidyl-transfer ribonucleic acid synthetase, in *Escherichia coli*. *Journal of Bacteriology* **138**, 264-67.
- Payne, M. S., Wu, S., Fallon, R. D., Tudor, G., Stieglitz, B., Turner, I. M., Jr. & Nelson, M. J. (1997). A stereoselective cobalt-containing nitrile hydratase. *Biochemistry* **36**, 5447-54.
- Pereira, R. A., Graham, D., Rainey, F. A. & Cowan, D. A. (1998). A novel thermostable nitrile hydratase. *Extremophiles* **2**, 347-57.
- Pettersen, E. F., Goddard, T. D., Huang, C. C., Couch, G. S., Greenblatt, D. M., Meng, E. C. & Ferrin, T. E. J. (2004). UCSF Chimera - A visualization system for exploratory research and analysis. *Journal of Computational Chemistry* **25**, 1605-12
- Pflugrath, P. (1999). The finer things in X-ray diffraction data collection. *Acta Crystallographica Section D: Biological Crystallography* **D55**, 1718-25.
- Podar, M., Eads, J. R. & Richardson, T. H. (2005). Evolution of a microbial nitrilase gene family: A comparative and environmental genomics study. *BioMed Central Evolutionary Biology* **5**, 42
- Pogorelova, T. E., Ryabchenko, L. E., Sunzov, N. I. & Yanenko, A. S. (1996). Cobalt-dependent transcription of the nitrile hydratase gene in *Rhodococcus rhodochrous* M8. *Federation of European Microbiological societies Microbiology Letters* **144**, 191-5.
- Pollak, P., Romender, G., Hagedorn, F. & Gelbke, H.P. (1991). Ullman's encyclopaedia of industrial chemistry, pp. 363-76.
- Popescu, V. C., Munck, E., Fox, B. G., Sanakis, Y., Cummings, J. G., Turner, I. M., Jr. & Nelson, M. J. (2001). Mossbauer and EPR studies of the photoactivation of nitrile hydratase. *Biochemistry* **40**, 7984-91.

- Precigou, S., Goulas, P. & Duran, R. (2001). Rapid and specific identification of nitrile hydratase (NHase)-encoding genes in soil samples by polymerase chain reaction. *Federation of European Microbiological societies Microbiology Letters* **204**, 155-61.
- Ramakrishna, C., Dave, H. & Ravindranathan, M. (1999). Microbial metabolism of nitriles and its biotechnological potential. *Journal of Scientific and Industrial Research* **58**, 925-47.
- Reysenbach, A. & Pace, N. (1995). Reliable amplification of hyperthermophilic archaeal 16S rRNA genes by the polymerase chain reaction. In *Archaea: a Laboratory Manual – Thermophiles*. (Robb, F. & A. Place, eds). pp. 101-5 Cold Spring Harbor, New York.
- Robertson, D. E., Chaplin, J. A., DeSantis, G., Podar, M., Madden, M., Chi, E., Richardson, T., Milan, A., Miller, M., Weiner, D. P., Wong, K., McQuaid, J., Farwell, B., Preston, L. A., Tan, X., Snead, M. A., Keller, M., Mathur, E., Kretz, P. L., Burk, M. J. & Short, J. M. (2004). Exploring nitrilase sequence space for enantioselective catalysis. *Applied and Environmental Microbiology* **70**, 2429-36.
- Russell, N. J. (1998). Molecular adaptations in psychrophilic bacteria: potential for biotechnological applications. *Advances in Biochemical Engineering/Biotechnology* **61**, 1-21.
- Russell, N.J. & Cowan, D.A. (2006) Handling of psychrophilic microorganisms. In *Extremophiles* (F.A. Rainey & Owen, A., eds) pp. 439-50. Academic Press. St. Louis, Missouri, USA.
- Ryabchenko, L. E., Podchernyaev, D. A., Kotlova, E. K. & Yanenko, A. S. (2006). Cloning the amidase gene from *Rhodococcus rhodochrous* M8 and its expression in *Escherichia coli*. *Russian Journal of Genetics* **42**, 886-92.
- Saitou, N. & Nei, M. (1987). The neighbor-joining method: A new method for reconstructing phylogenetic trees. *Molecular Biology and Evolution* **4**, 406-25.
- Sakai, N., Tajika, Y., Yao, M., Watanabe, N. & Tanaka, I. (2004). Crystal structure of hypothetical protein PH0642 from *Pyrococcus horikoshii* at 1.6 Å resolution. *Proteins* **57**, 869-73.
- Sali, A. & Blundell, T. L. (1993). Comparative protein modelling by satisfaction of spatial restraints. *Journal of Molecular Biology* **234**, 779-815.
- Sambrook, J. & Russell, D. W. (2001). *Molecular cloning: A laboratory manual*. (3rd edition) New York, USA.: Cold Spring Harbor Laboratory Press
- Santarossa, G., Lafranconi, P. G., Alquati, C., DeGioia, L., Alberghina, L., Fantucci, P. & Lotti, M. (2005). Mutations in the "lid" region affect chain

- length specificity and thermostability of a *Pseudomonas fragi* lipase. *Federation of European Biochemical Societies Letters* **579**, 2383-6.
- Schmeisser, C., Steele, H. & Streit, W. R. (2007). Metagenomics, biotechnology with non-culturable microbes. *Applied Microbiology and Biotechnology* **75**, 955-62.
- Sewell, B. T., Berman, M. N., Meyers, P. R., Jandhyala, D. & Benedik, M. J. (2003). The cyanide degrading nitrilase from *Pseudomonas stutzeri* AK61 is a two-fold symmetric, 14-subunit spiral. *Structure* **11**, 1413-22.
- Sewell, B. T., Thuku, R. N., Zhang, X. & Benedik, M. J. (2005). Oligomeric structure of nitrilases: Effect of mutating interfacial residues on activity. In *Annals of the New York Academy of Sciences*. **1056**, pp. 153-9.
- Shin, S., Lee, T.H., Ha, N.C., Koo, H., Kim, S.Y., Lee, H.S., Kim, Y. & Oh, B.H. (2002). Structure of malanomidase E2 reveals a novel Ser-cisSer-Lys catalytic triad in a new serine hydrolase fold that is prevalent in nature. *European Molecular Biology Organisation Journal* **21**, 2509-16.
- Singh, R., Sharma, R., Tewari, N. & Rawat, D. S. (2006). Nitrilase and its application as a 'green' catalyst. *Chemistry & Biodiversity* **3**, 1279-87.
- Skouloubris, S., Labigne, A. & De Reuse, H. (1997). Identification and characterisation of an aliphatic amidase in *Helicobacter pylori*. *Molecular Microbiology* **25**, 989-98.
- Skouloubris, S., Labigne, A. & De Reuse, H. (2001). The AmiE aliphatic amidase and AmiF formamidase of *Helicobacter pylori*: natural evolution of two enzyme paralogues. *Molecular Microbiology* **40**, 596-609.
- Smith, M., Jesse, J., Landers, T., Jordan, J., 1990. High efficiency bacterial electroporation: 1×10^{10} *E. coli* transformants/ μg . *Focus* **12** (2), 38-40.
- Song, L., Wang, M., Yang, X. & Qian, S. (2007). Purification and characterisation of the enantioselective nitrile hydratase from *Rhodococcus* sp. AJ270. *Biotechnology Journal* **2**, 717-24.
- Sorokin, D. Y., van Pelt, S. & Tourova, T. P. (2008). Utilization of aliphatic nitriles under haloalkaline conditions by *Bacillus alkalinitrilicus* sp. nov. isolated from soda solonchak soil. *Federation of European Microbiological societies Microbiology Letters* **288**, 235-40.
- Sorokin, D. Y., van Pelt, S., Tourova, T. P. & Evtushenko, L. I. (2009). *Nitriliruptor alkaliphilus* gen. nov., sp. nov., a deep-lineage haloalkaliphilic actinobacterium from soda lakes capable of growth on aliphatic nitriles, and proposal of *Nitriliruptoraceae* fam. nov. and *Nitriliruptorales* ord. nov. *International Journal of Systematic and Evolutionary Microbiology*. **59**, 248-53.

- Sorokin, D. Y., van Pelt, S., Tourova, T. P., Takaichi, S. & Muyzer, G. (2007). Acetonitrile degradation under haloalkaline conditions by *Natronocella acetinitrilica* gen. nov., sp. nov. *Microbiology* **153**, 1157-64.
- Soubrier, F., Levy-Schil, S., Mayaux, J. F., Petre, D., Arnaud, A. & Crouzet, J. (1992). Cloning and primary structure of the wide-spectrum amidase from *Brevibacterium* sp. R312: high homology to the amiE product from *Pseudomonas aeruginosa*. *Gene* **116**, 99-104.
- Stalker, D. M., Kiser, J. A., Baldwin, G., Coulombe, B. & Houck, C. M. (1996). *Cotton weed control using the BXN system*. In *Herbicide resistant crops*. pp. 93-105. (Duke, O., eds) CRC press, USA.
- Stalker, D. M., Malyj, L. D. & McBride, K. E. (1988a). Purification and properties of a nitrilase specific for the herbicide bromoxynil and corresponding nucleotide sequence analysis of the bxn gene. *Journal of Biological Chemistry* **263**, 6310-14.
- Stalker, D. M. & McBride, K. E. (1987). Cloning and expression in *Escherichia coli* of a *Klebsiella ozaenae* plasmid-borne gene encoding a nitrilase specific for the herbicide bromoxynil. *Journal of Bacteriology* **169**, 955-60.
- Stalker, D. M., McBride, K. E. & Malyj, L. D. (1988b). Herbicide resistance in transgenic plants expressing a bacterial detoxification gene. *Science* **241**, 419-23.
- Stevenson, D. E., Feng, R., Dumas, F., Groleau, D., Mihoc, A. & Storer, A. C. (1992). Mechanistic and structural studies on *Rhodococcus* ATCC 39484 nitrilase. *Biotechnology and Applied Biochemistry* **15**, 283-302.
- Studier, F. W. & Moffatt, B. A. (1986). Use of bacteriophage T7 RNA polymerase to direct selective high-level expression of cloned genes. *Journal of Molecular Biology* **189**, 113-30.
- Takashima, Y., Kawabe, T. & Mitsuda, S. (2000). Factors affecting the production of nitrile hydratase by thermophilic *Bacillus smithii* SC-J05-1. *Journal of Bioscience and Bioengineering* **89**, 282-4.
- Takashima, Y., Yamaga, Y. & Mitsuda, S. (1998). Nitrile hydratase from a thermophilic *Bacillus smithii*. *Journal of Industrial Microbiology and Biotechnology* **20**, 220-26.
- Tamura, K., Dudley, J., Nei, M. & Kumar, S. (2007). Molecular Evolutionary Genetics Analysis (MEGA) software version 4.0. *Molecular Biology and Evolution* **24**, 1596-99.
- Terwilliger, T. C., Grosse-Kunstleve, R. W., Afonine, P. V., Moriarty, N. W., Zwart, P. H., Hung, L.-W., Read, R. J. & Adams, P. D. (2008). Iterative model building, structure refinement and density modification with the

PHENIX AutoBuild wizard. *Acta Crystallographica Section D: Biological Crystallography* **64** (Pt 1), 61-9.

- Thiery, A., Maestracci, M., Arnaud, A., Galzy, P. & Nicolas, M. (1988). Purification and properties of an acylamide amidohydrolase (E.C.3.5.1.4) with a wide activity spectrum from *Brevibacterium* sp. R 312. *Journal of Basic Microbiology* **26**, 299-311.
- Thimann, K. V. & Mahadevan, S. (1964). Nitrilase, Occurrence, preparation, and general properties of the enzyme. *Archives of Biochemistry and Biophysics* **1405**, 133-41.
- Thompson, L., Knowles, C. J., Linton, E. & Wyatt, J. W. (1988). Microbial biotransformations of nitriles. *Chemistry in Britain* **24**, 900-10.
- Thuku, R. N., Brady, D., Benedik, M. J. & Sewell, B. T. (2009). Microbial nitrilases: versatile, spiral forming, industrial enzymes. *Journal of Applied Microbiology*. **106**, 703-27.
- Thuku, R. N., Weber, B. W., Varsani, A. & Sewell, B. T. (2007). Post-translational cleavage of recombinantly expressed nitrilase from *Rhodococcus rhodochrous* J1 yields a stable, active helical form. *Federation of European Biochemical Societies Journal* **274**, 2099-108.
- Torsvik, V. & Ovreas, L. (2002). Microbial diversity and function in soil: from genes to ecosystems. *Current Opinion in Microbiology* **5**, 240-45.
- Torsvik, V., Ovreas, L. & Thingstad, T. F. (2002). Prokaryotic diversity-magnitude, dynamics, and controlling factors. *Science* **296**, 1064-66.
- Vagin, A. A., Steiner, R. A., Lebedev, A. A., Potterton, L., McNicholas, S., Long, F. & Murshudov, G. N. (2004). REFMAC5 dictionary: organization of prior chemical knowledge and guidelines for its use. *Acta Crystallographica Section D: Biological Crystallography* **60**, 2184-95.
- Vejvoda, V., Kaplan, O., Bezouska, K., Pompach, P., Sulc, M., Cantarella, M., Benada, O., Uhnakova, B., Rinagelova, A., Lutz-Wahl, S., Fischer, L., Kren, V. & Martinkova, L. (2008). Purification and characterisation of a nitrilase from *Fusarium solani* O1. *Journal of Molecular Catalysis B: Enzymatic* **50**, 99-106.
- Wang, J. Y., Wang, D. X., Zheng, Q. Y., Huang, Z. T. & Wang, M. X. (2007). Nitrile biotransformations for the efficient synthesis of highly enantiopure 1-arylaziridine-2-carboxylic acid derivatives and their stereoselective ring-opening reactions. *Journal of Organic Chemistry* **72**, 2040-5.
- Wang, W. C., Hsu, W. H., Chien, F. T. & Chen, C. Y. (2001). Crystal structure and site-directed mutagenesis studies of N-carbamoyl-D-amino-acid amidohydrolase from *Agrobacterium radiobacter* reveals a homotetramer and insight into a catalytic cleft. *Journal of Molecular Biology* **306**, 251-61.

- Wayne, L. G. (1974). Simple pyrazinamidase and urease tests for routine identification of mycobacteria. *American review of respiratory disease*, **109**, 147-51.
- Weatherburn, M. (1967). Phenol-hypochlorite reaction for determination of ammonia. *Analytical Chemistry* **39**, 971-4.
- Wilson, S. A., Wachira, S. J., Norman, R. A., Pearl, L. H. & Drew, R. E. (1996). Transcription antitermination regulation of the *Pseudomonas aeruginosa* amidase operon. *European Molecular Biology Organisation Journal*, **15** (21) 5907-16.
- Wilson, S. A., Williams, R. J., Pearl, L. H. & Drew, R. E. (1995). Identification of two new genes in the *Pseudomonas aeruginosa* amidase operon, encoding an ATPase (AmiB) and a putative integral membrane protein (AmiS). *Journal of Biological Chemistry* **270**, 18818-24.
- Wintrode, P. L., Miyazaki, K. & Arnold, F. H. (2000). Cold adaptation of a mesophilic subtilisin-like protease by laboratory evolution. *Journal of Biological Chemistry* **275**, 31635-40.
- Woodward, J. D., Weber, B. W., Scheffer, M. P., Benedik, M. J., Hoenger, A. & Sewell, B. T. (2008). Helical structure of unidirectionally shadowed metal replicas of cyanide hydratase from *Gloeocercospora sorghi*. *Journal of Structural Biology* **161**, 111-19.
- Wu, S., Fallon, R. D. & Payne, M. S. (1997). Over-production of stereoselective nitrile hydratase from *Pseudomonas putida* 5B in *Escherichia coli*: activity requires a novel downstream protein. *Applied Microbiology and Biotechnology* **48**, 704-8.
- Xu, Y., Feller, G., Gerday, C. & Glansdorff, N. (2003). *Moritella* cold-active dihydrofolate reductase: are there natural limits to optimisation of catalytic efficiency at low temperature? *Journal of Bacteriology* **185**, 5519-26.
- Xuan, J. C. & Weber, I. T. (1992). Crystal structure of a B-DNA dodecamer containing inosine, d(CGCI AATTCGCG), at 2.4 Å resolution and its comparison with other B-DNA dodecamers. *Nucleic Acids Research* **20**, 5457-64.
- Yamada, H. & Kobayashi, M. (1996). Nitrile hydratase and its application to industrial production of acrylamide. *Bioscience, Biotechnology and Biochemistry* **60**, 1391-400.
- Yamaki, T., Oikawa, T., Ito, K. & Nakamura, T. (1997). Cloning and sequencing of a nitrile hydratase gene from *Pseudonocardia thermophila* JCM3095. *Journal of Fermentation and Bioengineering* **83**, 474-7.

- Yamamoto, K., Fujimatsu, I. & Komatsu, K. (1992a). Purification and characterisation of the nitrilase from *Alcaligenes faecalis* ATCC 8750 responsible for enantioselective hydrolysis of mandelonitrile. *Journal of Fermentation and Bioengineering* **73**, 425-30.
- Yamamoto, K. & Komatsu, K. (1991). Purification and characterisation of nitrilase responsible for the enantioselective hydrolysis from *Acinetobacter* sp. AK 226. *Agricultural and Biological Chemistry* **55**, 1459-66.
- Yamamoto, K., Oishi, K., Fujimatsu, I. & Komatsu, K.-I. (1991). Production of R-(-)-mandelic acid from mandelonitrile by *Alcaligenes faecalis* ATCC 8750. *Applied and Environmental Microbiology* **57**, 3028-32.
- Yamamoto, K., Ueno, Y., Otsubo, K., Kawakami, K. & Komatsu, K.-I. (1990). Production of S-(+)-ibuprofen from a nitrile compound by *Acinetobacter* sp. strain AK226. *Applied and Environmental Microbiology* **56**, 3125-9.
- Yamamoto, K., Ueno, Y., Otsubo, K., Yamane, H., Komatsu, K.-i. & Tani, Y. (1992b). Efficient conversion of dinitrile to mononitrile-monocarboxylic acid by *Corynebacterium* sp. C5 cells during tranexamic acid synthesis. *Journal of Fermentation and Bioengineering* **73**, 125-9.
- Yeom, S.-J., Kim, H.-J., Lee, J.-K., Kim, D.-E. & Oh, D.-K. (2008). An amino acid at position 142 in nitrilase from *Rhodococcus rhodochrous* ATCC 33278 determines the substrate specificity for aliphatic and aromatic nitriles. *Biochemical Journal* **415**, 401-7.
- Zheng, L., Gibbs, M. J. & Rodoni, B. C. (2008a). Quantitative PCR measurements of the effects of introducing inosines into primers provides guidelines for improved degenerate primer design. *Journal of Virological Methods* **153**, 97-103.
- Zheng, Y.G., Chen, J., Liu, Z.Q., Wu, M.H., Xing, L.Y. & Shen, Y.-C. (2008b). Isolation, identification and characterisation of *Bacillus subtilis* ZJB-063, a versatile nitrile-converting bacterium. *Applied Microbiology and Biotechnology* **77**, 985-93.
- Zhou, J., Bruns, M., & Tiedje, J. (1996). DNA recovery from soils of diverse composition. *Applied Environmental Microbiology* **62**, 316-22.
- Zhu, D., Mukherjee, C., Biehl, E. R. & Hua, L. (2007). Discovery of a mandelonitrile hydrolase from *Bradyrhizobium japonicum* USDA110 by rational genome mining. *Journal of Biotechnology* **129**, 645-50.
- Zhu, D., Mukherjee, C., Yang, Y., Rios, B. E., Gallagher, D. T., Smith, N. N., Biehl, E. R. & Hua, L. (2008). A new nitrilase from *Bradyrhizobium japonicum* USDA 110. Gene cloning, biochemical characterisation and substrate specificity. *Journal of Biotechnology* **133**, 327-33.